



University  
of Glasgow

Othman, Siti Sarah (2011) *Interactions of an attenuated AroA- derivative of Pasteurella multocida B:2 with mammalian cells and its potential for DNA vaccine delivery*. PhD thesis.

<http://theses.gla.ac.uk/2905/>

Copyright and moral rights for this thesis are retained by the author

A copy can be downloaded for personal non-commercial research or study, without prior permission or charge

This thesis cannot be reproduced or quoted extensively from without first obtaining permission in writing from the Author

The content must not be changed in any way or sold commercially in any format or medium without the formal permission of the Author

When referring to this work, full bibliographic details including the author, title, awarding institution and date of the thesis must be given

**Interactions of an attenuated AroA<sup>-</sup> derivative of  
*Pasteurella multocida* B:2 with mammalian cells  
and its potential for DNA vaccine delivery**



**SITI SARAH OTHMAN**

**(B Sc., M Sc.)**

**Institute of Infection, Immunity and Inflammation**

**College of Medical, Veterinary and Life Sciences**

**University of Glasgow**

**June 2011**

**A thesis submitted for the degree of**

***Doctor of Philosophy***

# Declaration

I hereby declare that the work presented in this thesis is my own, except where otherwise cited or acknowledged. No part of this thesis has been presented for any other degree. The research for this thesis was performed between November 2007 and June 2011.

Siti Sarah Othman

# Acknowledgements

*“Hutang emas boleh dibayar, hutang budi dibawa mati”*

“A debt of money can be repaid; a debt of kindness goes with one to the grave”  
(Malay proverb)

As the saying above, in my most humble form, I would like to express my gratitude to all the people who have made this thesis possible. First and foremost, I am utterly grateful to my supervisors Prof. John Coote and Dr. Roger Parton from accepting me as their last PhD student in their scientific careers, for their passionate supervision, profound enthusiasm, continued encouragement, stimulating discussion and guidance through the course of this study. I am also thankful for their time and patience in reading and giving critical comments on this thesis. All of these have inspired me to continue their contribution to the world of Science.

Special thanks are also due to my assessors Prof. Tim Mitchell and Dr. Robert Aitken for their encouragement, interesting suggestions and countless help when in need. I greatly appreciate and acknowledge the help of Prof. Paul Langford, Dr. Lawrence Tetley, Dr. Andrew Roe, Dr. Robert Davies and Dr. Arvind Mahajan for their guidance, materials contribution, collaboration and helpful advice during this study.

I would also like to express my most sincere thanks to Dr. Mara Rocchi who helped me to conduct part of my research in the Immunology Laboratory at Moredun Research Institute (MRI), Edinburgh.

Many thanks also go to Mrs. Denise Candlish, Mrs. Irene Houghton, Mrs. Margaret Mullin, Mrs. June Irvine, Mrs. Susan Bailie, Mrs. Mulu Gedle, Mr. Richard Irvine and all members of Division of Infection, Immunity and Inflammation, University of Glasgow for their technical help, collaboration and invaluable friendship. Sincerely, without them, this study would not have been as fun and enjoyable as it was.

‘Gems may be precious, but friends are priceless’. From the deepest core in my heart, I would like to express my gratitude to Miss Chonchanok Theethakaew, Mr. Teerasak E-komon, Mr. Jonathan Hounsome, Miss Alette Brinth, Miss Ashleigh

Holmes, Dr. Sarah Jones, Miss Satirah Zainal Abidin, Miss Sanna Taking, Captain Magnus Jeffrey and all members of Level 2, GBRC, University of Glasgow. Their friendship, encouragement, enthusiasm and sense of humour not only made this study interesting but made my stay in Glasgow a joyful and pleasurable experience.

I would never have embarked on the challenge of a post-graduate degree had it not been for the amazing support of my family. Especially to my husband, I would like to thank him for his unending patience. He, more than anyone, understands the emotional challenges that a Ph.D. entails. For my parents, *Mak* and *Abah*, their prayers, guidance and encouragement have made me become what I am today. Also to the rest of my family, I am so lucky to have had their love as the main support system in my life.

Finally, I would also like to acknowledge both benefactors, Universiti Putra Malaysia and Ministry of Higher Education, Malaysia for granting this opportunity to expand my training in Science.

Thus, here I end with a translated version of a short poem by one of Malaysia's famous poets, the late Usman Awang;

***Budi*** <sup>(good deed)</sup>, all the purity of life

Those who gave feel the great happiness

Those who accepted shoulder the burden of feeding

Live with it, live with it always

In a world getting poorer of it (Usman Awang, 1987)

A believer is never satiated with gainful knowledge; he goes acquiring it till his death and entry into Paradise.

~ Prophet Muhammad S.A.W. (Tirmidhi, 222) ~

## Abstract

The primary aim of this study was to investigate the potential of an *aroA* mutant of *Pasteurella multocida* B:2 (vaccine strain JRMT12) as a candidate for DNA vaccine delivery (bactofection). First, the invasive property of the vaccine strain was assessed for its interaction with different mammalian cell lines. Next, a eukaryotic expression plasmid that could be maintained in *Pasteurella* was modified to contain a prokaryotic reporter gene to help in determining the location and viability of the bacteria when moving from the extracellular environment into the intracellular compartment of the mammalian cells. This plasmid was further developed to function with a dual prokaryotic and eukaryotic reporter system in order to demonstrate expression of the plasmid DNA in the mammalian cells.

During interaction of strain JRMT12 with mammalian cell lines, the ability of the bacterium to adhere, invade and survive intracellularly was monitored and assessed. Three mammalian cell lines were used: a mouse macrophage-like cell line, J774.2; a bovine-lymphoma cell line, BL-3; and an embryonic bovine lung cell line, EBL. The JRMT12 strain was compared with strains of the wild-type *P. multocida* B:2 (85020), bovine *P. multocida* A:3, *Mannheimia haemolytica* A:1 and *Escherichia coli* XL-1 BLUE. Both *P. multocida* B:2 strains were capable of adhering to and invading J774.2, BL-3 and EBL cells. All of the *Pasteurella* and *Mannheimia* strains tested were able to adhere to EBL cells but only B:2 strains were taken up intracellularly in significant numbers. The vaccine strain, JRMT12 was found to survive intracellularly in EBL cells for at least 7 h although a steady decline in the number of viable intracellular bacteria was noted with time. In an invasion inhibition assay, the use of the microfilament formation inhibitor cytochalasin D suggested that the entry into mammalian cells was by an actin-dependent process. Cell viability assessment by trypan blue staining indicated that none of the bacterial strains was toxic for the mammalian cells. Upon entry into the mammalian cells the JRMT12 strain resided in a vacuolar compartment, as demonstrated by transmission electron microscopy. However, *P. multocida* A:3 and *M. haemolytica* A:1 were only found loosely adhering to the cell surface of EBL cells and were not detected intracellularly. Further morphological assessment by TEM showed that only a low percentage of mammalian cells

appeared to contain one or more JRMT12, suggesting that only certain cells in the population were capable of being invaded by, or taking up, the bacteria.

Attempts were made to construct a *Pasteurella* eukaryotic expression plasmid using a gene sequence from the *Pasteurella* shuttle plasmid pAKA16, developed previously in this laboratory, and the commercial eukaryotic expression plasmid pCMV-sCRIPT, but these were only partially successful. The origin of replication gene (*oriP*) in the *Pasteurella* shuttle plasmid was isolated and sequenced. Analysis of *oriP* showed sequence similarity with the known origins of replication in other *Pasteurella* plasmids. The *E. coli* plasmid origin of replication (*oriE*) was removed from pCMV-sCRIPT and the *oriP* gene was ligated into the *oriE*-free pCMV-sCRIPT but attempts to transform the resulting plasmid into *P. multocida* B:2 were not successful. An alternative approach to plasmid development was made using another commercial eukaryotic expression vector, pEGFP-N1. This plasmid has the same properties as pCMV-sCRIPT but has an additional, fluorescent reporter gene under the control of a eukaryotic promoter. It was found to be able to replicate in *P. multocida* B:2 but positive transformants were only recovered after prolonged incubation after electroporation. The plasmid was stably maintained in strain JRMT12 for at least 14 days with or without antibiotic selection. It was also successfully transfected into EBL cells, as shown by expression of green fluorescent protein (GFP) in individual cells. The *P. multocida* vaccine strain JRMT12 was also able to deliver the plasmid into EBL cells, although the number of EBL cells expressing GFP after bacterial delivery was lower than by direct transfection of the plasmid.

Next, plasmid pMK-Express, a *Pasteurellaceae* prokaryotic expression vector with a *gfp* reporter gene, was used. When this was electroporated into the vaccine strain, the strain was shown to express GFP maximally as measured by fluorimetry, during the early exponential phase of bacterial growth. The DsRed.M1 gene coding for red fluorescent protein (RFP) from plasmid pDsRed-Monomer was then used to replace the *gfp* gene in pMK-Express to make the construct pMK-RED. After electroporation of pMK-RED into the JRMT12, RFP expression was detected maximally during the early exponential phase of bacterial growth. The same strain expressing RFP could also be detected in the intracellular compartment of the EBL cells by fluorescence microscopy at 3 h post-invasion.



Finally, plasmid pSRG, our so-called “traffic light” plasmid with a dual reporter system was constructed. This was made from plasmid pEGFP-N1 (with its existing eukaryotic expression system for GFP expression) and the sodRED fragment (with a *Pasteurella* promoter controlling the DsRED.M1 gene for RFP expression) isolated from plasmid pMK-RED. This plasmid was stable in strain JRMT12 with or without antibiotic selection for 14 passages. RFP expression from JRMT12 was detected maximally during the early exponential phase of bacterial growth. Transfection of pSRG into EBL cells gave individual cells expressing GFP. Invasion assays with EBL cells and *P. multocida* B:2 JRMT12 pSRG<sup>+</sup> showed that RFP-expressing bacteria could be detected intracellularly at 3 h post-invasion. At this stage, some EBL cells harbouring RFP-expressing bacteria were observed to express GFP simultaneously. At 5 h post-invasion, some of the EBL cells were still harbouring RFP-expressing bacteria and at the same time expressing GFP themselves. Concurrently, some *Pasteurella* free-EBL cells were shown to express GFP. These experiments proved the functionality of the pSRG dual reporter system and the potential of *P. multocida* B:2 JRMT12 for bactofection and delivery of a DNA vaccine.

An apparent immunosuppressive effect of *P. multocida* B:2 on the proliferative response to concanavalin A (ConA) of peripheral blood mononuclear cells (PBMC) had been reported by Ataei (2007). The PBMC had been taken from calves infected with *P. multocida* B:2 or from normal calves and treated *in vitro* with extracts of *P. multocida* B:2. In the present study, *in vitro* assays with PBMC from normal calves were undertaken in an attempt to confirm these findings. A cell-free extract (CFE) of the vaccine strain JRMT12 was found to suppress the subsequent proliferation of PBMC in response to ConA in a dose-dependent manner. However, the results were not consistently reproducible and the same effect could not be demonstrated with CFE from the wild-type strain 85020.

# Table of contents

Declaration	II
Acknowledgements	III
Abstract	VI
Table of contents	IX
List of figures	XIII
List of tables	XV
Abbreviations	XVI
<b>1.0 INTRODUCTION</b>	<b>1</b>
1.1 History and taxonomy of the family <i>Pasteurellaceae</i>	1
1.2 The genus <i>Pasteurella</i>	1
1.3 <i>Pasteurella multocida</i>	2
1.3.1 The organism	2
1.3.1.1 Cell morphology and staining	3
1.3.1.2 Colonial morphology	3
1.3.1.3 Biochemical properties	3
1.3.2 Typing	3
1.3.2.1 Serotyping	4
1.3.2.2 Advanced typing methods	4
1.3.2.2.1 Identification by PCR	4
1.3.2.2.2 In situ hybridization	4
1.3.3 Diseases caused by <i>P. multocida</i> B:2 and other serotypes	5
1.3.4 Virulence factors	6
1.3.4.1 Capsule and lipopolysaccharides	6
1.3.4.2 Outer-membrane proteins	8
1.3.4.3 Fimbriae	8
1.3.4.4 Plasmids and transposons	9
1.3.4.5 Toxins	9
1.4 Haemorrhagic septicaemia (HS)	10
1.4.1 The disease	10
1.4.2 Global distribution	11
1.4.3 Epidemiological cycle	11
1.4.4 Progression of the disease	11
1.4.5 Treatment	12
1.5 Vaccination against HS	12
1.5.1 History and current status	12
1.5.1.1 Plain bacterin	13
1.5.1.2 Alum-precipitated vaccines (APV)	14
1.5.1.3 Aluminium hydroxide gel vaccines	14
1.5.1.4 Oil-adjuvant vaccines	14
1.5.2 Deficiencies of available vaccines	17
1.5.3 Live-attenuated vaccines	18
1.5.3.1 Streptomycin-dependent mutant	19
1.5.3.2 Deer strain live vaccine	19
1.5.3.3 Acapsular mutants	20
1.5.3.4 <i>aroA</i> mutant vaccines	20
1.6 DNA vaccines	21
1.6.1 Eukaryotic expression plasmids	22
1.6.1.2 Properties of eukaryotic expression plasmids	22

1.6.2	Mode of delivery-----	23
1.6.2.1	Gene gun -----	23
1.6.2.2	Liposomes -----	24
1.6.2.3	Cochleates-----	25
1.6.2.4	Microparticle encapsulation -----	26
1.6.2.5	Microneedles -----	28
1.6.2.6	Viral vectors-----	29
1.6.2.7	Bactofection -----	30
1.6.2.7.1	Adhesion, invasion and intracellular survival -----	31
1.6.2.7.2	Invasion by <i>P. multocida</i> -----	33
1.6.3	Advantages and disadvantages of DNA vaccines -----	34
1.7	Immunosuppression by <i>Pasteurella multocida</i> B:2 -----	35
1.8	Objectives of research and experimental plan -----	38
<b>2.0</b>	<b>MATERIALS AND METHODS -----</b>	<b>39</b>
2.1	General bacteriological procedures -----	39
2.1.1	Sources of bacteria -----	39
2.1.2	Plasmids -----	39
2.1.3	Bacterial growth and storage media-----	39
2.1.4	Growth of <i>E. coli</i> -----	39
2.1.5	Growth of <i>Pasteurella</i> species -----	42
2.1.6	Isolation of spontaneous streptomycin-resistant strains -----	42
2.2	Antibiotics-----	42
2.3	Plasmid DNA extraction -----	42
2.4	Restriction endonuclease digestion of DNA-----	43
2.5	Agarose gel electrophoresis-----	43
2.5.1	Sample preparation -----	43
2.5.2	Gel preparation-----	43
2.5.3	Electrophoresis -----	44
2.5.4	Visualisation of DNA-----	44
2.5.5	Purification of DNA from agarose gels -----	44
2.6	Estimation of DNA concentration -----	45
2.7	Concentration of DNA-----	45
2.8	Polymerase chain reaction (PCR) -----	46
2.8.1	PCR primers -----	46
2.8.2	Components of PCR -----	46
2.8.3	Conditions for PCR -----	48
2.8.4	Inverse PCR (IPCR) -----	48
2.8.5	Colony PCR -----	48
2.8.6	Purification of PCR products-----	48
2.9	DNA sequencing-----	49
2.10	Statistical analysis -----	49
2.11	Sequence analysis tools (bioinformatics) -----	50
2.12	Cloning-----	50
2.12.1	PCR product cloning -----	50
2.12.1.1	Cloning into pGEM-T EASY™ plasmid-----	50
2.12.2	Standard cloning protocol-----	51
2.12.2.1	DNA preparation-----	51
2.12.2.2	Ligation strategies -----	51
2.12.3	Dephosphorylation of linearized DNA -----	51
2.12.4	“Filling in” or “trimming” reactions for blunt end ligation -----	52
2.13	DNA transformation -----	52

2.13.1	Preparation of electro-competent cells	52
2.13.2	Electroporation procedure	53
2.13.3	Blue and white screening of recombinants	53
2.14	Conjugation	54
2.15	Mammalian cell lines	54
2.16	Cell viability assessment	54
2.17	<i>In vitro</i> assays	55
2.17.1	Adherence assay	55
2.17.2	Invasion assay	55
2.17.3	Intracellular survival assay	56
2.17.4	Invasion inhibition assay	56
2.17.5	Transfection assay	56
2.18	Fluorimetry assessment	57
2.19	Transmission electron microscopy (TEM)	57
2.20	Fluorescence imaging	58
2.20.1	Cell fixation	58
2.20.1.1	EBL cells	58
2.20.1.2	Fluorescence measurement and staining of bacterial strains	59
2.20.2	Fluorescence microscopy (FM)	59
2.21	Immunosuppression by <i>P. multocida</i> B:2	60
2.21.1	Preparation of bacterial cell-free extract (CFE)	60
2.21.2	Protein quantification	60
2.21.3	Isolation and preparation of peripheral blood mononuclear cells (PBMC)	61
2.21.4	Lymphocyte proliferation inhibition assay	61
<b>3.0</b>	<b>RESULTS</b>	<b>63</b>
3.1	Rate of bacterial killing by antibiotics	63
3.2	Interaction between mammalian cells and <i>Pasteurella</i> species	65
3.2.1	Effect of <i>P. multocida</i> B:2 on viability of J774.2 cells	65
3.2.2	Effect of <i>P. multocida</i> B:2 on viability of EBL cells	65
3.2.3	Invasion of J774.2 cells by <i>P. multocida</i> and <i>E. coli</i>	68
3.2.4	BL-3 cells	69
3.2.5	EBL cells	71
3.2.5.1	Establishment of an appropriate MOI between <i>Pasteurella</i> strains and EBL cells	71
3.2.5.2	Comparison of the extent of adherence and invasion between <i>P. multocida</i> B:2 strains and EBL cells.	71
3.2.5.3	Comparison of adherence and invasion between bovine <i>Pasteurellaceae</i> strains with EBL cells.	72
3.2.5.4	Intracellular survival of <i>P. multocida</i> B:2 JRMT12 in EBL cells.	74
3.2.5.5	Invasion inhibition assay of EBL cells with cytochalasin D.	76
3.2.6	The transmission electron microscopy (TEM) of the interaction of bacteria with EBL cells.	78
3.3	Construction of a <i>Pasteurella</i> eukaryotic expression plasmid	87
3.3.1	Inability of plasmid pCMV-sCRIP to replicate in <i>P. multocida</i> B:2 JRMT12	87
3.3.2	Development of plasmid pSJR	88
3.3.2.1	Isolation of <i>Pasteurella</i> origin of replication ( <i>oriP</i> ) from pAKA16	88
3.3.2.2	Characterisation of <i>oriP</i> locus	88

3.3.2.3	Isolation of the <i>oriP</i> gene from <i>oriP</i> fragment	92
3.3.2.4	Removal of pUC origin of replication ( <i>oriE</i> ) from pCMV-sSCRIPT	92
3.3.3	Analysis of pUC base eukaryotic expression plasmid, pEGFP-N1™	96
3.3.3.1	Electroporation into <i>P. multocida</i> B:2 JRMT12 and <i>E. coli</i> XL-1 Blue	96
3.3.3.2	Plasmid stability in <i>P. multocida</i> B:2 JRMT12	97
3.3.3.3	Growth curve of <i>P. multocida</i> B:2 JRMT12 pEGFP-N1™ <sup>+</sup>	98
3.4	Development of the <i>P. multocida</i> B:2 bactofection model system	102
3.4.1	Characterisation of plasmid pEGFP-N1™ in mammalian cells	102
3.4.1.1	Transfection of plasmid pEGFP-N1™ into embryonic bovine lung (EBL) cells.	102
3.4.1.2	Invasion of EBL cells with <i>P. multocida</i> B:2 JRMT12 pEGFP-N1™ <sup>+</sup>	104
3.4.2	Development of <i>P. multocida</i> B:2 JRMT12 expressing fluorescent proteins	106
3.4.2.1	<i>P. multocida</i> B:2 JRMT12 pMK-Express <sup>+</sup>	106
3.4.2.2	<i>P. multocida</i> B:2 JRMT12 pMK-RED <sup>+</sup>	112
3.4.3	Assessment of intracellular viability of <i>P. multocida</i> B:2 JRMT12 expressing fluorescent protein	120
3.4.3.1	Imaging of <i>P. multocida</i> B:2 JRMT12 pMK-RED <sup>+</sup> in EBL cells	120
3.4.4	Development of the ‘traffic light’ plasmid	124
3.4.4.1	Cloning of <i>P</i> <sup>sod-C</sup> /DsRed-Monomer ( <i>sodRED</i> ) fragment into plasmid pEGFP-N1™	124
3.4.4.2	Stability and expression of plasmid pSRG in <i>P. multocida</i> B:2 JRMT12	133
3.4.4.3	Transfection of plasmid pSRG into EBL cells	138
3.4.4.4	Localization of prokaryotic and eukaryotic fluorescent protein expression	143
3.5	Possible immunosuppressive effect of <i>P. multocida</i> B:2 infection	159
3.5.1	<i>In vitro</i> responses of PBMC	159
<b>4.0</b>	<b>DISCUSSION</b>	<b>166</b>
4.1	Interaction between mammalian cells and <i>Pasteurella</i>	166
4.2	Construction of a <i>Pasteurella</i> eukaryotic expression plasmid	175
4.3	Development of <i>P. multocida</i> B:2 bactofection model system	179
4.4	Development of bacterial DNA vaccines	189
4.5	Possible immunosuppressive effect of <i>P. multocida</i> B:2 infection	194
4.6	Summary and conclusion	201
<b>5.0</b>	<b>BIBLIOGRAPHY</b>	<b>202</b>
<b>6.0</b>	<b>APPENDIX</b>	<b>236</b>

## List of figures

Figure 1.	Example of gene guns.	23
Figure 2.	Liposomes for delivery of DNA vaccine.	24
Figure 3.	Compact microparticle encapsulation.	26
Figure 4.	Comparison of nanoparticle and microparticle.	27
Figure 5.	Nanoparticles in mammalian cells.	28
Figure 6.	Microneedle vaccine patch.	28
Figure 7.	Bactofection pathway for DNA vaccine delivery.	33
Figure 8.	Observation from infected calves (Ataei, 2007).	36
Figure 9.	Immunosuppressive effect of <i>P. multocida</i> B:2 cell-free extract on PBMC <i>in vitro</i> (Ataei, 2007).	37
Figure 10.	Viability assessments of J774.2 and EBL cells by trypan blue staining.	66
Figure 11.	TEM micrographs of EBL cells infected with bacteria.	80
Figure 12.	Cloning strategy: Development of plasmid pSJR.	89
Figure 13.	Agarose gel showing plasmid pAKA16 digested with <i>Pst</i> I.	90
Figure 14.	Agarose gel showing pGEM-oriP digested with <i>Eco</i> RI.	93
Figure 15.	Sequence of <i>ori</i> P fragment.	94
Figure 16a.	Agarose gel electrophoresis of <i>ori</i> P gene removed from pGEM-P with <i>Alw</i> NI and <i>Pci</i> I.	95
Figure 16b.	Agarose gel electrophoresis of pCMV-sCRIPt after digestion with <i>Alw</i> NI and <i>Pci</i> I.	95
Figure 17.	Growth curves of <i>P. multocida</i> B:2 JRMT12 pEGFP-N1 <sup>TM+</sup> .	100
Figure 18.	Transfection of plasmid pEGFP-N1 into EBL cells.	103
Figure 19.	Invasion of EBL by <i>P. multocida</i> B:2 JRMT12 pEGFP-N1 <sup>TM+</sup> .	105
Figure 20.	Assessment of GFP expression by <i>P. multocida</i> B:2 JRMT12 pMK-Express <sup>+</sup> during growth.	108

Figure 21.	Visualization of <i>P. multocida</i> B:2 JRMT12 pMK-Express <sup>+</sup> via fluorescence microscopy (FM).	111
Figure 22.	Cloning strategy: Development of plasmid pMK-RED.	113
Figure 23.	Assessment of RFP expression by <i>P. multocida</i> B:2 JRMT12 pMK-RED <sup>+</sup> during growth.	115
Figure 24.	Visualization of <i>P. multocida</i> B:2 JRMT12 pMK-RED <sup>+</sup> via FM.	118
Figure 25.	Imaging of <i>P. multocida</i> B:2 JRMT12 pMK-RED <sup>+</sup> in EBL cells.	122
Figure 26.	Cloning strategy: Development of ‘traffic light’ plasmid, pSRG.	126
Figure 27.	Agarose gel showing sodRED fragment PCR from plasmid pMK-RED using RED-A and RED-P primer pairs.	129
Figure 28.	Agarose gel showing plasmid pGEM <sup>®</sup> -T-Easy-sodRED from <i>E. coli</i> XL-1 Blue after digestion with <i>KpnI</i> .	129
Figure 29.	Agarose gel showing pGEM <sup>®</sup> -T-Easy-sodRED after digestion with <i>PciI</i> .	130
Figure 30.	Agarose gel showing pEGFP-N1 <sup>™</sup> after digestion with <i>PciI</i> and dephosphorylation with CIAP.	131
Figure 31.	Agarose gel showing pSRG after digestion with <i>EcoRI</i> .	131
Figure 32.	Complete sequence of sodRED fragment.	132
Figure 33.	Assessment of RFP expression by <i>P. multocida</i> B:2 JRMT12 pSRG <sup>+</sup> during growth.	134
Figure 34.	Visualization of <i>P. multocida</i> B:2 JRMT12 pSRG <sup>+</sup> via FM.	136
Figure 35.	Transfection of plasmid pSRG into EBL cells.	140
Figure 36.	Localization of prokaryotic and eukaryotic protein expression.	147
Figure 37.	Effect of CFE from <i>P. multocida</i> B:2 on the proliferative response of PBMC to ConA.	160
Figure 38.	Effect of new preparations of CFE <i>P. multocida</i> B:2 on proliferative response of PBMC to ConA.	163

## List of tables

Table 1.	Haemorrhagic septicaemia vaccination practices in Asia.	16
Table 2.	Bactofection using attenuated strains of pathogenic bacteria.	31
Table 3.	List of bacterial strains used in this study.	40
Table 4.	List of plasmids used in this study.	41
Table 5.	PCR primers used in this study.	47
Table 6.	Effect of antibiotics on viability of <i>P. multocida</i> B:2 JRMT12.	64
Table 7.	Invasion of <i>P. multocida</i> and <i>E. coli</i> strains with J774.2 mouse macrophage-like cells at different multiplicities of infection (MOI).	70
Table 8.	Uptake of <i>Pasteurella multocida</i> strains into bovine lymphoma (BL-3) cells at MOI 500:1.	70
Table 9.	Invasion of EBL cells by <i>P. multocida</i> B:2 JRMT12 at different MOIs.	73
Table 10.	Comparison of adherence and invasion rates between strains of <i>P. multocida</i> B:2.	73
Table 11.	Comparison of adherence and invasion rates between strains of <i>Pasteurellaceae</i> .	75
Table 12.	Period of intracellular survival of <i>P. multocida</i> B:2 JRMT12 in EBL cells at MOI 100:1.	75
Table 13a.	Effect of cytochalasin D at different concentrations on invasion of EBL by <i>P. multocida</i> B:2 JRMT12.	77
Table 13b.	Effect of cytochalasin D on invasion of EBL by <i>P. multocida</i> B:2 JRMT12.	77
Table 14a.	Assessment of the morphological features seen by TEM micrographs after infection of EBL cells with different <i>Pasteurellaceae</i> strains at MOI 100:1.	84
Table 14b.	Percentage distribution of total intracellular <i>P. multocida</i> B:2 JRMT12 within 90 individual EBL at 3 h after challenge.	85
Table 15.	Summary of <i>Pasteurella</i> interactions with mammalian cells.	172
Table 16.	Licensed veterinary products employing DNA plasmids.	191



## Abbreviations

A	= Adenine
A:1	= <i>Pasteurella multocida</i> biotype A capsular serotype 1
A:3	= <i>Pasteurella multocida</i> biotype A capsular serotype 3
aa	= Amino acid
APC	= Antigen presenting cell
APV	= Alum-precipitated vaccine
Ap	= Ampicillin
AR	= Atrophic rhinitis
<i>aroA</i>	= Aromatic amino acid metabolism gene
ATCC	= American Type Culture Collection
ATP	= Adenosine triphosphate
B:2	= <i>Pasteurella multocida</i> biotype B capsular serotype 2
BAEC	= Bovine aortic endothelial cell
BCG	= Bacille Calmette-Guerin
BHI	= Brain heart infusion
bp	= Base pair
BL-3	= Bovine lymphoma -3
BLAST	= Basic local alignment tool
BSA	= Bovine serum albumin
C	= Cytosine
°C	= Degrees Celsius
CCD	= Charge-coupled device
CD	= Cytochalasin D
CFE	= Cell-free extract
CFSE	= Carboxyfluorescein diacetate succinimidyl ester
CFU	= Colony forming unit
CIP	= Calf intestinal phosphatase
cm/mm	= Centimetre/millimetre
Cm	= Chloramphenicol
CMV	= Cytomegalovirus
ConA	= Concanavalin A
cpm	= Counts per minute
CTL	= Cytotoxic lymphocyte
Da	= Dalton
dATP	= Deoxyadenosine triphosphate

dCTP	= Deoxycytosine triphosphate
DC	= Dendritic cell
dGTP	= Deoxyguanine triphosphate
DIC	= Differential interference contrast
DMSO	= Dimethyl sulphoxide
DNA	= Deoxyribonucleic acid
dNTPs	= Deoxynucleoside triphosphates
dTTP	= Deoxythymidine triphosphate
E:2	= <i>Pasteurella multocida</i> biotype E capsular serotype 2
EBL	= Embryonic bovine lung
ECM	= Extracellular matrix
EDTA	= Ethylenediaminetetraacetic acid
Ems	= Emission
ELISA	= Enzyme-linked immunosorbent assay
Exc	= Excitation
FACS	= Fluorescence activated cell sorter
FBS	= Foetal bovine serum
FC	= Fowl cholera
FFL	= Filtered fluorescent light
FI	= Fluorescence intensity
FM	= Fluorescence microscopy
Fn	= Fibronectin
g/mg/μg	= Grams/milligrams/micrograms
G	= Guanine
GFP	= Green fluorescent protein
Gm	= Gentamycin
h	= Hour(s)
HBSS	= Hank's balanced salt solution
HEPES	= N-2-hydroxyethylpiperazine-N-2-ethanesulphonic acid
HS	= Haemorrhagic septicaemia
IFN $\gamma$	= Interferon gamma
Ig	= Immunoglobulin
IL-(X)	= Interleukin-(number)
i.m.	= Intramuscular
i.n.	= Intranasal
IPCR	= Inverse polymerase chain reaction
IPTG	= Isopropyl-B-D-thiogalactopyranoside

IU	= International units
kb	= Kilobase pair
kDa	= Kilo Dalton
kg	= Kilogram
Km	= Kanamycin
kV	= Kilo Volts
l/ml/ $\mu$ l	= Litres/millilitres/microlitres
<i>lac</i>	= Lactose operon gene
LB	= Luria-Bertani
LBV	= Live attenuated bacterial vaccine
LBV-B	= Live attenuated bacterial vaccine-bactofection
LLO	= Listeriolysin O
LPS	= Lipopolysaccharide
MDBK	= Madin-Darby bovine kidney
MEM	= Minimal Eagle' medium
MHC	= Major histocompatibility complex
M/mM/ $\mu$ M	= Molar/millimolar/micromolar
$\mu$ FD	= Microfarad
min	= Minute(s)
MOI	= Multiplicity of infection
MRF	= Minus restriction factor
mRNA	= Messenger RNA
mw	= Molecular weight
ng	= Nanogram
nm	= Nanometre
Nm	= Neomycin
nt	= Nucleotide
OAV	= Oil adjuvant vaccine
OD <sub>X nm</sub>	= Optical density at wavelength X nm
$\Omega$	= Ohm
OMP	= Outer-membrane protein
ORF	= Open reading frame
PAGE	= Polyacrylamide gel electrophoresis
PAR	= Progressive atrophic rhinitis
PBMC	= Peripheral blood mononuclear cell
PBS	= Phosphate-buffered saline
PCR	= Polymerase chain reaction

PFA	= Paraformaldehyde
PFGE	= Pulsed-field gel electrophoresis
Pg	= Picogram
pH	= Hydrogen ion concentration
P. m	= <i>Pasteurella multocida</i>
P	= Polymyxin B
PMM	= <i>Pasteurella</i> minimal medium
PMN	= Polymorphonuclear
PMPT	= passive mouse protection test
PMT	= <i>Pasteurella multocida</i> toxin
p.s.i.	= Pounds per square inch
RFP	= Red fluorescent protein
RFU	= Relative fluorescence unit
RNA	= Ribonucleic acid
rpm	= Revolutions per minute
RPMI	= Roswell Park Memorial Institute
rRNA	= Ribosomal RNA
rt	= Room temperature
s.c.	= Subcutaneous
SDS	= Sodium dodecyl sulphate
sec	= Second(s)
Sm	= Streptomycin
SOC	= Super optimal catabolite
T	= Thymine
TBE	= Tris borate EDTA
Tc	= Tetracycline
TCR	= T cell receptor
TE	= 10 mM Tris, 1 mM EDTA
TEM	= Transmission electron microscopy
Th (1/2)	= Helper T cell (1/2)
Tm	= Melting temperature
Tn5	= Transposon 5
TLR	= Toll-like receptor
TNF- $\alpha$	= Tumor necrosis factor alpha
tRNA	= Transfer RNA
Tris	= Tris (hydroxymethyl) aminoethane
U	= Units

UK	= United Kingdom
US	= United States
UTP	= Uridine triphosphate
UV	= Ultraviolet
V	= Volts
v/v	= Volume by volume
w/v	= Weight by volume
X-gal	= 5-bromo-4-chloro-3-indolyl- $\beta$ -D-galactosidase

# 1.0 INTRODUCTION

## 1.1 History and taxonomy of the family *Pasteurellaceae*

Members of the bacterial family *Pasteurellaceae* are small (0.2-2.0  $\mu\text{m}$ ), Gram-negative, chemoorganotrophic, non-motile, facultatively anaerobic coccobacilli or rods. Organisms belonging to the *Pasteurellaceae* can colonize mucosal surfaces of the respiratory, alimentary and genital tracts and cause diseases in different mammals, birds and reptiles (Jacques & Mikael, 2002). For years it was believed that the family consisted only of three genera: *Pasteurella* described by Trevisan in 1887, *Actinobacillus* by Brumpt in 1910 and *Haemophilus* by Winslow *et al.*, in 1917, but several other groups of organisms that exhibit complex phenotypic and genotypic relationships with these genera were also included (Boot & Bisgaard, 1995; De Alwis, 1999). After the designation of the organisms *Bisgaardia hudsonensis* (Foster *et al.*, 2011) into the new genus *Bisgaardia* in 2011, *Pasteurellaceae* now have 16 genera in the family. Other genera are *Mannheimia* (Angen *et al.*, 1999), *Gallibacterium* (Christensen *et al.*, 2003; 2004), *Actinobacillus* (Christensen & Bisgaard, 2006), *Volucribacter* (Christensen *et al.*, 2004b), *Nicoletella* (Kuhnert *et al.*, 2004) *Avibacterium* (Blackall *et al.*, 2005), *Pasteurella*, *Haemophilus*, *Lonepinella*, *Phocoenobacter*, *Aggregatibacter*, *Bibersteinia*, *Basfia*, *Chelanobacter* and *Histophilus*. The *Pasteurellaceae* family consisted of 62 species.

## 1.2 The genus *Pasteurella*

The phylogeny of the genus *Pasteurella* has been investigated by 16S rRNA sequence comparison and rRNA-DNA hybridization (De Ley *et al.*, 1990; Dewhirst *et al.*, 1992; Dewhirst *et al.*, 1993). The phylogenetic position of members of *Pasteurella* is shown by analysis of the 16S rRNA sequences of well-characterized strains. On the basis of this method, *Pasteurella* includes nine named species (*P. multocida*, *P. canis*, *P. stomatis*, *P. dagmatis*, *P. gallinarum*, *P. avium*, *P. volantium*, *P. langaa* and *P. anatis*) and two unnamed taxa (*Pasteurella species A* and *species B*). The type species of the genus *P. multocida* has been separated into three subspecies, *P. multocida subsp. multocida*, *P. multocida subsp. gallicida* and *P. multocida subsp. septica*. In addition, the exclusion of seven species: [*P.*] *aerogenes*, [*P.*] *pneumotropica*, [*P.*] *trehalosi*, [*P.*] *caballi*, [*P.*]

*mairii*, [*P.*] *bettyae* and [*P.*] *testudinis* from *Pasteurella* has been suggested. However, their names have not been formally changed and the genus name of these species is consequently denoted in brackets.

*Pasteurella* species exist as normal upper respiratory and gastrointestinal flora of dogs, cats, and other domestic and wild animals (Carter, 1967; Jones *et al.*, 1973; Francis *et al.*, 1975; as cited by De Alwis, 1999). These organisms are known to be widespread veterinary pathogens (Hubbert *et al.*, 1970; Jones *et al.*, 1973; Furie *et al.*, 1980) and some are being recognized as important human zoonotic pathogens (Hubbert *et al.*, 1970; Jones *et al.*, 1973; Johnson *et al.*, 1977; Furie *et al.*, 1980). Pasteur first isolated the causative agent of fowl cholera, *P. multocida*, in 1880 (Robinson, 1944). Thereafter, bacteria with the same growth characteristics were implicated in haemorrhagic septicaemia of cattle, in swine plague, and in rabbit septicaemia (Jones *et al.*, 1973). Isolates from all sources with common biochemical and morphological features were grouped together as “*P. septic*” in 1929 and *P. multocida* in 1939 (Weber, 1984). The organisms do not grow on MacConkey’s agar and they are non-haemolytic on blood agar. On nutrient agar they produce fine, translucent colonies with a characteristic musty odour.

### **1.3 *Pasteurella multocida***

#### **1.3.1 The organism**

Members of the bacterial genus *Pasteurella* usually are regarded as opportunistic, secondary invaders in vertebrates. *P. multocida* is the only representative of the genus regarded as a major pathogen, causing a clinical disease called pasteurellosis. It has been recognized as an important veterinary pathogen for over a century, and its importance as a human pathogen has been increasingly recognized in the last 50 years. The organism can occur as a commensal in the naso-pharyngeal region of apparently healthy animals and it can act as a primary or secondary pathogen in disease processes of a variety of domestic and feral mammals and birds (section 1.3.3).

The name ‘multocida’ originated from the words multus; (many) and cida: (killing) which means “many killing” (Carter, 1984). According to Rimler and Rhodes (1989), the organism was first isolated in 1879 by Toussiant. It had many

names (according to Frederiksen, 1989), beginning with *Micrococcus gallicidus*, which was given by Burriel in 1883, *Bacterium multocidum* (Lehmann and Neumann, 1899) and in 1925 Buchanan suggested *Pasteurella gallicida*. However after several disagreements, the name *Pasteurella multocida* was finally proposed by Rosenbusch and Merchant (1939) and is now widely used.

#### 1.3.1.1 Cell morphology and staining

*Pasteurella multocida* is a non-motile, non-spore forming, coccobacillus or short rod of 0.2-0.4 by 0.6-2.5 µm in size. The coccobacillus occurs either singly or in pairs and occasionally as chains or filaments. It is a Gram-negative organism and, as quoted by Adamson (1993), in tissue exudates and in recently isolated cultures will show bipolar staining with Giemsa or Wright's stain.

#### 1.3.1.2 Colonial morphology

Isolates of *P. multocida* from the respiratory tract of ruminants, pigs and rabbits may form large, watery, mucoid colonies, which may collapse after 48 hours of incubation. Rough colonies of *P. multocida* are formed from filamentous, non-capsulated cells (Rimler and Rhoades, 1989). Growth in broth usually causes turbidity, but granular growth may occur (Mutters *et al.*, 1985).

#### 1.3.1.3 Biochemical properties

*P. multocida* organisms are oxidase, catalase and indole positive. They ferment sugars such as glucose, sucrose, sorbitol and mannitol with acid, but with no gas production. Lactose, maltose and salicin are not fermented, while variable fermentation results are obtained with arabinose, trehalose and xylose. Gelatin is not liquefied (Holt, 1994).

### 1.3.2 Typing

Typing methods are used for detailed characterization to investigate the diversity of taxa of *Pasteurella* and for the study of pathogenicity and epidemiology.



### 1.3.2.1 Serotyping

Serotype designations of the *P. multocida* strains are based on capsular antigen-somatic antigen combinations (capsular antigens A to F and somatic antigens 1 to 16). Using a serotype designations system which is a combination of Carter (1955) capsular typing and Heddleston (1972) somatic typing, the Asian and African serotypes causing haemorrhagic septicaemia are designated B:2 and E:2 respectively.

### 1.3.2.2 Advanced typing methods

#### 1.3.2.2.1 Identification by PCR

*P. multocida* can be detected at the species level by a PCR targeting the *rrl* gene that codes for 23S rRNA. This PCR assay correctly identified all 144 isolates of *P. multocida* tested, including type strains of the three subspecies as well as the reference strains for the Heddleston and Carter typing schemes (Miflin & Blackall, 2001). In addition, the bacteria can also be detected using two sets of primers designed from *P. multocida* 6B; KTT72, KTSP61 and KMT1T7, KMT1SP6 (Townsend *et al.*, 1998). The first set of primers specifically amplified a DNA fragment from types B:2, B:5, and B:2,5 *P. multocida* and the second set of primers produced an amplification product unique to all *P. multocida* isolates. When PCR amplification was performed directly on bacterial colonies or cultures, it proved to be a rapid and sensitive method of *P. multocida* identification. Another PCR described by Kasten *et al.* (1997) was based on the gene for an outer-membrane protein known as the P6-like (PSL) protein (Kasten *et al.*, 1995) which shares significant similarities with the P6 protein of *Haemophilus influenzae*. The PSL *P. multocida* PCR has been shown to detect each reference strain of the 16 Heddleston somatic serovars, one field isolate of *P. multocida* and one live vaccine strain (Kasten *et al.*, 1997).

#### 1.3.2.2.2 In situ hybridization

An *in situ* hybridization test for *P. multocida* has been developed based on the recognition of a specific part of the 16S rRNA sequence and the presence of *P. multocida* was detected in sections of infected chicken and pig lungs (Mbutia *et al.*, 2001). The test was recommended for verification of pure cultures of *P. multocida* on smears as well as for histopathological detection of *P. multocida*

within infected tissues. Similar to the PCR tests described for *P. multocida*, the in situ hybridization test also detects biovar 2 strains of *P. avium* and *P. canis*, which are routinely misclassified and should be reclassified with *P. multocida* (Christensen *et al.*, 2002).

Other advanced typing methods have also been developed for identification of *P. multocida*. Restriction endonuclease analysis (REA) was used in epidemiological studies of porcine pasteurellosis and fowl cholera caused by *P. multocida* (Christensen *et al.*, 1998; Blackall *et al.*, 2000). The high genotypic resolution of random amplified polymorphic DNA (RAPD) represents the method of choice for fast screening of many isolates (Christensen & Bisgaard, 2006). Additionally, Gunawardana *et al.* (2000) has used Pulsed-Field Gel Electrophoresis (PFGE) to differentiate between *P. multocida* isolates from different outbreaks and thus produced another method that has been of great value for typing of *P. multocida*. Amplified Fragment Length Polymorphism (AFLP) has also been used to characterize the molecular epidemiology of avian isolates of *P. multocida* involved in fowl cholera (Amonsin *et al.*, 2002).

Briefly, as concluded by Christensen *et al.* (2006), identification and typing of *P. multocida* has been dominated by molecular-based techniques. The PCR-based tests are used for species identification and also for PCR-based 'serotyping' which are both capable of detecting the presence of the organism. REA, PFGE and other techniques have been refined to discriminate between closely-related isolates.

### **1.3.3 Diseases causes by *P. multocida* B:2 and other serotypes**

The numerous serotypes of *P. multocida* are associated with a variety of disease syndromes in a wide range of agricultural, domestic and feral animal species (De Alwis, 1992). In many occurrences, *Pasteurella* plays a secondary role in the pathogenesis of the disease or acts in combination with other agents. *Pasteurella multocida* serotypes B:2 and E:2 are associated with haemorrhagic septicaemia of cattle, water buffaloes, and occasionally other species, resulting in major economic losses, mainly in South East Asia (Carter and De Alwis, 1989; De Alwis, 1995). Capsule type A, serotypes 1, 3 and 4, are recognized as the primary cause of fowl cholera in poultry and wild birds (Rhodes and Rimler, 1989; Christensen & Bisgaard, 1997). Fowl cholera may appear as an acute

septicaemia characterized by disseminated intravascular coagulation, petechial or ecchymotic haemorrhages, multifocal necroses and fibrinous pneumonia. Chronic infections may involve a variety of types and local infections (Christensen & Bisgaard, 1997). Respiratory diseases in cattle, including bronchopneumonia in feedlot cattle and enzootic pneumonia of calves less than 6 months old, are mainly associated with capsule type A (Frank, 1989). Outbreaks of septicaemia in fallow deer have also been reported (Eriksen *et al.*, 1999). Infections of major economic importance in pigs include atrophic rhinitis and bronchopneumonia (Chanter and Rutter, 1989; Gardner *et al.*, 1994; Nagai *et al.*, 1994). Severe cases of atrophic rhinitis are mainly associated with capsule type D. Pulmonary lesions may result in blood-borne dissemination to the kidneys in pigs (Buttenschøn and Rosendal, 1990). *P. multocida* D was also proposed to be associated with porcine dermatitis and nephropathy syndrome (Lainson *et al.*, 2002). Atrophic rhinitis caused by *P. multocida* A:12, A:3 and other A and D serotypes has also been reported in goats and rabbits (Baalsrud, 1987; DiGiacomo *et al.*, 1989). In addition to major diseases in production animals, *P. multocida* has been recovered from a wide range of sporadic infections in many other species, including laboratory animals (Manning *et al.*, 1989), dogs and cats (Mohan *et al.*, 1997) and other mammals (DiGiacomo *et al.*, 1989).

#### 1.3.4 Virulence factors

Several factors that may be important for the virulence of *P. multocida* are lipopolysaccharide (LPS) (Rimler *et al.*, 1984), capsule (Tsuji *et al.*, 1989), outer-membrane proteins, fimbriae (Glorioso *et al.*, 1982), invasins and adhesins, toxins, plasmids and resistance to complement-mediated bacteriolysis. Many studies have been undertaken to determine the properties of each virulence factor and to investigate the correlation between antibiotic resistance profiles (Hirsh *et al.*, 1989; 1985), virulence attributes (Lee & Wooley, 1995) and the presence of plasmids.

##### 1.3.4.1 Capsule and lipopolysaccharides

There is general agreement in the literature that the capsule or outer layer of the cell is believed to be responsible for the serogroup specificity. It is composed of acidic polysaccharides and a variety of proteins. Both LPS and

polysaccharides can be adsorbed onto erythrocytes and are believed to play a role in passive haemagglutination. It was mentioned that LPS structure expressed by *P. multocida* has two main glycoforms, A and B (Harper *et al.*, 2011). Both glycoforms share the same outer core structure but differ in their inner core. Another study mentioned a low expression of a third LPS glycoform termed glycoform C found in the serovar 1 strain (Boyce *et al.*, 2009). The structure of glycoform C is similar to the one found in the LPS of *Haemophilus influenzae* and *Neisseria meningitidis*. It was suggested that the expression of glycoform C by these bacteria may allow the bacteria to avoid innate immune detection through molecular mimicry of the host carbohydrate (Harper *et al.*, 2011). In a recent review, it was suggested that LPS is an important virulence factor and minor changes in its structure could greatly affect the ability of *P. multocida* to cause disease (Harper *et al.*, 2011). A mutation in a gene *hptD*, encoding a heptosyltransferase (HptD) on a fowl cholera strain, *P. multocida* A:1 showed that this mutant was fully attenuated in chickens. HptD is required for the addition of heptose III to the tri-heptose side chain in the LPS inner core structures of glycoform A and B (Harper *et al.*, 2003). However, when the mutant strain was screened for attenuation in mice, it was not highly attenuated, indicating that the role of LPS in disease is host specific (Harper *et al.*, 2003).

The B serotype that causes HS does not possess the capsular hyaluronic acid responsible for the mucoid colonial character of the type A strain. The specific capsular substances were shown to be polysaccharide in nature by their capacity to adsorb to unmodified red blood cells. Knox & Bain (1960) recovered a fraction from serotype B:2 which contained protein, some polysaccharide and lipopolysaccharide (LPS). Bain & Knox (1961) found that phenol-extracted LPS of serotype B:2 yielded galactose, glucose, glucosamine and a heptose sugar. The LPS was toxic for rabbits and adsorbable to red blood cells. Rebers *et al.* (1967) isolated a LPS-protein complex from a B:2 strain and found that it had many of the properties of an endotoxin. It was immunogenic and immunologically specific in mice. The properties of the capsular antigens recovered from B:2 and E:2 strains by Penn and Nagy (1976) suggested that they were high molecular weight acidic polysaccharides. They were immunogenic for cattle but only weakly so for rabbits. Nagy and Penn (1974) had previously found that the purified capsular

antigens, presumably polysaccharides of types B and E HS strains, elicited antibodies in cattle that were protective, as tested by challenge.

#### 1.3.4.2 Outer-membrane proteins

This group of molecules includes components of importance for virulence, e.g., a 37.5-kDa porin of *P. multocida* affecting bovine neutrophils (Galdiero *et al.*, 1998). Outer-membrane proteins (OMPs) also include molecules with specific antigenic properties. In *P. multocida* serotype B:2,5, the presence of transferrin-binding proteins was discovered along with the pathways involved in iron regulation which are essential for bacterial growth and replication, as well as for establishment and progression of infection. *P. multocida* serogroup B bovine strain has been shown to produce transferrin binding proteins Tbp1 and Tbp2 (Veken *et al.*, 1994). Many of these OMPs are powerful antigens and some of them have been used in protection experiments against bacterial pathogens (Ratledge & Dover, 2000). A strain of *P. multocida* serotype A has been reported to excrete a siderophore called multocidin (Hu *et al.*, 1986). There is also agreement in the literature indicating that OMPs of *P. multocida* B:2 have the ability to immunize animals and to resist phagocytosis by murine peritoneal macrophages and are important contributors to the pathogenic process (De Alwis *et al.*, 1990; Srivastava, 1998; Basagoudanavar *et al.*, 2006). Further findings particularly in relation to the generation of immune response in cattle as well as in buffaloes reported that Montanide-adjuvanted OMPs derived from *P. multocida* type B grown in either iron-depleted or iron-sufficient medium could act as acellular vaccines against HS (Basagoudanavar *et al.*, 2006).

#### 1.3.4.3 Fimbriae

Glorioso *et al.* (1982) demonstrated fimbriae by electron microscopy on rabbit type A strains and found that the fimbriae were capable of adhering to rabbit pharyngeal cells. In addition, two types of fimbriae were identified on serogroup D strains, the first one similar to the type A fimbriae and the second were morphologically similar to the type 1 fimbriae of *E. coli* (Ruffolo *et al.*, 1997). Some fimbriae-like filamentous appendages have also been observed on the surface of HS-causing *P. multocida* B:2 (Tomer *et al.*, 2004). Strains belonging to other serotypes without fimbriae showed much less adhesive capacity to the host cell and suggested that fimbriae were involved in attachment of the

bacteria to their respective host. The attachment of *P. multocida* B:2 to the host cell could be inhibited by N-acetyl-D-glucosamine, which may suggest that this amino sugar could be the animal cell receptor to which the fimbriae adhere. Adhesiveness is reduced following treatment of the organism with pronase, heat or homogenisation, all of which would reasonably affect fimbrial function. Nevertheless, there is a poor correlation between possession of fimbriae and virulence in experimental models of disease. Indeed, toxigenic strains of *P. multocida* may have no detectable fimbriae or flagella and yet can colonize the porcine tonsil and respiratory tract both alone or concurrently with *Streptococcus suis* (Ackermann *et al.*, 1991).

#### 1.3.4.4 Plasmids and transposons

Various sizes of plasmids between 1.3 and 100 kbp have been found in *P. multocida* from different serotypes (Hunt *et al.*, 2000). These plasmids have been found related to resistance to streptomycin, sulfonamides, tetracycline, penicillins, kanamycin and chloramphenicol (Rimler & Rhoades, 1989; Hunt *et al.*, 2000). The distribution of identical non-conjugative R plasmids of *P. multocida* did not follow the clonal population structure (Ikeda & Hirsh, 1990). The only transposable element identified in *P. multocida* is transposon *Tn5706* (Hunt *et al.*, 2000).

#### 1.3.4.5 Toxins

Strains of *P. multocida* serogroup D, which cause atrophic rhinitis, produce a dermonecrotic toxin (PMT, for *P. multocida* toxin). It is the principle virulence factor in atrophic rhinitis and induces localised osteolysis in the nasal turbinates, primarily through increased osteoclastic bone resorption (Kock *et al.*, 1995). PMT is a potent mitogen and induces many cellular effects especially in the rearrangement of the actin cytoskeleton. It shares significant homology with the cytotoxic necrotizing factors (CNF1 and CNF2) of *E. coli* (Pei *et al.*, 2001). The homology is highest in an N-terminal region of PMT (residues 250-530). In CNF1, this region functions as a translocation-domain (Pei *et al.*, 2001) and is flanked by an N-terminal receptor binding domain and a C-terminal catalytic domain (Lemichiez *et al.*, 1997). Similarly, it has been shown that the receptor binding and catalytic domains of PMT are also located at the N- and C-termini, respectively, of the toxin (Baldwin *et al.*, 2004). Although toxin-related

sequences have occasionally been found in other serotypes, the synthesis of PMT is usually restricted to serogroup D. Recombinant toxin derivatives have been used as vaccine candidates (Nielsen *et al.*, 1991; Petersen *et al.*, 1991). Vaccine components for protection against atrophic rhinitis in pigs were developed by deletion mutagenesis of the gene encoding the PMT. Four purified toxin derivatives lacking different and widely separated regions in the amino acid sequence were characterized by a lack of toxic activity. One such component was shown to induce efficient protection of vaccinated female mice and their offspring against challenge with purified PMT.

The toxic effects of *P. multocida* serotype B:2,5 on macrophages *in vitro* and *in vivo* have been tested. HS-associated strains of *P. multocida* are reported to reproduce a vacuolating cytotoxin (Shah *et al.*, 1996). Mice were injected intraperitoneally with  $10^2$  cells of *P. multocida* B:2,5. Observation of peritoneal macrophages with electron microscopy after 6 h revealed strong induction of cytoplasmic vacuolation, macrophage lysis and death. When the HS-associated strains of *P. multocida* were then incubated with mouse macrophage cell line (RAW 264.7) at a ratio of 10:1 (bacteria:cell), vacuolation of macrophages were observed at 30 min post-invasion (Shah *et al.*, 1996).

## 1.4 Haemorrhagic septicaemia (HS)

### 1.4.1 The disease

Haemorrhagic septicaemia (HS) is an acute, fatal, septicaemic disease of cattle and buffaloes caused by the bacterium *Pasteurella multocida* serotypes B:2 or E:2. It is also a primary pasteurellosis and is reproducible in susceptible host species using pure cultures of the causative organism alone (De Alwis, 1999).

It has been shown that HS occurs most commonly in cattle and buffaloes. According to Carter (1991), buffaloes are more susceptible than cattle and the disease occurs more frequently in poor husbandry conditions. Clinical symptoms are often not observed but high temperature, loss of appetite, nasal discharge, increased salivation, and laboured breathing, with swelling in the submandibular region have been recorded. Moreover, Carter (1989) also stated that death usually occurs quickly and mortality is almost 100% in infected animals. True

recovery from clinical disease occurs only if the animal is treated in the very early stages, which is often impossible under prevailing field conditions.

#### **1.4.1 Global distribution**

Haemorrhagic septicaemia has been recorded in almost all parts of the world except for the UK and Oceania, including Australia, where it has never occurred (De Alwis, 1999). The disease is of great economic importance in Asia where cattle and buffaloes are abundant and are vital for draught power and milk production. In Malaysia, the disease was first reported as early as the 1880s (Bain, 1963). In the Peninsula of Malaysia, the disease is enzootic in Kelantan, Terengganu, Kedah, Perak, Pahang and Negeri Sembilan due to the high population of cattle and buffaloes (Chandrasekaran *et al.*, 1981).

#### **1.4.3 Epidemiological cycle**

Explosive outbreaks of HS may occur when it is first introduced to areas that have previously been free of the disease, or when it occurs as sporadic outbreaks in non-endemic areas. Previous studies have found that in endemic areas, large numbers of animals that survive after an outbreak of disease become latent carriers (Carter, 1989). They intermittently shed the organisms but, since the herd immunity is also high, there are no fresh clinical cases. A new outbreak occurs when a shedder come into contact with a susceptible animal, which may be one born after the previous outbreak or one introduced into the herd from elsewhere. According to De Alwis (1999), the chance of a fresh outbreak increases with time and with increase in size of the susceptible population.

#### **1.4.4 Progression of the disease**

In West Malaysia, Saharee and Salim (1991) have done a field observation of five outbreaks of disease involving 37 buffaloes and 7 cattle. They recorded a clinical course of 4-12 hours in per acute cases and 2-3 days in acute and sub-acute cases. On a herd basis, the outbreaks usually occur very fast and do not persist for long. Their observations indicated that 75% of outbreaks lasted for less than 15 days within a herd.

As recorded by De Alwis (1999), the clinical syndrome of HS may broadly be divided into three phases; phase one is dominated by increased temperature,



loss of appetite, general apathy and also depression. If closely monitored, a rise in rectal temperature to 40-41°C is recorded, which lasts throughout the course, dropping to subnormal levels during the terminal phase, a few hours before death. Phase two is dominated by a respiratory syndrome. There will be increased respiration rate (40/50 minute), laboured breathing, clear nasal discharge and salivation. Submandibular oedema may also begin to show during this phase. As the disease progresses, the nasal discharge becomes opaque and mucopurulent. Lastly, phase 3 is dominated by recumbency. The respiratory distress becomes more acute, the animal lies down, terminal septicaemia sets in and death follows; the case fatality is nearly 100%.

An earlier study by Graydon *et al.* (1993) stated that the disease is more acute and has a shorter course in buffaloes than in cattle. He also observed that upon experimental subcutaneous inoculation, buffaloes died 24-31 hours after inoculation, whereas the time of death for cattle was around 60 hours.

#### **1.4.5 Treatment**

As HS is a primary bacterial disease with no other biological agents involved, treatment may appear simple, using the wide range of antibiotics currently available. In spite of this, in reality, treatment is constrained by a host of practical considerations. It has been found in practice that animals can only be cured if they are treated at the very early stage of the disease (Carter, 1989).

### **1.5 Vaccination against HS**

Several types of vaccines have been used for prevention and control of the disease. Countries where the disease is endemic resort to routine prophylactic vaccination. Nonetheless, several disadvantages with the current vaccines have provoked scientists all over the world to try to develop an improved vaccine to overcome the weaknesses with the current vaccines.

#### **1.5.1 History and current status**

In 1907, Baldrey discovered the first vaccine for HS by preparing a killed vaccine (0.25% lysol-inactivated broth culture) (De Alwis, 1999). This vaccine conferred immunity against the disease for only 6 weeks. Later, in 1938, Delpy and Rastegar (as cited by De Alwis, 1999) prepared a vaccine that consisted of a

suspension of bacteria lysed in 5% saponin. It was then followed in 1959 by Dhana attempting to develop a vaccine from a capsular extract of the organism (De Alwis, 1999). The aim to produce better vaccines for HS continued and it was thought that a live vaccine might be an ideal vaccine to confine and control the disease more efficiently. Thus, an early development of live vaccine started with a streptomycin-dependent (StrD) mutant of *P. multocida* by Chengappa *et al.* (1979). This work progressed to use different serotypes of the pathogen to discover whether they can be cross-protective; Myint *et al.* (1987) first used a strain isolated from deer to be used as a live vaccine. There was then a debate on precautions, procedure and safety measures as to whether the live vaccine might confer the disease or in some other way generate an outbreak of HS by itself. Meanwhile, other scientists were considering other types of vaccine for HS, such as subunit vaccines. Sabri *et al.* (2000) used an OMP preparation from the pathogen as a subunit vaccine. However, the vaccine failed to contain the disease. To mimic the ability of the pathogen to infect the host without causing the disease has always been seen as an ideal way to confer protection against the disease. Consequently another live-attenuated vaccine was developed by Tabatabaei *et al.* (2002) by mutating a housekeeping gene, *aroA*, in order to develop an attenuated live *P. multocida* strain. The live vaccine strain proved to be very highly attenuated yet protective in mice and in cattle (Hodgson *et al.*, 2005; Dagleish *et al.*, 2007). The different types of HS vaccine are described below.

#### 1.5.1.1 Plain bacterin

One of the simplest vaccines comprised of killed whole-bacterial cells as the bacterin. Generally, bacterins need repeated vaccination in order to provide sufficient immunity. The most common type of bacterin is an inactivated broth culture. However, it triggers antibody poorly and it provides immunity for only about six weeks (OIE, 2004). An earlier study by Verma & Jaiswal (1997) which used another form of bacterin, an agar-wash formalin-killed vaccine shown to provide immunity for up to 4 months but later was found to cause a certain level of shock when administered to animals.

### 1.5.1.2 Alum-precipitated vaccines (APV)

This type of vaccine is the most widely used vaccine in Asia and Africa. It consists of a bacterin to which potash alum has been added to give a final concentration of 1%. If derived from aerated culture, the density of the bacterin should be adjusted to approximately 0.75 mg dry weight per ml, so that a 3 ml dose will contain a minimum of 2.0 mg bacteria (OIE, 2004).

The disadvantages of this type of vaccine are that it provides reliable immunity only for three to four months and shock reactions can also occur (Verma & Jaiswal, 1998). It is important to thoroughly mix the contents of the bottle before use because precipitation with alum causes the cells to settle at the bottom. If this precaution is not taken, animals receiving vaccines from the bottom of the bottle will receive a large dose of bacteria, and the chances of shock will be increased. Adding to that, in some countries where HS is endemic, the administration of the vaccine is also difficult because of poor husbandry condition with semi-wild buffaloes.

### 1.5.1.3 Aluminium hydroxide gel vaccines

This vaccine has common properties with the APV. The antigen solution is added to preformed aluminium hydroxide, aluminium phosphate, mixed aluminium hydroxide plus phosphate or gamma aluminium oxide (Edelman, 1980). According to Verma & Jaiswal (1998), this type of vaccine has been used extensively in Thailand and Laos and it has been able to produce immunity for up to 6 months, demanding twice-a-year vaccination. However, further vaccination did not confer a substantial immunity of more than 90 days even when used with immunomodulators such as vitamin E and levamisole (Verma & Jaiswal, 1998).

### 1.5.1.4 Oil-adjuvant vaccines

Oil-adjuvant vaccine is an alternative vaccine to overcome the disadvantages of alum precipitated vaccines such as short-term immunity. This vaccine can provide longer immunity for the host. In addition to that, this vaccine, which has been described in detail by Bain *et al.* (1982), is the most potent of the available vaccines. It consists of a dense bacterial suspension emulsified with a light mineral oil using various emulsifying agents (e.g., lanolin). The emulsion is of the water-in-oil type, and must contain approximately equal volumes of the

internal and the external phases. A well-made oil-adjuvant vaccine is white in colour and adheres evenly to clean glass. It is reported to confer immunity for six to nine months on primary vaccination of young animals, and up to one year with a booster (Thomas, 1970; De Alwis *et al.*, 1978).

When oil-adjuvant vaccines are injected, a vaccine depot is formed at the site of inoculation. This depot serves as a prolonged source of antigen. There is little production of antibody around the depot, the main sites of production being the local lymphatic chain and ultimately the reticulo-endothelial system. Talmage and Dixon (1953) showed that the antibody response to the protein antigen in this form remained constant for over 300 days. This contrasted with the antibody response to the same antigen in aqueous solution or alum precipitated, which declined after 10 days.

Although it is an alternative to the alum-precipitated vaccines, it also has some major set-backs. The disadvantages of this vaccine are that it has the added complexity of high viscosity, which make it quite unpopular even though improved oil-adjuvant vaccines with lower viscosities have been described. In addition, it also requires a high number of inactivated bacteria ( $10^{10}$  to  $10^{11}$  cells) which is not economical for production and is potentially reactogenic (Verma & Jaiswal, 1998). A summary of current vaccination practices against HS in Asia is shown in Table 1.

**Table 1. Haemorrhagic septicaemia vaccination practices in Asia.**

Country	Type of vaccine	Dose	Route	Duration of immunity
Cambodia	Alum-adjuvant vaccine; given twice a year	2 ml	s.c.	3-6 months
India	Alum-precipitated vaccine	3 ml	s.c.	4-6 months
Indonesia	Oil-adjuvant vaccine	3 ml	i.m.	up to 1 year
Iran	Alum-precipitated vaccine combined with Black leg vaccine; given twice a year	2-3 ml	s.c.	4-6 months
Malaysia	Alum-precipitated vaccine	5 ml	s.c.	4-6 months
	Oil-adjuvant vaccine	3 ml	i.m.	up to 1 year
Myanmar	Live vaccine; contains $10^7$ cfu/dose of <i>P. multocida</i> serotype B:3,4	2 ml	i.n.	1 year
Nepal	Alum-precipitated vaccine	5 ml	s.c.	6 months
Philippines	Killed alum adjuvant vaccine; booster every 6 months	5 ml	s.c.	4-6 months
Sri Lanka	Oil-adjuvant vaccine; given at 4-6 months, booster 3-6 months later, followed by annual vaccination	3 ml	i.m.	up to 1 year
Thailand	Aluminium hydroxide gel, contains $3 \times 10^{10}$ cfu/dose of <i>P. multocida</i> serotype B:2	3 ml	s.c.	3-4 months
Vietnam	Alum-precipitated vaccine; two injections per year	2 ml	s.c.	4-6 months

Table cited from Tabatabaei (2000) based on Verma and Jaiswal (1998) review. (s.c., subcutaneous and i.m., intramuscular)

### 1.5.2 Deficiencies of available vaccines

Since the current vaccines have notable defects, most countries in which HS is endemic have put a considerable amount of research to develop an improved vaccine. In addition to that, it is widely recognized that an ideal vaccine should possess certain characteristics, such as: easy and economical to produce, with sustainable production technology in the endemic countries; stable for use in the tropics; easy to handle in the field with a consistency that make it easy to administer; no adverse reactions, high level of immunity with a minimum delay after vaccination and lasting for at least one year. From De Alwis's (1999) suggestions on attempts to produce better HS vaccines, they can be classified into several groups, which are: use of other adjuvants; production of oil-adjuvant vaccines of low viscosity; production of vaccines based on purified extracts of the organism and on the identification of the protective antigens; and the use of live-attenuated vaccines.

Vaccination failure against HS is frequent in many countries. This is due to several factors. In some countries like Malaysia, vaccination campaigns are directed against several cattle diseases such as foot-and-mouth disease and HS. More than one vaccine is thus administered simultaneously. According to Joseph and Hedger (1984), there was no adverse effect towards simultaneous vaccination, hence indicating that cattle may be safely and effectively vaccinated simultaneously. However, another problem is the timing and the frequency of the vaccination. Failure to vaccinate at the critical time, such as prior to the stressful monsoon season, leads to disease outbreaks (Yeo & Mokhtar, 1993). Nevertheless, the major problem associated with vaccination failure is the low vaccination coverage, which has been reported in Malaysia, the Philippines and Indonesia (Syamsudin, 1993; Yeo & Mokhtar, 1993). Vaccination coverage of less than 80% may lead to the recurrence of disease outbreaks (Bain *et al.*, 1982). After several epidemiological studies, it was concluded that vaccination coverage of 70% leads to sporadic occurrence of HS while coverage of more than 80% will be able to significantly reduce the incidence of the disease (Syamsudin, 1993).

As well as having a vaccine that can eventually control HS, the mode of vaccine delivery to the animal is a major consideration (Sarah *et al.*, 2006). Injectable vaccines, such as oil-adjuvant vaccines, have been shown to stimulate immunity.

However, livestock production systems in many developing countries use either extensive or semi-extensive types of management with little animal handling (Zamri-Saad, 2005). This leads to difficulties in gathering animals for vaccine injection, thus most vaccination coverage, for example in Malaysia, is as low as 17% (Saharee and Salim, 1993). Disease outbreaks are often reported in the unvaccinated animals.

### 1.5.3 Live-attenuated vaccines

The advantages of a live-attenuated vaccine are (i), it mimics the early stages of a natural infection and (ii), use of the natural route of entry into the host might be expected to confer more solid and long-term protective immunity, particularly if it is amenable to oral or intra-nasal administration that would favour induction of mucosal immunity in a way similar to the natural infection. Not only would the live vaccine stimulate mucosal immunity of the exposed host, it might also transmit the attenuated organism to in-contact hosts and eventually stimulate the mucosal immunity of these animals. This was proven in a trial of live vaccine using low doses of *P. multocida* B:2 and challenge with a high doses of the same organism, when 100% of the non-exposed animals that were kept together with the intranasally-exposed group showed similar stimulation of the bronchus-associated lymphoid tissue (Zamri-Saad *et al.*, 2006). Concurrently, 60% of the in-contact animals carried the live *P. multocida* B:2 vaccine strain for a period of between 1 and 2 weeks after exposure to the exposed group (Zamri-Saad *et al.*, 2006). This is an important finding since there is a possibility of intranasal vaccination with live vaccine leading to self-vaccination of the in-contact animals.

De Alwis (1999) has suggested several characteristics for an ideal live vaccine: it must have all or at least most of the protective antigens present in the field strains; it must grow readily in ordinary culture media; it should be avirulent for cattle and buffaloes or have reduced virulence, i.e. the lethal dose must be much higher than the immunising dose; and it should be able to multiply sufficiently *in vivo* following vaccination, producing a full complement of the important immunogens, thereby stimulating an adequate immune response. The different types of live-attenuated vaccines used against HS are described in the next sections.

### 1.5.3.1 Streptomycin-dependent mutant

In this vaccine, *Pasteurella multocida* B:2 was mutagenised using N-methyl-N-nitrosoguanidine to produce a streptomycin-dependent mutant. After a single vaccination by the intranasal route using the rabbit as an animal model, it was shown to be fully protective against homologous challenge at 21 days post-vaccination (Wei & Carter, 1978). However, the vaccine needed a large number ( $3.75 \times 10^9$  organism per dose) of the mutant strain in order to produce a protective response and the inability of the organism to multiply in the absence of streptomycin was another disadvantage of the vaccine (Alwis *et al.*, 1980; Chengappa *et al.*, 1979). Yet, the development of this vaccine was a milestone in proving that a live strain of the pathogen could be used for vaccination.

### 1.5.3.2 Deer strain live vaccine

Jones & Hussaini (1982) isolated a *P. multocida* serotype B:3,4 from a fallow deer (*Dama dama*) in England after an outbreak of septicaemia. It was then used in experimental infection of cattle and buffaloes and succeeded in protecting calves for up to 9 months after they had been vaccinated subcutaneously or intradermally and later challenge subcutaneously with serotype B:2 (Myint *et al.*, 1987). Moreover the vaccine was reported to have a low virulence for cattle, possibly due to the lack of transferrin-binding proteins (Veken *et al.*, 1996). Myint and Carter have continued to investigate the vaccine, to prove its efficacy. By administering the vaccine intranasally as an aerosol spray, they have obtained encouraging results when applied to a population of cattle and buffaloes over six months of age in Myanmar (Myint *et al.*, 2005). They reported that the live B:3,4 organisms were able to induce efficient cross-protecting immunity by a single immunisation at a relatively small dose of  $2 \times 10^7$  viable organisms.

Yet the safety of the vaccine has been questioned. One study of isolates from the palatine tonsils of healthy fallow deer from an HS outbreak area in Denmark showed a 27% carrier rate of *P. multocida* B:3,4. The carrier isolates had identical ribotyping and pulse-field gel electrophoresis profiles to those of the strain used as the live vaccine for cattle and buffaloes in Asia (Aalbaek *et al.*, 1999). Thus here it was shown that the deer vaccine strain is a potential pathogen and vaccination of cattle and buffaloes would have to be done under



strictly controlled conditions. The question is how to prevent the spread of the organism if it is being administered to semi-wild cattle and buffaloes?

#### 1.5.3.3 Acapsular mutants

The search for an ideal live-attenuated vaccine continued when a *cexA* (gene involved in the export of capsule) mutant of *P. multocida* serotype B:2 was constructed by allelic exchange (Boyce & Adler, 2000). Immunisation (i.p.) with the vaccine conferred significant protection against wild-type challenge (i.p.) in a mouse model but only with high doses (e.g.  $>8 \times 10^5$ ) of the mutant (Boyce & Adler, 2001).

Boyce and Adler (2001) developed another acapsular mutant by constructing an inactivation of the *bcbH* gene (a gene predicted to be involved in polysaccharide biosynthesis) from the same organism. Immunisation with this mutant was able to confer significant protection against wild-type challenge in a mouse model, while immunisation with similar doses of either killed wild-type or killed mutant failed to confer protection (Boyce & Adler, 2001). There are no subsequent reports of the use of this vaccine in cattle or buffaloes.

#### 1.5.3.4 *aroA* mutant vaccines

Homchampa *et al.* (1992, 1994) first developed this particular type of vaccine against *Pasteurella* strains. They constructed *aroA* mutants of *P. multocida* serogroup A:1 and *P. haemolytica* biotype A:1 using recombinant DNA techniques. The mutants contained a  $Km^R$  cassette inserted into the *aroA* gene via a suicide vector approach. The mutants were shown to be attenuated in a mouse model when injected i.p. and protected the mice against wild-type challenge (i.p.). Further study by Homchampa *et al.* (1997) reported the cross-protective immunity conferred by a marker-free *aroA* mutant of *P. multocida* serotype A:1. They found that this new strain was highly attenuated in the mouse model. In addition, they also showed that with one or two doses of vaccine, this mutant strain could confer protective immunity against homologous and heterologous (serotype A:3 strain) challenge, but not against challenge by other biotypes. When tested further, the mutant was also able to protect chickens against intratracheal challenge with the wild type (Scott *et al.*, 1999).

The vaccine strain was also capable of providing cross-protection against heterologous challenge with strain serotype A:4.

Subsequently an *aroA* mutant derivative of *P. multocida* B:2 was developed by Tabatabaei *et al.* (2002). The mutant was constructed by allelic exchange and confirmed to be highly attenuated when tested in a mouse model of HS. Vaccination of the *aroA* strain ( $10^7$ - $10^9$  cfu/mouse) either i.p. or i.n. completely protected mouse against challenge with a high dose ( $>1,000 \times LD_{50}$ ) of the wild-type B:2 strain. It was further tested in cattle to confirm its attenuation and protection. When administered intramuscularly (i.m.) at  $10^8$  cfu/animal in two doses four weeks apart, it appeared to give the best combination of high immune response, safety and protection against challenge with  $10^7$  cfu/animal of the wild-type strain give by the i.m. route (Dagleish *et al.*, 2007). Whether this vaccine has overcome all the disadvantages of other types of HS vaccines is still too early to decide. More field trials are needed, especially in the countries where HS is endemic.

## 1.6 DNA vaccines

The historical basis for DNA vaccines rests on the observation that direct *in vitro* and *in vivo* gene transfer of recombinant DNA into mammalian cells by a variety of techniques resulted in expression of protein. Multiple approaches have been used in order to achieve this expression, such as using formulations of DNA with liposomes or proteoliposomes (Nicolau *et al.*, 1983; Mannino & Gould-Fogerite, 1988; Kaneda *et al.*, 1989), calcium phosphate-coprecipitated DNA (Benvenisty & Reshef, 1986), and a polylysine-glycoprotein carrier complex (Wu & Wu, 1987). It was shown in a land mark study by Wolff *et al.* (1990) that direct inoculation of plasmid DNA encoding several different promoter genes could induce protein expression within muscle cells when “plasmid” or “naked” DNA vaccination was done *in vivo* (Wolff *et al.*, 1990). The finding provided a strong basis that purified recombinant nucleic acids (“naked DNA”) can be delivered *in vivo* and can direct protein expression. These observations were further extended in a study by Tang *et al.* (1992) who injected mice with plasmid DNA encoding *hGH* (human growth hormone) and were able to elicit antigen-specific antibody responses. Subsequently, demonstrations by Ulmer *et al.* (1993) and Robinson *et al.* (1993) that DNA vaccines could protect mice or chickens, respectively, from

influenza infection provided a notable example of how DNA vaccination could mediate protective immunity. In further mouse experiments, it was proven that both antibody and CD8<sup>+</sup> cytotoxic T-lymphocyte (CTL) responses were elicited (Ulmer *et al.*, 1993), consistent with DNA vaccines stimulating both humoral and cellular immunity.

As shown above, plasmid DNA is a crucial tool in shuttling antigen genes *in vivo*, which results in the *in situ* production of antigen (for vaccines). Since expression is required in the mammalian host cells, a eukaryotic expression plasmid is necessary. Thus, several vital elements (listed in the next section) are needed when constructing this type of plasmid DNA for DNA vaccines, in order to increase the efficiency of antigen delivery.

### 1.6.1 Eukaryotic expression plasmids

#### 1.6.1.2 Properties of eukaryotic expression plasmids

For optimal expression of antigen in eukaryotic cells, there are certain requirements of the plasmid DNA, depending on the initial bacterial host and the targeted cells. An expression plasmid for a DNA vaccine needs: an origin of replication allowing for growth in bacteria (for easy *in vitro* manipulation); a bacterial antibiotic resistance gene (to aid in selection); a powerful promoter for optimal expression in mammalian cells; and stabilization of the mRNA transcript, achieved by incorporation of polyadenylation sequences such as those found in bovine growth hormone (BGH) or simian virus 40 genes (Gurunathan *et al.*, 2000; Grillot-Courvalin *et al.*, 2002).

It is generally believed that the level of gene expression *in vivo* obtained after DNA vaccination correlates with the immune response generated. Therefore, several laboratories have sought to improve gene expression and immune responses after plasmid DNA vaccination. These approaches have included optimizing gene regulatory elements within the plasmid backbone or modifying the plasmid backbone itself to enhance gene expression (Gurunathan *et al.*, 2000). One of the most important elements from the list above is the type of promoter used to express encoded protein. Viruses have a highly evolved structure and mechanism in order to transfect mammalian cells to transfer expressible genetic materials (Liu, 2003). An early study on DNA vaccines

demonstrated an expression plasmid expressing antigens from a eukaryotic viral promoter (Sizemore *et al.*, 1997). This work was followed by Darji *et al.* (2000) who had developed a DNA vaccine by manipulating plasmid pAH97, which also employs a cytomegalovirus promoter ( $P^{CMV}$ ) for expression of the encoded protein. Similar findings were demonstrated with a different type of expression plasmid with the same cytomegalovirus promoter ( $P^{CMV}$ ) for protein expression *in vivo* (Cossart & Lecuit, 1998; Grillot-Courvalin *et al.*, 2002). To date, commercial eukaryotic expression vectors mostly have employed a viral promoter from cytomegalovirus which had been proven to maximize protein expression especially when combined with the immediate early (IE) gene which is known to assist in augmentation of expression efficiency (Thomsen *et al.*, 1984).

### 1.6.2 Mode of delivery

Introducing the expression plasmid into eukaryotic cells requires an extensively appropriate delivery system in order to optimize DNA vaccines or even to make the vaccine work. There are multiple carrier-mediated approaches in order to deliver DNA vaccine into targeted cells.

#### 1.6.2.1 Gene gun

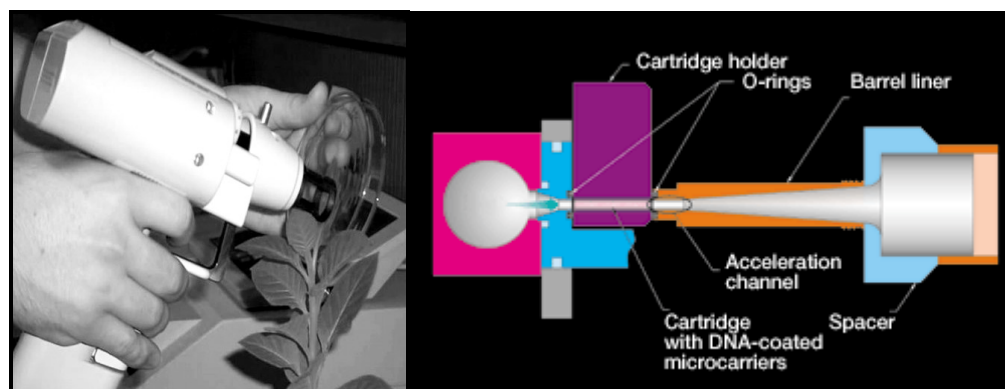


**Figure 1. Example of gene guns.**

Left: Helios Gene Gun (BioRad), a hand-held device for direct transfection of plasmid DNA into eukaryotic cells. Right: It uses an adjustable low-pressure helium pulse to sweep DNA-coated gold microcarriers from the inner wall of a small plastic cartridge directly into the target. (Pictures from BioRad, USA)

Gene gun technology as shown in Figure 1, uses a gas-driven biolistic bombardment device that propels gold particles coated with plasmid DNA directly into the tissues (Yang *et al.*, 1990; Williams *et al.*, 1991; Tang *et al.*,

1992; Fynan *et al.*, 1993). These gold particles are propelled directly into the cytosol of target cells, resulting in transgene expression levels higher than those obtained by comparable doses of injected “naked DNA”. As proved by Tang *et al.* (1992) plasmids coated onto gold beads resulted in foreign gene expression and the induction of an antibody response to the foreign gene product in mice. They used genetic immunisation as a means of generating a humoral immune response to a gene product, in this case the human growth hormone, by injecting plasmid DNA encoding the foreign gene into a host. This mode of immunization has been shown to elicit protective immunity in several animal models (Watts & Kennedy, 1999). For example, one study has reported that gold particles containing as little as 0.4 µg of DNA can induce protective immunity in mice when compared with hundreds of microgram of DNA in saline administered without a gene gun (Fynan *et al.*, 1993). Yoshida *et al.* (2000) indicated that a gene gun system developed in their study was highly reproducible and reliable to induce cytokine-T-lymphocyte (CTL) and specific antibodies in animal models when compared to intramuscular injection of plasmid DNA. However, this technique is not as cost-effective as other delivery methods and is one of the main reasons of the slow development of this technique (Donate *et al.*, 2011).

#### 1.6.2.2 Liposomes

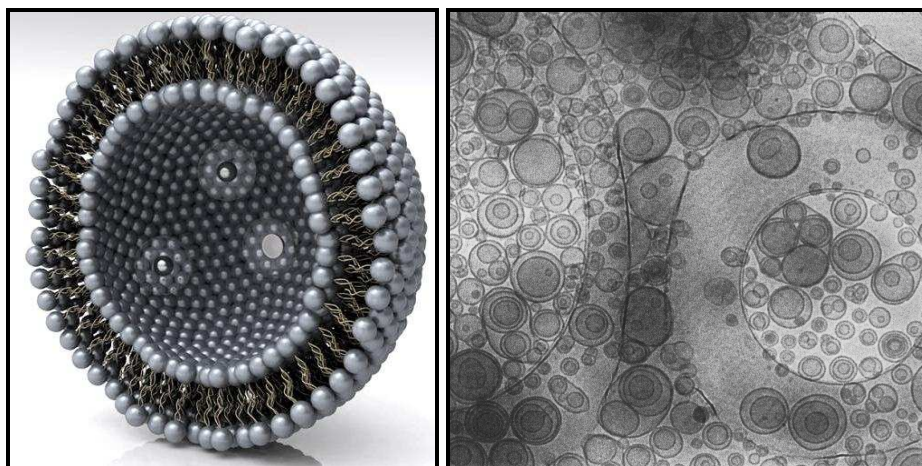


**Figure 2. Liposomes for delivery of DNA vaccine.**

Left: Image showing cross-section of the liposome bilayer structure. DNA or protein is carried in the aqueous core of the liposome (cited from <http://lyposphericnutrients.co.uk>). Right: An electron micrograph of liposomes during mammalian cell transfection (cited from <http://bioteach.ubc.ca/Bio-industry>).

Liposomes are bilayered membranes consisting of amphipathic molecules such as phospholipids, forming unilayered or multilayered (lamellar) vesicles (Figure 2).

Unilamellar vesicles have a single bilayer membrane surrounding an aqueous core and are characterized by either being small or large unilamellar vesicles. Multilayered vesicles have several lipid bilayers separated by a thin aqueous phase. Locally-injected liposomes are known to be taken up avidly by antigen-presenting cells infiltrating the site of injection or in the lymphatics, an event that has been implicated in their immunoadjuvant activity (Gregoriadis, 1990).

Liposomes would also protect their DNA content from deoxyribonuclease attack (Gregoriadis *et al.*, 1996). Because liposomes can be prepared with significant structural versatility based on vesicle surface charge, size, lipid content, and coentrapment of adjuvants, they offer considerable flexibility for vaccine optimization (Jain *et al.*, 2011). The full scope of the use of liposomes to increase the effect of DNA vaccines is currently an active area of investigation. Intramuscular injection of plasmid DNA incorporating hepatitis B surface antigen entrapped in liposomes elicited 100-fold increased antibody titers and increased levels of both interferon- $\gamma$  (IFN- $\gamma$ ) and interleukin-4 (IL-4) when compared with those in animals injected with “naked DNA” (Gregoriadis *et al.*, 1997). A similar result on antibody augmentation was seen when DNA/liposome complexes were administered intranasally (Klavinskis *et al.*, 1997). However, liposome potency depends on the composition of the lipid, bilayer fluidity number of lipid layers, size and physico-chemical characteristics as the modulation of these features bring about changes in immune responses to the associated antigens (Jain *et al.*, 2011). In a recent review, it was shown that using cationic liposomes alone is not sufficiently immunostimulatory. The need for combination of liposomes with immunostimulating ligands in order to enable the adjuvant system to work is considered as an additional task for further advancement of this technique (Christensen *et al.*, 2011).

#### 1.6.2.3 Cochleates

Developments from earlier structures of liposomes proved that lipid matrix-based subunit vaccines can be used to produce custom-designed vaccines. Cochleates are rigid, calcium-induced, spiral bilayers of anionic phospholipids. They have a unique structure that is different from that of liposomes. They are relatively stable after lyophilization or in harsh environments (Gurunathan *et al.*, 2000).

In oral delivery systems, cochleates have the advantage of preventing internal rapid degradation of naked DNA or protein and employing tools (such as pH and temperature) for target degradation of cochleate at specific sites such as organ, tissue or muscle; such tool could help in site-specific release of DNA or antigenic protein (Landry & Heilman, 2005). Upon contact with a lipid bilayer of a target cell, the cochleate vector structure delivers one or more of the nucleotide sequences with one or more proteins to the interior of the target cell. It is believed that, on contact with target cell membrane, a fusion event occurs between the membrane and the outer layer of the cochleate leading to delivery of the contents of the cochleate into the cytosol. Upon entry into the cell, the proteins, such as the surface glycoproteins of enveloped viruses, facilitate the integration of the nucleotide sequence into the genome of the host cell. It has been reported that DNA/cochleate formulations were able to induce strong CTL and antibody responses after parenteral or oral administration (Gould-Fogerite & Mannino, 1996; Gould-Fogerite *et al.*, 1998).

#### 1.6.2.4 Microparticle encapsulation

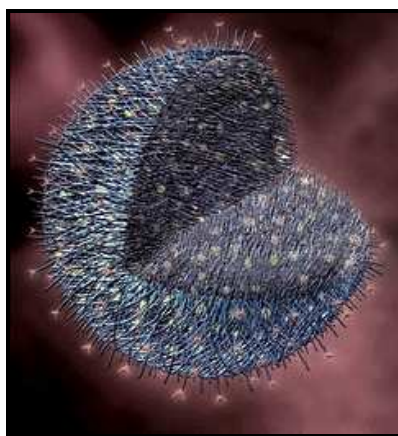


**Figure 3. Compact microparticle encapsulation.**

Illustration of compact microparticle encapsulation with embedded degradable polymer in its core for plasmid DNA packaging. (Re-drawn diagram is based on image from gizmodo.com)

Another potentially exciting means of DNA delivery is the use of biodegradable polymeric microparticles. Plasmid DNA trapped in these biodegradable microparticles, composed of polymers such as poly(lactic-co-glycolic acid) or chitosan (Figure 3), can be administered orally and has been shown to induce both mucosal and systemic immune responses (Herrmann *et al.*, 1999). The use of poly(lactic-co-glycolic acid)-entrapped DNA vaccines to induce protective

immune responses to rotavirus challenge after oral administration was demonstrated in two separate studies (Chen *et al.*, 1998; Herrmann *et al.*, 1999). The ability of polymer-entrapped DNA vaccines to induce systemic and mucosal immune responses after oral or intraperitoneal administration is similar to vaccine administration using cochleates. Most recent studies have manipulated this system for slow release of drugs at targeted sites *in vivo*. A PEG-PLA (polyethylene glycol-poly(lactide acid)) microparticle preparation was shown to deliver proteins in cell culture at 1 h of transfection and to persist *in vivo* in retinal cells for at least 9 weeks with no observed toxicity (Rafat *et al.*, 2010). Another study reported that an encapsulated poly (L-lactide) microparticle formulation for sustained intravitreal delivery of TG-0054, a highly water-soluble anti-angiogenic drug, was able to persist for 3 months *in vivo* and for 6 months *in vitro* in retina cell. This continuous choroidal delivery of thyroglobulin, TG-0054 has useful in treating choroid neovascularization in the retina (Shelke *et al.*, 2010).

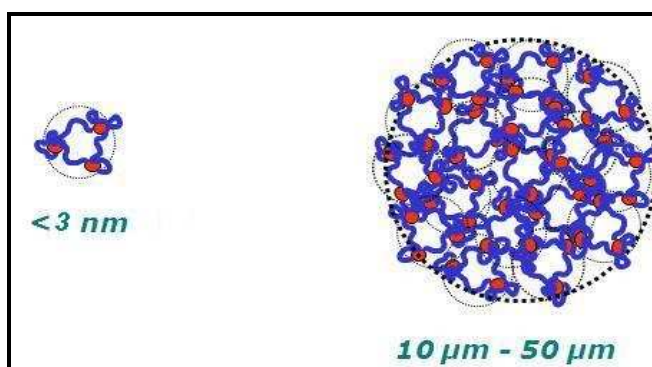


**Figure 4. Comparison of nanoparticle and microparticle.**

Image shows size comparison between plasmid DNA (red) in microparticle encapsulation (right) and plasmid DNA packaged in nanoparticles compartment (left).

Further developments of this method have adapted nanotechnology approaches to develop nano-scaled drug delivery vehicles termed as nanoparticles (1-2 nm). This vehicle has been developed to deliver naked DNA entrapped in its polymeric compartment. This system was shown to give more antigen production when compared with microparticle encapsulation (10-50  $\mu\text{m}$ ) (Figure 4) (Nandedkar, 2009). A possible explanation would be that smaller molecules are more likely to be taken up by antigen-presenting cells (APCs) at higher frequency which in turn, will increase the chances of DNA being delivered intracellularly (Foged *et al.*, 2005).



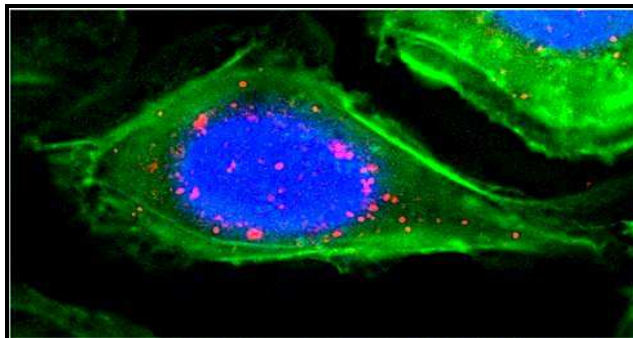


**Figure 5. Nanoparticles in mammalian cells.**

Fluorescence microscopy image above shows cytosolic accumulation through receptor (green) mediated endocytosis of targeted nanoparticles (pink) specifically targeted to a cell-surface antigen. (Image adapted from [www.bindbio.com](http://www.bindbio.com))

Nanoparticles also have the advantage of simplicity of preparation when compared to microparticles (Wendorf *et al.*, 2006). So far, this system has provided a novel delivery tool for naked DNA and an efficient antigen delivery and adjuvant system in the development of DNA and protein-based vaccines (Figure 5) (Akagi *et al.*, 2005). However, there is still the need to understand the role it plays after delivery, host-toxicity effects and also on its efficiency to trigger host-immune responses.

#### 1.6.2.5 Microneedles

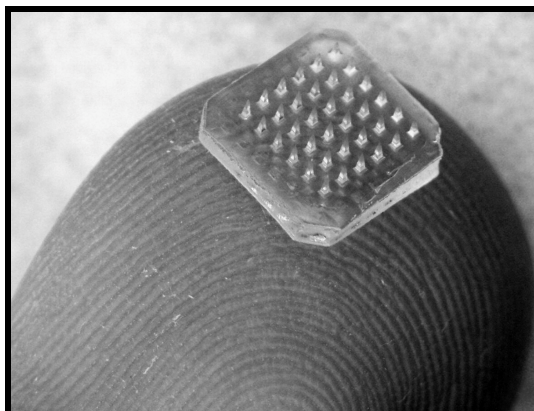


**Figure 6. Microneedle vaccine patch.**

Dissolvable microneedles of 650 microns in length and assembled into an array of 36 needles. (<http://gtresearchnews.gatech.edu/>)

The development of microneedles is mostly to address the pain caused by fine gauge needles used for intradermal administration of antigens (reviewed by Jain *et al.*, 2011) but they have also been used for DNA delivery (Chabri *et al.*, 2004; Gill & Prausnitz, 2007). It is a simple and cost-effective approach which employs

the microelectronics industry for inexpensive mass production. Microneedles typically measure hundreds of microns in lengths and are used as multi-needle arrays to pierce the skin in order to deposit antigen or DNA within the skin (Figure 6). It is a recent technology incorporating biodegradable polymer microneedles. Chabri *et al.* (2004) and Lee *et al.* (2008) have applied this method for transdermal DNA and protein delivery. Such microneedles have been shown to dissolve within the skin for bolus or prolonged delivery without leaving any biohazardous sharp medical waste. Other studies have focused on developing more versatile structures of the needle for greater future utilization (Wu *et al.*, 2007; Bal *et al.*, 2010). Although the system shows much promise, especially in the ease of vaccine administration, research is needed, especially on its efficiency to elicit acquired immunity in the host.

#### 1.6.2.6 Viral vectors

Development of a variety of expression strategies has made it possible to deliver foreign genes *in vivo* using viral vectors. Alphaviruses are arthropod-borne togaviruses with a positive-polarity and single-stranded RNA genome that can replicate in a large number of animal hosts. They have been reported to induce cellular immunity. For example, an attenuated Venezuelan equine encephalitis virus, a member of the alphavirus family, has been used to deliver and express the matrix/capsid (MA/CA) coding region of the HIV-1 *gag* gene into baby hamster kidney cells (Caley *et al.*, 1997). The virus managed to replicate rapidly *in vitro* and massive expression of the MA/CA protein was detected. When injected subcutaneously into BALB/c mice, it was observed to stimulate a comprehensive humoral and cellular immune response (Caley *et al.*, 1997). However, in another study using another family of alphavirus, Sindbis virus, as the vector to deliver DNA into mammalian cell lines, only short-term transgene expression was obtained (Lundstrom, 1997). Alphaviruses were also reported to induce apoptosis and had a cytotoxic effect in infected cells (reviewed in Lundstrom, 2005). In another study, a replicating attenuated adenovirus vector has been shown to generate strong immune responses against encoded heterologous antigens (Guroff, 2007). However, its rapid replicating nature in the host has raised general concerns about its safety. This and other factors such as their instability, cost and difficulty in production has slowed down the practicality of viruses as DNA delivery vectors (Seow & Wood, 2009). Further

studies are needed to engineer an attenuated viral vector with controllable replication and mutation to disable expression of potentially deleterious proteins.

#### 1.6.2.7 Bactofection

Bactofection is the technique of using bacteria for direct gene transfer into target organisms, organs or tissues. It has been the most studied method of delivery of DNA vaccines since the first breakthrough 30 years ago by Schaffner (1980). This bacteria-mediated transfer of plasmid DNA (bactofection) into mammalian cells is a potent approach to expressing plasmid-encoded heterologous proteins in a large set of different cell types, including phagocytic and non-phagocytic mammalian cells. Transfected bacterial strains deliver antigenic genes localized on plasmids into the cells, where these genes can be expressed intracellularly (Liu, 2011).

Some of the problem of using viral vectors could be overcome by using attenuated intracellular bacteria. Besides being much more stable (controlled attenuation), intracellular bacteria carrying the DNA undergo phagocytosis by APCs (antigen presenting cells) as during normal infection. Plasmid DNA is delivered into the host cell phagosome or cytosol. The released DNA is then transcribed, resulting in expression of encoded antigens which will induce host-adaptive immunity (reviewed by Weiss & Chakraborty, 2001). Table 2 below shows some example of bactofection models with attenuated strains of pathogenic bacteria that have been reported in recent years.

**Table 2. Bactofection using attenuated strains of pathogenic bacteria.**

Vector	Target gene	Disease	Model	Reference
<i>Listeria monocytogenes</i>	IL-12	<i>L. major</i> -infection	House mouse ( <i>Mus musculus</i> )	Shen <i>et al.</i> , 2004
<i>Salmonella typhimurium</i>	CD40L	B-cell lymphoma	<i>Mus musculus</i>	Urashima <i>et al.</i> , 2000
<i>S. typhimurium</i>	VEGFR-2 (FLK-1)	Various carcinomas	<i>Mus musculus</i>	Niethammer <i>et al.</i> , 2002
<i>L. monocytogenes</i>	CFTR	Cystic fibrosis	CHO-K1 cells	Krusch <i>et al.</i> , 2002
<i>S. typhimurium</i>	IFN- $\gamma$	Immunodeficiency	<i>Mus musculus</i>	Paglia <i>et al.</i> , 2000
<i>Salmonella choleraesuis</i>	Thrombospondin- 1	Melanoma	<i>Mus musculus</i>	Lee <i>et al.</i> , 2005

Table based on Pálffy *et al.* (2006).

#### 1.6.2.7.1 Adhesion, invasion and intracellular survival

One vital criterion for use of attenuated bacteria as a live-mobile carrier is their ability to adhere and to invade targeted mammalian cells in order to deliver plasmid DNA intracellularly. There is added value when the strains manage to survive or even replicate intracellularly and are able to control the release of the plasmid DNA at the appropriate time or place in order for the immunogenic protein to be expressed accordingly.

Various studies have shown attenuated strains of invasive bacteria such as *Shigella flexneri* (Sizemore *et al.*, 1995; Sizemore *et al.*, 1997), *Salmonella typhimurium* (Darji *et al.*, 1997; Paglia *et al.*, 1998), and *Listeria monocytogenes* (Dietrich *et al.*, 1998) being used for the delivery of plasmid DNA. For *S. typhimurium*, the bacteria are lysed within the phagosome, releasing plasmid DNA from this compartment into the cytoplasm via an unknown mechanism. Vaccination of mice with attenuated *S. typhimurium* transformed

with plasmid DNA encoding listeriolysin (a virulence factor of *L. monocytogenes*) induced specific antibody as well as T-cell responses to listeriolysin (Darji *et al.*, 1997). In a separate study, fluorescent dendritic cells (DC) were demonstrated after oral administration of *S. typhimurium* harboring plasmid DNA encoding green fluorescent protein. These data provided evidence that this delivery system could target relevant immune cells, leading to efficient induction of an immune response (Paglia *et al.*, 1998). For *Shigella* infection, after phagocytosis and lysis within host cells, antigenic material encoded by a eukaryotic expression plasmid is released directly into the cytoplasm. Immunization using attenuated *S. flexneri* transformed with a bacterial plasmid encoding  $\beta$ -gal led to induction of a strong antigen-specific humoral and cellular response (Sizemore *et al.*, 1997). In a separate study, it was shown that mice vaccinated with attenuated *Shigella* vaccine harbouring measles virus genes induced a vigorous measles virus antigen-specific response (Fennelly *et al.*, 1999). An attenuated *L. monocytogenes* has also been used for delivery of eukaryotic expression vectors to the cytoplasm of murine macrophage cell lines (Dietrich *et al.*, 1998). Whereas immunization with naked DNA has not been reported to lead to genomic integration with a significant frequency, delivery of DNA by *L. monocytogenes* can be a trigger for chromosomal integration in mammalian cells raising safety concerns with this system (Dietrich *et al.*, 1998; Courvalin *et al.*, 1995).

There seem to be agreement in the literature on the basic mechanism of the bactofection model system for the delivery of DNA vaccine, as illustrated in Figure 7 (Grillot-Courvalin *et al.*, 2002; Loessner *et al.*, 2008). Bactofection can be modelled with, for example, *Salmonella* or *Listeria*. After infecting the host, bacteria are normally taken up by the antigen presenting cells (APCs) via phagocytosis. However, in the case of *L. monocytogenes*, some of them can escape from the phagosome by the action of pore-forming listeriolysin O whereas *Salmonella* is still trapped in the phagosome. *L. monocytogenes* proliferates in the cell cytosol and proteins secreted by the bacteria are degraded by the proteosomes, enter the endoplasmic reticulum and are presented to the immune system preferentially by MHC class I molecules. Cytosolic *L. monocytogenes* causes polymerization of actin filaments which mediate its intracellular movement and direct transfer to neighboring host cells without exiting the cells (Figure 7). A portion of the *L. monocytogenes* population remains in the phagosome and shares the life-cycle of *Salmonella*, which proliferates in the

phagosome. Proteins secreted by the phagosomal bacteria are trapped and degraded in this compartment and presented on the APC cell surface by MHC class II molecules. At the same time, plasmid DNA carried by both bacteria are delivered into the cytoplasm after bacterial cell lysis in the phagosomal compartment. The plasmid is then transferred to the nucleus and processed for antigen expression. The mechanism of plasmid DNA delivery from the vacuoles to the nucleus, however, is still unknown (Becker & Guzmán, 2008).

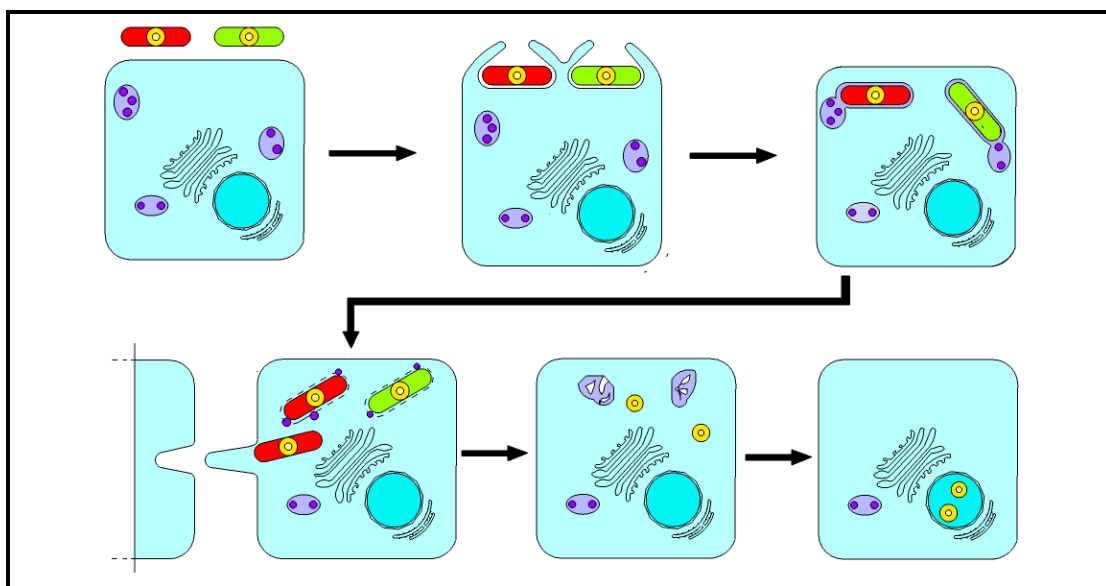


**Figure 7. Bacterofection pathway for DNA vaccine delivery.**

Schematic representation of bacteria-cell delivery process e.g. by *Salmonella* (green) and *Listeria* (red). After cell internalization and phagolysosome fusion, the escape of the bacteria or of their plasmid DNA content from the vacuole into the cytosol results in the transfer of the plasmid (yellow) to the cell nucleus. (Adapted from Grillot-Courvalin & Goussard, 2011).

#### 1.6.2.7.2 Invasion by *P. multocida*

*P. multocida* may also have the potential as a DNA vaccine delivery vector as it has been found intracellularly within a variety of eukaryotic cells. In one study, the pathogen was reported as multiplying intracellularly in liver and spleens of experimentally-infected turkeys in the early stages of infection, before spreading into the blood (Pabs-Garnon & Soltys, 1971). This report was supported by histological observations of liver and spleen from infected chickens and embryos (Ibrahim *et al.*, 2000). Another study showed that two serotype A 3,4 strains of *P. multocida* from turkeys that differed in virulence were able to invade epithelial cell monolayers grown in tissue culture. Both organisms were comparably adherent to turkey kidney cells (Lee *et al.*, 1994). The virulent strain was also able to invade porcine epithelial cells and feline epithelial cells

in cell culture. However, neither strain invaded rabbit epithelial cells (Lee *et al.*, 1994). More recently, the capsule of serotype A strains was found to be the adhesion factor for avian strain A:3 and A:1. These strains are capable of invading and multiplying in chicken embryo fibroblast cells (Al-haj Ali *et al.*, 2004). Association with and invasion of bovine aortic epithelial cell by *P. multocida* serotype B have also been demonstrated (Galdiero *et al.*, 2001). Rabier *et al.* (1997) demonstrated that a group A strain of *P. multocida* was capable of adhering to polarized epithelial MDCK cells and it was present on the apical cell surface and inside the cells near the apical border when analysed by confocal microscopy. Other studies have demonstrated that *P. multocida* serotype A was able to invade HeLa cells (Esslinger *et al.*, 1993, Esslinger *et al.*, 1994, Pruijboom *et al.*, 1996) and uptake of *P. multocida* B:2 into mouse a macrophage cell line has also been reported (Tabatabaei, 2000). In his study, an *aroA* mutant of *P. multocida* B:2 and the wild-type strain were taken up into the mouse macrophage-like cell line and were shown to survive intracellularly for at least 2 h after invasion.

### 1.6.3 Advantages and disadvantages of DNA vaccines

There are several reasons why DNA vaccination might provide important advantages over current vaccines: DNA vaccines mimic the effects of live attenuated vaccines in their ability to induce major histocompatibility complex (MHC) class I-restricted CD8<sup>+</sup> T-cell responses important for cell-mediated immune response. This may be advantageous compared with conventional protein-based vaccines, while removing some of the safety concerns associated with live vaccines; DNA vaccines can be manufactured in a relatively cost-effective manner and stored with relative ease, eliminating the need for a cold chain to maintain the stability of a vaccine during its distribution.

Concurrently, DNA vaccines do have some possible disadvantages. One concern is that there is a potential for integration of the delivered DNA into the host chromosome. Plasmid DNA-based vectors sometimes contain nucleic acid sequences from oncogenic viruses, and the possibility for chromosomal integration exists. A second concern of DNA vaccination is the possibility of generating antibodies to DNA. Immune responses to DNA occur in autoimmune diseases, such as systemic lupus erythematosus, and the potential exists that infection of bacterial DNA could induce an immune response that might cross-

react with host DNA (Watts & Kennedy, 1999). It has been reported that antibodies to DNA have been observed following immunisation of mice with bacterial DNA (Gilkeson *et al.*, 1993; Griffiths, 1995). However, this still represents a theoretical possibility that requires more attention. A third concern is the effect that long-term expression of injected DNA in muscle cells may have on immune responses to subsequent vaccination with a different DNA, and whether the immune responses to protective epitopes associated with this second immunisation will be compromised. It has also been reported that DNA vaccination strategies for non-protein based antigens, such as bacterial polysaccharides and lipids have been unsuccessful (Watts & Kennedy, 1999).

## 1.7 Immunosuppression by *Pasteurella multocida* B:2

Hornef *et al.* (2002) reported that different types of bacterial pathogens have adopted different strategies to interfere with host innate and adaptive immune mechanisms. Different bacterial components and products play different roles in modulating host immune reactions, most of them stimulatory but a minority are inhibitory (Schwab, 1975). To study the modulatory effects of bacterial pathogens on immune response, one can execute *in vitro* experiments such as a lymphocyte stimulation assay (also called antigen-stimulated lymphocyte proliferation or lymphoblastogenesis assays). The assay will assist in investigating stimulation and proliferation responses of mononuclear cells after treatment with different components of the bacteria. In the body, stimulation of primed (activated) lymphocytes occurs in lymphoid tissues in response to antigen presented to them. Yet, the ability of isolated lymphocytes (such as peripheral blood mononuclear cells, PBMC) to be stimulated (expressed as proliferation and/or cytokine secretion) when cultured in the presence of the antigen has been exploited as a tool to assess cellular responses *in vitro*.

The proliferative response of activated PBMC to antigen has been extensively used to study cellular immunity, as PBMC from infected or immune hosts will proliferate in response to antigen obtained from the organism that they have been exposed too. In a study on HS- and shipping fever-related *Pasteurella*, it was reported that PBMC from HS-immunised cattle exhibited a higher stimulation index when incubated with antigen preparations from homologous strains than with those from a heterologous, shipping fever strain. In contrast,



PBMC from cattle immunised with the shipping fever strain of *P. multocida* exhibited a higher stimulation index when incubated with an antigen preparation from the homologous strain than with antigen preparation from heterologous HS strains (Maheswaran & Thies, 1979).

Previous study by Ataei (2007) observed that *P. multocida* B:2 appeared to suppress proliferation of the lymphocyte population *in vivo* and *in vitro*. His initial observation on *P. multocida* B:2 suppression of lymphocyte proliferation in response to concanavalin A (ConA) was shown when PBMC were sampled from vaccinated (i.n.) (with a live-attenuated *aroA*<sup>-</sup> *P. multocida* strain) and non-vaccinated calves that had subsequently been challenged i.m. with a wild-type, virulent *P. multocida* B:2 strain. Figure 8 below shows a bar graph, adapted from his thesis, demonstrating *in vivo* suppression of lymphocyte proliferation in response to ConA.

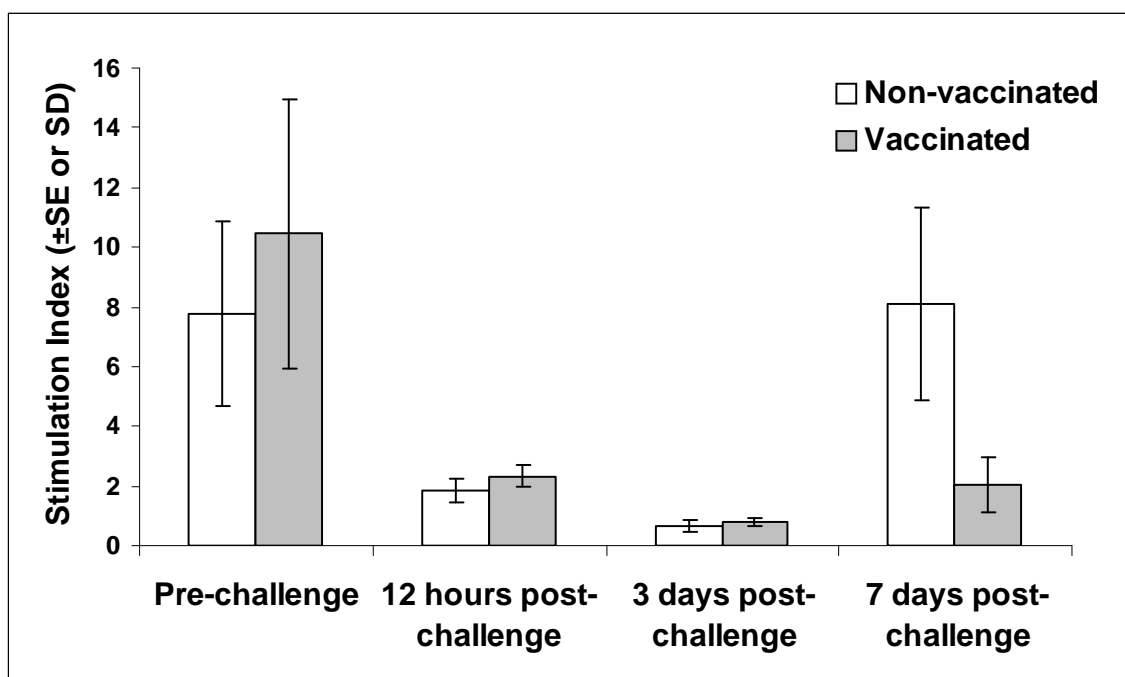


**Figure 8. Observation from infected calves (Ataei, 2007).**

Proliferative *in vitro* response to ConA of lymphocytes obtained from calves after challenge with *P. multocida* B:2 85020 (wild-type).

PBMC ( $2 \times 10^5$  cells/well) were prepared from vaccinated and non-vaccinated groups of calves on the day of challenge and at different times after challenge with virulent *P. multocida* B:2 85020. In vaccinated group, calves were vaccinated once with  $10^8$  cfu of *P. multocida* B:2 JRMT12 and all of the animals were challenged after 28 days.  $1 \mu\text{g/well}$  of concanavalin A (ConA) was added to the cells. All of the treated cells along with untreated cells as controls were incubated at  $37^\circ\text{C}$ . On the 3<sup>rd</sup> day, cells were pulsed with [methyl- $^3\text{H}$ ] thymidine and incubated for 18 h and the amount of incorporated thymidine was measured by scintillation. Proliferation of cells was detected by the level of thymidine incorporation and is shown as bars, which represent the stimulation index (SI). SI is the ratio of treated (ConA added) compared to untreated cells.

*P. multocida* B:2 suppression of lymphocyte proliferation *ex vivo* in response to ConA was clearly demonstrated from 12 hours post-challenge and suppression continued until at least day 3 post-challenge. At this time, there was little difference in proliferation levels when comparing vaccinated and non-vaccinated animals. Immunosuppression by *P. multocida* B:2 was still observed after 7 days post-challenge in PBMC from vaccinated animals while suppression was no longer evident in PBMC from non-vaccinated animals. The study was continued to further assess this immunosuppressive effect of a cell-free extract (CFE) of *P. multocida* B:2 or PBMC *in vitro*. Figure 9 (Ataei, 2007) shows that the proliferative response of calf PBMC to ConA was markedly suppressed when the cells were incubated with the optimal concentration (10  $\mu\text{g}/\text{well}$ ) of *P. multocida* B:2 CFE for one hour before adding the ConA. Incubation of PBMC with CFE alone (10  $\mu\text{g}/\text{well}$ ) showed no stimulatory effect on lymphocyte proliferation. The concentration of CFE and the 1  $\mu\text{g}/\text{well}$  concentration of ConA, together with incubation of PBMC for 1 h with extract before addition of ConA, were optimal conditions to demonstrate this suppressive effect.

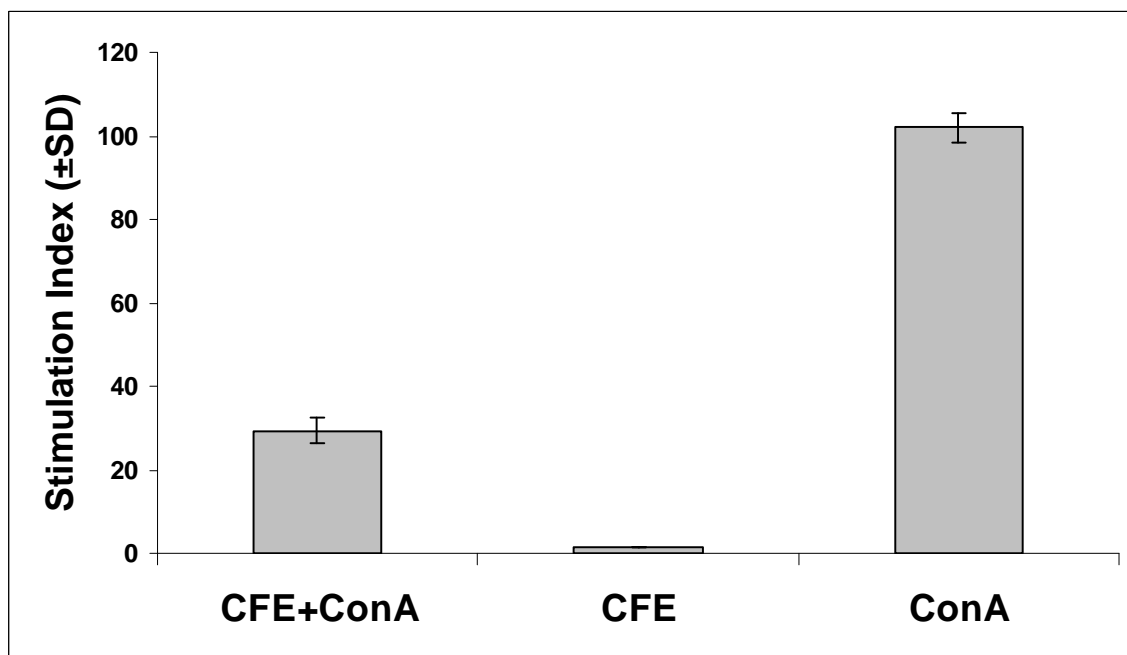


**Figure 9. Immunosuppressive effect of *P. multocida* B:2 cell-free extract on PBMC *in vitro* (Ataei, 2007).**

The effect of CFE of *P. multocida* B:2 on PBMC were obtained from normal calves and their proliferative response to ConA, was determined.

Bars represent the proliferative response of normal calf PBMC ( $2 \times 10^5$  cells/well) after incubation for 1 h with 10  $\mu\text{g}/\text{well}$  CFE before addition of 1  $\mu\text{g}/\text{well}$  ConA. Proliferation was detected by measurement of thymidine incorporation and expressed as stimulation index, which shows the ratio of incorporation in treated (CFE was added) compared to untreated cells.

The study was then continued to analyze the suppressive effect caused by different component of *P. multocida* B:2. It was determined that the active part of the suppressive agent was likely to be protein, because an outer membrane protein preparation of the bacteria markedly suppressed the proliferative response of PBMC to ConA. The investigation was extended using fluorescence-activated cell sorter (FACS) analysis to assess the specific effect of suppression of proliferation, on the different populations in the PBMC: B cell and T cell sub-populations (CD4<sup>+</sup>, CD8<sup>+</sup> and  $\gamma\delta^+$ ). In his conclusion, Ataei (2007) suggested that the *in vitro* experiments demonstrated that *P. multocida* B:2 contains a component(s) with the potential to inhibit the proliferative response of CD4<sup>+</sup> and CD8<sup>+</sup> -T cells. This observation is of concern and therefore, was subjected to further investigation in parallel with the development of *P. multocida* B:2 as a delivery vehicle for DNA vaccines.

## 1.8 Objectives of research and experimental plan

The long-term goal of the laboratory was to further characterize and develop the attenuated *P. multocida* B:2 *aroA* derivative created by Tabatabaei *et al.* (Tabatabaei, 2000; Tabatabaei *et al.*, 2002), to determine if it can, in addition to raising a protective immune response against *P. multocida* challenge, also raise an immune response to heterologous antigens expressed from a plasmid via a eukaryotic promoter. In order to achieve this eventual goal, several understandings need to be developed. These have been structured in the current study which aims;

- a) To compare the capacity of the wild-type and vaccine strain of *P. multocida* to invade and survive within the mammalian cells lines.
- b) To develop a suitable *Pasteurella* dual-expression plasmid that enables protein expression in both prokaryote and eukaryote.
- c) To demonstrate a bactofection model system of *Pasteurella* for infection of mammalian cells.
- d) To confirm and extend the observations concerned with the possible immunosuppressive effects of *P. multocida*.

## **2. MATERIALS AND METHODS**

### **2.1 General bacteriological procedures**

#### **2.1.1 Sources of bacteria**

Bacterial strains used in this study are listed in Table 3. All bacterial strains were available from culture collections within the Division of Infection and Immunity, University of Glasgow or were available commercially.

#### **2.1.2 Plasmids**

Plasmids used in this study are listed in Table 4.

#### **2.1.3 Bacterial growth and storage media**

The compositions of the following media are given in Appendix 1. Luria Bertani (LB) broth, Luria Bertani (LB) agar, Brain Heart Infusion (BHI) broth, BHI Agar, SOC, Terrific broth and Terrific agar. All media were sterilised by autoclaving at 15 p.s.i. (121 °C) for 15 min except where stated. Heat-labile ingredients such as antibiotics were sterilised by filtration through a sterile 0.22 µm filter (Sartorius, UK). Glassware was sterilised by heating to 160 °C for 2 h. All strains were stored frozen in 50% (v/v) glycerol at -80 °C in BHI broth for *Pasteurella* strains or LB broth for *Escherichia coli* strains.

#### **2.1.4 Growth of *E. coli***

*E. coli* strains were subcultured on LB agar medium and incubated at 37 °C overnight. Liquid cultures of the strains were grown in LB broth media in Universal containers overnight on an orbital shaker at 180-200 rpm at 37 °C. When required, antibiotic-resistant strains were grown on agar or in liquid media containing the appropriate antibiotic concentration.

**Table 3. List of bacterial strains used in this study.**

Strain	Relevant strain characteristics	Source
<i>Pasteurella multocida</i> serotype B:2 85020	Wild-type, isolated from a case of bovine haemorrhagic septicaemia in Sri Lanka	Institute of Infection, Immunity & Inflammation, University of Glasgow (Prof. John G. Coote)
<i>P. multocida</i> serotype B:2 JRMT12	AroA <sup>-</sup> derivative of 85020 strain	Institute of Infection, Immunity & Inflammation, University of Glasgow (Prof. John G. Coote)
<i>Mannheimia haemolytica</i> serotype A1	Wild-type, isolated from a case of bovine pneumonia in Glasgow	Institute of Infection, Immunity & Inflammation, University of Glasgow (Dr. Robert L. Davies)
<i>P. multocida</i> serotype A3 (MRI, 671/90)	Wild-type, isolated from bovine pneumonia in Scotland	Moredun Research Institute, Edinburgh (Dr. J. Christopher Hodgson)
<i>P. multocida</i> serotype B:2 JRMT12 Sm <sup>r</sup>	Spontaneous streptomycin resistant (Sm <sup>r</sup> ) derivative of JRMT12 strain	This study
<i>E. coli</i> XL-1 BLUE MRF' (Minus Restriction) [restriction minus (McrA <sup>-</sup> , McrCB <sup>-</sup> , McrF <sup>-</sup> , Mrr <sup>-</sup> , HsdR <sup>-</sup> ) derivative of the XL1-Blue strain]	$\Delta(mcrA)183 \Delta(mcrCB-hsdSMR-mrr)173 endA1 supE44 thi-1 recA1 gyrA96 relA1 lac [F' proAB lacIqZ\Delta M15 Tn10 (Tc^r)]$	Stratagene, Amersham Biosciences, UK
<i>E. coli</i> DH5 $\alpha$	F'/endA1 hsdR17 (r <sub>k</sub> <sup>-</sup> m <sub>k</sub> <sup>-</sup> ) supE44 thi <sup>-1</sup> recA1 gyrA (Nal <sup>r</sup> ) relA1 $\Delta(lacIZYA-argF)U169 deoR (F80dlacD(lacZ)M15)$	Invitrogen, UK
<i>E. coli</i> SM10 $\lambda$ pir	recA::RP4-2-Tc::Mu, $\lambda$ pir, R6K, thi, thr, leu, tonA, lacY, supE	Institute of Infection, Immunity & Inflammation, University of Glasgow (Prof. John G. Coote)

**Table 4. List of plasmids used in this study.**

Plasmid	Relevant characteristics	Origin
pAKA16	<i>P. multocida</i> shuttle vector (Ap <sup>R</sup> )	Azad <i>et al.</i> (1994)
pAKA19	<i>P. multocida</i> suicide vector (Ap <sup>R</sup> )	Azad <i>et al.</i> (1994)
pGEM-T-EASY	<i>E. coli</i> cloning vector (Ap <sup>R</sup> )	Promega, UK
pCMV-Script	<i>E. coli</i> eukaryotic expression vector (Km <sup>R</sup> )	Stratagene, UK
pEGFP-N1	Eukaryotic expression vector with green fluorescent protein (GFP) reporter gene (Km <sup>R</sup> )	CLONTECH Laboratories Inc., USA
pMK-Express	<i>Pasteurellaceae</i> prokaryotic expression vector with GFP reporter gene (Km <sup>R</sup> )	Bossé <i>et al.</i> (2009)
pMC-Express	<i>Pasteurellaceae</i> expression vector with GFP reporter gene (Cm <sup>R</sup> )	Bossé <i>et al.</i> (2009)
pDsRed-Monomer	<i>E. coli</i> expression vector with red fluorescent protein (RFP) gene (Ap <sup>R</sup> )	CLONTECH Laboratories Inc., USA
pMK-Red	pMK-Express with GFP gene replaced by RFP gene from pDsRed-Monomer vector	This study
pSRG	Dual expression vector modified from pEGFP-N1. Containing RFP gene directed by a prokaryotic promoter and GFP gene directed by a eukaryotic promoter.	This study

Ap<sup>R</sup> : Ampicillin resistanceKm<sup>R</sup> : Kanamycin resistanceCm<sup>R</sup> : Chloramphenicol resistance

### 2.1.5 Growth of *Pasteurella* species

*P. multocida* B:2, *P. multocida* A:3 and *M. (Pasteurella) haemolytica* A:1 strains from the frozen glycerol stocks were subcultured routinely on BHI agar medium. Liquid cultures of the strains were grown in the BHI broth medium in Universal containers overnight on an orbital shaker at 180-200 rpm at 37°C. Where necessary, antibiotic-resistant strains were grown on agar or in liquid media containing the appropriate antibiotic concentration.

### 2.1.6 Isolation of spontaneous streptomycin-resistant strains

*P. multocida* 85020 and JRMT12 were grown overnight (to approx.  $10^{12}$  cells/ml) in BHI broth with shaking at 37°C. A 100 µl portion of each culture was spread on BHI agar supplemented with streptomycin (100 µg/ml). The seeded plates were allowed to dry and then incubated at 37°C for 48-72 h. Streptomycin resistant colonies were picked, and their phenotype confirmed by overnight subculture on agar medium containing the same concentration of streptomycin.

## 2.2 Antibiotics

Antibiotics used in this study were: ampicillin (Ap), chloramphenicol (Cm), kanamycin (Km), streptomycin (Sm), gentamicin (Gm) polymyxin B (Pm) and neomycin (Nm). All antibiotics were obtained from Sigma, UK.

Sterile antibiotic solution was added to broth or agar media after the media had been autoclaved and then cooled to 50°C. The concentrations of the antibiotics used in selective media were (µg/ml): Ap (50), Cm (3.5, 12.5), Km (50), Sm (100), Gm (50-350), Pm (50-350) and Nm (50).

## 2.3 Plasmid DNA extraction

Plasmid DNA was isolated according to the QIAprep<sup>®</sup> Miniprep Purification System (Qiagen) (Appendix 3) procedure, based on alkaline lysis of bacterial cells followed by selective adsorption of plasmid DNA onto a silica gel membrane in high-salt buffer and subsequent elution in low-salt buffer. This procedure is a modification of the alkaline lysis method of Birnboim & Doly (1979). Bacteria are lysed under alkaline conditions, and the lysate is subsequently neutralised and adjusted to high-salt binding conditions in one step, and the lysate cleared by

centrifugation. The plasmid DNA, from the resulting supernatant is adsorbed on to the silica-gel membrane of QIAprep columns and RNA, cellular proteins and metabolites are not retained on the membrane upon washing but are found in the flow-through. After washing with washing buffer to remove salts, high-quality plasmid DNA is then eluted from the QIAprep column with distilled water. The purified plasmid DNA is stored at  $-20^{\circ}\text{C}$ .

## **2.4 Restriction endonuclease digestion of DNA**

All restriction endonuclease enzymes were purchased from Promega or New England Biolabs (NEB, UK) and used according to manufacturer's instructions. Restriction enzyme digestion was routinely performed in a 20  $\mu\text{l}$  volume containing approximately 2  $\mu\text{g}$  of DNA, 8 to 20 units of enzyme (2  $\mu\text{l}$ ) and reaction buffer diluted to 1 fold. Sterile distilled water, reaction buffer (10x), DNA solution and restriction enzyme were added sequentially to a sterile centrifuge tube placed on ice and mixed gently by tapping the tube. The reaction mixtures were incubated at  $37^{\circ}\text{C}$  for 4 h to 24 h and analyzed by gel electrophoresis in 0.7% (w/v) agarose.

## **2.5 Agarose gel electrophoresis**

### **2.5.1 Sample preparation**

The sample DNA (5-30  $\mu\text{l}$ ) was mixed with 6x loading buffer (Appendix 2) in a ratio 5:1 prior to loading into the wells. The mixture was centrifuged briefly to remove bubbles before loading onto the gel. Two different DNA ladders were used, depending on the topological forms and the fragment sizes of DNA. For sizing the digested or linearised DNA fragments above 1 kb, 1 kb DNA Ladder (NEB, UK) was used and for linearised DNA fragments below 1 kb, 100 bp DNA Ladder (NEB, UK) was used (Appendix 2).

### **2.5.2 Gel preparation**

Agarose (Roche, UK) was suspended in 1x Tris-borate-EDTA (TBE) buffer (Appendix 2) at a suitable concentration and heated until the agarose was completely dissolved. The solution was allowed to cool and SybrSafe (Invitrogen, UK) was added to a final concentration of 0.1  $\mu\text{g}/\text{ml}$ . A gel tray was prepared and the gel was cast to the desired thickness. Upon setting, the gel was



immersed in 1x TBE buffer in a horizontal multi-sub midi-electrophoresis tank (Wolf Laboratories Limited, UK).

### **2.5.3 Electrophoresis**

Electrophoresis was carried out at 80 V for 75 min using a Power Pac Basic (Bio-Rad, UK) that is able to provide constant voltage throughout the running time.

### **2.5.4 Visualisation of DNA**

An UV transilluminator (UVIpro, UVItec) was used to visualise the SybrSafe-stained DNA. Images were stored electronically using the provided software, UVtec (UVItec). Images were printed using a video graphic printer (UP-860, Sony, Japan). Electronic images were edited using Adobe Photosuite CS (Adobe Suite, USA).

### **2.5.5 Purification of DNA from agarose gels**

QIAquick Gel Extraction kit (Qiagen, UK) (Appendix 3) was used according to the manufacturer's instructions. The DNA band of interest was excised from a SybrSafe-stained agarose gel with a sharp scalpel under long-wave UV light. The size of the gel slice was minimised by ensuring there was little extra agarose around a band. The gel slice was weighed in a colourless tube and 3 volumes of buffer QG were added to 1 volume of gel (100 mg  $\approx$  100  $\mu$ l). The tubes were incubated at 50°C for 10 min or until the gel slice was completely dissolved. The tubes were mixed by vortexing every 2-3 min during the incubation to help the gel to dissolve. The colour of the mixture should be yellow (similar to the buffer QG without dissolved agarose) after the gel slice was completely dissolved. If the colour of the mixture was violet, 10  $\mu$ l of 3M-sodium acetate, pH 5.0 was added and then the colour turned to yellow. The yellow colour indicates a pH  $\leq$ 7.5 where the adsorption of DNA to the QIAquick membrane in a later step is most efficient.

The dissolved gel samples, maximum volumes of 800  $\mu$ l, were applied to the QIAquick column to bind DNA and then centrifuged at 13 000 x g in a 1.5 ml centrifuge tube using a tabletop microcentrifuge (Biofuge, Heraeus, Germany) for 1 min. Sample volumes of more than 800  $\mu$ l were simply loaded in 800  $\mu$ l batches and recentrifuged. The flow-through was discarded and the QIAquick

column placed back in the same collection tube. To remove all traces of agarose, 0.5 ml of buffer QG was added to QIAquick column and centrifuged at 13 000 x g for 1 min. To wash the column, 0.75 ml of buffer PE was added to QIAquick column and then centrifuged at 13 000 x g for 1 min. The flow-through was discarded and, to remove completely the residual ethanol from buffer PE, the QIAquick column was centrifuged for an additional 1 min at 13 000 x g. The QIAquick column was then placed into a clean 1.5 ml centrifuge tube and 50 µl buffer EB added to the centre of the QIAquick membrane followed by centrifugation at 13 000 x g for 1 min to elute DNA. The average eluate volume was 48 µl from 50 µl elution buffer volume, and the maximum elution efficiency was achieved between pH 7.0 and 8.5.

## 2.6 Estimation of DNA concentration

DNA concentration was measured using NanoDrop™ 1000 (Thermo Scientific, UK). A 1-2 µl volume was placed at the measuring point before the DNA concentration was estimated by measuring the absorbance at 260 nm. The software was then used to calculate the DNA concentration using the Beer-Lambert equation which is modified to use an extinction coefficient with units of ng-cm/µl. This extinction coefficient gives a manipulated equation:

$$c = (A * e)/b$$

Where c is the nucleic acid concentration in ng/µl, A is the absorbance in AU, e is the wavelength-dependent extinction coefficient in ng-cm/µl and b is the path length in cm. The generally accepted extinction coefficients for DNA are 50 ng-cm/µl for double-stranded DNA and 33 ng-cm/µl for single-stranded DNA.

Alternatively, the approximate concentration of DNA fragments was determined visually on agarose gel, by comparison of their staining intensities with those of known quantities of marker DNA of a similar size.

## 2.7 Concentration of DNA

DNA that had gone through the gel extraction procedure was cleaned and concentrated before further manipulation. Qiagen Min-Elute (Appendix 3) kit with a pre-chilled collection column was used in this case. A three-fold volume of binding buffer (ER) was mixed with the sample before addition to the silica-

gel column followed by centrifugation at 13 000 x g for 1 min. The column was then washed with wash buffer (PB) and DNA was eluted out with an elution buffer (EB) at a lower volume to increase the DNA concentration.

## 2.8 Polymerase chain reaction (PCR)

The PCR conditions were optimised, where necessary, according to the orthogonal array method described by Cobb & Clarkson (1994). The annealing and elongation thermal parameters were then adjusted to obtain optimal conditions. A Hybaid thermal cycler was used for all reactions. The products of the PCR were stored at -20°C or used immediately.

### 2.8.1 PCR primers

All primers were designed manually and assessed by online software such as Primer 3. During primer design, care was taken to avoid potential internal secondary structure and where possible a GC clamp was engineered at the 3' end of the primer. Additionally, primers were also checked for sequence overlapping, possible dimerisation and compatibility of melting temperature ( $T_m$ ) between paired primers.  $T_m$  values were calculated according to the equation:

$$T_m (\text{°C}) = 4 (G+C) + 2 (A+T) - 5 \text{°C}$$

Primers (50 nmol, desalted) were obtained from Invitrogen (UK) and resuspended in sterile distilled water to give final concentrations of 100 pmol/μl or 25 pmol/μl for PCR. Table 5 shows the primers used in this study.

### 2.8.2 Components of PCR

The reaction mixture (50 μl) contained (final concentration) 10 mM Tris-HCl (pH 8.4), 50 mM KCl, 3.0 mM MgCl<sub>2</sub>, 0.2 mM of each deoxynucleoside triphosphate (dNTPs) (NEB, UK), 20 μM each primer, 1.0 U of *Taq* DNA polymerase (NEB, UK) and 1-5 μl of template DNA preparation. The PCR assays were performed in 0.5 ml thin-walled dome cap tubes (Thistle Scientific, UK).

Table 5. PCR primers used in this study.

Primer designation	Primer sequence	Comments
Inverse PCR primer Forward 5' to 3' (IPCR F)	GTACC GAGCTC GAATTC ATCG	Amplifies oriP fragment from multiple cloning site (MCS) of pAKA16. Internal restriction sites in the primer, <i>SacI</i> and <i>EcoRI</i>
Inverse PCR primer Reverse 3' to 5' (IPCR R)	ATCCTCTAGAGTCGACCTGCG	Amplifies oriP fragment from MCS of pAKA16. Internal restriction site in the primer, <i>Sall</i>
oriP primer Forward 5' to 3' (oriP F)	CAGNNCTGCGAATGACTTCCTACCG	Amplifies <i>oriP</i> gene from oriP fragment with an additional restriction site, <i>AlwNI</i>
oriP primer Reverse 5' to 3' (oriP R)	ACATGTAACCGCAGGCGTTTTGAC	Amplifies <i>oriP</i> gene from oriP fragment with an additional restriction site, <i>PciI</i>
RED primer Forward 5' to 3' (RED F)	CTACATGTCCGCGCCAACCG	Amplifies sodRED cassette from pMK-RED with an additional restriction site, <i>PciI</i>
RED primer Reverse 5' to 3' (RED R)	GCACATGTTCTACTGGGAG	Amplifies sodRED cassette from pMK-RED with an additional restriction site, <i>PciI</i>

### 2.8.3 Conditions for PCR

The following thermo-cycling parameters were used unless stated otherwise:

Initial activation step at 94°C for 2 min, 30 cycles of denaturation at 94°C for 1 min, annealing between 55°C to 70°C for 1 min, extension at 72°C for 2.5 min with a final extension at 72°C for 10 min. The amplified products were analysed by electrophoresis in a 0.7% (w/v) agarose gel (section 2.5).

### 2.8.4 Inverse PCR (IPCR)

Ochman *et al.* (1988) described IPCR as a method for the rapid *in vitro* amplification of DNA sequences that flank a region of known sequence. The method manipulates PCR, but it has the primers oriented in the reverse direction of the usual orientation. The template for the reverse primers was a restriction fragment that had been ligated upon itself to form a circle.

Plasmid pAKA16 was digested with restriction enzyme *Pst*I and a 1800 bp fragment containing the origin of replication was isolated. The fragment was then ligated (section 2.10.2.2) and, after deactivation of T4 DNA ligase, the mixture was used as a template for PCR (section 2.8.2). The IPCR programme on the thermal-cycler was the same as stated in section 2.8.3.

### 2.8.5 Colony PCR

This type of PCR was normally used to screen bacterial clones for positive transformants with correctly ligated inserts in plasmid products. In colony PCR, the PCR components were the same as in section 2.8.2. However, instead of adding prepared DNA, a small amount of colony growth was added to the mixture. A slight modification of the PCR conditions, whereby an initial step of 95°C for 5 min was used to assist in bacterial cell-wall breakage. After that, cycles were performed as described in 2.8.3.

### 2.8.6 Purification of PCR products

PCR products were purified using QIAquick PCR purification kit (Qiagen, UK) according to manufacturer's instructions (Appendix 3). This protocol was used to purify fragments ranging in size from 100 bp to 10 kb away from primers, nucleotides, polymerase and salts.

Initially, 5 volumes of buffer PB were added to 1 volume of the PCR sample and mixed. The sample was then applied to the QIAquick column to bind DNA, and this was centrifuged on a tabletop microcentrifuge (Biofuge, Heraeus, Germany) for 1 min at 13 000 x g. The flow-through was discarded and the QIAquick column returned to the same tube. Buffer PE (0.75 ml) was then added to the column to wash the column by centrifugation at 13 000 x g for 1 min. The flow-through was again discarded and the column was re-centrifuged at the same speed for 1 min. This was done to completely remove residual ethanol from the column. The column was then placed in a clean 1.5 ml centrifuge tube and 30-50 µl of buffer EB was added to the centre of the column membrane. The column was left for 1 min and then centrifuged again as in previous steps to finally elute DNA. PCR products were used immediately or stored at -20°C.

## 2.9 DNA sequencing

DNA was purified with the relevant cleaning kit (eg: plasmid, PCR product). The sample of DNA and appropriate concentrations of primers were sent to The Sequencing Unit at the University of Dundee to perform DNA sequencing. A MegaBACE1000 (96 capillary) sequencer, which used Big Dye (Applied Biosystems) and ET-Dye Terminator (Amersham Bioscience) chemistries, was employed based on the dideoxy method developed by Sanger *et al.* (1977). Each dideoxy nucleotide contained a specific fluorescent dye that could be excited by a laser. The signals were then collected and analysed by specific software. A coloured electropherogram was produced. The data were downloaded and saved on to a CD. For data analysis, BioEdit (version 7.0.9.0) software was utilised. Preparations of clean template DNA produced a read of around 700 bases, including 400-700 bases of accurate sequence. The length of accurate sequence was primarily determined by the quality of the template DNA and the efficiency of primer annealing.

## 2.10 Statistical analysis

The means, standard deviation and standard error values of results data were calculated in Microsoft Excel when needed. Student's t-test was also applied on associated data.

## 2.11 Sequence analysis tools (bioinformatics)

Two primary sequence databases; GenBank, which is maintained by the National Centre for Biotechnology Information (NCBI) and the Nucleotide Sequence Database maintained by the European Molecular Biology Laboratory (EMBL) were used to annotate and highlight the important properties of the raw sequence data. ENTREZ, a WWW-based data retrieval tool (NCBI), was employed to search multiple biological databases and retrieve relevant information including nucleotide and whole genomes. Entrez can be accessed via the NCBI web site at the following URL: <http://www.ncbi.nlm.nih.gov/Entrez/>.

Sequence similarity searches of databases were performed to extract the similarities using Basic Local (Linear) Alignment Search Tool (BLAST) and FASTA programs. Information about these extracted sequences can be used to predict the structure or function of the query sequence. BLAST utilizes statistical theory to produce bit score and expert value (E-value) for each alignment pair (query to hit). The bit score indicates how good the alignment is; the higher the score, the better the alignment. The E-value indicates the statistical significance of a used pairwise alignment and reveals the size of the database and the scoring system. The lower the E-value, the more significant the hit. A sequence alignment that has E-value of 0.05 means that this similarity has a 5 in 100 (1 in 20) chance of occurring by chance alone. The  $p$  value of a similarity score is the high probability of obtaining the score in a chance similarity between two unrelated sequences of similar composition. Low  $p$  value corresponds to significant matches that are likely to have a real biological significance. In general, the score is calculated by an equation that considers identical or similar residues and any gaps in the aligned sequences using BLOSUM62 to assign a score for aligning any possible pair of residues.

## 2.12 Cloning

### 2.12.1 PCR product cloning

#### 2.12.1.1 Cloning into pGEM-T EASY™ plasmid

The pGEM-T EASY™ plasmid is a linearized plasmid DNA with a single 3'-terminal thymidine at both ends. The T-overhangs at the insertion site increase the

efficiency of ligation of purified PCR products by preventing recircularization of the plasmid and providing a compatible overhang for PCR products generated by thermostable polymerases. The ligation and transformation procedures were performed according to the manufacturer's instructions (Appendix 3).

## 2.12.2 Standard cloning protocol

### 2.12.2.1 DNA preparation

Plasmid and insert DNA were subjected to restriction enzyme digestion to obtain complementary cohesive overhangs and the resultant fragments were gel-purified (section 2.5.5). DNA concentrations were estimated according to section 2.6 and ratios determined as follows:

$$\text{ng of insert} = [(\text{ng plasmid} \times \text{kb size of insert}) / \text{kb size of plasmid}]$$

$$\times [\text{molar ratio of Insert/Plasmid}]$$

Insert: Plasmid ratios of 2:1 and 3:1 were commonly used.

### 2.12.2.2 Ligation strategies

Ligation reactions were performed in a total volume of 10  $\mu\text{l}$  using 3 units of T4 DNA ligase and 2x ligase buffer (Promega, USA). After incubation at 16°C for 18 h for a blunt-end ligation, or at room temperature (22°C) for 3 h or 4-8°C overnight for a sticky-end ligation, the ligation reaction was terminated by heating the reaction mix at 70°C for 10 min, and then the products were stored at -20°C until further use.

## 2.12.3 Dephosphorylation of linearized DNA

In order to prevent linearized vectors from self-ligation or recircularization during cloning, the 5'-phosphate groups of double-stranded DNA fragments were removed by treatment with calf intestinal phosphatase (CIP) (NEB, UK), according to the protocol of Sambrook *et al.* (1989).

Plasmid DNA (2-4  $\mu\text{g}$ ) was digested to completion with the appropriate restriction enzyme in a 40  $\mu\text{l}$  volume. Then 2.5  $\mu\text{l}$  (1 U/  $\mu\text{l}$ ) of CIP and 4.5  $\mu\text{l}$  10 X CIP buffer (NEB, UK) were added to the digestion mix which was then incubated at 37°C for 1-2 h. The CIP was heat inactivated at 75°C for 15 min and the



dephosphorylated DNA fragments were purified using QIAGEN MinElute Reaction Cleanup kit according to manufacturer's instructions (Appendix 3).

#### 2.12.4 “Filling in” or “trimming” reactions for blunt end ligation

For ease of cloning, incompatible DNA ends were converted into blunt ends. This was carried out by “filling in” of 3' recessed ends (e.g. produced by *EcoRI*) or “trimming” of 3' protruding ends of DNA (e.g. produced by *PstI*).

Plasmid DNA was digested to completion with the appropriate restriction enzyme in a 40 µl volume and fragments were separated by agarose gel electrophoresis. DNA fragments of interest were purified as in section 2.5.5 and taken up in 30-50 µl distilled water in a fresh microcentrifuge tube where DNA polymerase buffer (Invitrogen, UK) was added. dNTPs mix (a mixture of 25 mM dATP, dCTP, dGTP and dTTP, obtained from NEB, UK) was added to the tube at a final concentration of 1mM each (filling reaction) or 2 mM (trimming reaction). To this was added 1-2 µl of Klenow fragment of *E. coli* DNA polymerase I (Invitrogen, UK). The mixtures were incubated for 15 min at room temperature. DNA polymerase enzyme was inactivated by heating the reaction mixture to 75°C for 10 min before proceeding with the ligation or cloning protocols.

### 2.13 DNA transformation

Electroporation, rendering prokaryotic and eukaryotic cells permeable to nucleic acid by exposure to electrical fields is a commonly used technique (Dower *et al.*, 1988). Both *E. coli* and *P. multocida* strains have been transformed to reasonable efficiencies with this technique (Dower *et al.*, 1988; Jablonski *et al.*, 1992).

#### 2.13.1 Preparation of electro-competent cells

An overnight culture of *E. coli* or *P. multocida* was diluted 1 in 100 in pre-warmed 500 ml of LB or BHI broth respectively in a 2 L dimpled flask. The flask was shaken vigorously at 37°C until an OD<sub>540nm</sub> of 0.5-0.7 was achieved. The flask was then chilled on ice for 20 min and cells harvested at 4 000 x g for 15 min in a mid bench 4K15 Centrifuge (Sigma) at 4°C. The pellet was resuspended in 500 ml of cold sterile distilled water and centrifuged as before. Next, the pellet was resuspended in 250 ml of cold sterile distilled water, centrifuged as before and

resuspended in 10 ml of cold sterile 10% (v/v) glycerol. Following a final centrifugation, the cells were resuspended in 1.5 ml of cold sterile 10% (v/v) glycerol and 100  $\mu$ l aliquots were snap frozen in liquid nitrogen. Cells remained cold (on ice) at all times during the procedure and were stored at  $-80^{\circ}\text{C}$ . Cells remained electro-competent for up to three months as long as the storage temperature was maintained at  $-80^{\circ}\text{C}$ .

### 2.13.2 Electroporation procedure

The *E. coli* and *P. multocida* strains were transformed by electroporation procedures described by Dower *et al.* (1988) and Jablonski *et al.* (1992). Prior to electroporation, a 2 mm electroporation cuvette (Bio-Rad, UK) and the safety chamber were chilled at  $-20^{\circ}\text{C}$ . An amount of 1-5  $\mu$ l of DNA (ligation mixture or plasmid preparation) and 50  $\mu$ l of just thawed competent cells were added to the cuvette. The cuvette was tapped gently to ensure that the mixture settled at the bottom of the cuvette. A Bio-Rad pulse controller (MicroPulser Electroporator, Bio-Rad) was set at 2.0 kV (field strength  $10\text{ kV}/\text{cm}^2$ ) for *E. coli* and 2.5 kV (field strength  $12.5\text{ kV}/\text{cm}^2$ ) for *P. multocida*. The cells were pulsed once with a time constant of 4-5 ms for *E. coli* and 5-6 ms for *P. multocida* strains. Immediately following electroporation, 1 ml of pre-warmed SOC medium (Appendix 1) for *E. coli* or BHI broth for *P. multocida* strains was added and the cells were incubated at  $37^{\circ}\text{C}$  with shaking at 180 rpm for 1 h (*E. coli*) or 3-4 h (*P. multocida*) to allow expression of plasmid-encoded antibiotic resistance. Aliquots of 50-100  $\mu$ l transformed cells were then spread onto selective plates containing appropriate antibiotic and the plates were incubated at  $37^{\circ}\text{C}$  to obtain transformant colonies.

### 2.13.3 Blue and white screening of recombinants

Following incubation of transformed cells in SOC medium, 100  $\mu$ l aliquots were spread onto pre-warmed LB agar plates containing appropriate antibiotics, 2 mg/ml of isopropyl-D-thiogalactopyranoside (IPTG, Sigma) and 40 mg/ml of 5-bromo-4-chloro-3-indolyl-D-galactoside (X-gal, Sigma). The plates were then incubated at  $37^{\circ}\text{C}$  overnight. Resultant white colonies (potentially containing insert) were sub-cultured and plasmid DNA was purified according to section 2.3. The plasmid was then subjected to restriction enzyme analysis (section 2.4) to assess the presence of insert.

## 2.14 Conjugation

The following method was adapted from Bradley *et al.* (1980). Each strain was grown overnight at 37°C, 180 rpm in 5 ml BHI for *P. multocida* recipient strain or LB broth for *E. coli* donor strain containing appropriate antibiotic. An aliquot (0.5 ml) of overnight culture was inoculated into 10 ml pre-warmed BHI or LB broth respectively and incubation continued for 2 h with *E. coli* and 4 h for *P. multocida* or until both cultures reached an optical density (OD<sub>540nm</sub>) of 0.5-0.6 ( $\pm 5 \times 10^7$  cells/ml). The cells were harvested by centrifugation at 4500 x g for 5 min and washed with the same respective medium and then resuspended in 200 µl of medium. Equal volumes (50-100 µl) of the culture of donor and recipient strains were mixed gently in a centrifuge tube. Aliquots were then transferred onto BHI agar plates containing selective antibiotics and left to dry at room temperature before incubating at 37°C, face up, for 48 h.

## 2.15 Mammalian cell lines

The mouse macrophage-like cell line, J774.2 and the bovine lymphoma cell line, BL-3, were maintained in RPMI 1640 medium (Sigma, UK) and the embryonic bovine lung cell line, EBL, was maintained in MEM 2279 medium (Sigma, UK). All media contained calf serum (10% v/v) and 10 mM glutamine and supplemented with antibiotics (1% penicillin and 1% streptomycin). Approximately  $10^5$  cells/ml were seeded in tissue culture plates or flasks and incubated for 48 to 72 h at 37°C, 5% CO<sub>2</sub> until cell numbers had increased to  $5 \times 10^5$  cells/ml or a confluent monolayer had formed in the case of EBL cells. Cell numbers and viability were confirmed by trypan blue exclusion counts (section 2.16). Frozen stock was prepared by mixing  $1 \times 10^5$  cells/ml of the mammalian cells in 1 ml of dimethyl sulphoxide (DMSO) containing calf serum (90% v/v) in a storage vial and stored in a liquid nitrogen tank for future use.

## 2.16 Cell viability assessment

Cell viability was measured using the trypan blue exclusion method. For cell counting, a mixture containing 10 µl of trypan blue (0.4% w/v) (Sigma, UK) and 10 µl of the cell suspension was placed in an improved Neubauer (1/400 mm<sup>2</sup> x 0.1 mm depth) counting chamber. After 10 min, the chamber was viewed by

light microscopy and examined under x10 objective lens. For each sample, the number of cells in four squares was determined, the average number of cells per single square was determined and multiplied by  $2 \times 10^4$  to give the number of cells per ml. Viability of cells was determined by blue stained cells being counted as dead cells while clear cells were counted as viable.

## **2.17 *In vitro* assays**

### **2.17.1 Adherence assay**

*P. multocida* strains were harvested from 18-h cultures in BHI broth, washed twice in Phosphate-buffered saline (PBS) (Appendix 2) and resuspended in MEM medium without antibiotics. The density of each strain was adjusted to an optical density corresponding to approximately  $1 \times 10^7$  colony forming units (CFU)/ml to allow a final multiplicity of infection (MOI) of 100 bacteria/mammalian cell. One microlitre of bacterial suspension was added to each well of 24-well tissue culture plates containing J774.2 suspension, BL-3 suspension or EBL monolayer. The plates was centrifuged at  $1200 \times g$  for 5 min in a Heraeus 3 S-R centrifuge and then incubated in a CO<sub>2</sub> incubator at 37°C for 2 h. The EBL monolayer was washed once with PBS and trypsinized by addition of 1 ml of 0.5% trypsin-EDTA (pH 7.0) (Sigma, UK) per well and incubated for 5 min at 37°C with 5% CO<sub>2</sub>. All mammalian cells were harvested in PBS into universal tubes and the plates washed again with PBS to recover remaining cells. Pooled suspensions were centrifuged at  $1200 \times g$  for 5 min at room temperature, pellets resuspended with PBS and then re-centrifuged (to remove remaining bacteria and, for EBL cells, any traces of trypsin-EDTA). Cells were then resuspended in mammalian cells assay medium (Appendix 4) and an aliquot was removed for trypan blue staining (section 2.16) to assess cell viability. The remaining cells were lysed by addition of digitonin (100 ug/ml) and incubation for 30 min at 37°C with 5% CO<sub>2</sub>. The adherent bacteria were estimated by serial dilution of the suspension, plating aliquots onto BHI and LB agar and incubating at 37°C overnight before counting.

### **2.17.2 Invasion assay**

The invasion assay was performed according to the adherence assay with an additional step. After incubation of the bacteria/mammalian cell mixture in the

24-well plate for 2 h, the wells were washed gently with PBS to remove the unattached bacteria, for EBL cells. For J774.2 cells, the cells were centrifuged at 1200 x g for 5 min in a Heraeus 3 S-R centrifuge and the pellet was resuspended with J774.2 assay medium (Appendix 4). The washing step was repeated twice. A millilitre of assay medium with antibiotics [polymyxin (50 ug/ml) and gentamicin (50 ug/ml)] was added to each well to kill any remaining extracellular bacteria. The plate was then incubated for 1 h at 37°C with 5% CO<sub>2</sub>. The methods for assessment of mammalian cell viability and quantification of intracellular bacteria were done as above.

### **2.17.3 Intracellular survival assay**

The intracellular survival assay was done according to the invasion assay with an additional incubation step. After the antibiotic treatment for 1 h in the second incubation period of the invasion assay, the experimental wells were washed twice with PBS. A millilitre of EBL assay medium (Appendix 4) with various concentrations of antibiotics [polymyxin (0-50 ug/ml) and gentamicin (0-50 ug/ml)] was added to the designated wells. The plates were further incubated up to 4 h at 37°C with 5% CO<sub>2</sub>. The methods for assessment of EBL cell viability and quantification of intracellular bacteria were done as above.

### **2.17.4 Invasion inhibition assay**

Bacterial strains were prepared as in the adherence assay. The EBL cell monolayers in the wells of the tissue culture plates were treated with 1 ug/well of cytochalasin D for 1 h. The wells were then washed twice with PBS, and MEM medium without antibiotics was added prior to addition of the bacteria. The invasion assay was then performed as described above.

### **2.17.5 Transfection assay**

Briefly, for one well of a 6 well plate, 100 µl Opti-MEM (Invitrogen, UK) was mixed with 4 µl Lipofectamine 2000 (Invitrogen, UK) in a sterile centrifuge tube prior to incubation at room temperature for 5 min. In a separate sterile centrifuge tube, a total of 1 µg DNA was added to 100 µl Opti-MEM and mixed by gentle tapping. Following incubation, the entirety of the Lipofectamine 2000/Opti-MEM mixture was added to the centrifuge tube containing DNA. The contents were mixed by gentle tapping and incubated at room temperature for

20 min. Cell culture medium on cells was discarded and replaced with 2 ml/well of antibiotic-free, supplemented growth medium. 200 µl of transfection mixture was added per well and cells incubated overnight at 37°C, 5% (v/v) CO<sub>2</sub>. At 24 h post-transfection, growth medium was discarded and replaced with 1.5 ml of fresh growth medium. Transfected cells were maintained for 24 h at 37°C, 5% (v/v) CO<sub>2</sub> before viewed under an inverted microscope (Zeiss Axiovert 40 CFL). Phase contrast light images were captured at x20 and x40 magnification using a Zeiss AxioCam MRcS camera attached to a Zeiss Axiovert 40 CFL Microscope and images were processed with Zeiss Axiovision software.

## 2.18 Fluorimetry assessment

The patterns of GFP expression in bacterial strains expressing fluorescent protein were monitored using a fluorimeter (FLUOstar OPTIMA, BMG Labtech, UK). A sterile flask containing 100 ml of fresh broth supplemented with antibiotics at a final concentration of 50 µg/ml was inoculated with 1 ml of an overnight culture of *P. multocida* B:2 or *E. coli* XL-1 BLUE. It was then left shaking at 180 rpm, 37°C. 1 ml of growth culture was taken at every hour interval and its optical density at 600 nm (OD<sub>600nm</sub>) were measured using a cell density meter (WPA CO8000, Biochrom Ltd., UK) in a polystyrene cuvette (FisherBrand, UK). The suspension were then transferred into a centrifuge tube and centrifuged at 13 000 x g for 1 min. The pellet was resuspended in 1 ml of PBS and the OD<sub>600nm</sub> was measured again and a 200 µl aliquot placed in a well of a 96 well flat-bottom dish (Corning, USA) in triplicate before assessing the fluorescence intensity (FI) via the fluorimeter set with a fluorescent light filter: Excitation 485-12 nm, Emission 590 nm. All samples were compared with bacteria only to eliminate background. Samples were taken at hourly intervals until OD<sub>600nm</sub> reached stationary phase (~2.0).

## 2.19 Transmission electron microscopy (TEM)

All bacterial strains and EBL cells were prepared as described in the adherence assay. The bacteria/EBL cells mixture was incubated for 4 h at 37°C with 5% CO<sub>2</sub>. After trypsinization, cell viability was assessed and the remainder of the cells were centrifuged at 1200 x g for 5 min. The pellet was fixed with 2% (v/v) glutaraldehyde in 0.1 M sodium cacodylate buffer (pH 7.2) at 4-8°C overnight,

washed three times with 0.1 M cacodylate buffer and embedded in 2% agar gel. One millimeter cubes were dehydrated in graded alcohol 70-100%, post-fixed in 1% osmium tetroxide and embedded in epoxy resin. Ultra-thin sections were obtained by a MT-2B ultramicrotome and stained with lead citrate and 0.5% (w/v) uranyl acetate. Sections were examined with a LEO 912AB transmission electron microscope operating at 80 kV at 1000x magnification.

## 2.20 Fluorescence imaging

### 2.20.1 Cell fixation

#### 2.20.1.1 EBL cells

EBL cells were treated according to the invasion assay above (section 2.14.2). The only difference for fluorescence microscopy (FM) slide preparation was that the EBL cells were seeded in a chamber-slide (NUNC, UK) rather than a 6-well plate. This is because cells can be fixed directly to the slide after removing the removable well off the chamber slide. This method proved to be more efficient than the conventional method by increasing the quantity of cells to be analyzed after fixation.

As mentioned in the above method (section 2.14.2), after antibiotic treatment to eliminate extracellular and adherent bacteria, the monolayer was washed twice with PBS. CellMask plasma membrane stain (GE Healthcare, UK) (5 µg/ml) (diluted according to manufacturer's instructions) was added at 200 µl per well. The chamber-slide was then incubated for 7 min at 37°C supplemented with 5% CO<sub>2</sub>. The staining solution was removed from the well and the cells washed two to three times with PBS. About 200 µl of pre-warmed paraformaldehyde (PFA) (4% v/v) was added to each well and incubated for 30 min at 37°C supplemented with 5% CO<sub>2</sub>. PFA was then removed from the well by washing three times with PBS. The removable wells were then removed from the chamber-slide and the slide was left to dry.

Fluorescence mounting medium (DAKO, UK) was used to cover the fixation area on the chamber-slide. A cover slip was then gently applied on top of the medium to avoid air bubble formation. Any gap between the cover slip and the chamber-slide was then sealed-off using a nail polish to prevent air pockets from forming.

The slide was left for 10 min to properly fix the mounting media. It was then cleaned and labelled before arranging in a slide box and stored in the dark.

#### 2.20.1.2 Fluorescence measurement and staining of bacterial strains

An overnight culture of *P. multocida* B:2 strains with respective plasmid was diluted (1:100) in 100 ml of pre-warmed BHI broth in a 500 ml dimpled flask. The flask was shaken vigorously at 37°C until an OD<sub>540nm</sub> of 0.3-0.5 was obtained. One millilitre of the bacterial suspension was taken and centrifuged at 13 000 x g for 1 minute. The pellet was then resuspended in 1 ml of PBS and its OD<sub>540nm</sub> was again measured. An aliquot of 200 µl was transferred from the PBS suspension into a flat-bottom 96-well plate. All samples were done in triplicate. Fluorescence intensity (FI) was then measured using a fluorimeter (Fluostar, UK) according to a customized set-up (section 2.18).

A vial of Cy5Dye (Amersham, UK) was mixed with 100 µl of PBS according to the manufacturer's instructions and was ready for use. The dye was then mixed with bacterial suspension at a ratio of 1:20 (25 µl of dye to 500 µl of bacterial suspension). The mixture was then incubated in the dark at room temperature for an hour to allow staining of bacterial free-peptide groups on the outer membrane. After incubation, the suspension was pelleted at 13 000 x g for 1 min and washed with 1 ml of PBS before being re-centrifuged. The washing step was repeated until the suspension was no longer coloured.

For fixation, an aliquot of the suspension was mixed with 4% (v/v) of paraformaldehyde (PFA) (1:1). About 20 µl of the fixation mixture was spotted onto a clean spot-slide which was then left at room temperature to dry. Fluorescence mounting medium (DAKO) was used to cover the fixation area on the spot-slide. A cover slip was then gently applied on top of the medium to avoid air bubble formation. Any gap between the cover slip and the slide was then sealed-off using nail polish. The slide was left for 10 min to properly fix the mounting media. It was then cleaned and labelled before arranging in a slide box and stored in the dark.

#### 2.20.2 Fluorescence microscopy (FM)

Fluorescence imaging was carried out using the Zeiss Axiomager M1 upright fluorescence microscope (Carl Zeiss, UK) connected to a Hamamatsu Orca 03 and



QIClick digital charge-coupled device (CCD) camera. The system allows visualization of fluorescence at high spatial resolution (1200 x 1300 pixels) and high bit depth (12-bit gray scale). Acquisition, visualization, measurement and restoration of the images were then processed with Volocity software (Perkin Elmer, UK).

## **2.21 Immunosuppression by *P. multocida* B:2**

### **2.21.1 Preparation of bacterial cell-free extract (CFE)**

CFE of different bacterial strains were prepared from 18 h broth cultures. Cells were collected by centrifugation at 3 000 x g for 30 min at 4°C (RC-5B, Sorvall, UK) and washed three times with PBS. A thick suspension of bacteria in 5 ml PBS was lysed by sonication using a Vibra Cell ultrasonic processor (Jencons-PLS, Leighton Buzzard, UK) for three 60-s bursts with intermittent cooling on ice. The broken-cell suspension was centrifuged at 3 000 x g for 30 min at 4°C, and the supernatant was filtered through a 0.2 µm-pore size membrane (Sartorius, UK). The protein concentration was determined by Bradford assay (section 2.21.2) and adjusted to a desired concentration by adding sterile PBS.

### **2.21.2 Protein quantification**

The Bradford assay was used to measure the protein content of all CFE preparations in this study. The Bradford reagent (Bio-Rad, UK) was used to provide a quantitative measurement of protein concentration of samples containing soluble proteins. When Coomassie dye binds protein in an acidic environment, an immediate absorbance shift occurs from 465 nm to 595 nm with a simultaneous colour change of the reagent from green/blue to blue. The Bradford's reagent was diluted 1 in 5 with sterile distilled water and filtered through a 0.45 µm-pore size membrane filter (Sartorius, UK) before use. The method required a standard curve that was established with different concentrations of bovine serum albumin (BSA) (NEB, UK) in PBS. A solution of 2 mg/ml of BSA was prepared in PBS and 2-fold dilutions of this in PBS were prepared in a 96-well flat bottom plate. PBS alone was used as a blank or negative control. To a new 96-well flat bottom plate, 25 µl of each dilution of BSA and sample were mixed with 200 µl of diluted Bradford's reagent. After incubation for 10 min at room temperature, the absorbance values were read at

OD<sub>620nm</sub> in a plate reader (FluoStar, UK). The sample-adjusted value was obtained after subtraction of the background value of the medium and the protein concentrations of the sample was then determined from the BSA standard curve.

### **2.21.3 Isolation and preparation of peripheral blood mononuclear cells (PBMC)**

PBMC was isolated by the procedure of Vanden Bush with some modifications (Vanden Bush & Rosenbusch, 2002). Blood samples were provided by Dr Mara Rocchi from the Moredun Research Institute (MRI), Edinburgh. Samples were collected from the jugular vein of calves in heparinised Vacutainers (Becton Dickinson, Meylan, France) containing 170 I.U. heparin and kept on ice until being centrifuged at 1730 x g for 20 min at 20°C (Heraeus, multifuge 3 S-R). The buffy coat was transferred into a universal tube containing Hank's balanced salt solution (HBSS, Invitrogen, UK) without Ca<sup>2+</sup> and Mg<sup>2+</sup>, at room temperature. Then the mixture was layered carefully on top of an equal volume of NycoPrep™ 1.077 A (Fresenius Kabi Norge, Norway) and centrifuged at 600 x g for 20 min at 20°C. The interface opaque band was transferred to HBSS and washed once by centrifugation at 200 x g at 4°C for 10 min. To lyse the contaminating erythrocytes, the pellet was suspended in red blood cell lysis buffer (Appendix 4) and kept for 10 min on ice and then washed with HBSS by centrifugation at 200 x g at 4°C for 10 min. The pellet was then suspended in complete RPMI medium (Sigma, UK) supplemented with 10% heat-inactivated fetal bovine serum (Sigma, UK), 2 mM L-glutamine (Gibco, UK), 100 U of penicillin per ml, 100 µg/ml of streptomycin, 0.5% (w/v) nystatin, 1% (w/v) gentamycin, and 30 mM HEPES (Sigma, UK), to reach a final concentration of 1.0 x 10<sup>6</sup> viable cells/ml, as estimated by trypan blue staining and haemocytometer cell count, (Life Technologies, UK) (Appendix 4).

### **2.21.4 Lymphocyte proliferation inhibition assay**

To investigate inhibitory effects of *P. multocida* B:2 on the proliferative response of PBMC to concanavalin A (ConA), 50 µl of the required concentration of a CFE was added to the designated wells and 100 µl of PBMC was added subsequently. The cells were pre-incubated with CFE for 1 h in the CO<sub>2</sub> incubator. After incubation, 50 µl of RPMI containing the required concentration

of ConA was added to the wells. Plates were incubated at 37°C in a humidified atmosphere of 5% (v/v) CO<sub>2</sub> and 95% air (Wolf Laboratories, Galaxy R). On the third day of incubation, each well was pulsed with 37 KBq [methyl-<sup>3</sup>H] thymidine (Amersham, UK) in 20 µl RPMI and incubated for another 18 h. The cultures were then harvested onto printed filtermat (glass fibre filter size 90-120 mm) (Wallac, Finland) by a semi-automated 96-well plate harvester (Tomtec M111) and allowed to dry at 37°C. Dried filtermats then were bagged (Sample bag, Perkin Elmer, UK) with 4 ml of liquid scintillation cocktail (Betaplate Scint, PerkinElmer, UK) and sealed. The amount of incorporated [methyl-<sup>3</sup>H] thymidine was determined by a scintillation counter (Microbeta TriLux, PerkinElmer) and expressed as counts per minute (cpm). The stimulation index (SI) was expressed as: cpm of treated cultures/cpm of control cultures without treatment.

## 3. RESULTS

### 3.1 Rate of bacterial killing by antibiotics

In order to establish whether *P. multocida* was able to enter and survive within mammalian cells, it would be necessary to ensure that all extracellular bacteria were killed before cells were lysed and intracellular bacteria released. As a preliminary to this, the optimum concentration of antibiotics to kill >99.9% of bacteria in 1 h was established. A sterile flask containing 20 ml of fresh BHI broth was inoculated with 1 ml of an overnight culture of *P. multocida* B:2 JRMT12 in BHI broth. It was then incubated for 4 h (log-phase) at 37°C in an orbital incubator at 150 rpm. The bacterial cells were then collected by centrifuging at 3 000 x g for 30 min and the resulting pellet was resuspended in 1 ml of PBS and diluted down to 10<sup>5</sup> CFU/ml. It was then added into a sterile BHI broth supplemented with the antibiotics gentamicin and polymyxin B sulphate, either separately or together, at concentrations ranging from 50 µg/ml to 350 µg/ml. At 30, 60 and 120 min, samples were taken and plated onto BHI agar. The numbers of bacterial colonies were recorded after overnight incubation at 37°C. The antibiotics gentamicin and polymyxin B sulphate have been reported to have little effect on mammalian cells in 1 h (Rudin *et al.*, 1970; Feingold *et al.*, 1974).

According to the data in Table 6, the viability of the strain decreased rapidly upon treatment with either gentamicin or polymyxin B or when both antibiotics were used together. However, when the two antibiotics were used together, no viable bacteria was detected, even after 30 min with the lowest concentration of antibiotics. Hence, it can be concluded that *P. multocida* B:2 JRMT12 were eliminated completely (>99.99% killing) after 30 min of incubation with both antibiotics at 50 µg/ml. The study was then followed by testing the antibiotics, gentamicin or polymyxin B either single or together, at a final concentration of 50 µg/ml towards the parent strain (85020) of JRMT12 and other strains of *Pasteurellaceae* (*P. multocida* A3 and *M. haemolytica* A1) to observe the bacterial rate of killing. All three strains showed similar results to those for *P. multocida* B:2 JRMT12 (data not shown). This information gave confidence that the combination antibiotics at 50 µg/ml for 1 h would ensure killing of extracellular bacteria in subsequent invasion assays.

**Table 6. Effect of antibiotics on viability of *P. multocida* B:2 JRMT12.**

Time (min)	Antibiotics ( $\mu\text{g/ml}$ )											
	Polymyxin B (Pm)				Gentamicin (G)				Pm & G			
	50	100	250	350	50	100	250	350	50	100	250	350
30	2	3	N	N	3	N	N	N	N	N	N	N
60	N	N	N	N	2	N	N	N	N	N	N	N
120	N	N	N	N	N	N	N	N	N	N	N	N

Bacteria were diluted to  $10^5$  CFU/ml in BHI broth containing a final concentration of 50-350  $\mu\text{g/ml}$  each of gentamicin or polymyxin, alone or in combination. Cells were incubated at  $37^\circ\text{C}$  for 30, 60 and 120 min. Viable *P. multocida* B:2 were enumerated by plating 100  $\mu\text{l}$  samples onto BHI agar in triplicate and incubated at  $37^\circ\text{C}$ , overnight. Control without antibiotic was executed in parallel. Values are average number of colonies detected on BHI agar.

N : no colony detected

## 3.2 Interaction between mammalian cells and *Pasteurella* species

### 3.2.1 Effect of *P. multocida* B:2 on viability of J774.2 cells

To obtain meaningful data on the adherence and invasive capacities of *Pasteurella* strains, it was necessary to show that bacteria were not killing a large percentage of mammalian cells during the 2 h incubation period used for the adherence and invasion assays. To determine the effect of *P. multocida* B:2 on viability of mouse macrophage-like cells, J774.2, the cells were collected by centrifugation at 1500 x g at 3 h post-infection with bacteria at MOI 100:1, resuspended in assay medium and stained with trypan blue (0.4% w/v) (Sigma, UK) (section 2.16). Macrophage viability in the presence of bacteria was compared to the control J774.2 cells where no bacteria were present throughout the experiment. From graph A in Figure 10, it was demonstrated that none of the strains caused any toxicity affecting macrophage viability during the invasion assay. When compared to the control cells (J774.2 only), all the experimental cells (J774.2 + bacteria) gave a similar percentage of total cell viability at 80% - 85% after 3 h of incubation. There was also no significance difference in cell viability observed from J774.2 cells mixed with either the wild-type or mutant *P. multocida* B:2.

### 3.2.2 Effect of *P. multocida* B:2 on viability of EBL cells

To determine the effect of *P. multocida* B:2 on the viability of embryonic bovine lung (EBL) cells, the cells were trypsinized at 3 h post-infection with bacteria at MOI 100:1 and resuspended in EBL assay medium and stained with trypan blue (0.4% w/v) (Sigma, UK). EBL viability in the presence of bacteria was compared to that of the control cells where no bacteria were present throughout the experiment. According to graph B in Figure 10, none of the *Pasteurella* strains showed a toxic effect towards EBL viability during the time period of the standard invasion assay. All control and experimental cells were found to be at least 80 % to 90 % viable after incubation for 3 h.

**Figure 10. Viability assessments of J774.2 and EBL cells by trypan blue staining.**

Approximately  $10^5$  cells were infected with log-phase *Pasteurella* and *E. coli* strains at MOI of 100:1 (bacteria:mammalian cell) according to the standard invasion assay procedure (section 2.14.2). After incubation for 3 h, cells were stained with trypan blue and counted in a haemocytometer under 10 x objective lens (section 2.16). Viability of cells was determined by blue stained cells being counted as non-viable while clear cells were counted as viable. Data represent the means ( $\pm$  SEM) of three independent assays with duplicate samples.

**A:**

Percentage of viable and non-viable J774.2 cells in;

Uninfected controls [J774.2 (J7) only],

J774.2 cells infected with *P. multocida* B:2 JRMT12 [J7 + JRMT12],

J774.2 cells infected with *P. multocida* B:2 85020 [J7 + 85020],

J774.2 cells infected with *P. multocida* A3 [J7 + A3],

J774.2 cells infected with *E. coli* XL-1 BLUE [J7 + XL].

**B:**

Percentage of viable and non-viable EBL cells in;

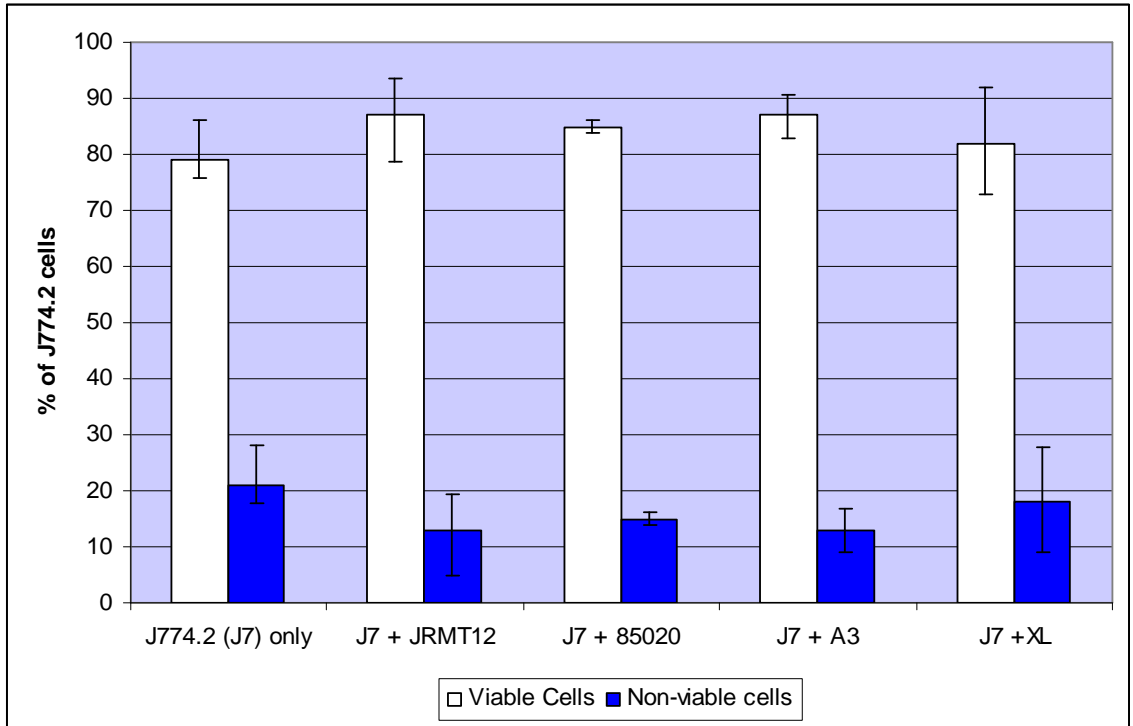
Uninfected controls [EBL (E) only],

EBL cells infected with *P. multocida* B:2 JRMT12 [E + JRMT12],

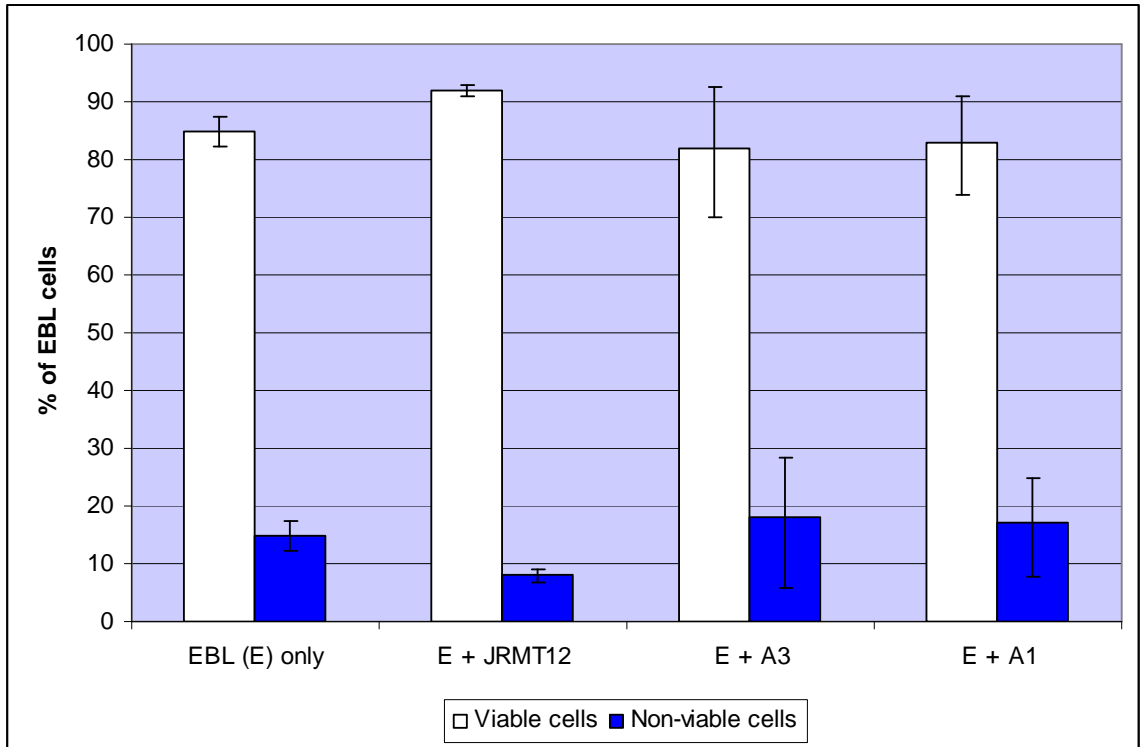
EBL cells infected with *P. multocida* A3 [E + A3],

EBL cells infected with *M. haemolytica* A1 [E + A1].

A



B





### 3.2.3 Invasion of J774.2 cells by *P. multocida* and *E. coli*

Detection within cultured mouse macrophage-like cells (J774.2) of the parent strain (85020) an attenuated derivative strain (JRMT12) of *P. multocida* B:2 and *P. multocida* A3 was determined by infecting the cells at ratios of 500:1 and 100:1 bacteria per J774.2 cell (section 2.17.2). In order to enhance cell-to-cell contact, the mixture was centrifuged at 1500 x g for 3 min, followed by incubation for 2 h. Macrophages were then washed to remove the majority of extracellular bacteria and the residual extracellular bacteria were killed with a combination of gentamicin and polymyxin B sulphate each at a final concentration of 50 µg/ml for 1 h. After the incubation period, suspensions were washed 3 times with PBS to remove antibiotics before exposing the cells to digitonin (100 µg/ml) in assay medium for 30 min to lyse the mammalian cells and release any intracellular bacteria. Serial 10-fold dilutions were prepared from each sample in PBS and 100 µl portions were spread on BHI agar and incubated at 37°C for 48 h. *E. coli* XL-1 Blue was also included in the experiments as a presumed negative control for invasion and intracellular survival.

Table 7 shows numbers of viable intracellular bacteria in J774.2 cells after incubation for 3 h and at two different multiplicities of infection. Uptake of the putative control strain, *E. coli* XL-1 Blue, was noted at 0.061 viable bacteria/J774.2 cell. Because of the nature of macrophages, all strains do get phagocytosed and taken up. The uptake of *P. multocida* A3 was similar to that of *E. coli* XL-1 Blue. However, for the mutant strain, JRMT12, and parent strain, uptake was approximately 10-fold higher than that for the *E. coli* XL-1 Blue and *P. multocida* A3 strains. At MOI 500:1, JRMT12 uptake rate is 0.559 viable bacteria/J774.2 cell and at MOI 100:1 it reduced slightly to 0.483 viable bacteria/J774.2 cell. Similar results were obtained with the wild type strain, 85020. At MOI 500:1, 85020 uptake rates was 0.459 viable bacteria/ J774.2 cell and it reduced slightly to 0.346 viable bacteria/ J774.2 cells when mixed at MOI 100:1. There was no significant difference in the rate of uptake even when the MOI was reduced to 100:1. This results strongly indicated that the B:2 strains were invading or inducing their uptake over and above the baseline phagocytic capacities of the J774.2 cells. This ability could be one of the virulence properties possessed by the B:2 strain.

### 3.2.4 BL-3 cells

The capacity of *P. multocida* strains to invade or be taken up by a bovine lymphoma (BL-3) cell line was also investigated. BL-3 cells were chosen as they were derived from one of the hosts of this pathogen.

BL-3 cells were maintained and cultivated as described in section 2.15 and the invasion assay was carried out as detailed in sections 2.17.2 and 3.2.1. The experiment was done once comparing the wild-type B:2 85020 and its mutant derivative JRMT12 (Table 8). The invasion rate was not significantly different between the two strains, and gave similar values to those observed with the J774.2 cells. Since BL-3 cells are not phagocytic, the detection of the bacteria in the intracellular compartment of these cells confirmed that the B:2 strains had the capacity to promote their uptake into BL-3 cells. This invasive capacity was further examined using a bovine embryonic lung cells which represented more closely a cell barrier likely to be encountered by *P. multocida* B:2 during natural infection.

**Table 7. Invasion of *P. multocida* and *E. coli* strains with J774.2 mouse macrophage-like cells at different multiplicities of infection (MOI).**

Strains	Bacterial invasion (No. of viable intracellular bacteria/ J774.2 cell)	
	MOI (500:1)	MOI (100:1)
<i>P. multocida</i> B:2 AroA <sup>-</sup> (JRMT12)	0.56 ± 0.13	0.48 ± 0.20
<i>P. multocida</i> B:2 wt (85020)	0.46 ± 0.23	0.35 ± 0.12
<i>P. multocida</i> A3	0.05 ± 0.02	0.06 ± 0.04
<i>E. coli</i> XL-1 Blue	0.06 ± 0.03	0.09 ± 0.03

Invasion is expressed as no. of viable bacteria/J774.2 cell that resist exposure to polymyxin B and gentamicin each at a final concentration of 50 µg/ml for 1 h after an infection period of 2 h. Data represent the means (± SEM) of three independent assays with duplicate samples.

wt: wild-type

**Table 8. Uptake of *Pasteurella multocida* strains into bovine lymphoma (BL-3) cells at MOI 500:1.**

Strains	Bacterial invasion (No. of viable intracellular bacteria/BL-3 cell)
<i>P. multocida</i> B:2 AroA <sup>-</sup> (JRMT12)	0.72
<i>P. multocida</i> B:2 wild-type (85020)	0.39

Invasion is expressed as no. of viable bacteria/BL-3 cell that resist exposure to polymyxin B and gentamicin at a final concentration of 50 µg/ml for 1 h after an infection period of 2 h.

### 3.2.5 EBL cells

The embryonic bovine lung cell line, EBL (DSMZ ACC192 BgVV, Jena, Germany) was maintained and cultivated as mentioned in section 2.15. A feature of *P. multocida* B:2 during HS disease is the rapid spread of infecting bacteria from the respiratory tract to the blood and lymph to cause a fatal septicaemia in less than 48 h. This may, in part, be caused by invasion of the respiratory epithelium by the *P. multocida* B:2 cells. Thus, using a mammalian cell line *in vitro* that is derived from the bovine respiratory system should parallel stages of the actual of infection *in vivo*.

#### 3.2.5.1 Establishment of an appropriate MOI between *Pasteurella* strains and EBL cells

The extent of *P. multocida* B:2 invasion of EBL cells at different MOI ratios was the first experiment applied to this cell line. The invasion assay using JRMT12 and parent strain was performed according to section 2.17.2 at 4 different MOIs: 25:1, 50:1, 100:1 and 200:1 bacteria per cell. Table 9 shows that uptake of *P. multocida* B:2 JRMT12 at MOI 25:1 and 50:1 was poor compared to the uptake seen at MOIs of 100:1 and 200:1. From these observations, the minimum MOI necessary to achieve a significant invasion efficiency of JRMT12 into EBL cells was 100:1.

#### 3.2.5.2 Comparison of the extent of adherence and invasion between *P. multocida* B:2 strains and EBL cells

As detailed in section 2.17.1, adherence of *Pasteurellaceae* strains towards EBL cells was determined by infecting the mammalian cells with bacteria in a 24-well tissue culture plate at an MOI of 100:1 bacteria per cell. The plate was briefly centrifuged to encourage close contact between EBL and bacterial strains. After exposure of the bacteria to EBL for 2 h, the cells were washed to remove any unattached bacteria. The cells were then exposed to digitonin for 30 min at a final concentration of 100 µg/ml to lyse the mammalian cells and release attached bacteria and any possible intracellular bacteria. Serial 10-fold dilutions were prepared for each sample in PBS and aliquots (100 µl) were spread onto a BHI agar and incubated at 37°C for 24 h to 48 h. Bacterial counts would represent adherent plus intracellular bacteria. An adherence experiment was

normally done in parallel with an invasion experiment as the invasion assay has an additional step added where a parallel batch of cells was incubated with polymyxin B and gentamicin at a final concentration of 50 µg/ml for 1 h after the initial incubation for 2 h.

Table 10 shows a comparison of adherence and invasion between the wild-type and mutant strains of *P. multocida* B:2 and EBL cells. Although this represents only a single assay, it appeared that JRMT12 bacteria adhered to EBL cells at higher rate than wild type 85020 cells and this was reflected in a slightly higher invasive capacity. This higher invasion capacity is in keeping with previous data (Tables 7 & 8) where JRMT12 also showed a slightly higher invasive capacity than 85020 for J774.2 and BL-3 cells.

### 3.2.5.3 Comparison of adherence and invasion between bovine *Pasteurellaceae* strains with EBL cells

In order to confirm the ability of the mutant strain to adhere and to invade EBL cells, both the adherence and invasion assay were repeated and two other bovine *Pasteurellaceae* strains, *P. multocida* A3 and *M. haemolytica* A1 were used for comparison. Data in Table 11 shows that all bovine *Pasteurellaceae* strains were able to adhere to EBL cells at roughly the same rate of between 6 and 8 bacteria per EBL cell after incubation for 2 h. However, in an invasion assay done in parallel with the adherence assay (Table 11 A), only the B:2 strain was detected intracellularly, at 0.76 bacteria per EBL cell, a value similar to those previously recorded (Tables 9 & 10). These data were then further confirmed when invasion assays were repeated with the bovine *Pasteurellaceae* strains. *P. multocida* B:2 JRMT12 was shown to be viable intracellularly in EBL cells at 0.67 bacteria per EBL cell (Table 11 B) and intracellular bacteria were again undetectable (for *P. multocida* A3) or present at a very low level (for *M. haemolytica*). These findings showed that all bovine *Pasteurellaceae* strain tested in this studies were able to adhere to EBL cells but only the B:2 strains were detected intracellularly. This strongly suggested that the B:2 strain may possess invasive properties which allow intracellular access to mammalian cells.

**Table 9. Invasion of EBL cells by *P. multocida* B:2 JRMT12 at different MOIs.**

<b>MOI (bacteria/EBL)</b>	<b>Bacterial invasion (No. of viable intracellular bacteria/EBL)</b>
25:1	0.04 ± 0.01
50:1	0.07 ± 0.01
100:1	0.84 ± 0.06
200:1	0.25 ± 0.08

Invasion is expressed as no. of bacteria/EBL that resisted exposure to polymyxin B and gentamicin at a final concentration of 50 µg/ml for 1 h after an infection period of 2 h. Data represent the means (± SEM) of three independent assays with duplicate samples.

**Table 10. Comparison of adherence and invasion rates between strains of *P. multocida* B:2.**

<b>Strains</b>	<sup>a</sup> <b>Bacterial adhesion (No. of bacteria/EBL)</b>	<sup>b</sup> <b>Bacterial invasion (No. of viable intracellular bacteria/EBL)</b>
<i>P. multocida</i> B:2 aroA <sup>-</sup> (JRMT12)	23.2	1.58
<i>P. multocida</i> B:2 wild-type (85020)	13	1.12

<sup>a</sup> Adhesion is expressed as no. of bacteria/EBL after exposure of EBL to bacteria for 2 h at MOI 100:1.

<sup>b</sup> Invasion is expressed as no. of viable intracellular bacteria/EBL that resist exposure to polymyxin B and gentamicin each at a final concentration of 50 µg/ml for 1 h after an infection period of 2 h at MOI 100:1.

#### 3.2.5.4 Intracellular survival of *P. multocida* B:2 JRMT12 in EBL cells

It was of interest to determine the length of time bacteria remain viable intracellularly. In this section, an intracellular survival assay with the mutant strain JRMT12 was done, with a prolonged incubation time (total of 7 h) after the antibiotic treatment step in the invasion assay (section 2.17.3) before viable intracellular bacteria numbers were determined.

Besides assessing intracellular survival, the observation were extended in an attempt to record any intracellular growth and replication of internalised *P. multocida* B:2 which might have occurred within the EBL cells. Three conditions were used to measure intracellular bacteria. After the standard invasion assay, some cells were further incubated without antibiotics for up to 4 h and some cells were further incubated for the same length of time in the presence of polymyxin B and gentamicin (P&G) at a final concentration of each of 10 µg/ml or 50 µg/ml. These latter two conditions were employed as a precaution. If, without the presence of antibiotic, any extracellular bacteria left after the initial antibiotic treatment had survived, they would replicate and invalidate the assessment of intracellular bacteria. Thus, P&G at 50 µg/ml was added during the prolonged incubation to eliminate any extracellular bacteria that might be left or might be released by dying mammalian cells. However, there was also the possibility that external antibiotic may enter mammalian cells during prolonged incubation (Eltahawy, 1983) and thus kill the intracellular bacteria. Thus, a batch of the cells was incubated with medium supplemented with P&G at only 10 µg/ml of each in order to slow down or eliminate replication of any extracellular bacteria but also to minimise the possibility of uptake of antibiotic into mammalian cells and eradicating internalised bacteria. However, the data obtained (Table 12) showed that, after 5 or 7 hours of incubation, all three conditions showed a similar rate of decrease with time of the number of viable intracellular bacteria per cell when compared to the initial time (3 h) of the standard invasion assay, although there was some variation in the total number of intracellular bacteria recorded in the different batches of cells. This suggested that internalised bacteria might not be able to replicate intracellularly but were gradually eradicated by the EBL cells.

**Table 11. Comparison of adherence and invasion rates between strains of *Pasteurellaceae*.**

Strains	Bacterial adhesion (No. of bacteria/EBL)	Bacterial invasion (No. of viable intracellular bacteria/EBL)	
		A	B
<i>P. multocida</i> B:2 AroA <sup>-</sup> (JRMT12)	6.94 ± 6.08	0.76 ± 0.07	0.67 ± 0.46
<i>P. multocida</i> A3	7.52 ± 5.79	< 0.0001	< 0.0001
<i>M. haemolytica</i> A:1	6.59 ± 5.13	< 0.0001	0.002 ± 0.002

Adhesion is expressed as no. of bacteria/EBL cell after 2 h exposure of the EBL cells to bacteria at MOI of 100:1.

Invasion is expressed as no. of bacteria/EBL cell that resist exposure to polymyxin B and gentamicin each at a final concentration of 50 µg/ml for 1 h after an infection period of 2 h at MOI 100:1. **A:** Invasion assays executed in parallel with adherence assays. **B:** Individual invasion assays without assessing adherence rate. Data represent the means (± SEM) of three independent assays with duplicate samples.

**Table 12. Period of intracellular survival of *P. multocida* B:2 JRMT12 in EBL cells at MOI 100:1.**

Invasion time (h)	No. of viable intracellular bacteria/EBL			
	Standard invasion assay	No antibiotic added after washing	P&G 10 µg/ml added after washing	P&G 50 µg/ml added after washing
3	1.49 ± 0.55			
5		0.33 ± 0.07	1.47 ± 0.93	0.56 ± 0.25
7		0.22 ± 0.05	0.59 ± 0.27	0.24 ± 0.24

Internalized viable bacteria were evaluated as no. of bacteria/EBL after incubation of EBL with bacteria for 2 h followed by exposure to polymyxin B and gentamicin (P&G) each at a final concentration of 50 µg/ml for 1 h prior to further incubation for 2 h and 4 h in the presence of either 0, 10 or 50 µg/ml each of polymyxin B and gentamicin in the medium. Data represent the means (± SEM) of three independent assays with duplicate samples.



These findings have important implications for the delivery of the inbound plasmid during bactofection (section 1.6.2.7), where the bacteria presumably need to die and undergo lysis for the release of the plasmid into the mammalian cells. Hence, gradual death of the bacteria intracellularly, as indicated by the data should help in gradual release of plasmid into the cytoplasm of the mammalian cells. Moreover, for the three antibiotic conditions used, the data suggested that the rate of decline of viable intracellular bacteria per EBL during prolonged incubation (total 7 h) was not influenced by the absence or presence of the antibiotics.

### 3.2.5.5 Invasion inhibition assay of EBL cells with cytochalasin D

In order to further examine the findings that *P. multocida* B:2 JRMT12 was invasive, an experiment to inhibit the actin-dependent phagocytosis of the mammalian cell might confirm not only the active uptake of bacteria but also a possible mechanism of entry into the host cell for this particular species. Cytochalasin D (CD) is a cell permeable mycotoxin, which causes both the association and dissociation of actin subunits. Pre-incubation of EBL cells with this mycotoxin would disrupt actin polymerization and actin filament formation necessary for phagocytosis. The invasion inhibition assay (section 2.17.4) was slightly modified from the standard invasion assay. The EBL cells were pre-incubated with the mycotoxin before addition of bacteria. In one assay, CD was left with the cells throughout the experiment but, in another, CD was completely removed by washing before addition of bacteria. Table 13a shows the effect of cytochalasin D at different concentrations on invasion of EBL cells by the mutant JRMT12 strain. The data showed that CD was active at 1 µg/ml in preventing invasion. In Table 13b, EBL cell were pre-incubated with 1 µg/ml of CD. CD was then removed by washing the cells 3 times with PBS before adding the bacteria at MOI 100:1 (bacteria/EBL). Incubation was then followed as for the standard invasion assay but also prolonged as for the intracellular survival assay (total 7 h). It was observed that there was a steady decline in intracellular bacteria over the 7 h period in EBL not treated with CD. It was also clear that the effect of CD was not reversible, at least during the 2 h period when washed EBL cells were incubated with bacteria prior to antibiotic treatment. Thus, these confirmed the decline in viable intracellular bacteria with time and the CD treatment confirmed the active nature of bacterial uptake by EBL cells.

**Table 13a. Effect of cytochalasin D at different concentrations on invasion of EBL by *P. multocida* B:2 JRMT12.**

Cytochalasin D (µg/ml)	Bacterial invasion (No. of viable intracellular bacteria/EBL)
0	1.95
1	0.03
2	0.07
4	0.02
8	0.01

Invasion is expressed as no. of viable intracellular bacteria/EBL that resist exposure to polymyxin B and gentamicin each at a final concentration of 50 µg/ml for 1 h after an infection period of 2 h. EBL were pre-exposed to cytochalasin D for 1 h before adding the bacteria. Cytochalasin D was present throughout the experiment.

**Table 13b. Effect of cytochalasin D on invasion of EBL by *P. multocida* B:2 JRMT12.**

Cytochalasin D (µg/ml)	Bacterial invasion (No. of viable intracellular bacteria/EBL)		
	3 h	5 h	7 h
0	0.22 ± 0.07	0.11 ± 0.04	0.01 ± 0.01
1	< 0.0001	< 0.0001	< 0.0001

After cytochalasin D treatment, monolayers were washed 3 times with PBS then treated with bacteria for the standard invasion procedure. Incubation was continued for 5 h and 7 h. Data represent the means (± SEM) of three independent assays with duplicate samples.

### 3.2.6 The transmission electron microscopy (TEM) of the interaction of bacteria with EBL cells

To corroborate the invasive capacity of *P. multocida* B:2 towards mammalian cells and also to investigate intracellular location and possible fate of the bacteria once internalized, samples were taken for TEM after bacterial invasion of the EBL cells, at 2 and 3 h (section 2.19).

EBL cells were treated with either *P. multocida* B:2 (JRMT12), *P. multocida* A3 or *M. haemolytica* A:1 in a 24-well tissue culture plate at MOI 100:1. Samples were taken for fixation with glutaraldehyde and osmium tetroxide after incubation periods of 2 h and 3 h. After dehydration via graded alcohol steps, samples were embedded in epon araldite resin and serial ultra thin sections were stained with uranyl acetate and lead citrate before examination with the LEO 912AB transmission electron microscope.

Micrograph images A and B (Figure 11) show examples of normal EBL cells not infected with bacteria. As early as 2 h after infection, some of the JRMT12 cells were found to adhere closely to EBL membrane. Micrograph C (Figure 11) shows a *P. multocida* B:2 JRMT12 bacterium in the process of being taken up by an EBL cell. Intracellular localization of *P. multocida* B:2 JRMT12 in EBL cells was observed after 3 h of incubation. For example, in micrograph image D (Figure 11), bacteria were shown to be present in the vacuoles of the mammalian cells and many of the internalized bacteria appeared to be ruptured and in the process of degradation. At 2 h after infection, *P. multocida* A3 and *M. haemolytica* A1 were found around the EBL cells either near the surface or not associated with it (Figure 11: E & F). However, a search for intracellular bacteria of these 2 strains proved unsuccessful, in keeping with the apparent lack of uptake of these strains in the previous invasion assays (section 3.2.5.3).

Table 14a shows morphological assessment of 90 EBL cells for each bacterial strain after incubation for 3 h. Out of 90 EBL cells infected with the JRMT12 strain, 11% of the mammalian cells were shown to possess bacteria internally in vacuoles and 29% of the mammalian cells showed closely adherent bacteria around their cell surface. For the other two *Pasteurella* strains, although previous data from the adherence assay showed a similar capacity to adhere to EBL cells as the *P. multocida* B:2 (section 3.2.5.3), from the TEM observations,

only 3% of the EBL cells had adherent *P. multocida* A3 and only 4% of EBL cells had adherent *M. haemolytica*. The reason for this difference is not clear. As noted above, no internalised *P. multocida* A3 or *M. haemolytica* A1 bacteria were detected. In keeping with the results presented in section 3.2.2, 95.96% of EBL cells were viable by trypan blue staining at the time that the samples were taken for TEM.

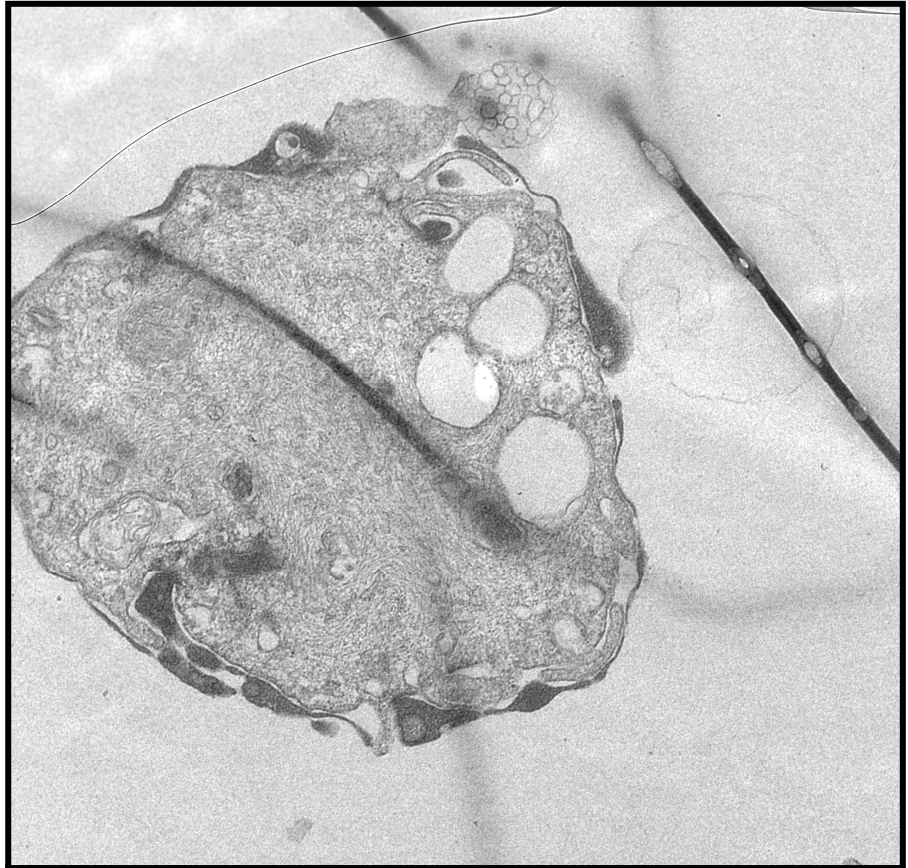
EBL cells infected with strain JRMT12, as reported in Table 14a, were scrutinized closely in the electron microscope to determine the approximate number of bacteria per individual EBL cell (Table 14b). Out of 90 EBL cells containing bacteria only 3% possessed between 12 and 16 visible bacteria and 8% between 2 and 8 visible bacteria. Thus, 89% of the mammalian cells appeared to have no intracellular bacteria in these thin sections. This agrees with the data in Tables 7, 8 and 9 from the invasion assays which showed an average of between 0.8 and 1.5 bacteria per EBL cell. The TEM data showed that <10% of EBL cells actually internalised bacteria but, when they did, several bacteria were present.

**Figure 11. TEM micrographs of EBL cells infected with bacteria.**

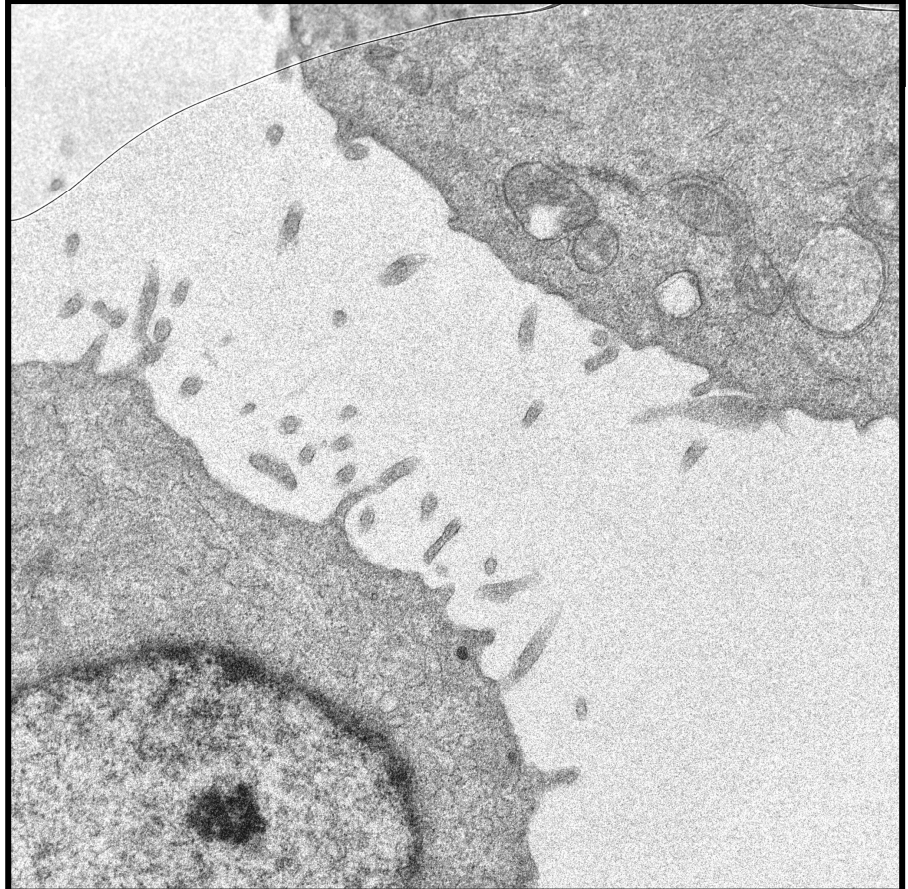
EBL cells were infected with *P. multocida* B:2 JRMT12, *P. multocida* A3 and *M. haemolytica* A1 at MOI 100:1 (bacteria per cell). Cells were centrifuged at 1200 x g for 3 min and incubated for 2 h. This was followed by washing of the cells to remove most of the extracellular bacteria and prepared for TEM at 2 h (A, C, E & F). In some experiments, after washing, cells were further incubated for 1 h with media supplemented with P&G at a final concentration of 50 µg/ml. Cells were then washed and prepared for TEM at 3 h (B & D). The main features to note are the localization of intracellular bacteria and non-internalized bacteria.


- A:** EBL cells after 2 h of incubation. Normal appearance of the cell with existing vacuoles.
- B:** EBL cells after 3 h of incubation.
- C:** An EBL cell infected with *P. multocida* B:2 JRMT12 at MOI 100:1 after 2 h of incubation. The bacterium is adhering to the EBL cell surface and EBL cell shows extended membrane projections in the process of engulfing it (arrowed).
- D:** An EBL cell infected with *P. multocida* B:2 JRMT12 at MOI 100:1 after 3 h of incubation. Bacteria localized in the vacuoles of an EBL cell (arrowed).
- E:** An EBL cell infected with *P. multocida* A3 at MOI 100:1 after 2 h of incubation. Arrows show extracellular bacteria around the EBL cell.
- F:** An EBL cell infected with *M. haemolytica* A1 at MOI 100:1 after 2 h of incubation. Arrows show extracellular bacteria around the EBL cell.

A



B

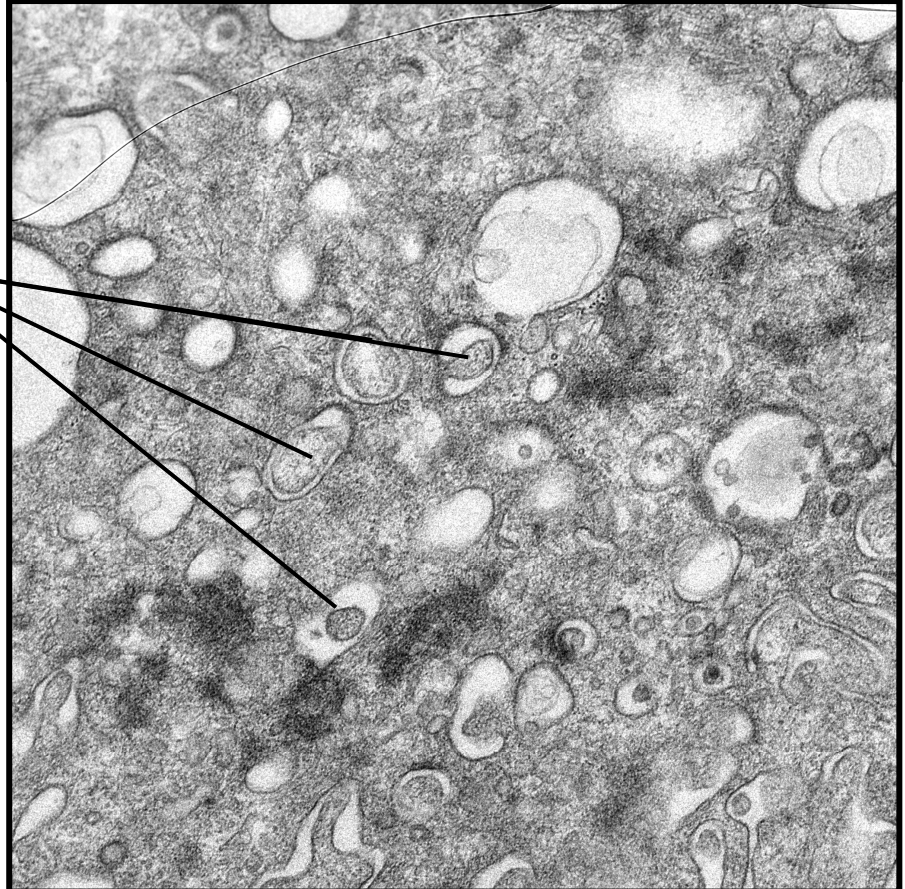


Microscope	Accelerating Voltage	Energy Loss	Magnification	Scale Bar
	-	-	-	—1 $\mu$ m—

C



D



Microscope Accelerating Voltage Energy Loss Magnification

-

-

-

-

1  $\mu$ m

E



F

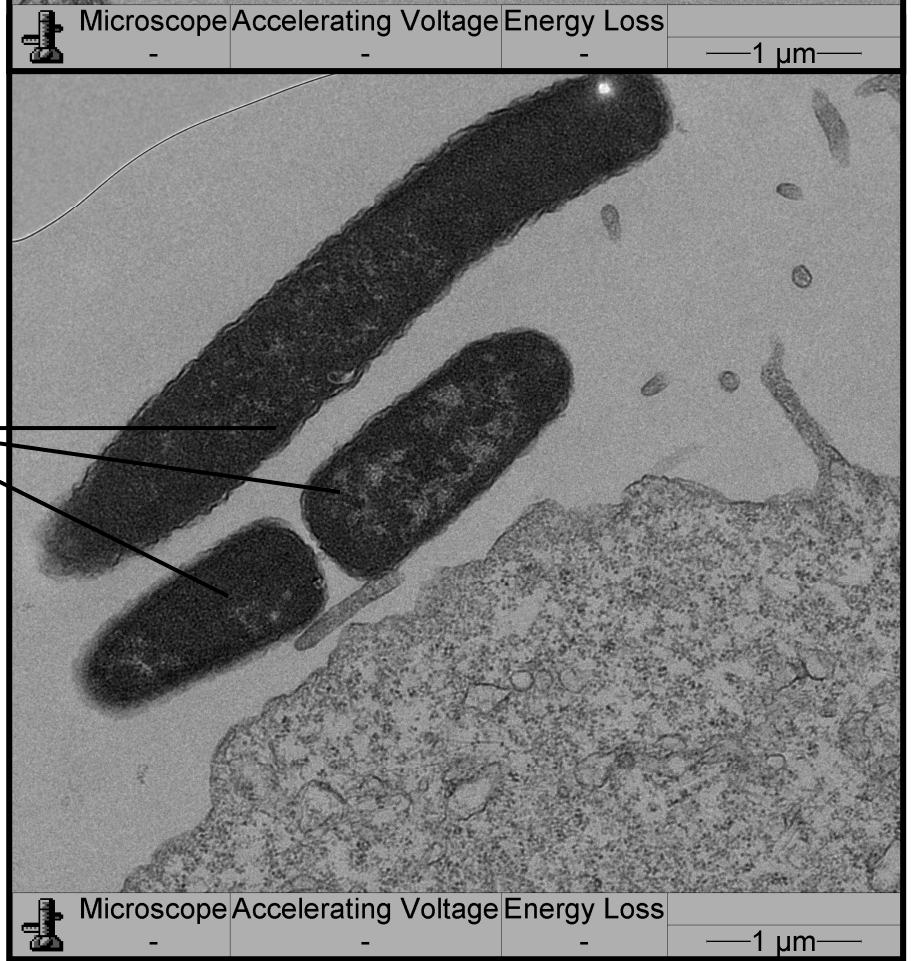




**Table 14a. Assessment of the morphological features seen by TEM micrographs after infection of EBL cells with different *Pasteurellaceae* strains at MOI 100:1.**

Treatments	Intracellular localisation of bacteria	Percentage of EBL cells with intracellular bacteria in the vacuoles	Percentage of non-viable EBL	Percentage of EBL with bacteria attached on the outer surface
<i>P. multocida</i> B:2 JRMT12 + EBL	Observed	11 ± 2	5 ± 1	29 ± 14
<i>P. multocida</i> A:3 + EBL	----	----	5 ± 1	3 ± 1
<i>M. haemolytica</i> A:1 + EBL	----	----	4 ± 0	4 ± 4
EBL only	----	----	4 ± 0	----

Cells were centrifuged briefly after mixing and incubated for 2 h. After removal of most of the extracellular bacteria by washing, EBL assay medium with P&G at final concentrations of 50 µg/ml was added to the cells and incubation continued for 1 h. Samples for TEM were taken after 3 h of incubation. For each strain, 90 individual EBL cells were examined. Cells were assessed to be non-viable if the cell membrane was discontinuous or ruptured. Data represent the means (± SEM) of three independent assays with duplicate samples.

---- Not found

**Table 14b. Percentage distribution of total intracellular *P. multocida* B:2 JRMT12 within 90 individual EBL at 3 h after challenge.**

No. of <i>P. multocida</i> B:2 JRMT12 within individual EBL	Percentage of total number of EBL
0	89
1	0
2	3
3	1
8	4
9	0
10	0
11	0
12	1
13	0
14	0
15	1
16	1

Cells were briefly centrifuged after mixing and incubated for 2 h. After removal of most of the extracellular bacteria by washing, EBL assay media with P&G at final concentration of 50 µg/ml were supplemented to the cells and incubated for 1 h. Samples for TEM were taken for fixation at this point. 90 individual EBL cells were examined.

To conclude the first part of the study, it was confirmed that both *P. multocida* B:2 strains were capable of adhering to and invading J774.2, BL-3 and EBL cells. It was also noted that, although all *Pasteurella* strains tested were able to adhere to EBL cells, only the B:2 strains were taken up intracellularly. *P. multocida* B:2 JRMT12 was able to survive intracellularly for at least 7 h although a steady decline of the number of viable intracellular bacteria was noted with time. The use of the actin microfilament formation inhibitor cytochalasin D indicated that the entry into mammalian cells might be by actin-dependant process even in the non-phagocytic EBL cell line. From the cell viability assessment, mammalian cells were shown to be free from toxicity due to the pathogens added. TEM micrographs for strain JRMT12 showed bacteria both closely-associated with the cell surface and also located intracellularly, with most bacteria found in the vacuoles of the mammalian cells after 3 h of incubation. The other 2 strains of *Pasteurella* used were not detected intracellularly but were found loosely adhering at the cell surface of EBL cells after 2 h of incubation. Further, morphological assessment by TEM showed JRMT12 apparatus co-localising in a low percentage of mammalian cells rather than being invasive individually towards the majority of mammalian cells. These observations on the fate of *P. multocida* B:2 JRMT12 upon interaction with EBL cells were important preliminary observations that established that the B:2 strain should act as a suitable carrier vehicle to deliver plasmids to mammalian cells.

### 3.3 Construction of a *Pasteurella* eukaryotic expression plasmid

In order to develop a bactofection system for *P. multocida* B:2 JRMT12, one needs to understand the fate of the plasmid carried by the bacterium after it enters into mammalian cells. This understanding would be enhanced by actual visualization of fluorescence proteins from reporter genes. To achieve this, a eukaryotic expression plasmid that can stably replicate in *P. multocida* B:2 JRMT12 is needed for fluorescent protein expression in mammalian cells.

Eukaryotic expression plasmids have long been developed to study intracellular trafficking in mammalian cells and also for intracellular protein expression. A range of commercial plasmids has been designed to assist in achieving these purposes. They are mostly derivatives that carry a eukaryotic promoter for protein expression within the mammalian cell coupled to a ColE1 origin of replication that allows manipulation and propagation in *E. coli*. However plasmids originated with either ColE1 or pUC-based replication functions have not been reported to replicate in *Pasteurellaceae* family.

This section explains the strategy for developing a eukaryotic expression plasmid that can replicate and be maintained in *Pasteurella*. As illustrated in Figure 12, two plasmids were manipulated in this strategy to develop a *Pasteurella* eukaryotic expression plasmid, pSJR. Plasmid pAKA16 (Azad *et al.*, 1994) is a shuttle cloning plasmid developed in this laboratory for gene transfer to *M. haemolytica* and *P. multocida*. This plasmid was derived from a bovine isolate of *M. haemolytica* serotype A1 and was proven for its stability and ready amplification in *E. coli* and high mobilization frequency to *M. haemolytica* (Azad, 1992). Plasmid pCMV-sCRIPT (Stratagene, UK) is derived from a high-copy number pUC-based plasmid and is designed to allow replication in *E. coli* and replication and protein expression in mammalian systems.

#### 3.3.1 Inability of plasmid pCMV-sCRIPT to replicate in *P. multocida* B:2 JRMT12

Plasmid pCMV-sCRIPT was electroporated into *P. multocida* B:2 JRMT12 (section 2.13.2). No colonies were detected on the antibiotic selection agar after incubation for 24 h after electroporation. The experiment was repeated several

times and each experiment included a control *Pasteurella* plasmid, pAKA16, electroporated into the same electro-competent host used. The control plasmid was successfully recovered from *P. multocida* after each experiment. This was taken as confirmation that plasmid pCMV-sCRIPT, which is a pUC-based plasmid, failed to replicate and to be maintained stably in *P. multocida* B:2 JRMT12.

### 3.3.2 Development of plasmid pSJR

#### 3.3.2.1 Isolation of *Pasteurella* origin of replication (*oriP*) from pAKA16

From the strategy (Figure 12), the origin of replication for the *Pasteurella* plasmid, *oriP* needed to be isolated from plasmid pAKA16 and ligated into plasmid pCMV-sCRIPT. Based on the pAKA16 map that Azad (1992) developed, several restriction enzymes were selected in order to isolate the *oriP* region. Restriction enzymes *Apa*LI, *Nde*I and *Ava*I were used to isolate the *oriP* region. However, after determination of plasmid size by gel electrophoresis after digestion, inaccuracies in location or existence of the restriction enzyme sites were detected and only undigested plasmids were recovered.

As shown in Figure 12, *Pst*I sites (fuchsia lines) are located at one side of the *mob* gene and another one is in the multiple cloning site (MCS) of pAKA16. After digestion and agarose gel electrophoresis analysis, a *Pst*I fragment containing the *oriP* gene (1800 bp) was visible (Figure 13). The fragment was purified for further manipulation.

#### 3.3.2.2 Characterisation of *oriP* locus

In order to sequence the *oriP* locus, primers were designed based on the only known sequence on the *oriP* fragment, the multiple cloning site (MCS). The MCS that was cloned in by Azad (1992) in developing plasmid pAKA16 was originally from plasmid pIC2OH and the full sequence of the MCS was published by Marsh *et al.* (1984). The location of the MCS is at one end of the *oriP* fragment. By using inverse PCR, possibilities to sequence the whole fragment and introduce required restriction enzyme sites were higher. The *oriP* *Pst*I fragment from pAKA16 was ligated as described in section 2.12.2.2 and used as a template for inverse PCR (section 2.8.4) with inverse PCR primers (Table 5). PCR products were purified and cloned into plasmid pGEM-T-EASY™ (section 2.12.1.1).

Figure 12. Cloning strategy: Development of plasmid pSJR.

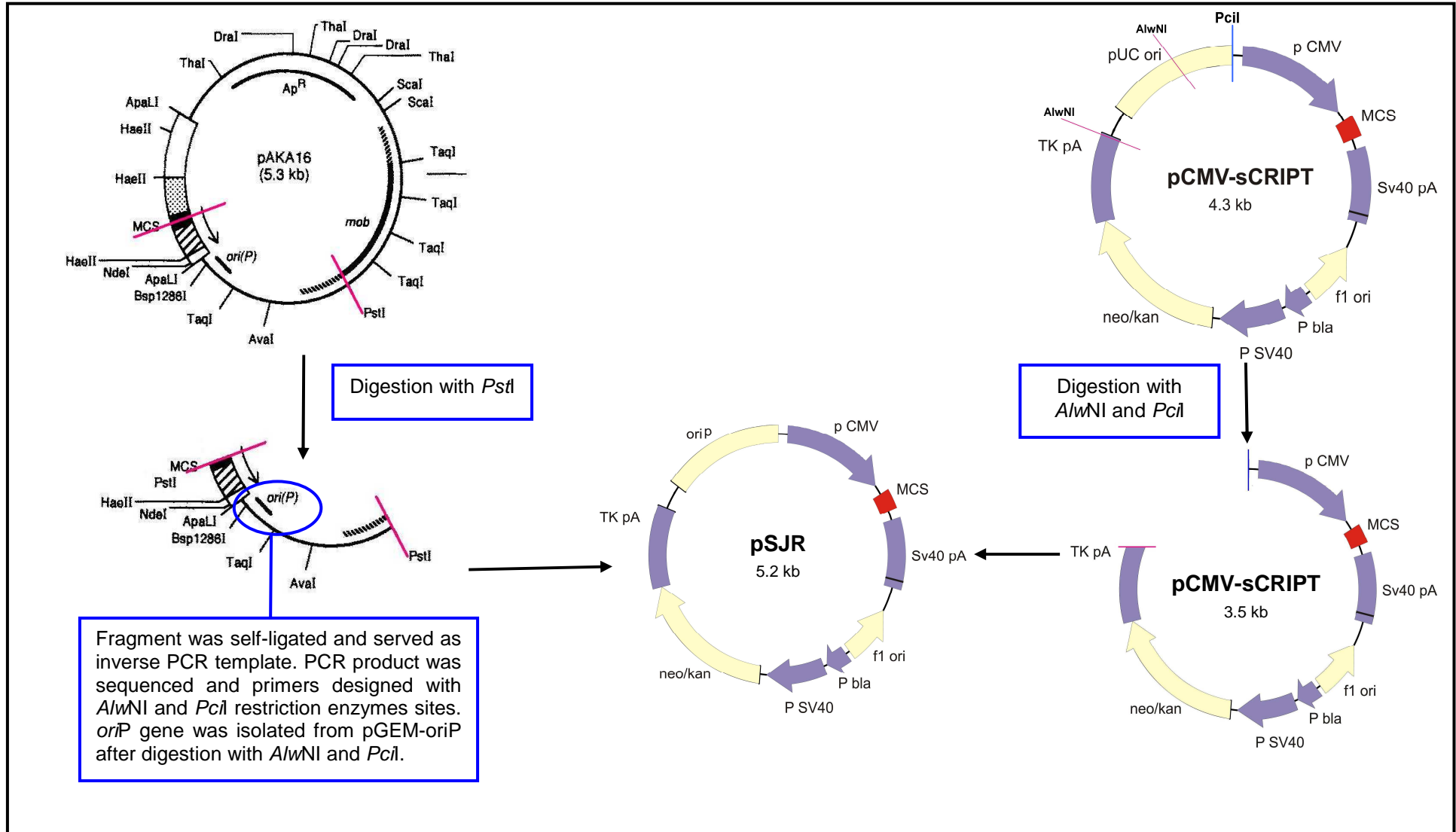
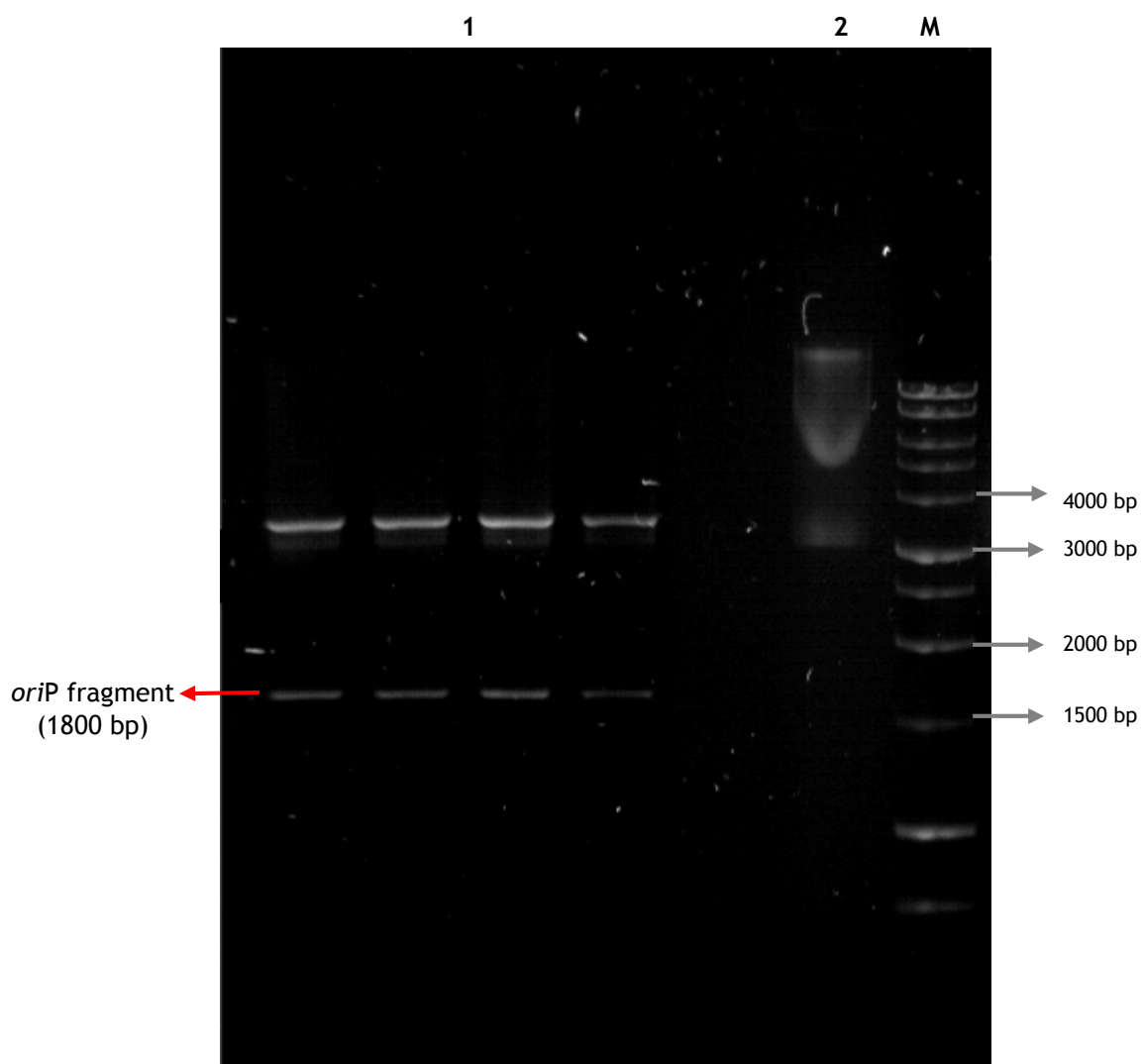


Figure 13. Agarose gel showing plasmid pAKA16 digested with *Pst*I.



1: Digested pAKA16 with *Pst*I

2: Undigested pAKA16

M: 1 kb DNA ladder

After transformation into *E. coli* DH5 $\alpha$ , positive transformants were selected from the antibiotic selection plate. Plasmid purification and restriction enzyme analysis were executed to confirm the existence of the *oriP* fragment in the resulting plasmid, pGEM-*oriP* (Figure 14).

The *oriP* gene was sequenced with inverse PCR primers and sequencing results were then analyzed with BioEdit (ver. 7.9.0) and sequences were compared in NCBI databases using BLAST (Figure 15). Six colour indicators were used to describe the sequence. The sequence in the yellow box was recognized as part of the MCS and *lacZ* gene from pIC20H and the sequence upstream of this part of the fragment was used to design the inverse PCR primers (A and B). The blue boxes highlighted open reading frames (ORF) found in this fragment. The first ORF was found just before the sequence in grey box and the second ORF was located just before the sequence in the purple box. The sequences in these boxes are designated as the putative *oriP* gene. This assumption is supported with further evidence of an homologous region from the sequence in the red box towards similar sequences in the origin of replication from other *Pasteurella* plasmids. This was confirmed when the sequence of the whole fragment was compared with origin of replication from plasmid pJR1 (AY232670) from *P. multocida*, plasmid pD70 (DQ125466) from *M. haemolytica*, plasmid pIG1 (U57647) from *P. multocida* and plasmid pAB2 (Z21724) from *M. haemolytica*. Numbers in bracket indicate PubMed accession numbers. All plasmids showed a 99% match towards the sequence in the red box. A direct repeat was also recognized in the middle of the homologous sequence (green box).

Direct repeats and inverted repeats (not found in this sequence) are some of the distinctive traits characteristic of the origin of replication in *Pasteurella* plasmids. After nucleotide BLAST analysis, the sequence in the purple box was highly matched with part of the mobilization gene, *mbeAy* from plasmid pIG1 (U57647). The top un-highlighted sequence of the fragment was equivalent to the sequence in the ROB  $\beta$ -lactamase region in plasmid pAB2 (Z21724). This possible designation was supported by the strategy used in developing plasmid pAKA16 (Appendix 6) which showed that the MCS of pIC20H was cloned in near to the  $\beta$ -lactamase region of the original plasmid.



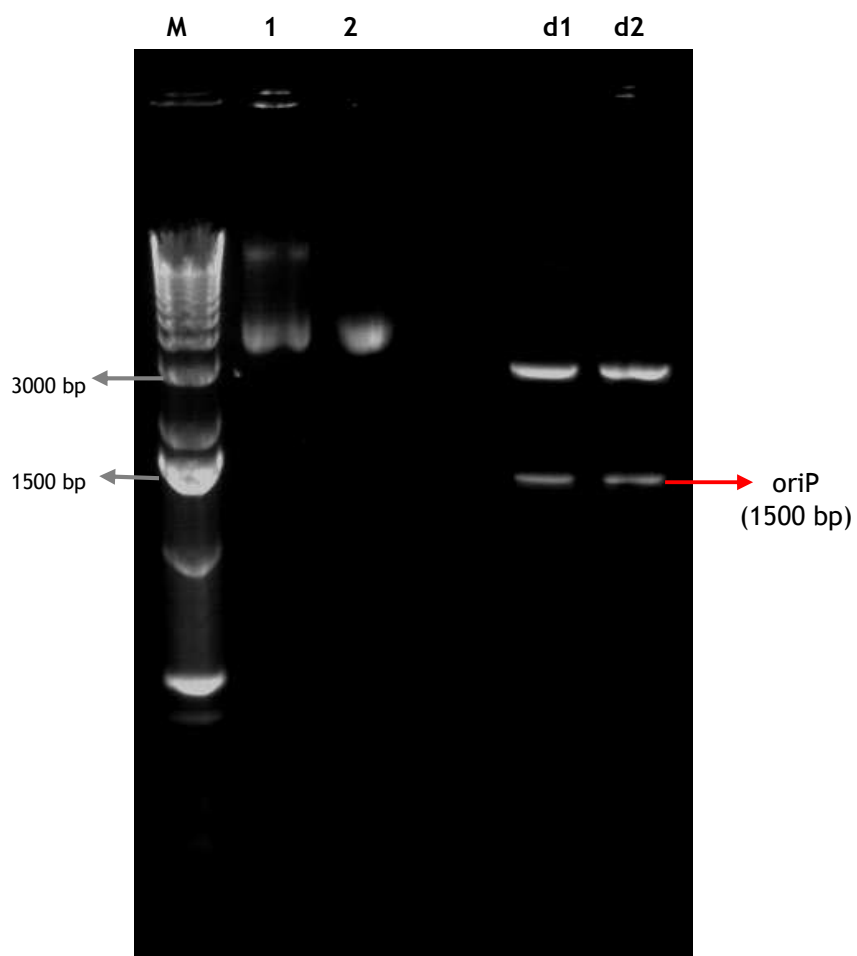
### 3.3.2.3 Isolation of the *oriP* gene from *oriP* fragment

The strategy outlined in Figure 12 shows that the *oriP* fragment from the inverse PCR product was cloned into plasmid pGEM-T-EASY™ (section 2.12.1.1). A new set of primers were designed based on the *oriP* fragment sequence (Figure 15). The primers sequences are underlined as indicated in the figure legend. In order to facilitate ligation of the *oriP* insert into plasmid pCMV-sCRIPt, restriction enzyme sites were incorporated into the *oriP* primers. An *AlwNI* site was included into the forward *oriP* primer and a *PciI* site was included into the reverse *oriP* primer. PCR was performed as in section 2.8 and PCR products were purified and cloned into plasmid pGEM-T-EASY™ (2.12.1.1). Positive transformants (pGEM-P) were digested with both restriction enzymes, *AlwNI* and *PciI*. After analysis with agarose gel electrophoresis, a ~400 bp band was identified and purified. This band represented the digested *oriP* gene ready for ligation into pCMV-sCRIPt (Figure 16a).

### 3.3.2.4 Removal of pUC origin of replication (*oriE*) from pCMV-sCRIPt

As shown in Figure 12, the *oriE* locus was removed from pCMV-sCRIPt using restriction enzyme digestion. Enzyme *AlwNI* cuts twice at the *oriE* locus at 3409 bp and 3817 bp and the enzyme *PciI* cuts at 4909 bp. Double digestion with both of these enzymes removed the whole *oriE* gene from the plasmid. Digested pCMV-sCRIPt was then dephosphorylated with calf intestinal alkaline phosphatase (CIAP) and purified, before ligation with the *oriP* locus cut from pGEM-P (Figure 16b).

The *oriP* gene prepared as above was ligated with prepared pCMV-sCRIPt. Numerous attempts at ligation were done but after transformation or electroporation, either in *E. coli* or *P. multocida*, positive transformants were never recovered. Thus, either the ligation failed to work or the putative *oriP* locus was unable to function as a replication origin. The latter possibility is more likely, as gel analysis of the ligation mixture showed an obvious higher molecular weight band at 3900 bp as well as the 400 bp fragment of *oriP* and the 3500 bp fragment of pCMV-sCRIPt (data not shown).

**Figure 14. Agarose gel showing pGEM-oriP digested with *Eco*RI.**

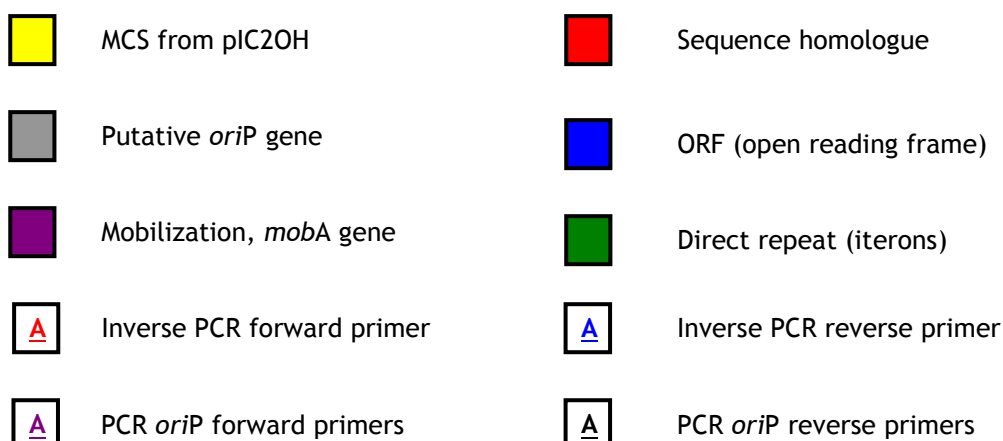
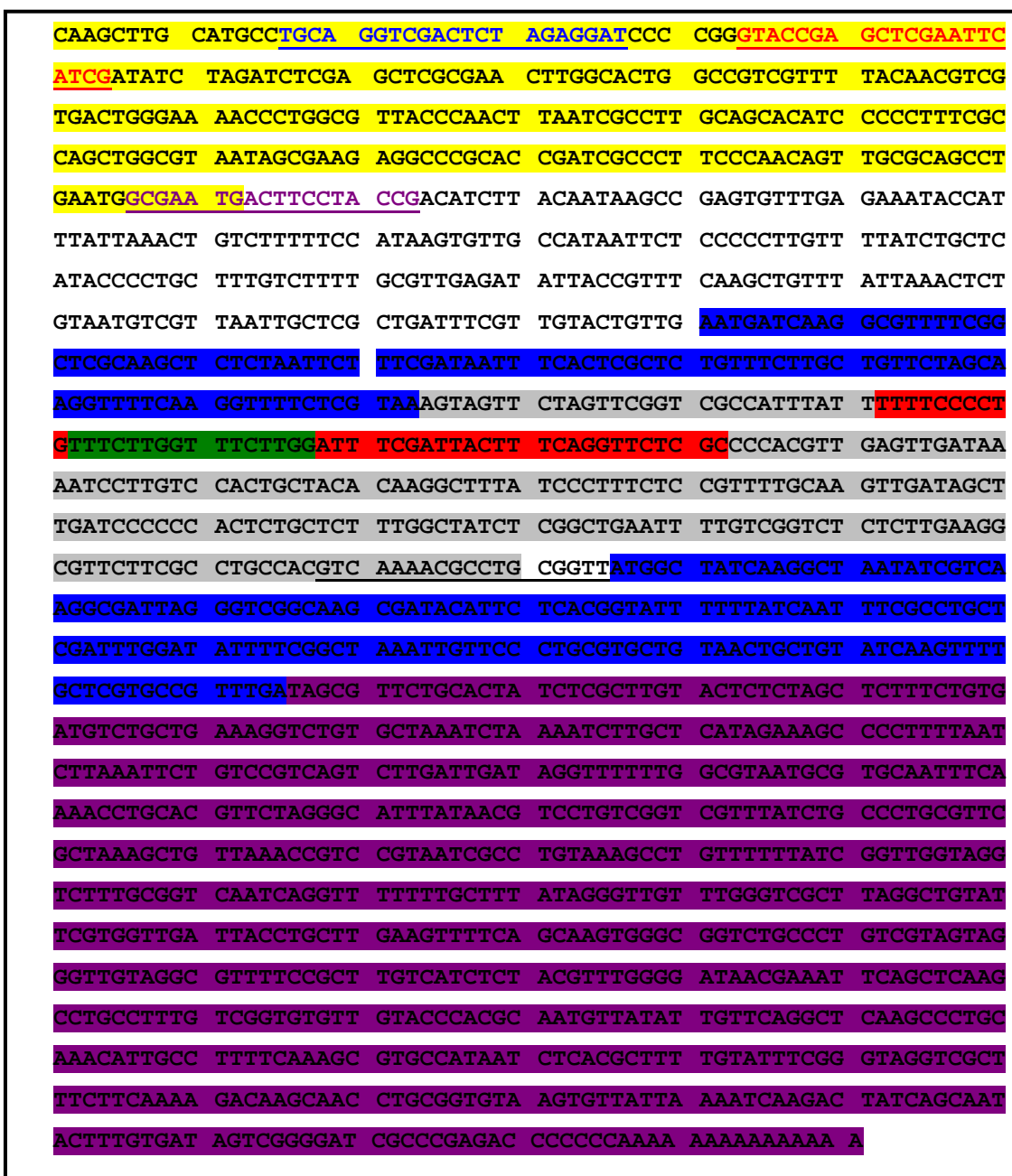
**M:** 1 kb DNA ladder

**1:** undigested pGEM-oriP

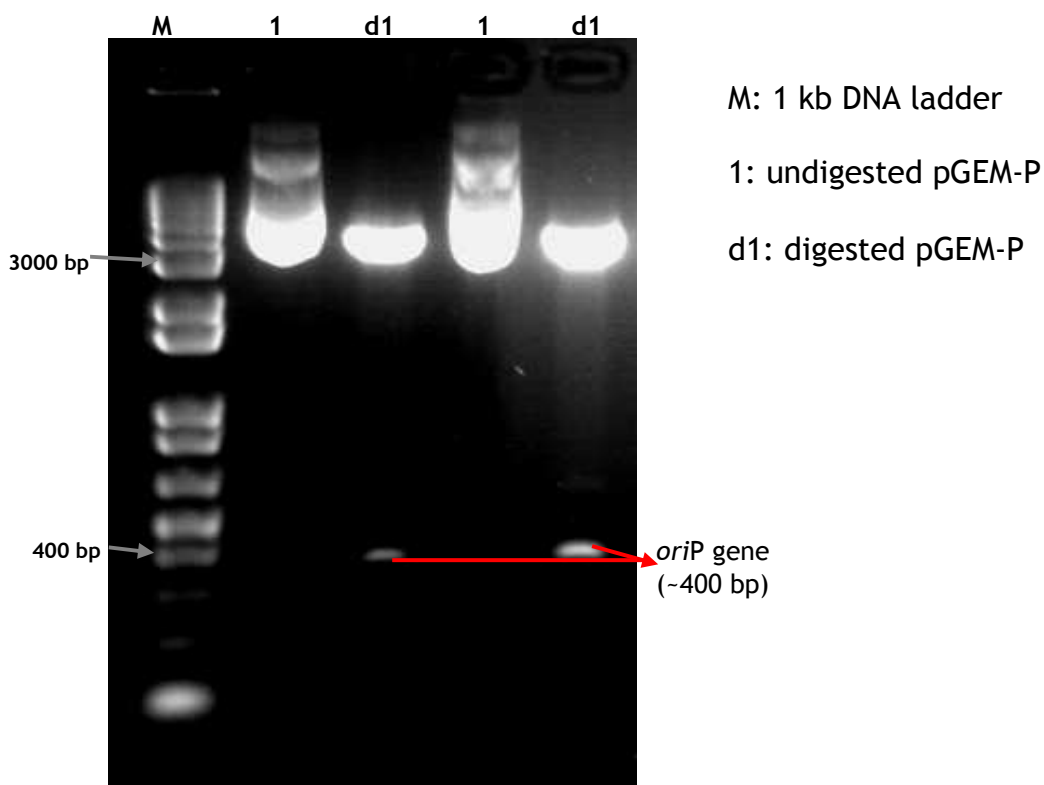
**2:** undigested pGEM-oriP

**d1:** digested pGEM-oriP

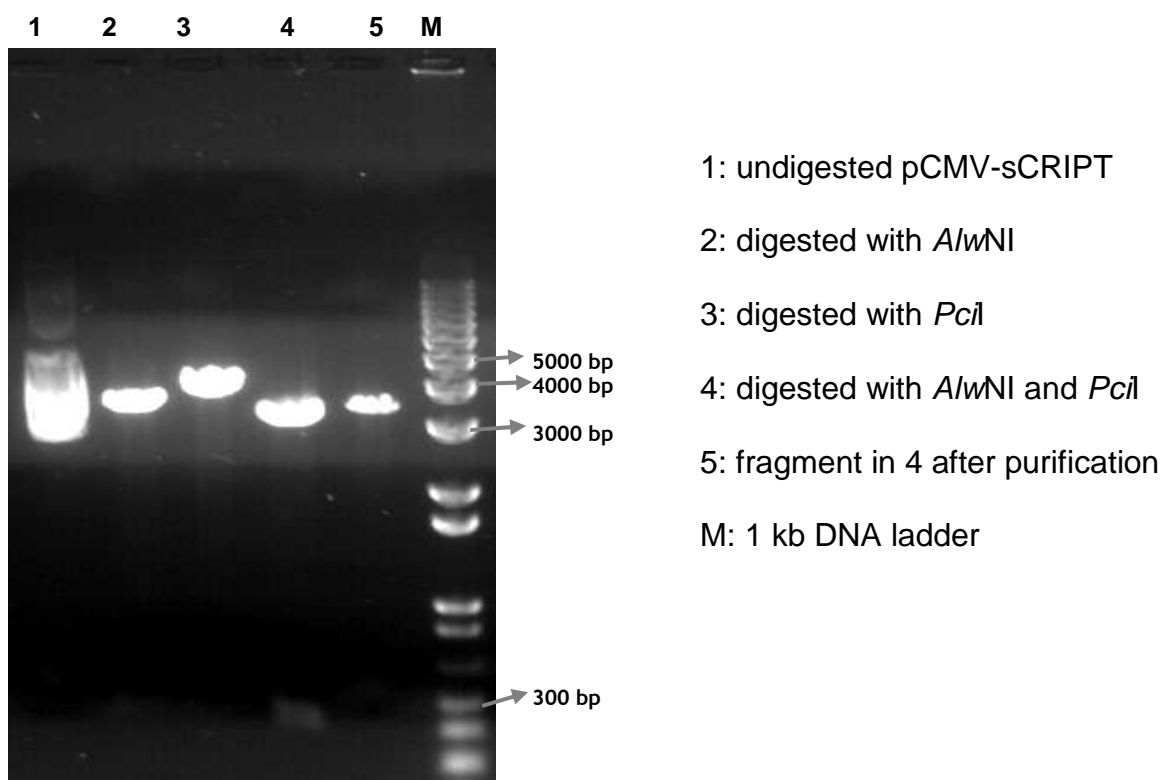
**d2:** digested pGEM-oriP

Figure 15. Sequence of *oriP* fragment.

**Figure 16a. Agarose gel electrophoresis of *oriP* gene removed from pGEM-P with *A/wNI* and *PciI*.**



**Figure 16b. Agarose gel electrophoresis of pCMV-sCRIPT after digestion with *A/wNI* and *PciI*.**



### 3.3.3 Analysis of pUC base eukaryotic expression plasmid, pEGFP-N1™

After numerous attempts to develop a *Pasteurella* eukaryotic expression plasmid from pCMV-sCRIPt had been unsuccessful, it was decided to change to another eukaryotic expression plasmid. The plasmid pEGFP-N1™ (Clontech, US) (Appendix 4) was available in the laboratory. The plasmid has a similar backbone to pCMV-sCRIPt but, in addition to that, it incorporated a reporter gene, EGFP, downstream of the viral immediate early promoter of cytomegalovirus (CMV). The EGFP gene encodes a red-shifted variant of wild type green fluorescent protein (GFP) which has been optimized for brighter fluorescence and higher expression in mammalian cells (excitation wavelength (Exc.) = 488 nm and emission wavelength (Ems.) = 507 nm). A MCS is located upstream of EGFP gene and a gene cloned here will be expressed as a fusion to the N-terminus of EGFP. However EGFP can still be expressed from the eukaryotic promoter individually without any protein coding gene fused at its N-terminal end.

#### 3.3.3.1 Electroporation into *P. multocida* B:2 JRMT12 and *E. coli* XL-1 Blue

Although previous work had indicated that pCMV-sCRIPt was unable to replicate in *Pasteurella*, it was decided to conduct a more thorough examination with pEGFP-N1 in the hope that a few break-through clones would be detected that managed to overcome the replication barrier in *Pasteurella*. In order to detect the ability of plasmid pEGFP-N1™ to replicate and survive stably in *P. multocida* B:2 JRMT12, the plasmid was electroporated into this strain (2.13.2). Electroporation was also done, in parallel, with plasmid pAKA16 as a control and positive transformant were readily selected. With pEGFP-N1™, however, no colonies were detected on the antibiotic selective agar after 18 h of incubation at 37°C. However, when the plate was further incubated up to 36 h, small colonies were detected from the antibiotic (Km 50 µg/ml) selection plate. A dozen colonies were selected and transferred onto a duplicate plate and incubated for another 36 h. They were then transferred into BHI broth (Km 50 µg/ml) and incubated overnight at 37°C with shaking at 180 rpm. Plasmid DNA was purified from individual cultures and analyzed with restriction enzyme digestion. All the 12 colonies originally selected proved to harbour plasmid pEGFP-N1™.

Electroporation was then repeated using several types of plasmid, pEGFP-N1™ purified from *P. multocida* B:2 JRMT12, pEGFP-N1™ purified from *E. coli* XL-1 Blue, pGEM-oriP (section 3.3.2.2), pCMV-sCRIPt and pAKA16 (as a positive control). The experiment was repeated, first, to confirm the repetition of previous electroporation, and second, to assess whether pEGFP-N1™ purified from *P. multocida* B:2 JRMT12 was able to replicate more easily in *Pasteurella* than the original plasmid and produce faster-growing colonies. This would determine if any modification had been made towards the plasmid after replication in the mutant strain. In addition, this repeat experiment would verify whether or not pGEM-oriP and pCMV-sCRIPt would manage to replicate in JRMT12. In parallel, all the above plasmids were also electroporated into *E. coli* XL-1 Blue.

After electroporation, positive transformants were selected from BHI agar (*P. multocida* B:2 JRMT12) or LB agar (*E. coli* XL-1 Blue) supplemented with either ampicillin (50 µg/ml) for plasmid pAKA16 and pGEM-oriP or kanamycin (50 µg/ml) for plasmid pEGFP-N1™ and pCMV-sCRIPt. Observation after 18 h of incubation showed that all plasmids were successfully electroporated into *E. coli* XL-1 Blue without any significant difference in the number of colonies on individual selective plates. For *P. multocida* B:2 JRMT12, colonies were detected only with pAKA16 after incubation for 18 h. When incubation was extended to 36 h, small colonies started to be visible on all other plates including those with plasmid pCMV-sCRIPt, and at a similar number (data not shown).

Plasmid pEGFP-N1™ either purified from *P. multocida* B:2 JRMT12 or from *E. coli* XL-1 Blue, and electroporated into the mutant strain, showed no significant difference in either the number of colonies formed or the rate of colony formation on the selective agar plates after 36 h. After plasmid purification and restriction enzyme digestion analysis, it was proven that all plasmids were successfully electroporated into *P. multocida* B:2 JRMT12 and *E. coli* XL-1 Blue.

### 3.3.3.2 Plasmid stability in *P. multocida* B:2 JRMT12

Plasmid pEGFP-N1™ has the advantage of harbouring a fluorescence reporter gene, *gfp* (EGFP) downstream of its immediate early viral expression promoter (<sup>P</sup>CMV<sub>IE</sub>). Hence, among the plasmids tested above in section 3.3.3.1, this

plasmid is a more suitable candidate for following the fate of the plasmid after bacterial invasion into the intracellular compartment of mammalian cells. Therefore, *P. multocida* B:2 JRMT12 pEGFP-N1<sup>TM+</sup> was tested for its stability to harbour pEGFP-N1<sup>TM</sup>.

*P. multocida* B:2 JRMT12 pEGFP-N1<sup>TM+</sup> was plated onto a BHI agar with and without kanamycin (50 µg/ml). After incubation for 24 h, selected colonies were picked from both plates and were streaked onto fresh plates. After a further 24 h, a dozen colonies were picked from both plates and inoculated into BHI broth with or without kanamycin (50 µg/ml) respectively. Plasmids were purified and analyzed by restriction enzyme digestion for confirmation of identity. Strains were subcultured everyday for 14 days and plasmids were purified and analyzed every alternate day. After 14 days, all 12 colonies of *P. multocida* B:2 JRMT12 pEGFP-N1<sup>TM+</sup> taken from BHI agar without antibiotic were found to be still harbouring the plasmid, pEGFP-N1<sup>TM</sup>. This demonstrates that pEGFP-N1<sup>TM</sup> was stable in *P. multocida* B:2 JRMT12 even in the absence of an antibiotic selection.

#### 3.3.3.3 Growth curve of *P. multocida* B:2 JRMT12 pEGFP-N1<sup>TM+</sup>

The growth curve of *P. multocida* B:2 JRMT12 pEGFP-N1<sup>TM+</sup> was compared to the *E. coli* XL-1 BLUE pEGFP-N1<sup>TM+</sup> strain. Figure 17, graph A shows the growth curves of *P. multocida* B:2 JRMT12 pEGFP-N1<sup>TM+</sup> cultured in BHI broth supplemented with kanamycin (50 µg/ml) and *E. coli* XL-1 BLUE pEGFP-N1<sup>TM+</sup> cultured in LB broth supplemented with kanamycin (50 µg/ml). Both strains showed a similar pattern in their growth curve. Next, *P. multocida* B:2 JRMT12 and *P. multocida* B:2 JRMT12 pEGFP-N1<sup>TM+</sup> were compared. In parallel, the mutant strain harbouring the plasmid was cultured in BHI broth with and without kanamycin (50 µg/ml) and the mutant strain without plasmid was cultured in BHI broth without antibiotic.

Graph B shows that as expected, the mutant strain without plasmid entered exponential phase more quickly than the mutant strain harbouring pEGFP-N1<sup>TM</sup>. However, comparison of *P. multocida* B:2 JRMT12 pEGFP-N1<sup>TM+</sup> growth in BHI broth with and without antibiotic supplementation showed that the strain cultured in media without antibiotic entered exponential phase slightly quicker than the strain cultured in media supplemented with antibiotic, though the difference in the exponential phase was insignificant. The presence of plasmid in

*P. multocida* B:2 JRMT12 pEGFP-N1<sup>TM+</sup> was determined at the end of this experiment from both conditions. In fact, cells harvested at the same OD<sub>600nm</sub> showed the presence of pEGFP-N1<sup>TM</sup> DNA at similar concentrations (data not shown). These findings demonstrated that *P. multocida* B:2 JRMT12 was able to stably maintain pEGFP-N1<sup>TM</sup>, even without the presence of kanamycin, for at least 14 days.



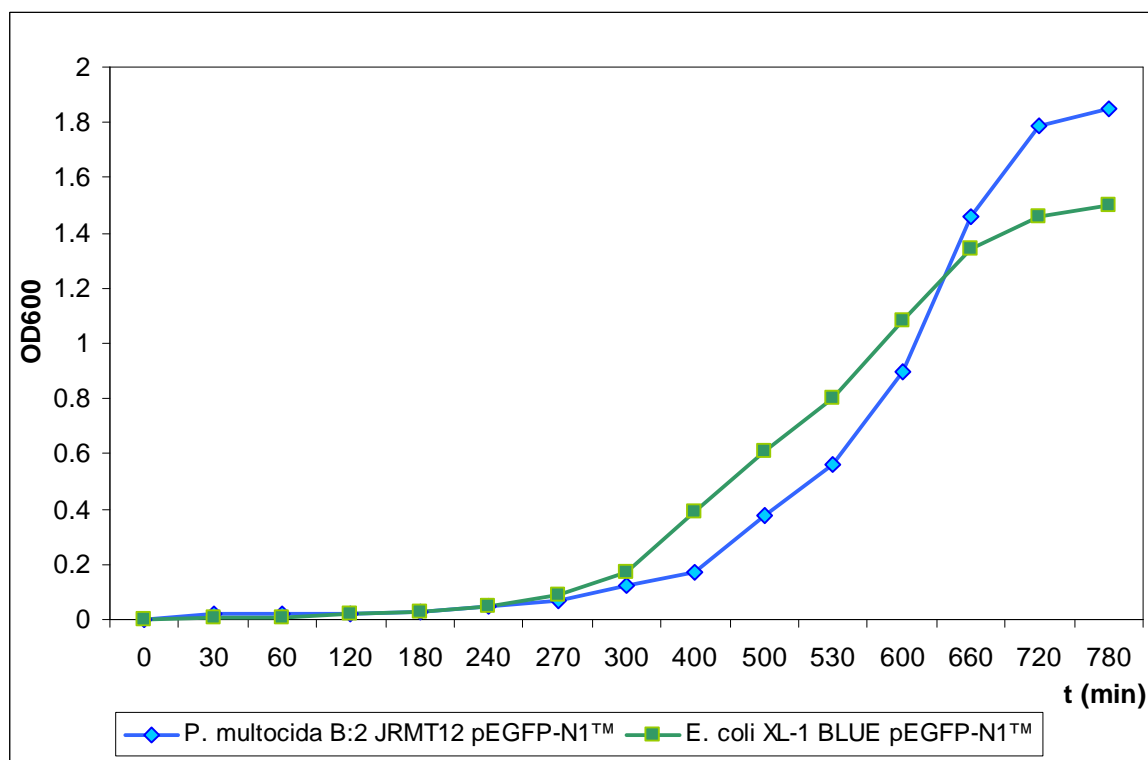
**Figure 17. Growth curves of *P. multocida* B:2 JRMT12 pEGFP-N1<sup>TM+</sup>.**

Overnight cultures were diluted to OD<sub>600nm</sub> ~0.08 with sterile media (BHI broth for *P. multocida* and LB broth for *E. coli*). 1 ml of culture was removed at regular intervals and OD<sub>600nm</sub> measured, the remaining culture was incubated at 37°C. Readings were taken until the growth cultures entered stationary phase. All experiments were done in parallel.

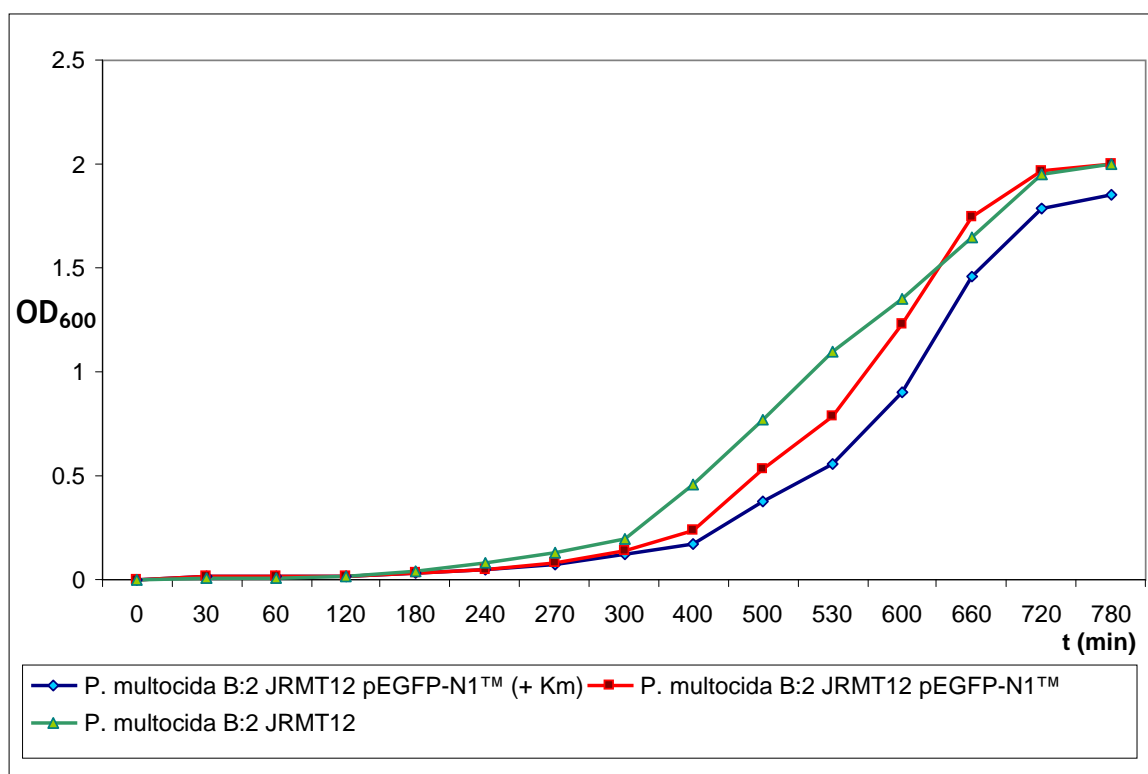
Graph A shows a comparison of *P. multocida* B:2 JRMT12 pEGFP-N1<sup>TM+</sup> with *E. coli* XL-1 BLUE pEGFP-N1<sup>TM+</sup>. Strains were cultured with BHI broth supplemented with kanamycin (50 µg/ml) or LB broth supplemented with kanamycin (50 µg/ml), respectively.

Graph B shows a comparison of *P. multocida* B:2 JRMT12 and *P. multocida* B:2 JRMT12 pEGFP-N1<sup>TM+</sup>. The mutant strain harbouring pEGFP-N1<sup>TM</sup> was cultured in BHI broth with and without kanamycin (50 µg/ml) and the mutant strain without plasmid was cultured in BHI broth without antibiotic.

A



B



## 3.4 Development of the *P. multocida* B:2 bactofection model system

### 3.4.1 Characterisation of plasmid pEGFP-N1™ in mammalian cells

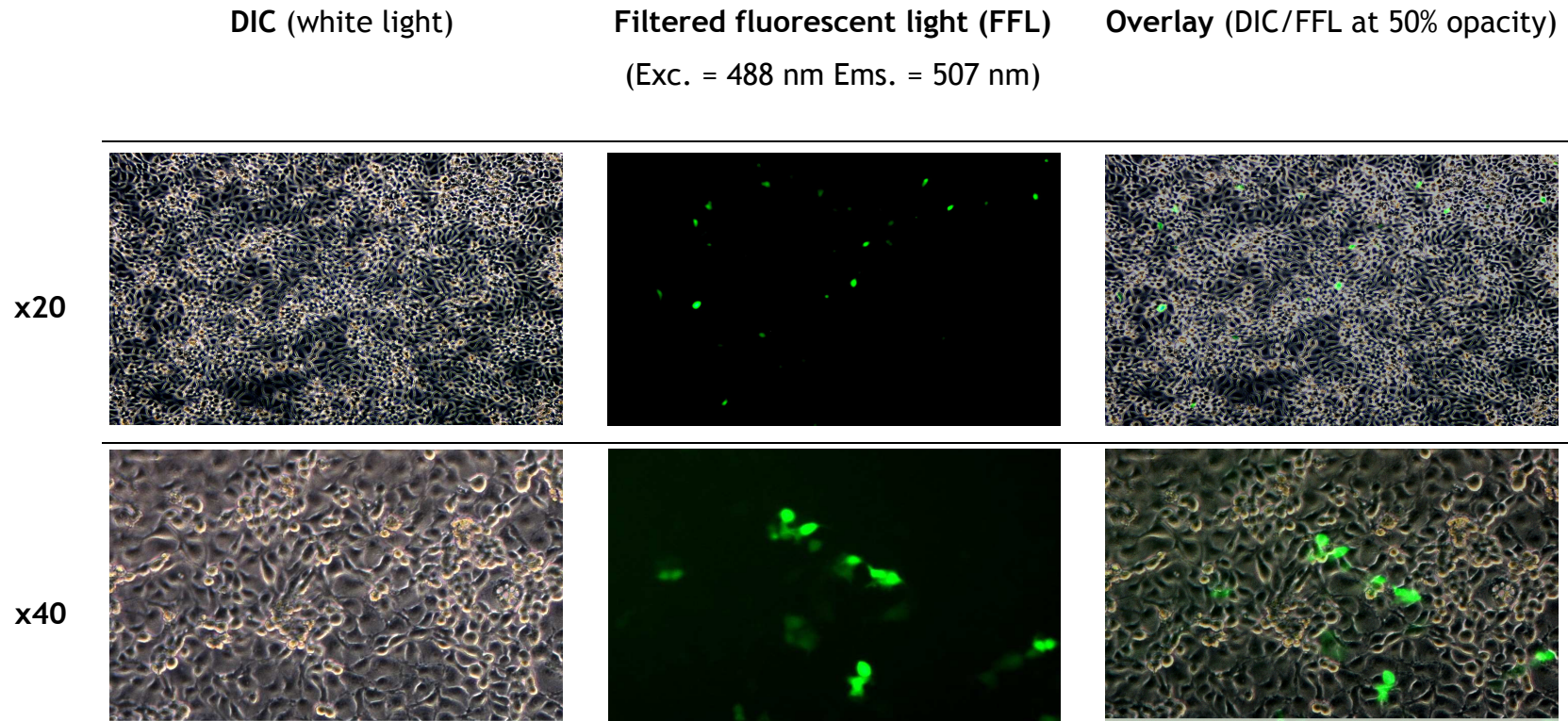
#### 3.4.1.1 Transfection of plasmid pEGFP-N1™ into embryonic bovine lung (EBL) cells.

Eukaryotic expression vector, pEGFP-N1™ (CLONTECH) is a pUC-based plasmid, but was shown to adapt to replication in *P. multocida* (section 3.3.3). In order to examine the ability of EBL cells to express GFP from the gene controlled by a viral promoter (<sup>P</sup>CMV<sub>IE</sub>) on pEGFP-N1™, the plasmid (1 µg/well) was transfected into EBL cells assisted by lipofectamine 2000 (Invitrogen, UK) (section 2.17.5). Cells were plated and allowed to adhere overnight at 37°C, in 5% (v/v) CO<sub>2</sub>. The following day, plasmid DNA was introduced to cells using the lipofectamine 2000 transfection reagents.

Figure 18 shows two different sets of transfected EBL cells at different magnifications. Both were taken at 48 hours after transfection with plasmid pEGFP-N1. At each magnification, images were taken of the same field under differential interference contrast (DIC) light (white) and filtered fluorescent light (Exc. = 488 nm, Ems. = 507 nm). Both images were then brought together to produce an overlay image. Images at each magnification were taken from a different experiment.

When the monolayer was observed under x20 optical objective, some EBL cells were shown to express GFP when viewed under the filtered fluorescent light. In the overlay it was difficult to tell exactly which cells were expressing the GFP. In another experiment, images of the EBL cell monolayer were taken at x40 magnification. At this magnification, cells were more clearly focused and overlay of the images showed individual EBL cells that were expressing GFP. These images demonstrated that approximately 5% of the transfected EBL cells were able to express *gfp* from plasmid pEGFP-N1.

**Figure 18. Transfection of plasmid pEGFP-N1 into EBL cells.**

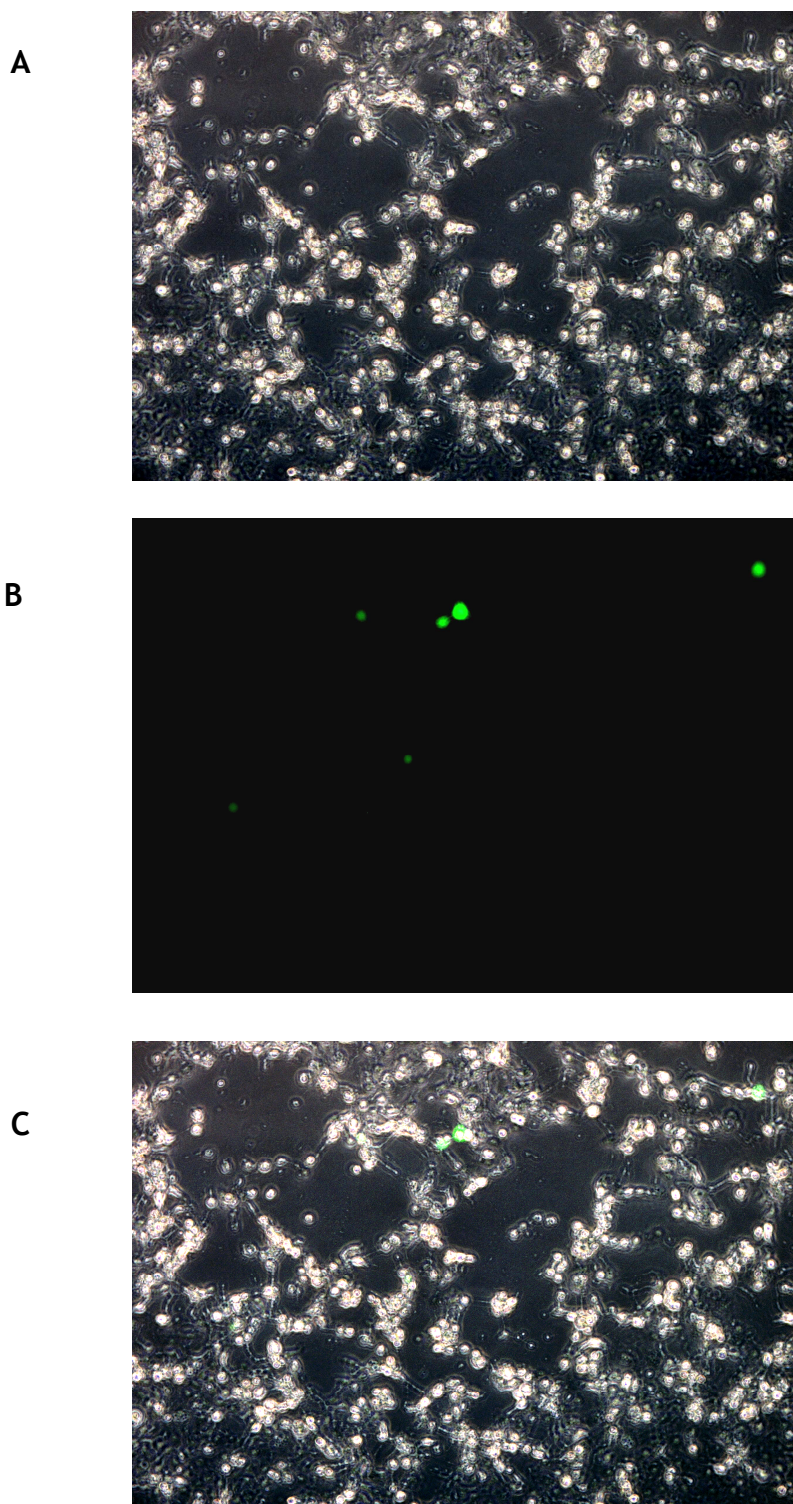


Plasmid pEGFP-N1 was transfected into EBL cells (section 2.17.5). After 48 h of incubation, cells were viewed under x20 and x40 magnification with using a Zeiss AxioCam MRcS camera attached to a Zeiss Axiovert 40 CFL Microscope and images were processed with Zeiss Axiovision software under DIC (white light) and filtered light [Excitation (Exc.) = 488 nm, Emission (Ems.) = 507 nm] to view EBL cells expressing GFP (section 2.17.5). Each magnification represents cells from two different experiments.

### 3.4.1.2 Invasion of EBL cells with *P. multocida* B:2 JRMT12 pEGFP-N1<sup>TM+</sup>

Plasmid pEGFP-N1<sup>TM</sup> was electroporated into *P. multocida* B:2 JRMT12 (section 3.3.3.1). EBL cells were then infected with this strain in a standard invasion assay (section 2.14.2). However, in this assay, instead of cell lysis by digitonin at the final step, monolayers were supplemented with fresh EBL assay medium followed by further incubation for 24 h at 37°C, under 5% (v/v) CO<sub>2</sub>. Cells were then viewed under DIC light (white) and filtered fluorescent light (Exc. = 488 nm, Ems. = 507 nm) at x20 magnification.

Figure 19 shows images of EBL cells taken at 24 h post-invasion with *P. multocida* B:2 JRMT12 pEGFP-N1<sup>TM+</sup>. Images were taken at x20 magnification of the same field under DIC light (white) (A) and filtered fluorescent light (Exc. = 488 nm, Ems. = 507 nm) (B). The overlay image (C) showed less than 5% of the EBL cells expressing gfp. In this images <1% seem to be expressing GFP compared with 5% in previous figure. Even though plasmid delivery via bactofection was not as efficient as transfecting the plasmid directly into EBL cells, these data showed that this *P. multocida* strain was capable of releasing the plasmid into the cell cytosol of EBL cells to allow GFP expression from the viral promoter by the EBL cells at 24 h post-invasion.

**Figure 19. Invasion of EBL by *P. multocida* B:2 JRMT12 pEGFP-N1<sup>TM+</sup>.**

Images of a EBL cell monolayer in an experimental well on a 6-well tissue culture plate taken 24 h after invasion of EBL cells by *P. multocida* B:2 JRMT12 carrying pEGFP-N1<sup>TM</sup>. Images were taken under **A**: DIC light (white) and **B**: filtered fluorescent light (Exc. = 488 nm, Ems. = 507 nm) at x20 magnification. Both images were then overlaid (**C**) to display the cells expressing GFP.

### 3.4.2 Development of *P. multocida* B:2 JRMT12 expressing fluorescent proteins

In order to develop a model system to more clearly understand the process of bactofection with *P. multocida*, it was decided to create a pEGFP-N1™ derivative that expressed another fluorescent protein under the control of a constitutive prokaryotic promoter. This would represent a marker for the bacterium containing the plasmid and would allow the fate of the bacteria, once inside the EBL cells, to be followed more closely. Two broad-host-range plasmids (Appendix 5) were obtained as a courtesy from Prof. Paul R. Langford, Imperial College London. Plasmid pMK-Express and pMC-Express (Bossé *et al.*, 2009) contained versatile restriction sites, expressed kanamycin (pMK-Express) or chloramphenicol (pMC-Express) resistance for the selection of plasmid-containing strains, and a *A. pleuropneumoniae sodC* promoter active in other *Pasteurellaceae* bacteria which controlled a *gfpmut3* gene coding for *Aequorea victoria* green fluorescent protein (GFP: Exc. = 501 nm, Ems. = 511 nm).

Both plasmids were electroporated (section 2.13.2) separately into *P. multocida* B:2 JRMT12. Plasmid pMK-Express appeared to replicate more stably in *P. multocida* B:2 JRMT12 than plasmid pMC-Express. Plasmid DNA purified from *P. multocida* B:2 JRMT12 pMK-Express<sup>+</sup> was more defined and concentrated when compared to the latter (results not shown). Thus, the mutant strain harbouring plasmid pMK-Express was utilized further in this study.

#### 3.4.2.1 *P. multocida* B:2 JRMT12 pMK-Express<sup>+</sup>

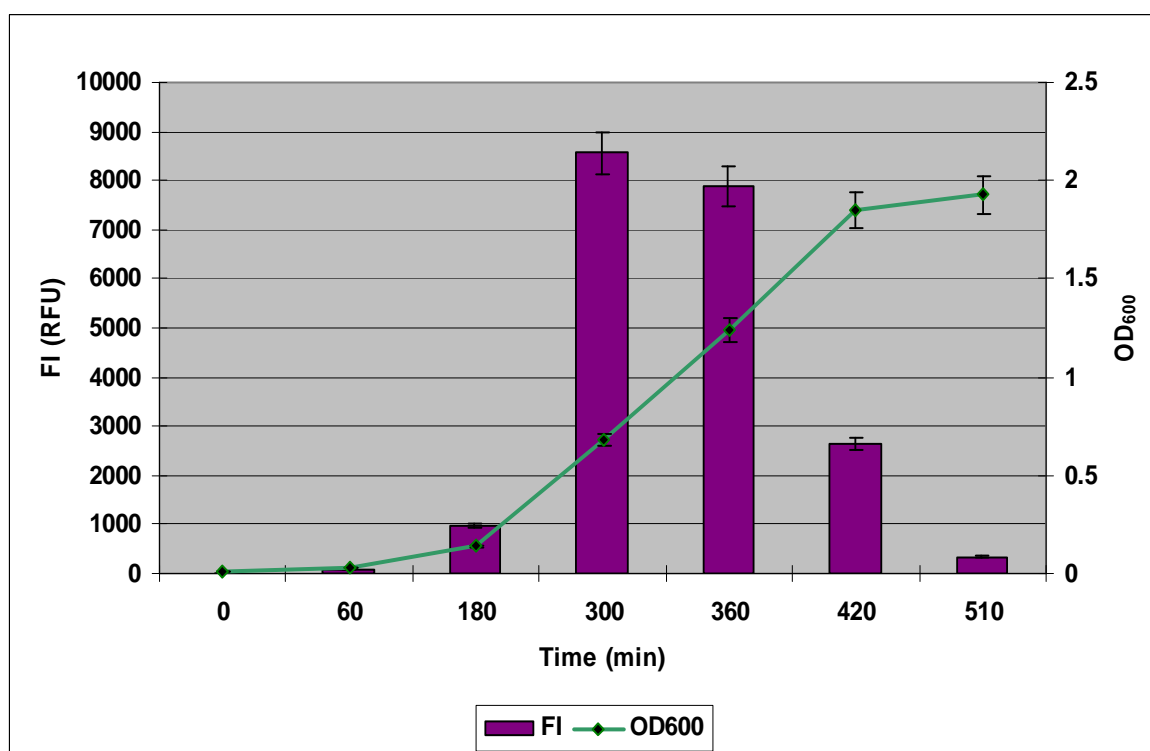
Several positive transformants were picked after the electroporation procedure and plasmid pMK-Express was purified from them. All strains harbouring this plasmid underwent GFP expression assessment (section 2.18). One strain was chosen which showed significant GFP expression. Figure 20 shows a bar graph of fluorescence intensity (FI) of this strain over time, accompanied by a line graph which shows the bacterial growth curve (OD<sub>600nm</sub>) over the same time period. Bacteria were sampled at intervals to determine OD<sub>600nm</sub> and FI. During lag phase (0-120 min), bacteria were observed to express low levels of GFP. GFP expression increased gradually as the growth curve entered the exponential phase, after 180 min of culture, and continued to increase until 300 min of culture which produced the highest peak of FI at 8571 RFU when OD<sub>600nm</sub> had

reached 0.68. After that, the GFP expression gradually declined, especially when the growth curve entered stationary phase. After 420 min of culture, FI had dropped to more than 50% of the peak value. It continued to drop further in the stationary phase. These data indicated that the bacteria expressed GFP optimally during early to mid exponential phase, between  $OD_{600nm}$  0.14 to 0.68.



**Figure 20. Assessment of GFP expression by *P. multocida* B:2 JRMT12 pMK-Express<sup>+</sup> during growth.**

GFP expression during the growth curve of *P. multocida* B:2 JRMT12 pMK-Express<sup>+</sup> was monitored using a fluorimeter. The fluorescence intensity (FI) in relative fluorescence units (RFU) of the bacteria (bar graph) and the bacterial density (OD<sub>600nm</sub>) (line graph) were measured at intervals. For each FI reading, the background fluorescence from *P. multocida* B:2 JRMT12 has been subtracted. Experiments were performed in triplicate and the error bars indicate standard deviations of the means.



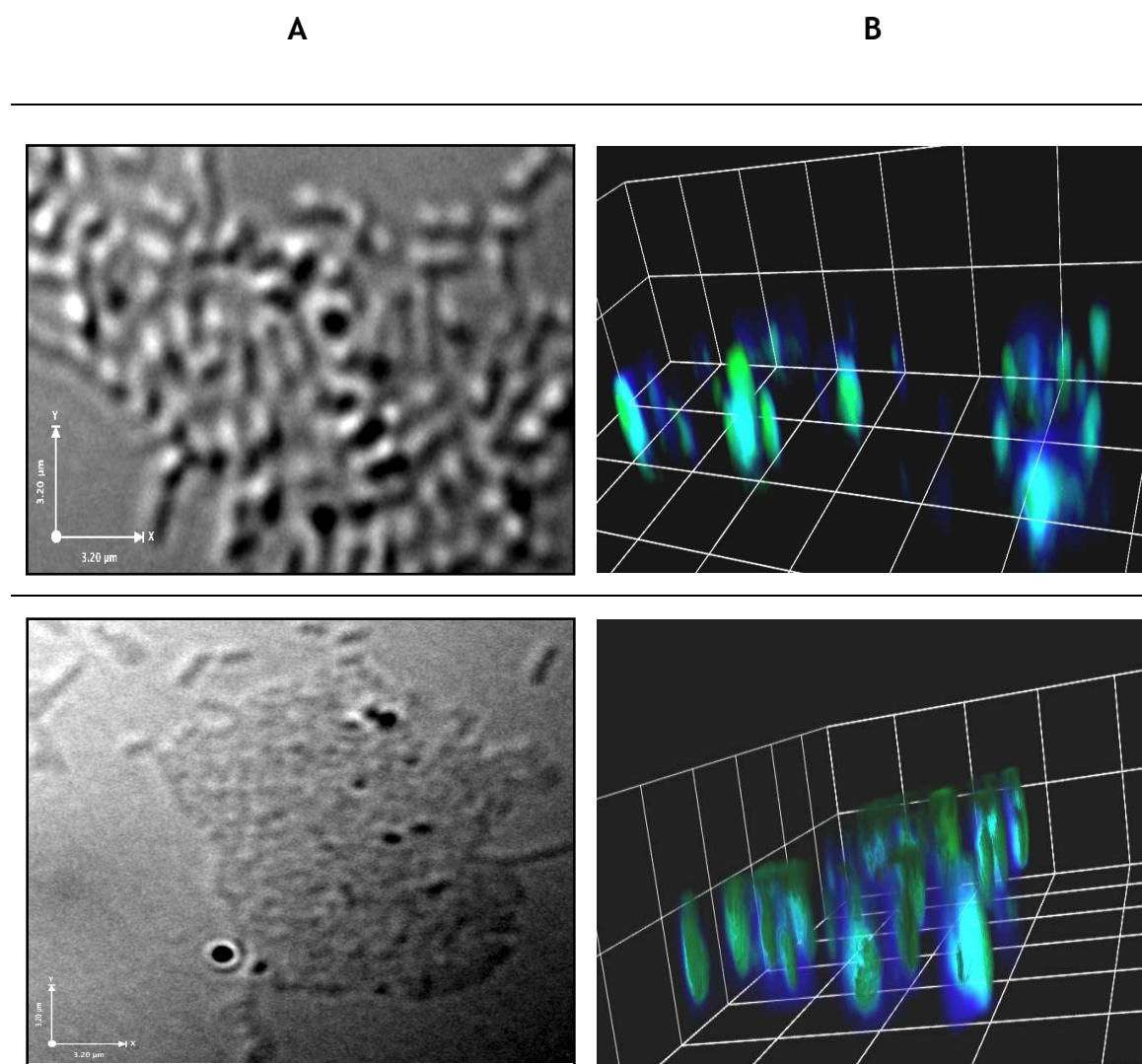
The next step was to visualize *P. multocida* B:2 JRMT12 pMK-Express<sup>+</sup> using fluorescence microscopy (FM). The strain was prepared as mentioned above. However, this time, sampling of the bacteria was only undertaken between OD<sub>600</sub> 0.14 to 0.68 in order to capture the bacteria during maximum GFP expression. After obtaining maximum GFP expression by measuring FI by fluorimetry, bacteria were counterstained with Cy5 Dye (Amersham, UK) according to manufacturer's instructions. The Cy5 Dye is a monofunctional NHS-Ester for the labelling of free amino groups on the bacterial surface. It can be detected under fluorescence filter light between Exc. 649 nm and Ems. 670 nm. Bacteria were then mixed with 4% of paraformaldehyde (PFA) before fixing onto a poly-L-lysine coated microscope slide. The slide was left to air dry and mounted with DAKO fluorescence mounting medium (DAKO, USA) in preparation for FM. A cover slip was then applied on top of the slide and stored in the dark until viewing (section 2.20.1.2).

It can be seen from Figure 21, that two sets of images were viewed under the 100 x objective lens of a Zeiss AxioImager M1 fluorescence microscope (Carl Zeiss) using a Hamamatsu Orca 03 and a QIClick digital charge-coupled device (CCD) camera. Images were then captured and processed with Volocity software (Perkin Elmer, UK). Left and right images were taken of the same field but under different light paths, **A** are images taken under DIC light (white) and **B** are images taken under filtered fluorescent light (Exc. = 649 nm, Ems. = 670 nm) (blue) to visualize the counterstain, Cy5 Dye (Amersham, UK) and filtered fluorescent light (Exc. = 488 nm, Ems. = 507 nm) (green) to visualize bacteria expressing GFP. This helped to determine whether GFP expression was within the bacteria cell.

The top pair of images were of *P. multocida* B:2 JRMT12 pMK-Express<sup>+</sup> bacteria from a culture grown to OD<sub>600nm</sub> 0.2. The strain was sampled at this OD<sub>600nm</sub> and processed as above before fixing onto a spot slide and mounted for fluorescence microscopy viewing. The left image shows a cluster of coccobacilli under the DIC light. The right image is a 3D image under filtered fluorescence light of GFP expression (green) within the bacterial cell membranes (counterstained blue with Cy5 dye stain). If observed closely, it can be seen that not all bacteria were expressing *gfp* at this OD<sub>600nm</sub>. However, this corroborates with the previous fluorimeter data which indicated only low level of *gfp* expression during the

early stages of exponential phase, e.g. at  $OD_{600nm}$  0.2. The bottom images were of *P. multocida* B:2 JRMT12 pMK-Express<sup>+</sup> sampled at  $OD_{600nm}$  and processed as above. The left image shows a cluster of coccobacilli under the DIC light. The right image is a 3D image under filtered fluorescence light of GFP expression (green) within the bacterial cell membranes (counterstained blue with Cy5 dye stain). At  $OD_{600nm}$  0.6, the strain showed heavier clustering and greater GFP expression by *P. multocida* B:2 JRMT12 pMK-Express<sup>+</sup> at this stage, where more bacteria were observed to be expressing GFP at the same time. This finding was promising for the next stage of the investigation, to allow visualization of the JRMT12 strain during the various stages of invasion. All 3D images (B) were developed from multiple 2D images captured from the prepared slide. The vertical elongated shape of the bacteria is presumably an artefact of iterative restoration during image manipulation using Volocity software (Perkin Elmer, UK).

**Figure 21. Visualization of *P. multocida* B:2 JRMT12 pMK-Express<sup>+</sup> via fluorescence microscopy (FM).**



Images of *P. multocida* B:2 JRMT12 pMK-Express<sup>+</sup> fixed with 4% PFA on a poly-L-lysine microscope slide, mounted with DAKO mounting medium and viewed under 100x objective lens with a Zeiss AxioImager M1 fluorescence microscope (Carl Zeiss). Images were captured using Hamamatsu Orca 03 and QIClick digital charge-coupled device (CCD) cameras and processed with Velocity software (Perkin Elmer, UK). Left and right images were taken of the same field under different light paths. Top images were *P. multocida* B:2 JRMT12 pMK-Express<sup>+</sup> at OD<sub>600nm</sub> 0.2 and bottom images were *P. multocida* B:2 JRMT12 pMK-Express<sup>+</sup> at OD<sub>600nm</sub> 0.6. **A:** Image taken under DIC light (white) **B:** Image taken under filtered fluorescent light (Exc. = 649 nm, Ems. = 670 nm) (blue) to visualize the counterstain, Cy5 Dye (Amersham, UK) and filtered fluorescent light (Exc. = 488 nm, Ems. = 507 nm) (green) to visualize bacteria expressing GFP.

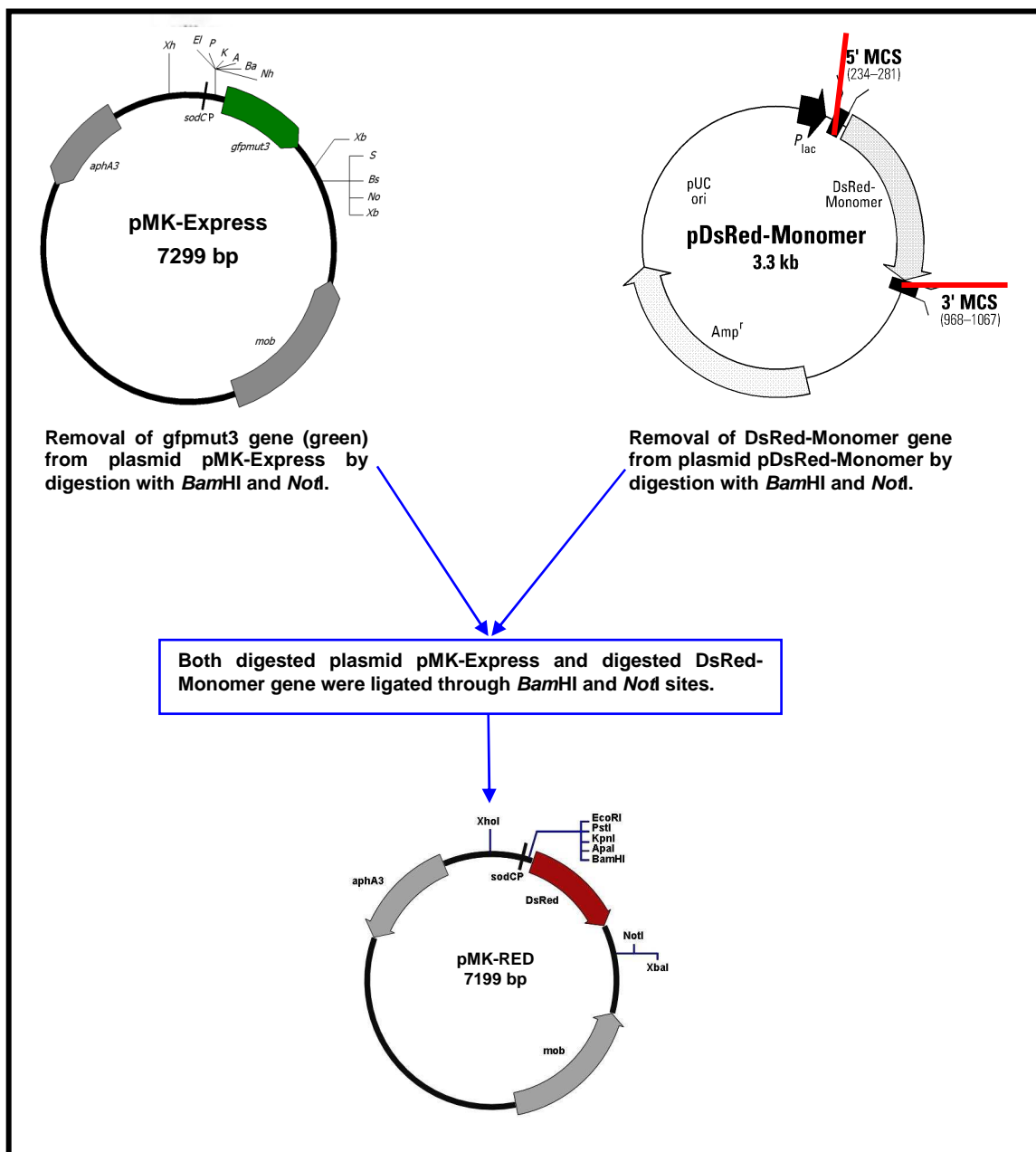
### 3.4.2.2 *P. multocida* B:2 JRMT12 pMK-RED<sup>+</sup>

In a previous section (3.3.3), plasmid pEGFP-N1™ was confirmed as a suitable eukaryotic expression plasmid for *P. multocida* B:2 JRMT12. This plasmid carries the EGFP gene with a modified Shine-Dalgarno sequence to make it suitable for expression in mammalian cells. This is accomplished using the cytomegalovirus promoter (<sup>P</sup>CMV<sub>IE</sub>). *P. multocida* B:2 JRMT12 harbouring this plasmid carried it into EBL cells during invasion and released the plasmid intracellularly followed by GFP expression in the mammalian cells (section 3.4.1.2). In order to visualize bacteria intracellularly and to follow their fate after uptake, strain JRMT12 expressing a different type of fluorescent protein to the one expressed by the mammalian cell was required. Hence, it was decided as a first step to replace the *gfpmut3* gene on pMK-Express with DsRed-Monomer gene which coded for red fluorescent protein (RFP) from plasmid pDsRed-Monomer (ClonTech, UK). This would then put the *rfp* gene under the control of prokaryotic *sodC* promoter.

Plasmid pDsRed-Monomer (Appendix 5) is a prokaryotic expression vector that encodes DsRed-Monomer (DsRed.M1), a monomeric protein derived from the tetrameric *Discosoma* sp. red fluorescent protein DsRed. This modified protein contains 45 amino acid substitutions, increasing its stability. The excitation wavelength (Exc.) maximum is 557 nm and emission wavelength (Ems.) maximum is 585 nm. In this plasmid, DsRed-Monomer coding sequence is flanked at the 5' and 3' ends by separate and distinct multiple cloning sites (MCS) which facilitate the isolation of the gene. This protein can be expressed by *E. coli* from the *lac* promoter, but this promoter would not function well in *P. multocida*.

The strategy employed (Figure 22) was to remove the *gfpmut3* gene from plasmid pMK-Express and replace it with the DsRed-Monomer gene from plasmid pDsRed-Monomer. The GFP gene, *gfpmut3*, and the DsRed.M1 gene were removed from their respective plasmids by digestion (section 2.4) with *Bam*HI and *Not*I sites. The digested pMK-Express (6583 bp) and DsRed.M1 gene (700 bp) were then ligated (section 2.12.2.2) giving a 7283 bp plasmid called pMK-RED. This plasmid was then electroporated into *P. multocida* B:2 JRMT12 (section 2.13.2).

Figure 22. Cloning strategy: Development of plasmid pMK-RED.

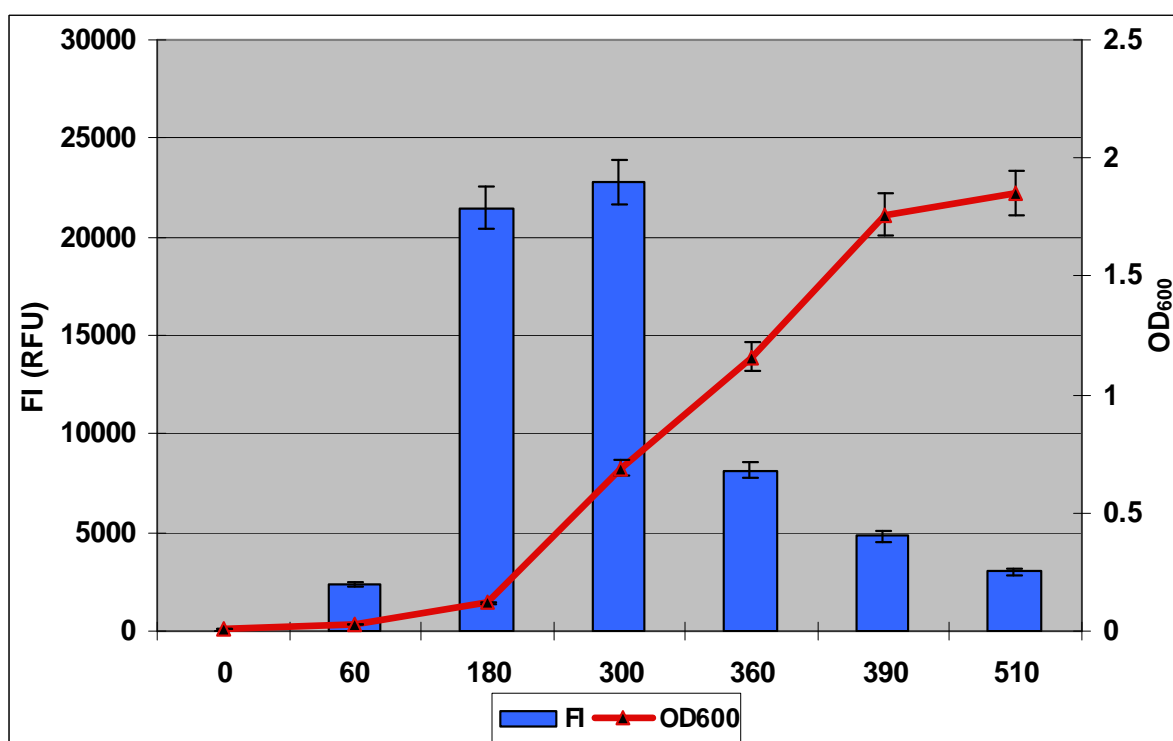


Several positive transformants were picked after the electroporation procedure and plasmid pMK-RED was purified from them. After confirmation of plasmid identity, a strain harbouring this plasmid was chosen to undergo assessment of RFP expression. *P. multocida* B:2 JRMT12 pMK-RED<sup>+</sup> was assessed for its ability to express RFP using a fluorimeter (FLUOstar OPTIMA, BMG Labtech). The procedure is similar to the one noted in section 3.4.2.1. The only difference is the set programme of the FLUOstar OPTIMA. For RFP detection, the fluorescent light filter was set at excitation maximum at 544 nm and emission maximum at 590 nm. All samples were compared with *P. multocida* B:2 JRMT12 to eliminate background. Samples were taken at hourly intervals until the OD<sub>600nm</sub> showed that the culture had reached stationary phase (~2.0).

Figure 23 shows a bar graph of fluorescence intensity (FI) of this strain over time (min) accompanied by a line graph showing the bacterial growth curve (OD<sub>600nm</sub>). During the lag phase (0-120 min), bacteria were observed to express some RFP. This markedly increased as the growth curve entered the exponential phase, after 180 min of culture, at OD<sub>600nm</sub> 0.12, where the FI was at 21483 RFU, and continued to increase slightly until 300 min which gave the highest peak of FI at 22809 RFU when OD<sub>600nm</sub> had reached 0.69. After that, RFP expression declined, especially when the growth curve entered the stationary phase. These data indicated that the bacteria expressed RFP best during exponential phase in a similar manner to expression of GFP from the same plasmid backbone (section 3.4.2).

**Figure 23. Assessment of RFP expression by *P. multocida* B:2 JRMT12 pMK-RED<sup>+</sup> during growth.**

RFP expression during the growth curve of *P. multocida* B:2 JRMT12 pMK-RED<sup>+</sup> was monitored using a fluorimeter. The fluorescence intensity (FI) of the bacteria (bar graph) and the bacterial density (OD<sub>600nm</sub>) (line graph) were measured at intervals. For each FI reading, the background fluorescence from *P. multocida* B:2 JRMT12 has been subtracted. Experiments were performed in triplicate and the error bars indicate standard deviations of the means.





The next step was to visualize *P. multocida* B:2 JRMT12 pMK-RED<sup>+</sup> using fluorescence microscopy (FM). The strain was prepared as mentioned above, and sampling of the bacteria culture was undertaken between OD<sub>600</sub> 0.12 to 0.69 during the maximum expression of RFP. After measuring RFP using the fluorimeter, bacteria were counterstained with Cy5 Dye (Amersham, UK) according to manufacturer's instruction. This was done to ease visualization of the bacteria expressing the RFP. Bacteria were then mixed with 4% paraformaldehyde (PFA) before fixing onto a spot slide. The slide was left to air dry and mounted with DAKO fluorescence mounting medium (DAKO, USA) in preparation for viewing by fluorescence microscopy. A cover slip was then applied on top of the slide and stored in the dark until viewing. As a control, *E. coli* XL-1 Blue containing pDSRed-Monomer was grown under similar conditions, but in LB medium.

In Figure 24, images in row I were taken from a spot slide of *P. multocida* B:2 JRMT12 pMK-RED<sup>+</sup> when the OD<sub>600nm</sub> of the culture had reached 0.6. Images were taken of the same field on the slide under 3 different light paths to ease visualization. In **A**, the image taken under DIC (white) light showed a heavy cluster of bacteria. This was expected because of the high density of growth at OD<sub>600nm</sub> 0.6. When the same field of the slide was captured in **B** under filtered fluorescent light (Exc. = 649 nm, Ems. = 670 nm) (blue) to visualize the counterstain, Cy5 Dye, on the bacterial cell surface a more distinguishable shape of the bacteria was recognized. This image was taken at 0.6  $\mu$ m splicing through the field, in order to view a single layer of the bacteria, using the optical sectioning function of the Volocity software (Perkin Elmer, UK). The image was set to section optically at 0.3  $\mu$ m intervals from top to bottom; an image was captured at every 0.3  $\mu$ m of depth, with a total section stacking of 3.0  $\mu$ m. The Volocity software was then further utilized to deconvolve the captured images by focusing the light emitted to the exact spot where it was originally from. This was to eliminate background light diffraction. In **C**, the image was taken under filtered fluorescent light (Exc. = 557 nm, Ems. = 585 nm) (red), to visualize bacteria expressing RFP from plasmid pMK-RED, and under filtered fluorescent light (Exc. = 649 nm, Ems. = 670 nm) (blue) to show the counterstain and to localize the RFP expression within the bacteria. This image was also taken at 0.6  $\mu$ m splicing and then deconvolved using the Volocity software. Image **C** showed

purplish pink coccobacilli of *P. multocida* B:2 JRMT12 pMK-RED<sup>+</sup> mostly expressing RFP at OD<sub>600nm</sub> 0.6.

The images in row II show *E. coli* XL-1 Blue pDsRed-Monomer<sup>+</sup>. This was used as a control for visualization of RFP expression from the DsRed-Monomer gene in another Gram-negative bacterium. The images of the same field were taken under three different light paths, as above. Image A was taken under DIC (white) light and showed a heavy cluster of bacteria similar to that of *P. multocida*, although the cells appeared larger and less concentrated. The same field of the slide, captured in image B, was taken under filtered fluorescent light (Exc. = 649 nm, Ems. = 670 nm) (blue) to visualize the counterstain, Cy5 Dye. The bacterial shape was again more clearly recognized. This image was again taken at 0.6  $\mu$ m splicing through the slide in order to view a single layer of the bacteria with background light diffraction eliminated as above. Image C was taken under filtered fluorescent light (Exc. = 557 nm, Ems. = 585 nm) (red) to visualize *E. coli* expressing RFP from plasmid pDsRed-Monomer and under filtered fluorescent light (Exc. = 649 nm, Ems. = 670 nm) (blue) to show the counterstain and to localize the RFP expression in the bacteria. The image was also taken at 0.6  $\mu$ m splicing and then deconvolved using the Volocity software. Image C showed purplish-pink rod-shaped *E. coli* XL-1 Blue pDsRed-Monomer<sup>+</sup> expressing RFP when the culture was sampled at OD<sub>600nm</sub> 0.6.

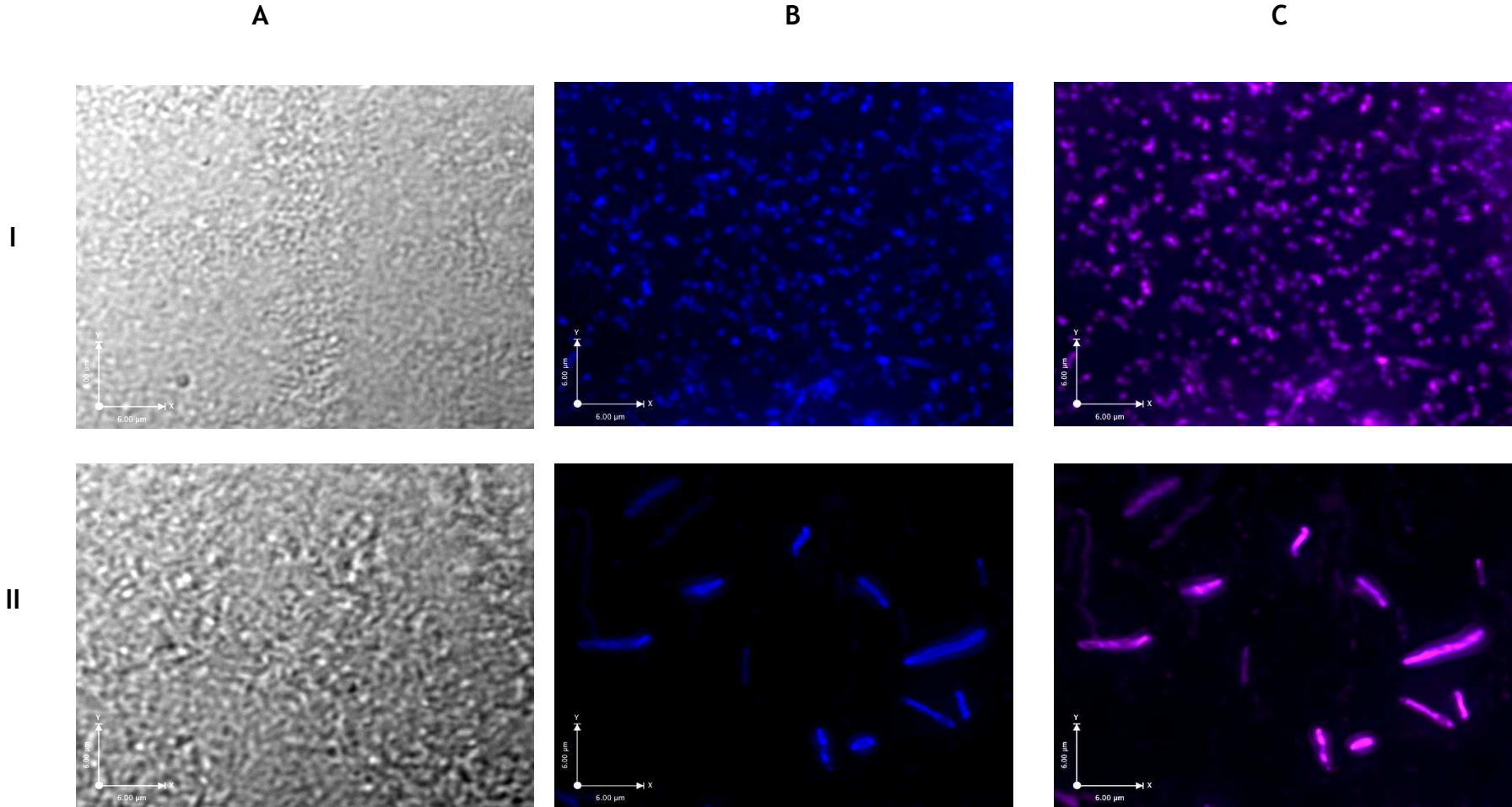
**Figure 24. Visualization of *P. multocida* B:2 JRMT12 pMK-RED<sup>+</sup> via FM.**

Images of *P. multocida* B:2 JRMT12 pMK-RED<sup>+</sup> (I) and *E. coli* XL-1Blue pDsRed-Monomer<sup>+</sup> (II) counterstained with Cy5 Dye (Amersham, UK) and fixed with 4% (w/v) PFA on a spot-slide, then mounted with DAKO mounting medium and viewed under a 100x objective lens with a Zeiss Axiolmager M1 fluorescence microscope (Carl Zeiss). Images were captured using Hamamatsu Orca 03 and QIClick digital charge-coupled device (CCD) cameras and processed with Volocity software (Perkin Elmer, UK). Images were taken of the same field under three different light paths;

A: Image taken under DIC (white) light.

B: Image taken under filtered fluorescent light (Exc. = 649 nm, Ems. = 670 nm) (blue)

C: Image taken under filtered fluorescent light (Exc. = 557 nm, Ems. = 585 nm) (red) and filtered fluorescent light (Exc. = 649 nm, Ems. = 670 nm) (blue).



The images in Figure 24 confirmed the ability of DsRed-Monomer gene to be expressed by *P. multocida*. Plasmid pMK-RED was derived by removing the DsRed-Monomer gene from pDsRed-Monomer and placing it upstream of the  $P_{sodC}$  promoter in plasmid pMK-Express to replace the deleted *gfpmut3* gene. After electroporation of the plasmid into *P. multocida* B:2 JRMT12, fluorimeter assessment of RFP expression showed highest fluorescence production during the exponential phase at  $OD_{600nm}$  0.6. Images captured with the fluorescence microscopy (FM) showed individual bacteria expressing RFP and counterstained with Cy5 dye.

### **3.4.3 Assessment of intracellular viability of *P. multocida* B:2 JRMT12 expressing fluorescent protein**

In the previous section, plasmid pMK-RED was constructed and assessed for the ability of *P. multocida* B:2 JRMT12 to express RFP from this plasmid. RFP fluorescence was visualized in the mutant strain using FM. In the next step, the ability of the plasmid to express RFP in JRMT12 in the intracellular environment of mammalian cells was assessed using the invasion assay.

#### **3.4.3.1 Imaging of *P. multocida* B:2 JRMT12 pMK-RED<sup>+</sup> in EBL cells**

In order to visualize *P. multocida* B:2 JRMT12 pMK-RED<sup>+</sup> after invasion of EBL cells at high definition, an invasion assay at MOI 100:1 (bacteria/cell) was prepared as in section 2.17.2 and 2.20.1.1. Prepared slides were then viewed under the x100 objective lens of a Zeiss AxioImager M1 (Carl Zeiss). Images were captured using Hamamatsu Orca 03 and QIClick digital charge-coupled device (CCD) cameras and processed with Volocity software (Perkin Elmer, UK).

A single EBL cell is shown in Figure 25 as representative of the cells examined. All images of the cell were taken under the x100 objective lens of the same field but under different light paths. Images were then deconvolved using Volocity software. In **A**, the EBL cell was visualized under DIC (white) light. In **B**, the EBL cell was observed under filtered fluorescent light (Exc. = 649 nm, Ems. = 670 nm) (blue) to visualize the counterstain, CellMask™ (GE Healthcare, UK), which stained the plasma membrane of live cells. This stain is composed of an amphipathic molecule providing a lipophilic moiety to improve membrane loading and a negatively-charged hydrophilic dye for stable fixation in the

plasma membrane. In this image, the nucleus of the cell, the cytoplasm and the cell outline are distinguishable. In **C** the EBL cell was observed under filtered fluorescent light (Exc. = 557 nm, Ems. = 585 nm) (red) to visualize internalized RFP-expressing bacteria in the EBL cell cytoplasm. The red coccobacilli shaped spots show the presence of *P. multocida* B:2 JRMT12 pMK-RED<sup>+</sup> expressing RFP from the DsRed-Monomer gene. In order to corroborate the presence of the bacterium internally within the mammalian cell, image **D** was captured under filtered fluorescent light (Exc. = 649 nm, Ems. = 670 nm) (blue) and filtered fluorescent light (Exc. = 557 nm, Ems. = 585 nm) (red) at selected depths by Volocity optical sectioning. The cell was sectioned optically at 0.3  $\mu\text{m}$  intervals from top to bottom; the images shown were captured at every 0.3  $\mu\text{m}$  depth as shown in the table (bottom, right). First (0  $\mu\text{m}$ ) and last (3.0  $\mu\text{m}$ ) images indicate the top and bottom of the EBL cell. The 2<sup>nd</sup> (0.3  $\mu\text{m}$ ) until the 10<sup>th</sup> (2.7  $\mu\text{m}$ ) images show the optical sectioning of the cell. There are a number of bacteria present intracellularly in this cell. For example, the yellow circles point out an area where the fluorescence intensity (FI) of the RFP is greatly enhanced as the depth of the section increases. This was at the highest FI within 0.9  $\mu\text{m}$  to 1.5  $\mu\text{m}$  depth of the optical section. The intensity gradually decreased as the optical sectioning progressed deeper than that. This confirmed the RFP expression in this area by *P. multocida* B:2 JRMT12 pMK-RED<sup>+</sup>. Another example is outlined by the green circles. In this area, the RFP became visible just after the optical sectioning reached 2.1  $\mu\text{m}$  and 2.4  $\mu\text{m}$ . However, as the image progressed to a higher depth, some of the RFP fluorescence disappeared but, for other spots, their intensity was greatly enhanced. Both examples serve to illustrate that the bacterium persisted intracellularly within the EBL cell at 3 h of the standard invasion assay. It should be noted that some spots were present at 0  $\mu\text{m}$  and appeared to persist in most of the sections. It is not clear what these spots may represent as a surface-located bacterium, visible at 0  $\mu\text{m}$ , would not be expected to show fluorescence in later sections. For this experiment, out of 60 EBL cells examined, 37% of the EBL cells showed the presence of *P. multocida* B:2 JRMT12 pMK-RED<sup>+</sup> intracellularly.

**Figure 25. Imaging of *P. multocida* B:2 JRMT12 pMK-RED<sup>+</sup> in EBL cells.**

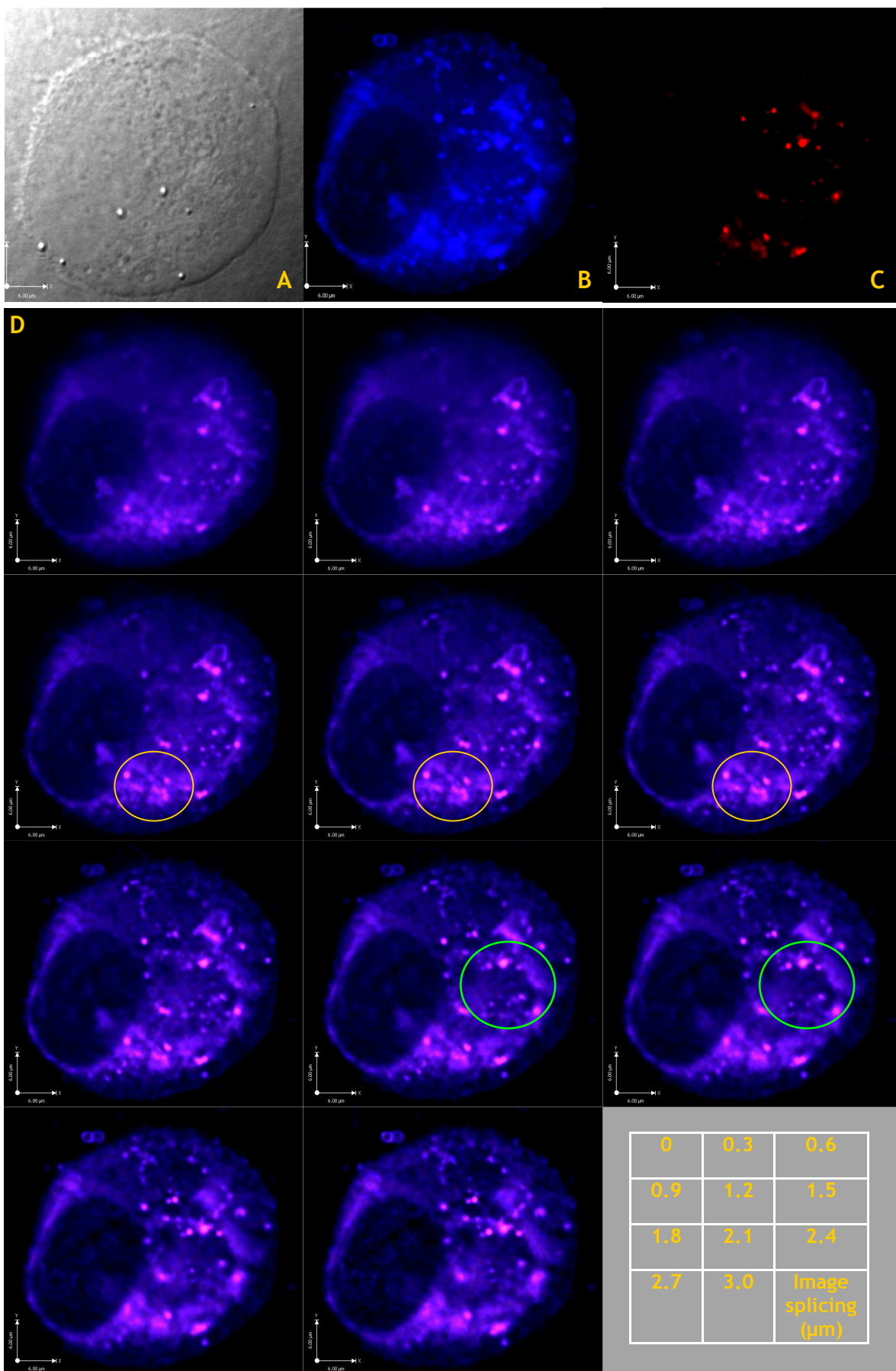
Slides for visualization of *P. multocida* B:2 JRMT12 pMK-RED<sup>+</sup> after invasion of EBL cells were prepared as in section 2.16.1.1. Prepared slides were then viewed under the x100 objective lens of a Zeiss AxioImager M1 FM (Carl Zeiss). Images were captured using Hamamatsu Orca 03 and QIClick digital charge-coupled device (CCD) cameras and processed with Volocity software (Perkin Elmer, UK). The image of a representative single EBL cell taken under different light paths is shown.

**A:** EBL cell taken under the DIC (white) light.

**B:** EBL cell taken under filtered fluorescent light (Exc. = 649 nm, Ems. = 670 nm) (blue) to visualize the counterstain, CellMask™ plasma membrane stain (GE Healthcare).

**C:** EBL cell taken under filtered fluorescent light (Exc. = 557 nm, Ems. = 585 nm) (red) to visualize internalized bacteria expressing RFP in the cytoplasm of the EBL cell.

**D:** EBL cell taken under filtered fluorescent light (Exc. = 649 nm, Ems. = 670 nm) (blue) and filtered fluorescent light (Exc. = 557 nm, Ems. = 585 nm) (red) at selected depths by manipulation of optical sectioning. The slide was set to be sectioned optically at 0.3 μm from top to bottom; the images shown were captured at every 0.3 μm depth to a total section stacking of 3.0 μm. The table (bottom, right) shows the section depth (μm) of each image.





### 3.4.4 Development of the 'traffic light' plasmid

Work detailed in the previous section showed that the JRMT12 strain expressing RFP from plasmid pMK-RED could be visualized intracellularly in EBL cells using FM. In section 3.4.1.2, it was shown that the bacterium could carry plasmid pEGFP-N1™ into EBL cells, followed by visualization of EBL cells expressing GFP from the plasmid when observed with FM. In order to develop an understanding of how bacteria behave after entry into mammalian cells, it was thought useful to develop a plasmid with both a prokaryotic and a eukaryotic expression system with each expression system having a different reporter gene to differentiate their activation.

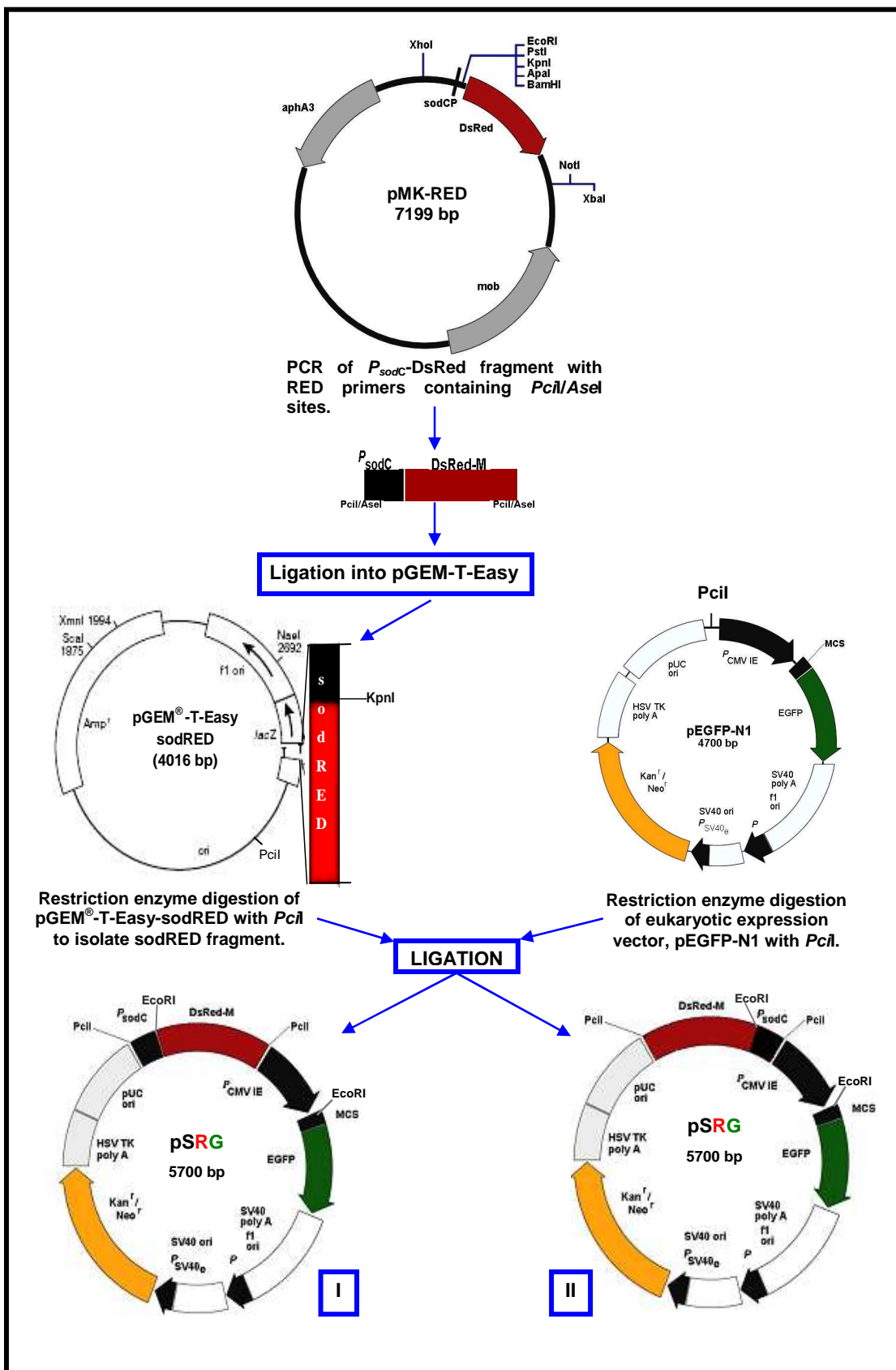
In this section, both systems were to be distinguished by different types of fluorescent protein expressed. To this end, it was decided to use a prokaryotic expression system and the DsRed-monomer gene which coded for RFP and a eukaryotic expression system with the EGFP gene which coded for GFP. The plasmid carrying both systems was termed 'traffic light' plasmid because, when it is present in viable bacteria, the prokaryote expression system would be active from a constitutive promoter and the bacteria would be seen as red by FM after expressing RFP. This would include a situation where mammalian cells internalized the bacteria, for as long as the bacteria remained viable and intact. After the plasmid was released in the mammalian cells via bacterial lysis, the eukaryotic expression system would be activated and the mammalian cells would express GFP and be visualized as green cells. If the bacteria were destroyed, the RFP expression would no longer be possible. The JRMT12 strain carrying this plasmid into EBL cells provides a method to monitor bacterial invasion and intracellular survival via RFP expression and the GFP reporter, of eukaryotic expression to show the potential for delivery of a DNA vaccine by bactofection.

#### 3.4.4.1 Cloning of $P_{sod-C}$ /DsRed-Monomer (sodRED) fragment into plasmid pEGFP-N1™

The cloning strategy is illustrated in Figure 26. Plasmid pMK-RED was used as a template for PCR with RED primers (Table 5) following the method in section 2.8.3 to amplify the sodRED fragment. Both forward and reverse primers have a restriction enzyme site at each end of the sequence, either *Asel* or *Pcil*. The PCR products (Figure 27) were purified (section 2.8.6) and then cloned into the PCR

cloning plasmid pGEM<sup>®</sup>-T-Easy (section 2.12.1.1) to increase the concentration of purified DNA in order to generate a good quantity of completely-digested fragment after either *PciI* or *AseI* restriction enzyme digestion. All the criteria above were crucial in acquiring a successful ligation (Figure 26).

Figure 26. Cloning strategy: Development of 'traffic light' plasmid, pSRG.



The ligation mixture containing linearised pGEM-T-Easy and the PCR product, derived using RED-P or RED-A primers (Figure 27), was transformed into *E. coli* XL-1 Blue. After plating on LB agar supplemented with ampicillin (50 µg/ml), some colonies were selected for further analysis. However, successful transformants were only found to harbour pGEM<sup>®</sup>-sodRED that was digested through *PciI* sites rather than *Asel* sites. Plasmid DNA was then purified from selected transformants and digested (section 2.4) with *KpnI*, a single site on sodRED MCS which will linearize pGEM<sup>®</sup>-sodRED at 4016 bp (Figure 28). After confirmation, plasmids harbouring the sodRED fragment (1016 bp) were digested with *PciI*. The restriction digest map is shown in Figure 29. The restriction enzyme, *PciI*, cuts the plasmid once at 517 bp and cuts twice at each end of the insert, thus giving 3 fragments after digestion. From the agarose gel image, the sodRED fragment was circled in red; gel extraction was performed to isolate the digested fragment (section 2.5.5).

In parallel, plasmid pEGFP-N1<sup>™</sup> was also digested with the same restriction enzyme *PciI* (section 2.4) and dephosphorylated with enzyme CIAP (section 2.12.3). The plasmid was then isolated by gel extraction (section 2.5.5) and purified for ligation. The agarose gel image in Figure 30 shows the undigested plasmid pEGFP-N1<sup>™</sup> as a control and the digested and dephosphorylated pEGFP-N1<sup>™</sup>. DNA concentrations were then estimated (section 2.6) for the digested insert fragment, sodRED, and the digested plasmid pEGFP-N1<sup>™</sup> to aid the ligation strategy (section 2.12.2.2). Ligation mixtures (1:1, 1:2, 1:4, 1:8 vector:fragment concentration) were then transformed into *E. coli* XL-1 Blue. In Figure 26, the cloning strategy shows two diagrams of plasmid pSRG after the ligation step showing two possible orientations of the sodRED fragment in plasmid pSRG (diagrams I and II). After transformation, plasmid DNA was purified from positive transformants (colonies derived from the antibiotic selection plate) and subjected to restriction enzyme analysis with *EcoRI* to assess the presence of sodRED fragment and to determine its orientation. The enzyme *EcoRI*, cuts the plasmid twice, once at the MCS after the eukaryotic promoter <sup>P</sup>CMV<sub>IE</sub> and the other at the MCS in the middle of the sodRED cassette (Figure 26). This would give two distinct sizes of fragment that would determine the orientation of the insert in plasmid pSRG (5700 bp). After agarose gel analysis, all positive clones were showed to be in the second orientation (diagram II, Figure 26). Figure 31 shows the plasmid restriction map with the *EcoRI* sites and fragment sizes after

digestion. The agarose gel image demonstrates two of the positive clones after digestion with *EcoRI* showing the fragment sizes that classified them as in the second orientation in pSRG. For further confirmation, the sodRED fragment was isolated from plasmid pSRG by digestion with *PciI* and sequenced (section 2.9). The complete sequence of the sodRED fragment is shown in Figure 32. The plasmid was electroporated into electro-competent *P. multocida* B:2 JRMT12 (section 2.13.2) for further manipulation.

**Figure 27. Agarose gel showing sodRED fragment PCR from plasmid pMK-RED using RED-A and RED-P primer pairs.**

- M1: 1 kb DNA ladder
- M2: 100 bp DNA ladder
- 1 : sodRED fragment from PCR with RED-P primers
- 2 : sodRED fragment from PCR with RED-A primers

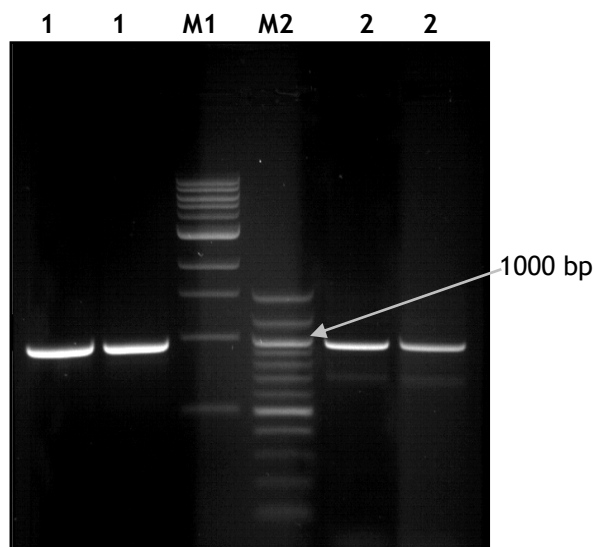
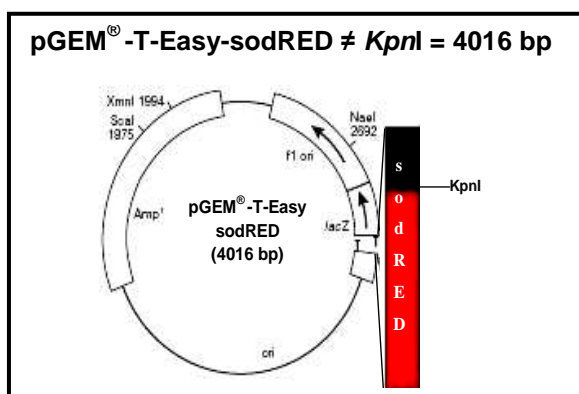


**Figure 28. Agarose gel showing plasmid pGEM<sup>®</sup>-T-Easy-sodRED from *E. coli* XL-1 Blue after digestion with *Kpn*I.**



- A: undigested pGEM<sup>®</sup>-T-Easy-sodRED
- dA: digested pGEM<sup>®</sup>-T-Easy-sodRED with *Kpn*I
- M: 1 kb DNA ladder

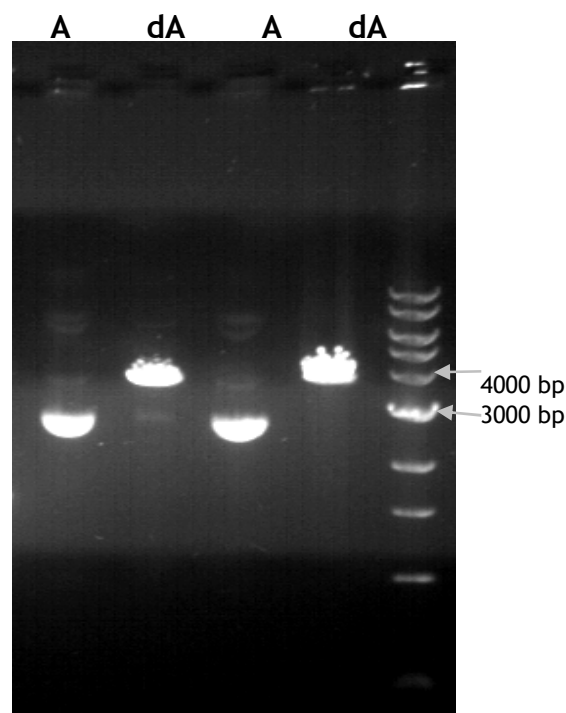
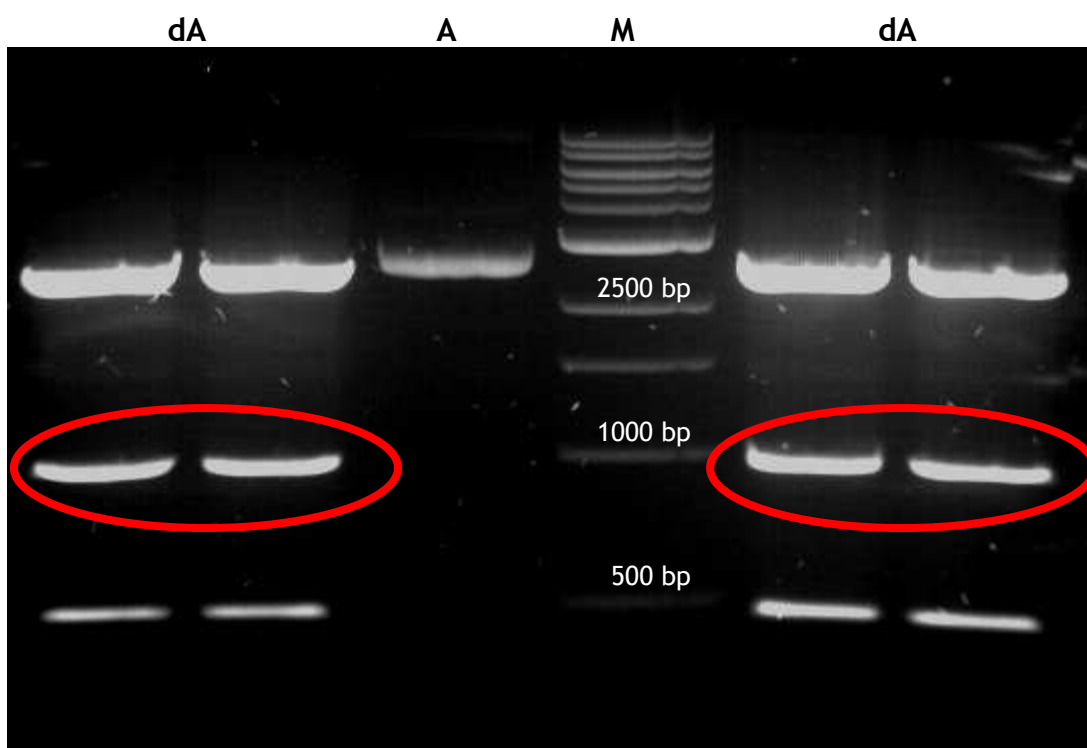
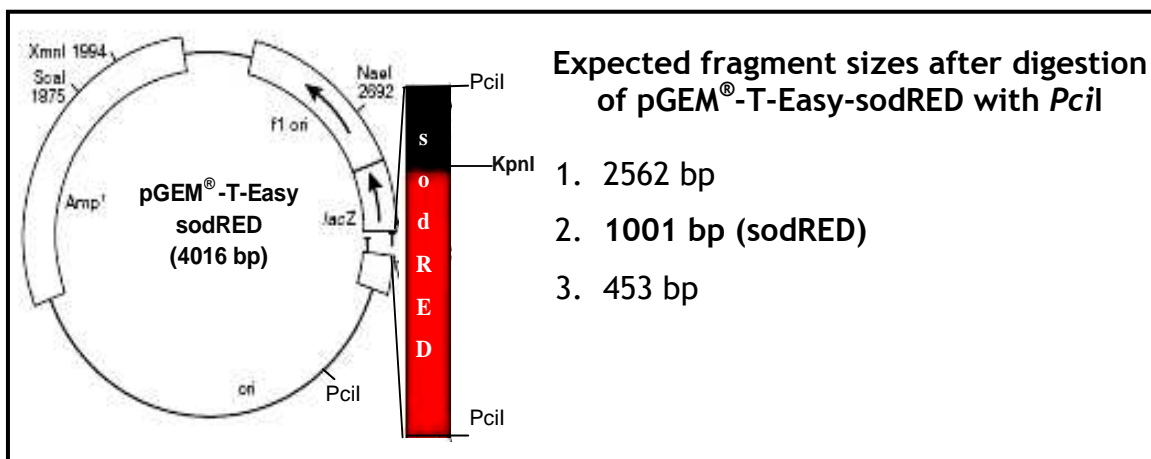


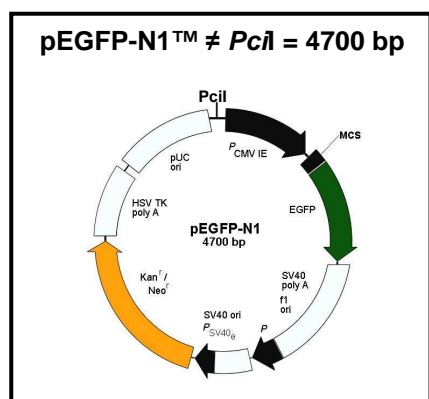
Figure 29. Agarose gel showing pGEM<sup>®</sup>-T-Easy-sodRED after digestion with *Pci*I.



M: 1 kb DNA ladder  
 A: undigested pGEM<sup>®</sup>-T-Easy-sodRED  
 dA: digested pGEM<sup>®</sup>-T-Easy-sodRED with *Pci*I

 sodRED fragment

**Figure 30. Agarose gel showing pEGFP-N1™ after digestion with *PciI* and dephosphorylation with CIAP.**



- A:** Plasmid pEGFP-N1™
- dA:** pEGFP-N1™ digested with *PciI* and dephosphorylated with CIAP
- M:** 1 kb DNA ladder

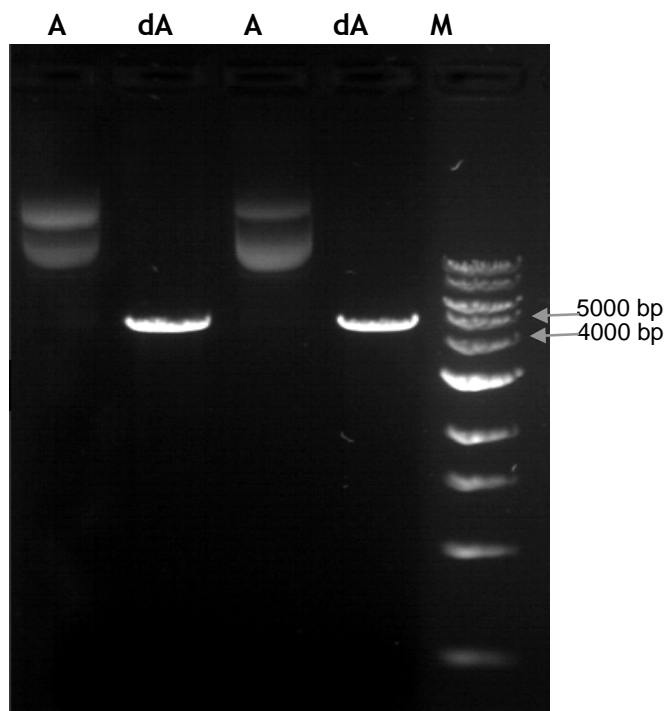
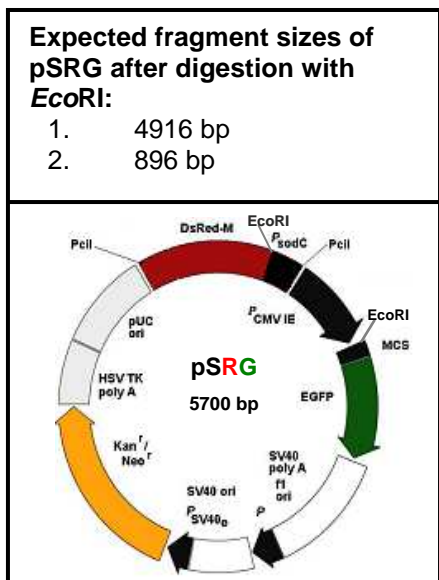


**Figure 31. Agarose gel showing pSRG after digestion with *EcoRI*.**



- A:** undigested pSRG
- dA:** digested pSRG with *EcoRI*
- M1:** 1 kb DNA ladder
- M2:** 100 bp DNA ladder

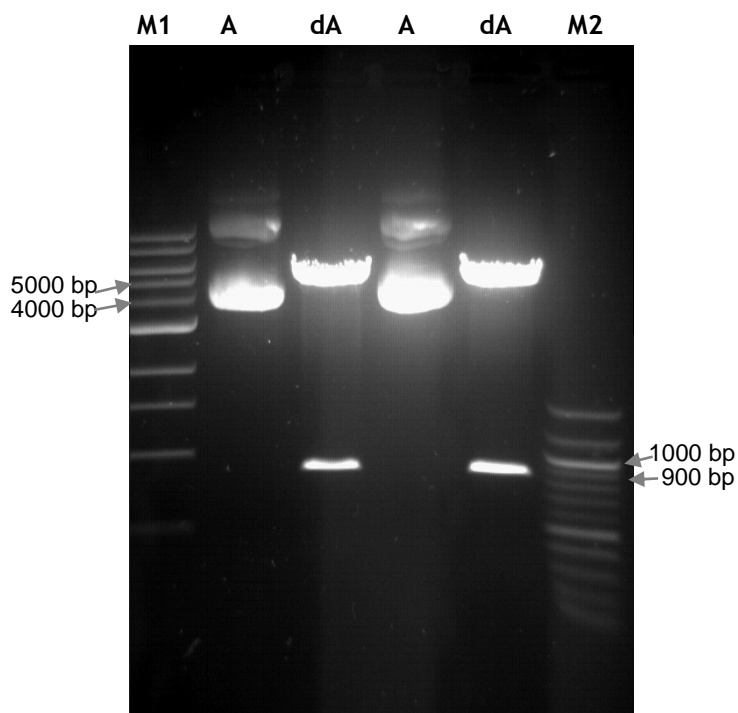




Figure 32. Complete sequence of sodRED fragment.



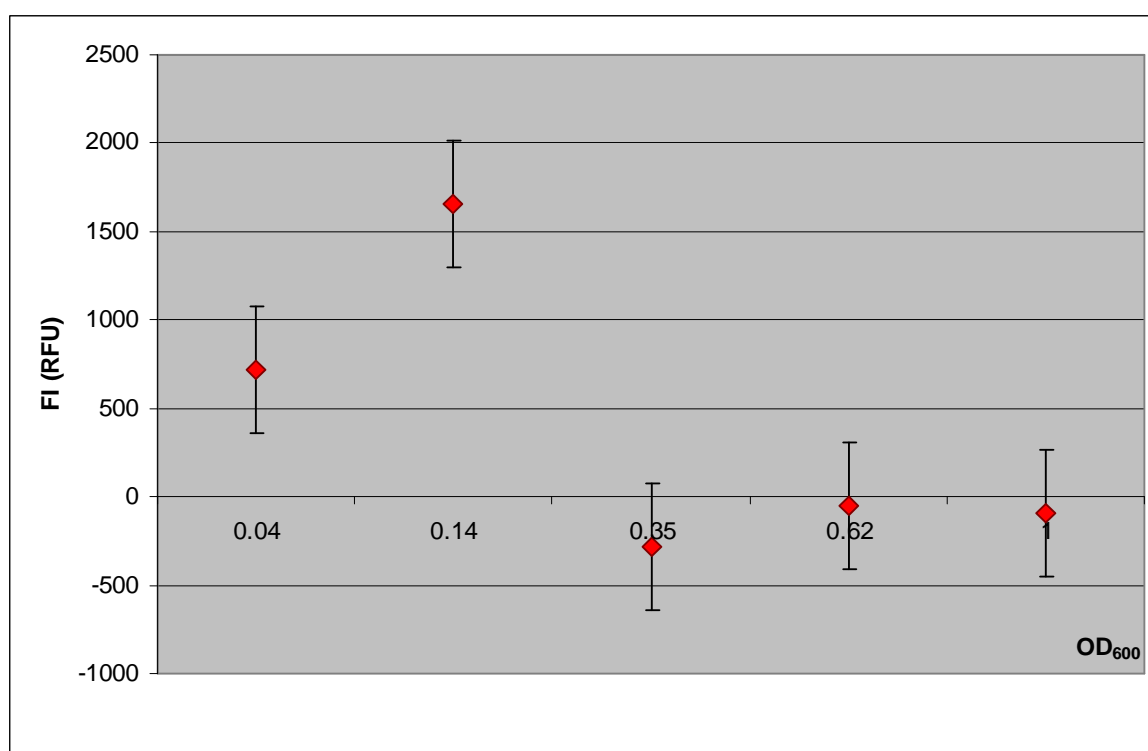
#### 3.4.4.2 Stability and expression of plasmid pSRG in *P. multocida* B:2 JRMT12

After electroporation of plasmid pSRG into *P. multocida* B:2 JRMT12, positive transformants were selected from BHI agar supplemented with kanamycin (50 µg/ml). Once the strains were confirmed to harbour pSRG, they were assessed for plasmid stability after routine subculture and also assessed for their capability to express RFP from the plasmid. For plasmid stability, *P. multocida* B:2 JRMT12 pSRG<sup>+</sup> was plated on BHI agar with and without kanamycin (50 µg/ml). After incubation for 24 h, selected colonies from both plates were streaked to a fresh plate. After a further 24 h, a dozen colonies were picked from both plates and inoculated into BHI broth with or without kanamycin (50 µg/ml) respectively. After 24 h, plasmids were purified and analyzed by restriction digestion with *Eco*RI for confirmation. Strains were subcultured into fresh broth medium everyday for 14 days and plasmids from each culture were purified and analyzed every alternate day. After 14 days, *P. multocida* B:2 JRMT12 pSRG<sup>+</sup> cultured without antibiotic was found to be still harbouring the plasmid, pSRG, in each of the 12 colonies originally subcultured. This demonstrated that pSRG is stable in *P. multocida* B:2 JRMT12 even after the bacterium has undergone very many cell division.

RFP expression was then assessed in a stable isolate of *P. multocida* B:2 JRMT12 pSRG<sup>+</sup> according to the procedure given in section 3.4.2.1. Figure 33 shows FI (RFU) of *P. multocida* B:2 JRMT12 pSRG<sup>+</sup> plotted against bacterial density (OD<sub>600nm</sub>). At OD<sub>600nm</sub> 0.04, the strain was clearly expressing RFP. As expected, this increased with increasing bacterial density showing 1657 RFU when the OD<sub>600nm</sub> had reached 0.14. After that, the RFP expression was seen to decline markedly, even at OD<sub>600nm</sub> of 0.35. This graph indicated that the RFP expression from this strain peaked in the early exponential phase of the growth. This was a similar result to that obtained with JRMT12 pMK-RED (Figure 23).

**Figure 33. Assessment of RFP expression by *P. multocida* B:2 JRMT12 pSRG<sup>+</sup> during growth.**

An overnight culture was diluted to  $OD_{600nm} \sim 0.08$  with sterile BHI and incubated at 37°C. 1 ml of culture was removed at regular intervals and  $OD_{600nm}$  measured. The 1 ml sample was then centrifuged at 13 000 x g for 1 min. After resuspending the bacterial pellet in 1 ml PBS, 200  $\mu$ l aliquots were analyzed in triplicate for fluorescence in a fluorimeter plate reader (RFP: Exc.= 557 nm, Ems.= 585 nm) *P. multocida* B:2 JRMT12 acted as a control for background fluorescence; fluorescence was plotted against  $OD_{600nm}$  using Microsoft Excel software and data were corrected for background fluorescence. Experiments were performed in triplicate and the error bars indicate standard deviations of the means.



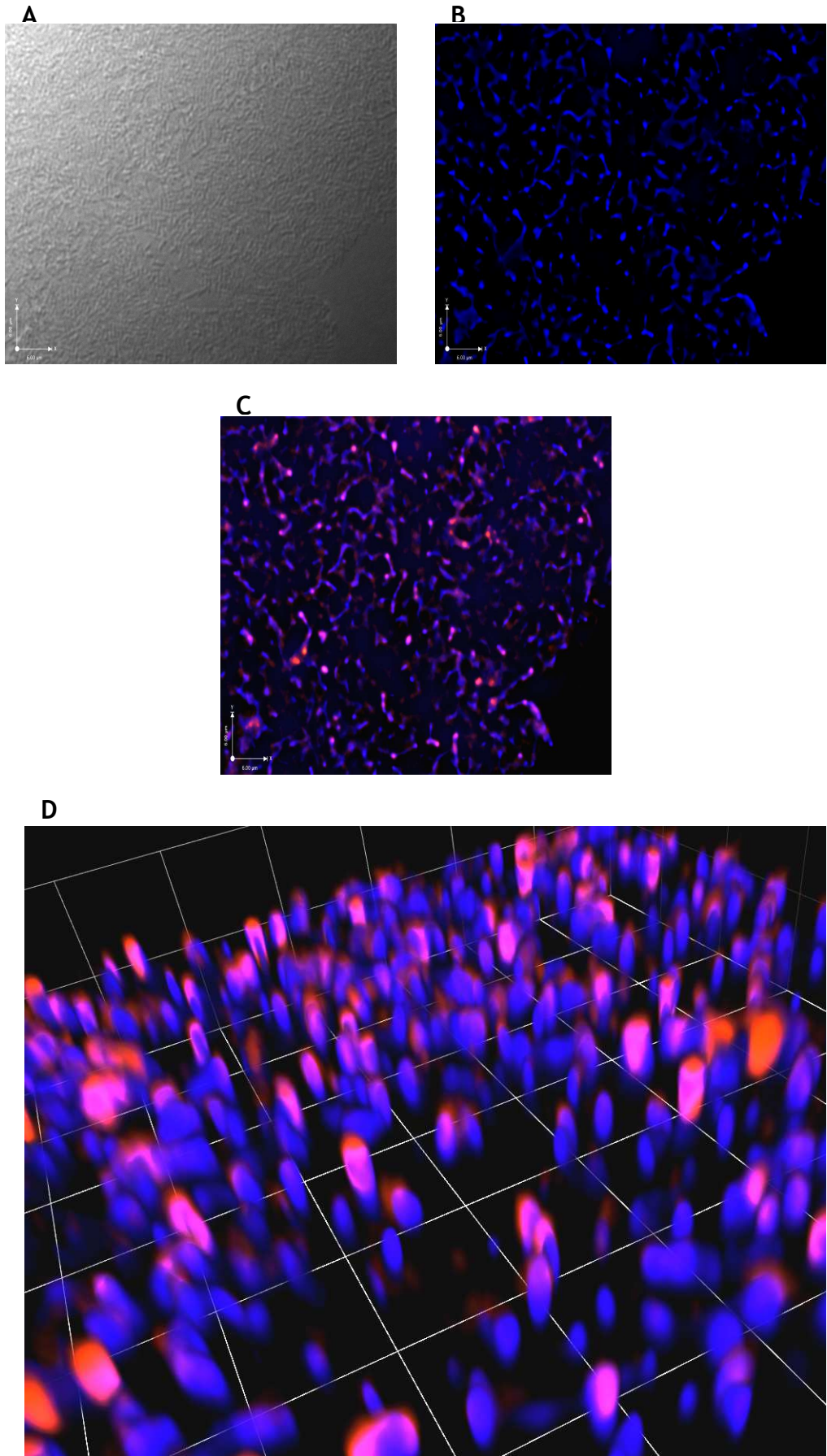
The next step was to visualize RFP expression in *P. multocida* B:2 JRMT12 pSRG<sup>+</sup> using fluorescence microscopy (FM). The strain was prepared as in section 3.4.2.1, and sampling of the bacteria was done between OD<sub>600nm</sub> 0.04 to 0.30 in order to capture the bacteria during maximum RFP expression. After obtaining maximum RFP expression at OD<sub>600nm</sub> 0.3 by measuring FI using the fluorimeter, bacteria were counterstained with Cy5 Dye (Amersham, UK) according to the manufacturer's instructions. Bacteria were then mixed with 4% (w/v) of paraformaldehyde (PFA) before fixing onto a poly-L-lysine coated microscope slide. The slide was left to air dry and mounted with DAKO fluorescence mounting medium (DAKO, USA) in preparation for FM. A cover slip was applied on top of the slide which was stored in the dark until viewing.

In Figure 34, a set of images were captured from the spot slide prepared with *P. multocida* B:2 JRMT12 pSRG<sup>+</sup> taken at OD<sub>600nm</sub> 0.3. Images were taken of the same field using the 100x objective lens under three different light paths to ease visualization. Image A, taken under DIC (white) light, showed a heavy cluster of bacteria. When the same field of the slide was captured in B, where the image was taken under filtered fluorescent light (Exc. = 649 nm, Ems. = 670 nm) (blue) to visualize the counterstained, Cy5 Dye, the shape of the bacteria was more defined. This image was taken at 0.6 µm splicing through the slide in order to view a single layer of the bacteria. As before, the slide was set to be sectioned optically at 0.3 µm intervals from top to bottom; an image was captured at every 0.3 µm depth at a total section stacking of 3.0 µm. The Volocity software was then utilized to deconvolve images captured by reversing the optical distortion to produce a sharper and clearer image. This technique also eliminates background light diffraction. Image C was taken under filtered fluorescent light (Exc. = 557 nm, Ems. = 585 nm) (red) to visualize bacteria expressing RFP from plasmid pSRG and under filtered fluorescent light (Exc. = 649 nm, Ems. = 670 nm) (blue) to show the counterstain in order to localize the RFP expression in the bacteria. The image showed purplish pink coccobacilli of *P. multocida* B:2 JRMT12 pSRG<sup>+</sup> expressing RFP. Image D shows a 3D image of image C to generate a 3D modelling of the RFP-expressing bacteria. The vertical elongated shape of the bacteria is presumably an artefact of iterative restoration after image manipulation using Volocity software (Perkin Elmer, UK).

**Figure 34. Visualization of *P. multocida* B:2 JRMT12 pSRG<sup>+</sup> via FM.**

Images of *P. multocida* B:2 JRMT12 pSRG<sup>+</sup> counterstained with Cy5 Dye (Amersham, UK) and fixed with 4% (w/v) PFA on a poly-L-lysine coated microscope slide, then mounted with DAKO mounting media and viewed under a 100x objective lens with a Zeiss AxioImager M1 fluorescence microscope (Carl Zeiss). Images were captured using Hamamatsu Orca 03 and QIClick digital charge-coupled device (CCD) cameras and processed with Volocity software (Perkin Elmer, UK). Images were taken of the same field under three different light paths;

- A:** DIC light (white),
- B:** filtered fluorescent light (Exc. = 649 nm, Ems. = 670 nm) (blue) to visualize the counterstain, Cy5 Dye (Amersham, UK),
- C:** two filtered lights; filtered fluorescent light (Exc. = 557 nm, Ems. = 585 nm) (red) to visualize bacteria expressing RFP from plasmid pSRG and filtered fluorescent light (Exc. = 649 nm, Ems. = 670 nm) (blue) to visualize the counterstain, Cy5 Dye. This helps to show that RFP expression was within the bacteria cell membrane,
- D:** 3D imaging of the 2D image from C using Volocity software (Perkin Elmer, UK).



### 3.4.4.3 Transfection of plasmid pSRG into EBL cells

EBL cells were prepared as in section 3.4.1.1 for transfection of plasmid pSRG. Figure 35 shows two different sets of transfected EBL cells. All images were captured from the prepared chamber-well slide (section 2.20.1.1). Slides were viewed under the x100 objective lens of a Zeiss AxioImager M1 FM (Carl Zeiss). Images were then captured using Hamamatsu Orca 03 and QIClick digital charge-coupled device (CCD) cameras, deconvolved and processed with Volocity software (Perkin Elmer, UK).

In Figure 35, images in set I (top row) were taken at 24 h post-transfection and those in set II were taken at 48 h post-transfection with pSRG. All images in a set were taken of the same field but under different light paths. In set I, cells of the monolayer were captured under DIC (white) light in image A. The cells were outlined in blue with the plasma membrane stain in image B. Overlay of the filtered light generated image C which showed localization of GFP in each EBL cell. Parts of the three cells expressing GFP were visible in this image. After optical sectioning, the images in D showed fluorescent intensity throughout these cells at every 0.4  $\mu\text{m}$  of splicing. GFP expression was visible throughout the images but decreased in later sections (stack 17-20) as the splicing went nearer to the surface indicating GFP expression was indeed intracellular in the EBL cells. Image E shows 3D imaging of the 2D image from C. At 48 h post-transfection, slides were again prepared as in section 2.20.1.1. Set II shows images of EBL cells on part of the monolayer captured at the same field under different light paths. One prominent EBL cell in image A was outlined in blue with the plasma membrane stain in image B and the overlay of the filtered light in image C showed localization of GFP within the EBL cell. Fluorescence intensity captured at each 0.4  $\mu\text{m}$  optical splicing throughout the cell. Image D showed the intensity of GFP fluorescence throughout the cell although it again decreased as the splicing went nearer to the cell surface (stack 18-20). This again indicated internal expression of GFP by the EBL cells. Image E shows 3D imaging of the 2D image from C.

Detailed observation of both slides found that out of 60 EBL cells examined, 67% of EBL cells were found to express GFP as early as 24 h after transfection. Another 60 EBL cells were assessed from slides prepared at 48 h post-

transfection and 82% were found to express GFP. The duration of GFP expression by the cells was not determined.



**Figure 35. Transfection of plasmid pSRG into EBL cells.**

Slides for visualization of pSRG during transfection of EBL cells at high definition were prepared as in section 3.4.1.1. Prepared slides were then viewed under the x100 objective lens of a Zeiss AxioImager M1 FM (Carl Zeiss). Images were then captured using Hamamatsu Orca 03 and QIClick digital charge-coupled device (CCD) cameras and processed with Volocity software (Perkin Elmer, UK). Images show two sets of EBL cells:

- I: EBL cells transfected with plasmid pSRG at 24 h post-transfection.
- II: EBL cells transfected with plasmid pSRG at 48 h post-transfection.

For both sets of images, the same field was taken under different light paths;

**A:** EBL cell taken under DIC (white) light.

**B:** EBL cell taken under filtered fluorescent light (Exc. = 649 nm, Ems. = 670 nm) (blue) to visualize the counterstained plasma membrane stain.

**C:** EBL cell taken under filtered fluorescent light (Exc. = 488 nm, Ems. = 507 nm) (green) to visualize expression of gfp in the cytoplasm of EBL cell and filtered fluorescent light (Exc. = 649 nm, Ems. = 670 nm) (blue) to visualize the counterstained plasma membrane stain.

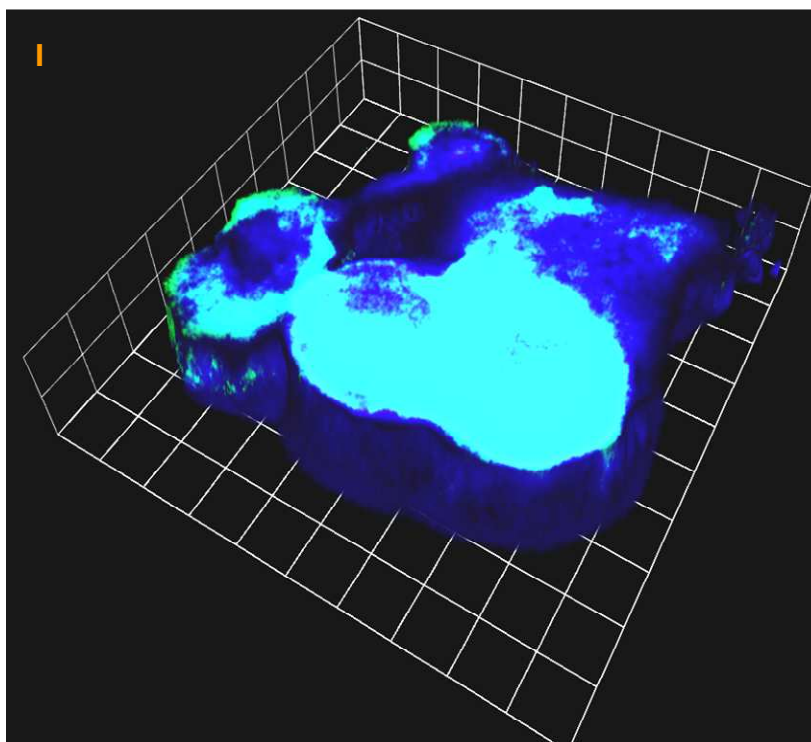
**D:** EBL cell taken under filtered fluorescent light (Exc. = 649 nm, Ems. = 670 nm) (blue) and filtered fluorescent light (Exc. = 488 nm, Ems. = 507 nm) (green) at selected depths by manipulation of optical sectioning. The slide was set to be sectioned optically at 0.4  $\mu\text{m}$  intervals from top to bottom; the images shown were captured at every 0.4  $\mu\text{m}$  of depth at a total section stacking of 8.0  $\mu\text{m}$ . The table below shows the optical section number for every stack in the image, with stack 1 at 0.4  $\mu\text{m}$  and stack 20 at 8.0  $\mu\text{m}$ .

**E:** 3D image of C.

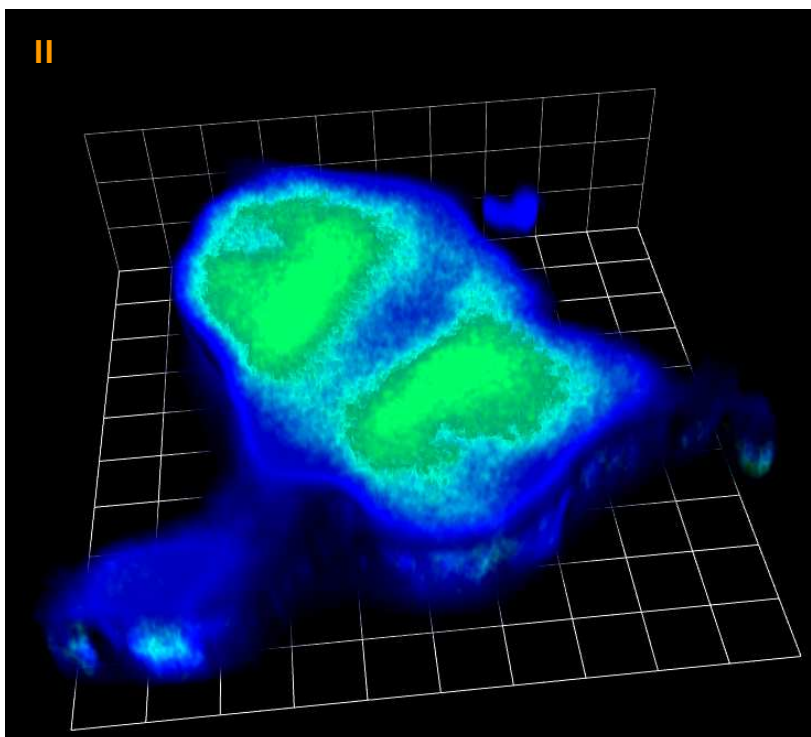
1	2	3	4
5	6	7	8
9	10	11	12
13	14	15	16
17	18	19	20



E



II



3D image of the 2D image of C. Image was generated using the Volocity software (Perkin Elmer, UK).

#### 3.4.4.4 Localization of prokaryotic and eukaryotic fluorescent protein expression

By this stage, it had been shown that plasmid pSRG was able to express fluorescent proteins using either prokaryotic or eukaryotic promoter systems. *P. multocida* B:2 JRMT12 was able to express RFP from the plasmid's sodRED cassette using the constitutive *sodC* promoter and EBL cells were able to express GFP from the plasmid's eukaryote promoter (<sup>P</sup>CMV<sub>IE</sub>) and *gfpmut3* gene. In the next step, it was hoped to monitor the activity of the traffic light plasmid, pSRG, during invasion of EBL cells by *P. multocida* B:2 JRMT12 pSRG<sup>+</sup>.

Cells and bacteria were prepared as in section 3.4.3.1 with the modification that the bacterium, *P. multocida* B:2 JRMT12 pSRG<sup>+</sup>, was grown to OD<sub>600nm</sub> 0.3 (at maximum RFP expression) before the invasion assay. Slides were prepared as in section 2.20.1 for FM and viewed under the x100 objective lens of the Zeiss AxioImager M1 microscope (Carl Zeiss).

Four sets of images are displayed in Figure 36. Sets I and II were captured from slides prepared after 3 h of the standard invasion time, while sets III and IV were captured from slides prepared at 5 h post-invasion. All images in a set were captured in the same field of the slides but under different light paths. In set I, image A shows a single EBL cell taken under white light. When the light path was changed to blue-filtered fluorescent light in image B, the plasma membrane was stained blue. In image C, an overlay of blue- and red-filtered fluorescent light showed the cell membrane as blue and the internalized *P. multocida* B:2 JRMT12 pSRG<sup>+</sup> as red. In order to confirm the internal location of RFP expression in the EBL cell, the slides underwent optical sectioning. Image D shows optical sections of the slide of 20 slices at every 0.4 μm of depth. Referring to the table below the figure description, at stack 7 (2.8 μm), RFP started to become visible, indicating internalized bacteria. The intensity of the red fluorescence increased as the optical sections went deeper into the cell. The maximum appearance of red fluorescence was observed between stack 10 (3.6 μm) and stack 15 (5.6 μm). Image E shows a 3D image of image C using Volocity software (Perkin Elmer, UK). However, when the fluorescent light path was changed to green to visualize GFP, no green fluorescence was found to be expressed by this EBL cell. Hence, at 3 h post-invasion, internalized bacteria were found in this EBL cell but no

expression of GFP was detected. This could be interpreted as indicating that the bacteria were still intact and had not released plasmid into the intracellular environment of the EBL cell.

As in set I, images in set II were also captured at 3 h post-invasion. In image **A**, a single EBL cell is clearly defined under the white light. In image **B**, filtered fluorescent blue light demonstrated the cell membrane in blue when stained by the plasma membrane stain. Image **C** was taken under red and blue filtered fluorescent light to visualize RFP expression (red) which appeared to be localised to the membrane boundaries that were stained blue. By switching the filtered fluorescent light path into green and blue, in image **D**, the EBL cell was seen to express GFP within the cell cytoplasm. Image **E** shows the stack of images when the slide underwent optical sectioning of 20 slices at every 0.4  $\mu\text{m}$ . The existence of a few *P. multocida* B:2 JRMT12 pSRG<sup>+</sup> internally were demonstrated in stack 5 (1.6  $\mu\text{m}$ ) until stack 17 (6.4  $\mu\text{m}$ ) (the table below the figure legend shows the numbered stack images in **E** and **F**). The intensity of red fluorescent was still however confined mainly to the periphery of the cell. The same optical sectioning was applied when the filtered fluorescent light path was switched to green and blue. In image **F**, the intensity of green fluorescence was clearly displayed in stack 7 (2.4  $\mu\text{m}$ ) progressing through until stack 15 (5.6  $\mu\text{m}$ ) before it declined. Observation of fluorescence intensity between the sections of this stack suggested that the localization of GFP occurred in the cytoplasm of the EBL cell and not in the nucleus. Image **G** and image **H** show 3D images of **C** and **D**, respectively. The data could be interpreted to indicate that, in this EBL cell, free plasmid was available for expression of GFP in the cytoplasm of the cell. The presence of only a few RFP-expressing bacteria within this cell might mean that others had been lysed so that they were no longer able to express RFP, but had released plasmid into the cytoplasm. The clear presence of bacteria at the periphery of the EBL cell, expressing rfp, might indicate that these bacteria had not yet been taken up the cell.

Seventy EBL cells were assessed from slides prepared at 3 h post-invasion. 56% of these cells were found not to be expressing GFP and no RFP-expressing bacteria were found intracellularly. 44% of the EBL cells were found to harbour a number of RFP-expressing *P. multocida* B:2 JRMT12 pSRG<sup>+</sup> intracellularly and, of this 44%, 12 EBL cells were already expressing GFP. No EBL cells expressing GFP

without harbouring any RFP-expressing *P. multocida* B:2 JRMT12 pSRG<sup>+</sup> intracellularly were found at this stage.

In set III, images were captured at 5 h post-invasion. Under DIC (white) light in image **A**, a single EBL cell on a monolayer was captured. When viewed under filtered fluorescent light blue, the labelled membrane boundaries were visible as a blue fluorescence (Image **B**). When viewed with two different filtered fluorescent light paths, red and blue, the image in **C** showed internalized bacteria (red) within membrane boundaries (blue) at 2.8  $\mu\text{m}$  splicing after optical sectioning. In **D**, the EBL cell was viewed green and blue under filtered fluorescent light. Extended focus of the image showed green fluorescence in the EBL cell cytoplasm within membrane boundaries. In image **E**, putting the stack together (extended focus) and viewing the cell under all three filtered fluorescent light paths, red, green and blue, the image showed internalized bacteria as red fluorescence and *gfp* expression as green fluorescence within membrane boundaries outlined in blue fluorescence. Image **F** and image **G** show 3D images of image **C** and **D** respectively. In these images, localization of RFP and GFP expression is clearly displayed within the labelled (blue) membrane boundaries.

As above, set IV displayed images captured at 5 h post-invasion. Image **A** showed a single EBL cell taken under DIC (white) light. In image **B**, the same cell was viewed under filtered fluorescent light blue to visualize the labelled cell membrane. When switching to both green and blue filtered fluorescent light, the image in **C** showed expression of GFP by the EBL cell displayed as green fluorescence within the cell membrane (blue). **D** shows images of optical sectioning of the slide. As demonstrated in the image stack, the localization of green fluorescence was gradually enhanced between stack 9 (3.2  $\mu\text{m}$ ) and stack 16 (6.0  $\mu\text{m}$ ). Images between this stack showed clear discrimination of the cell cytoplasm and its nucleus, indicating that GFP was expressed only in the EBL cell cytoplasm. Image **E** shows a 3D image of image **C** using Volocity software (Perkin Elmer, UK). When cell were viewed under two filtered fluorescent light paths, red and blue, the image showed only the EBL cell with membrane boundaries outlined in blue fluorescence (image not shown). These data showed that, at this stage, internalized RFP-expressing bacteria had been lysed so that they

were no longer able to express RFP but had released the plasmid into the EBL cytoplasm for eukaryotic GFP expression.

Sixty EBL cells were assessed from slides prepared at 5 h post-invasion. 47% of the EBL cells were found not to be expressing GFP and no RFP-expressing bacteria were found intracellularly. 53% of the EBL cells were found to be expressing GFP. Out of that 53%, 12 cells were found to be still harbouring some RFP-expressing *P. multocida* B:2 JRMT12 pSRG<sup>+</sup> intracellularly. Unfortunately, time constraints and technical difficulties with the stock of EBL cells meant that these experiments could not be repeated in another invasion assay.

**Figure 36. Localization of prokaryotic and eukaryotic protein expression.**

The images show EBL cells after invasion with *P. multocida* B:2 JRMT12 pSRG<sup>+</sup>. Slides for visualization of EBL cells at high definition were prepared as in section 2.16.1.1. Prepared slides were then viewed under the x100 objective lens of a Zeiss Axiolmager M1 microscope (Carl Zeiss). Images were captured using a Hamamatsu Orca 03 and QIClick digital charge-coupled device (CCD) cameras and processed with Volocity software (Perkin Elmer, UK). Images were captured at 3 h (I and II) and 5 h (III and IV) post-invasion.

(I) EBL cell captured at 3 h post-invasion. Images were taken of the same field but under different light paths.

**A:** EBL cell taken under the DIC (white) light.

**B:** EBL cell taken under filtered fluorescent light (Exc. = 649 nm, Ems. = 670 nm) (blue) to visualize the counterstain, CellMask™ plasma membrane stain (GE Healthcare).

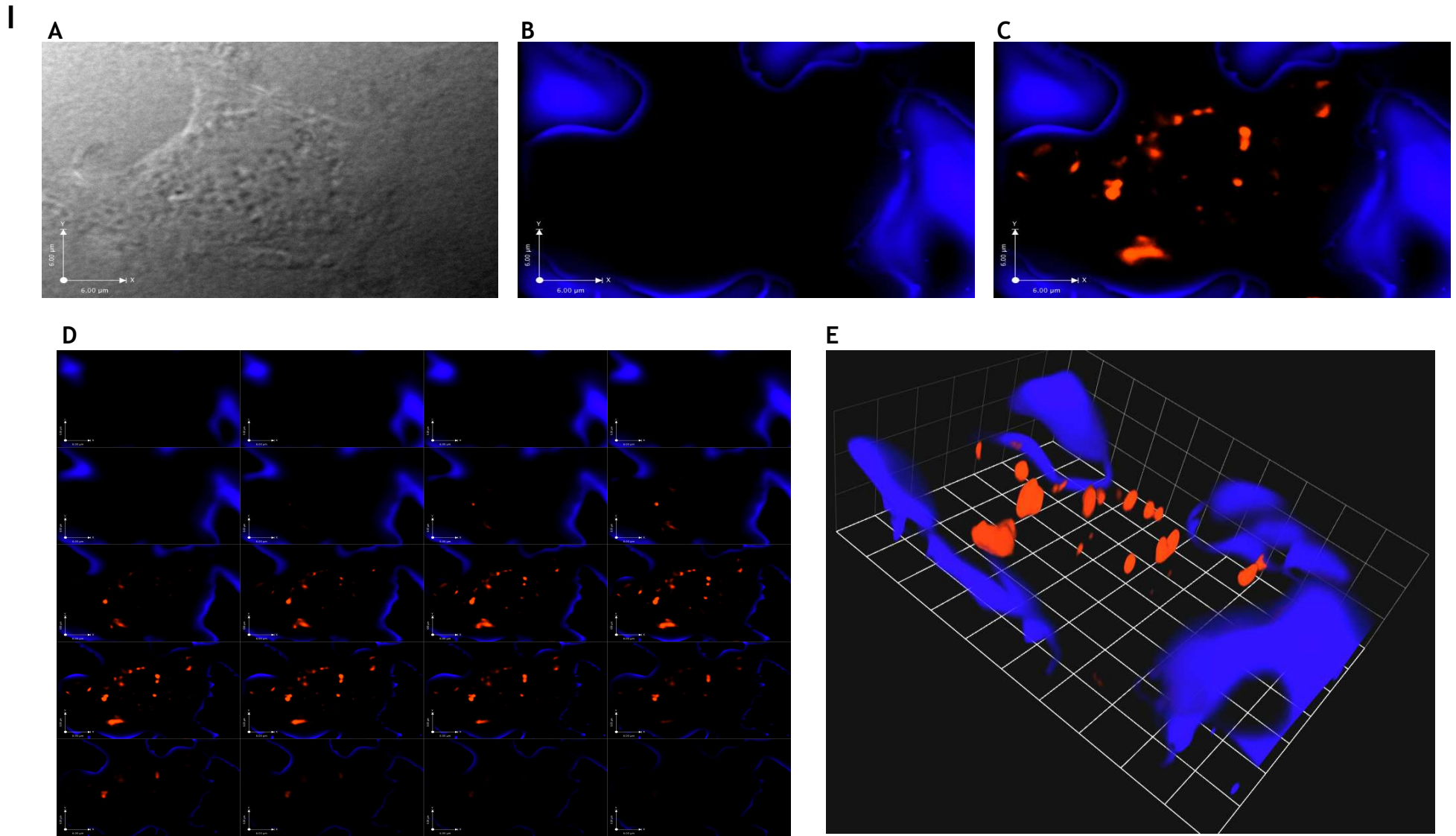
**C:** EBL cell taken under filtered fluorescent light (Exc. = 557 nm, Ems. = 585 nm) (red) to visualize internalized RFP-expressing bacteria and filtered fluorescent light (Exc. = 649 nm, Ems. = 670 nm) (blue) to visualize the counterstained plasma membrane.

**D:** EBL cell taken under filtered fluorescent light (Exc. = 649 nm, Ems. = 670 nm) (blue) and filtered fluorescent light (Exc. = 557 nm, Ems. = 585 nm) (red) at selected depths by manipulation of optical sectioning. The slide was set to be sectioned optically at 0.4 μm intervals from top to bottom; images shown were captured at every 0.4 μm of depth at a total section stacking of 8.0 μm. The box below shows optical section number for every stack in the images.

**E:** 3D image of C.

1	2	3	4
5	6	7	8
9	10	11	12
13	14	15	16
17	18	19	20





(II) EBL cell captured at 3 h post-invasion. Images were taken of the same field but under different light paths.

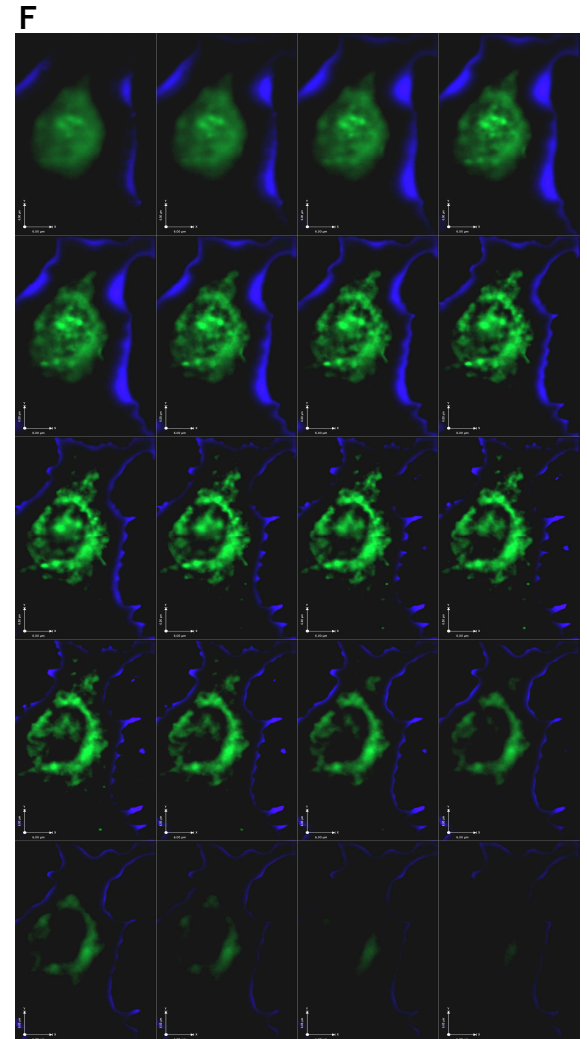
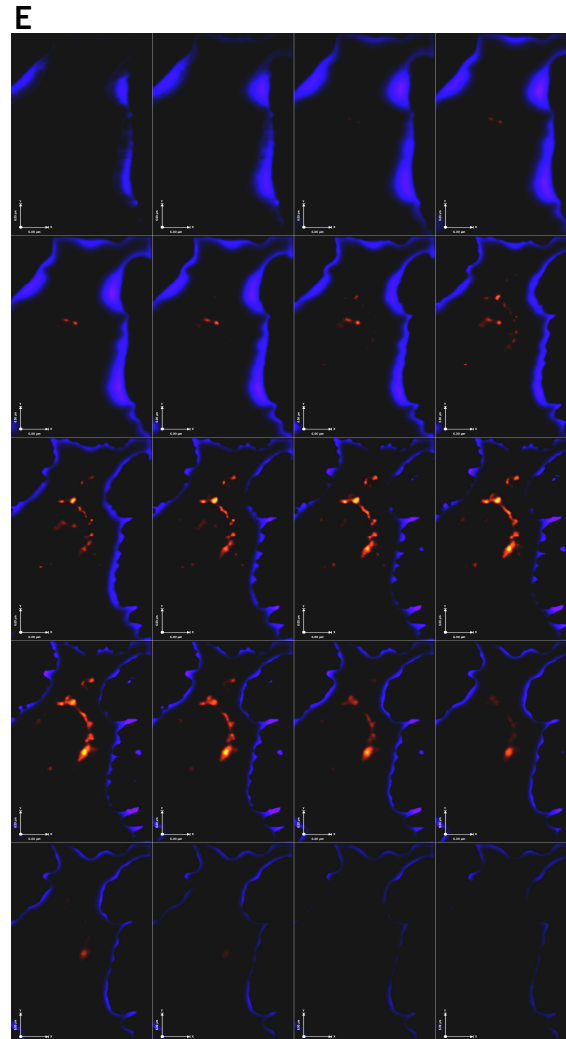
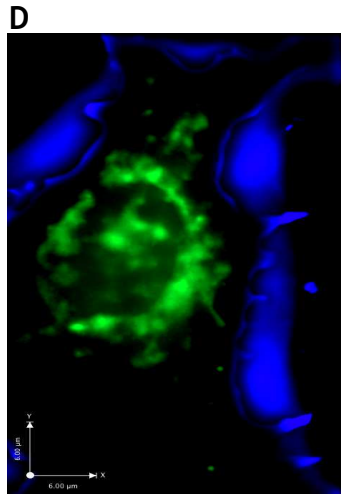
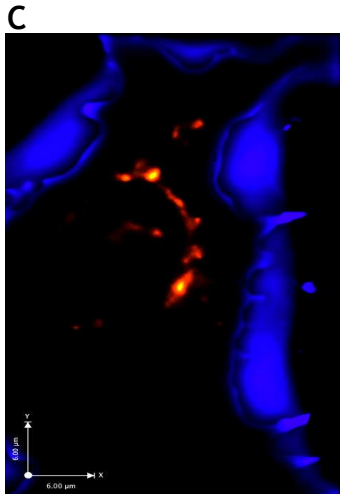
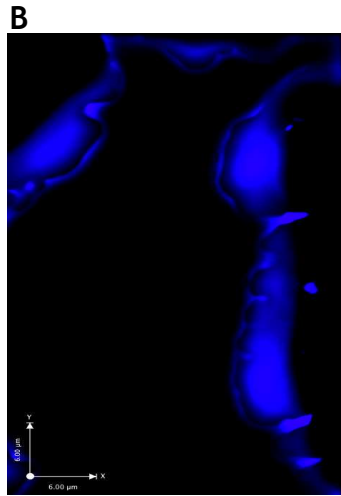
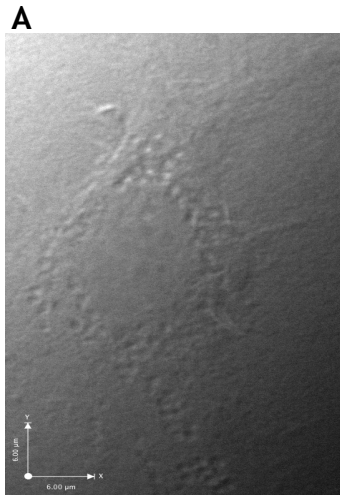
- A:** EBL cell taken under the DIC (white) light.
- B:** EBL cell taken under filtered fluorescent light (Exc. = 649 nm, Ems. = 670 nm) (blue) to visualize the counterstain, CellMask™ plasma membrane stain (GE Healthcare).
- C:** EBL cell taken under filtered fluorescent light (Exc. = 557 nm, Ems. = 585 nm) (red) to visualize internalized bacteria expressing RFP and filtered fluorescent light (Exc. = 649 nm, Ems. = 670 nm) (blue) to visualize the counterstained plasma membrane.
- D:** EBL cell taken under filtered fluorescent light (Exc. = 488 nm, Ems. = 507 nm) (green) to visualize expression of GFP and filtered fluorescent light (Exc. = 649 nm, Ems. = 670 nm) (blue) to visualize the counterstained plasma membrane.
- E:** EBL cell taken under filtered fluorescent light (Exc. = 649 nm, Ems. = 670 nm) (blue) and filtered fluorescent light (Exc. = 557 nm, Ems. = 585 nm) (red) at selected depths by manipulation of optical sectioning. The slide was set to be sectioned optically at 0.4 μm intervals from top to bottom; images shown were captured at every 0.4 μm of depth at a total section stacking of 8.0 μm. The box below shows optical section number for every stack in the images.
- F:** EBL cell taken under filtered fluorescent light (Exc. = 649 nm, Ems. = 670 nm) (blue) and filtered fluorescent light (Exc. = 488 nm, Ems. = 507 nm) (green) at selected depths by manipulation of optical sectioning. The slide was set to be sectioned as in E. The box below shows optical section number for every stack in the images.

**G:** 3D image of C.

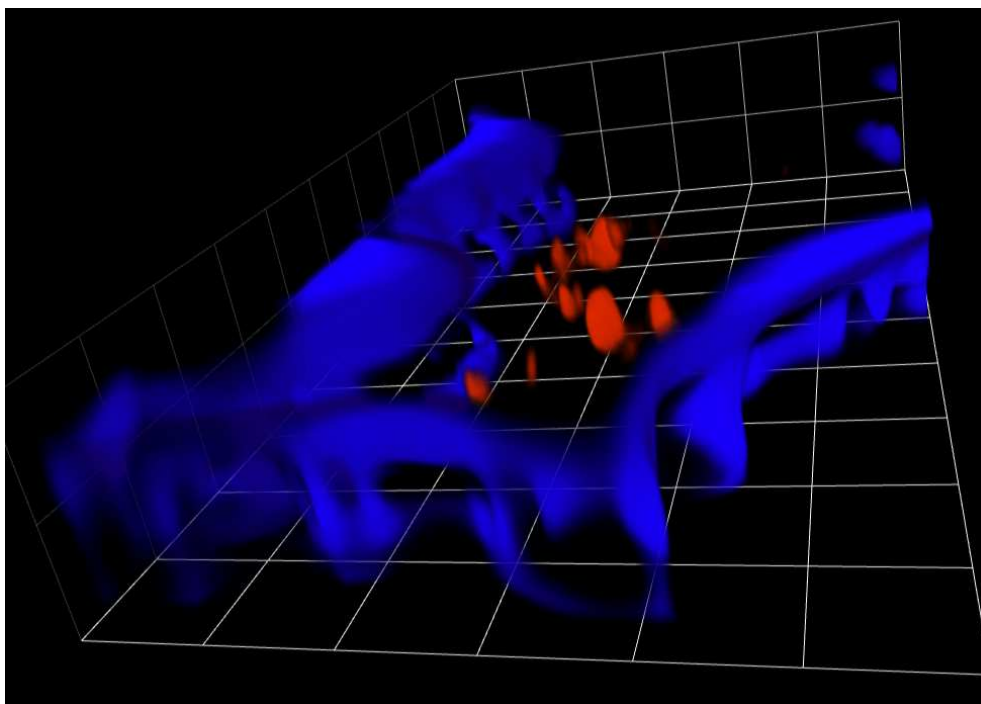
**H:** 3D image of D.

1	2	3	4
5	6	7	8
9	10	11	12
13	14	15	16
17	18	19	20

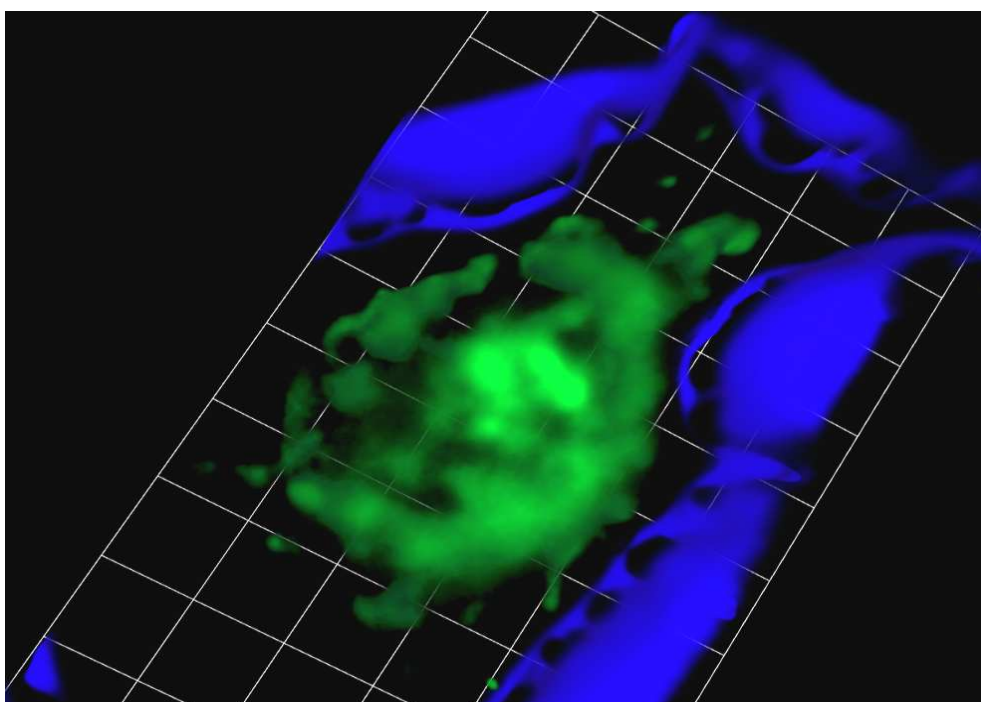
II



**G:** 3D image of C generated using Volocity software.



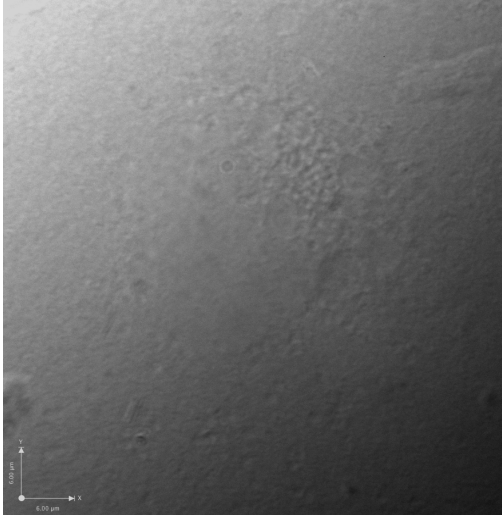
**H:** 3D image of D generated using Volocity software.



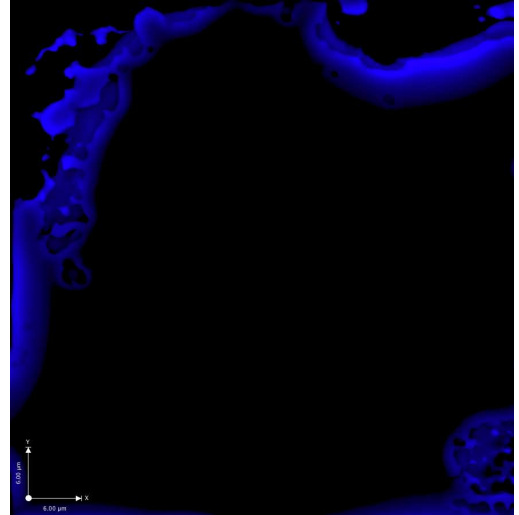
(III) EBL cell captured 5 h post-invasion. Images were taken of the same field but under different light paths.

- A: EBL cell taken under the DIC (white) light.
- B: EBL cell taken under filtered fluorescent light (Exc. = 649 nm, Ems. = 670 nm) (blue) to visualize the counterstain, CellMask™ plasma membrane stain (GE Healthcare).
- C: EBL cell taken under filtered fluorescent light (Exc. = 557 nm, Ems. = 585 nm) (red) to visualize RFP-expressing bacteria at 2.8  $\mu\text{m}$  depth by manipulating optical sectioning and filtered fluorescent light (Exc. = 649 nm, Ems. = 670 nm) (blue) to visualize the counterstained plasma membrane.
- D: EBL cell taken under filtered fluorescent light (Exc. = 488 nm, Ems. = 507 nm) (green) to visualize expression of GFP and filtered fluorescent light (Exc. = 649 nm, Ems. = 670 nm) (blue) to visualize the counterstained plasma membrane.
- E: EBL cell taken under filtered fluorescent light (Exc. = 649 nm, Ems. = 670 nm) (blue) to visualize the counterstained plasma membrane, filtered fluorescent light (Exc. = 557 nm, Ems. = 585 nm) (red) to visualize RFP-expressing bacteria and filtered fluorescent light (Exc. = 488 nm, Ems. = 507 nm) (green) to visualize expression of GFP.
- F: 3D image of C.
- G: 3D image of D.

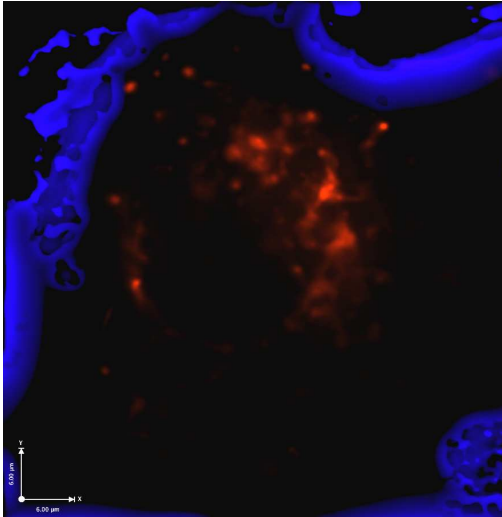
III A



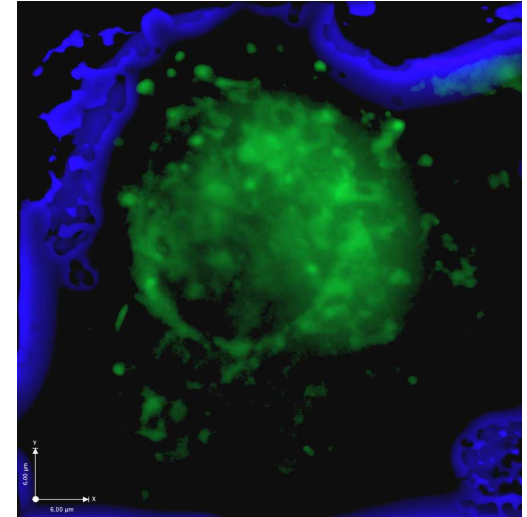
B



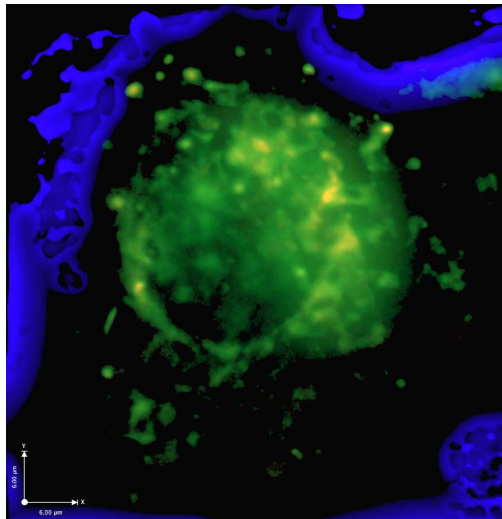
C



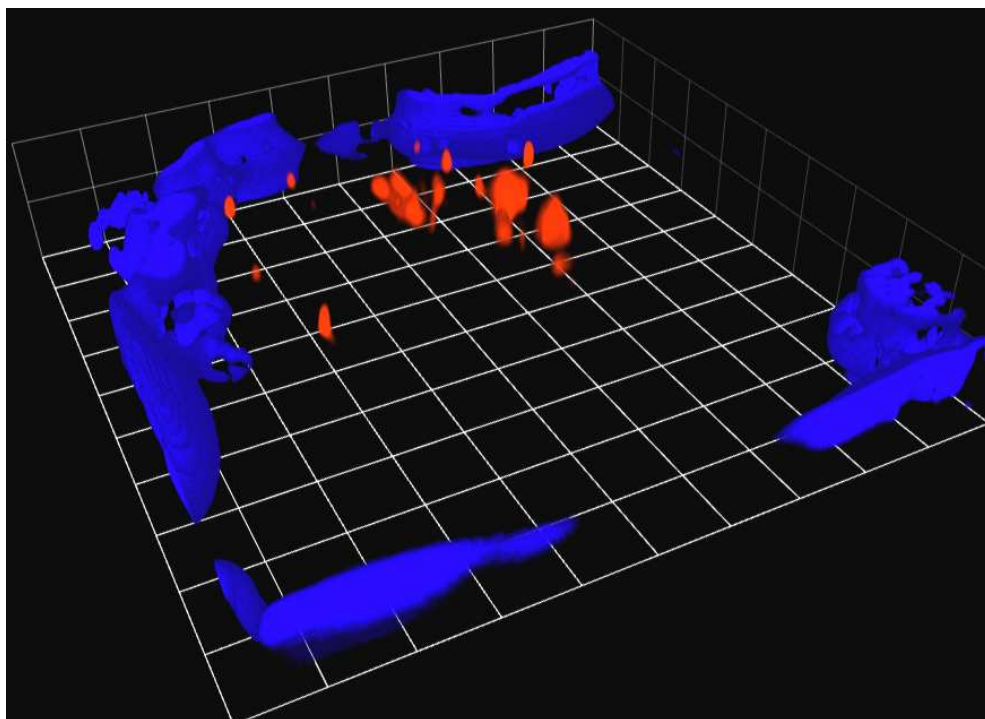
D



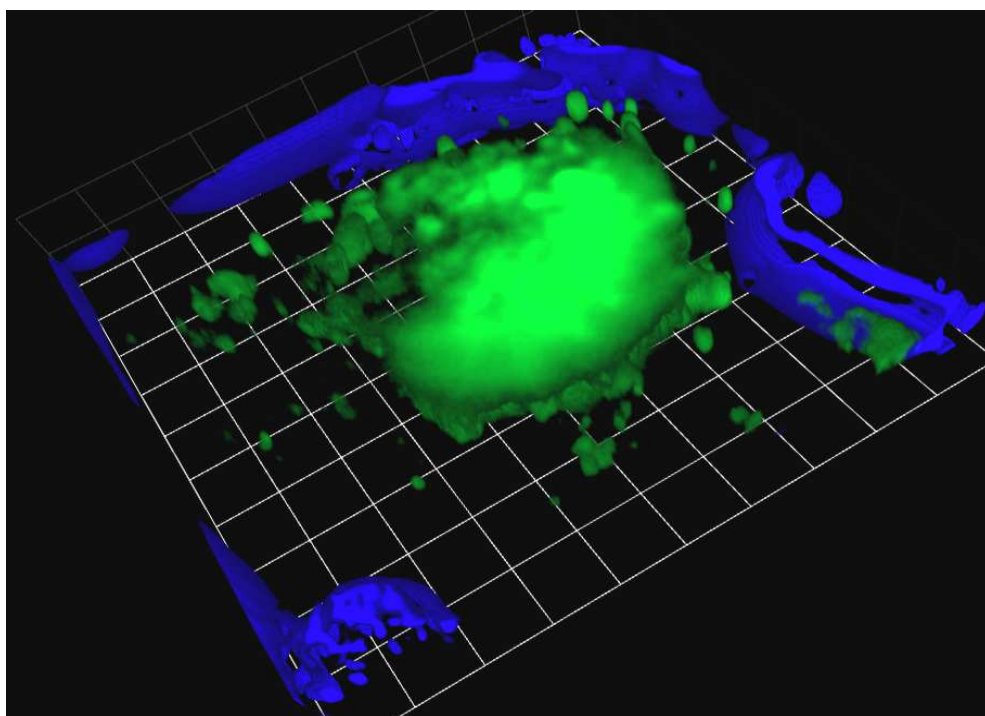
E



F



G



(IV) EBL cell captured at 5 h post-invasion. Images were taken of the same field but under different light paths.

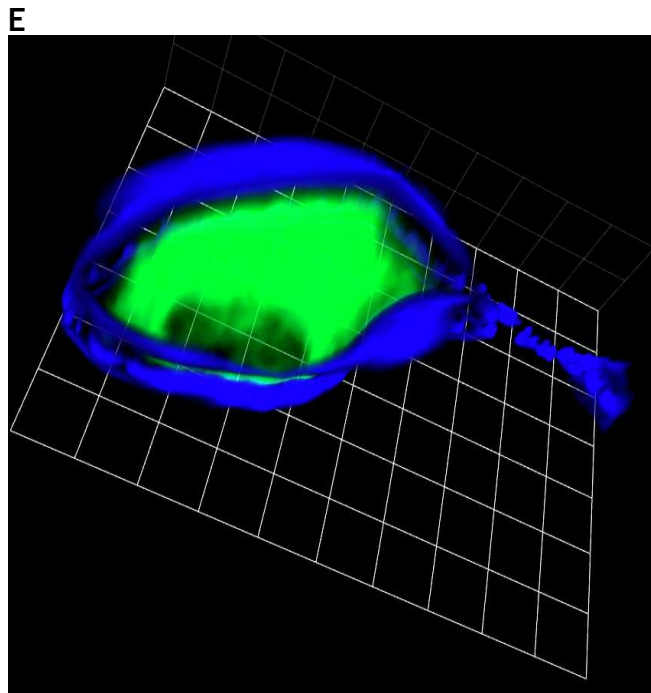
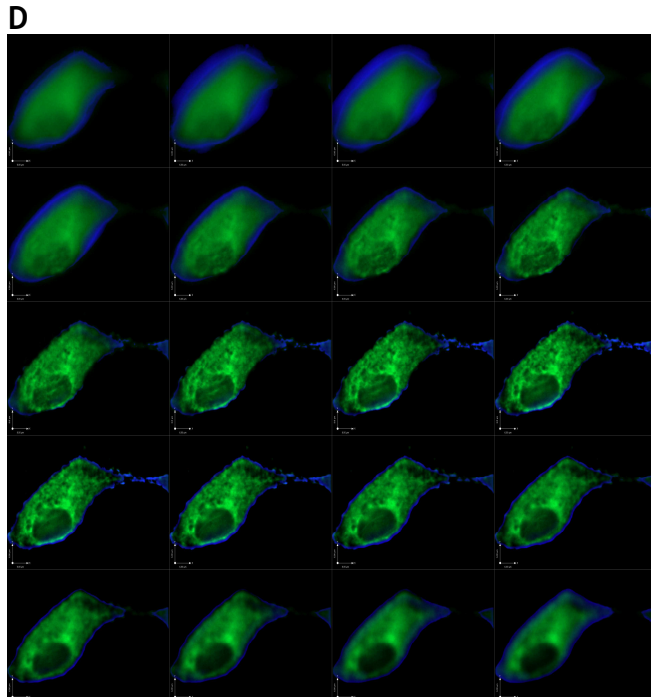
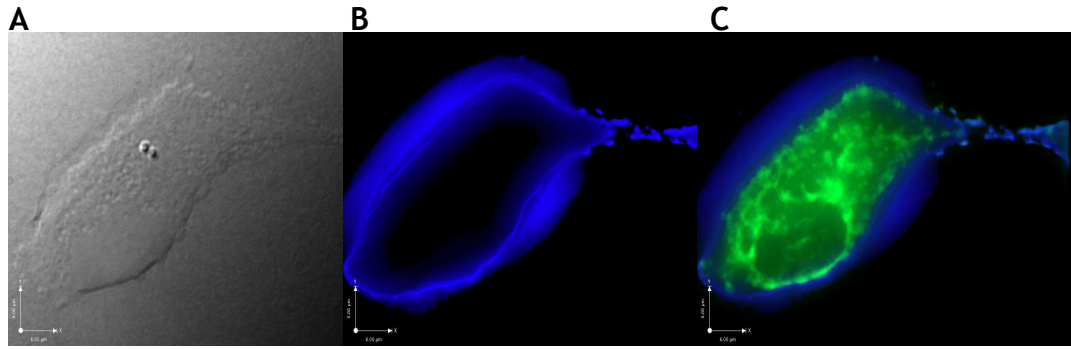
- A:** EBL cell taken under the DIC (white) light.
- B:** EBL cell taken under filtered fluorescent light (Exc. = 649 nm, Ems. = 670 nm) (blue) to visualize the counterstain, CellMask™ plasma membrane stain (GE Healthcare).
- C:** EBL cell taken under filtered fluorescent light (Exc. = 488 nm, Ems. = 507 nm) (green) to visualize expression of GFP in the cytoplasm of EBL cell and filtered fluorescent light (Exc. = 649 nm, Ems. = 670 nm) (blue) to visualize the counterstained plasma membrane.
- D:** EBL cell was taken under filtered fluorescent light (Exc. = 649 nm, Ems. = 670 nm) (blue) and filtered fluorescent light (Exc. = 488 nm, Ems. = 507 nm) (green) at selected depths by manipulation of optical sectioning. The slide was set to be sectioned optically at 0.4 μm intervals from top to bottom; images shown were captured at every 0.4 μm of depth at a total section stacking of 8.0 μm. The table below shows optical section number for every stack in the images.

1	2	3	4
5	6	7	8
9	10	11	12
13	14	15	16
17	18	19	20

- E:** 3D image of C.



IV



Images I and III showed the capability of *P. multocida* B:2 JRMT12 pSRG<sup>+</sup> to express RFP from plasmid pSRG within EBL cells. Images II, III and IV showed the apparent capacity of JRMT12 to release plasmid pSRG into EBL cytoplasm and the capacity of EBL cells to express GFP from pSRG released from internalized *P. multocida* B:2 JRMT12 pSRG<sup>+</sup>. The images also illustrated that *P. multocida* B:2 JRMT12 pSRG<sup>+</sup> was able to express RFP even at 5 h post-invasion (image III). It also demonstrated that pSRG were delivered into the EBL cytoplasm during the initial invasion period, allowing the mammalian cells to express GFP as early as 3 h (images I and II) post-invasion.

From observation of the slides, at 3 h post-invasion, three categories of EBL cells were found. Some EBL cells were found without any bacteria internally (no RFP expression), some EBL cells were found with internalized bacteria but the mammalian cells were not expressing GFP and some EBL cells, at the lowest percentage, were found to harbour internalized *P. multocida* B:2 JRMT12 pSRG<sup>+</sup> and at the same time expressed GFP. At 5 h post-invasion, three categories of EBL cells were also found, some without any bacteria internally, some EBL cells were found to harbour internalized viable *P. multocida* B:2 JRMT12 pSRG<sup>+</sup> expressing RFP and at the same time they expressed GFP and some EBL cells were found without any RFP expression but they expressed GFP. The last category could not be found at 3 h post-invasion and the second category of EBL cells found at 3 h post-invasion could not be found at 5 h post-invasion. Taken together, these data present good evidence that JRMT12 can carry plasmid pSRG into EBL cells and, while the bacteria remain viable, they will express RFP. Loss of RFP expression at 5 h post-invasion plus expression of GFP would indicate release of pSRG into the cytoplasm from the non-viable bacteria, where it was able to express GFP from the <sup>P</sup>CMV<sub>IE</sub> promoter.

### 3.5 Possible immunosuppressive effect of *P. multocida* B:2 infection

Previous work by Ataei (2007) showed an apparent immunosuppressive effect of *P. multocida* B:2 on the proliferative response to concanavalin A (ConA) of peripheral blood mononuclear cells (PBMC) taken from infected animals or from normal animals when treated *in vitro* with *P. multocida* cells and cell-free extracts (CFE). In order to confirm these findings PBMC obtained from normal calves were cultured *in vitro* and treated with CFE of *P. multocida* B:2 strains.

#### 3.5.1 In vitro responses of PBMC

An *in vitro* system to assess possible suppression of lymphocyte proliferation in response to ConA was developed as described in section 2.21. The first assay was done with CFE prepared from *P. multocida* B:2 JRMT12 (this study) and also with a batch of CFE from the wild-type strain (85020) that had been used previously by Ataei (2007). Aliquots of this preparation had been stored at  $-80^{\circ}\text{C}$ . PBMC were obtained from normal calves at the Moredun Research Institute (MRI), Edinburgh. Figure 37 shows the PBMC response towards different concentrations of ConA after pre-treatment for 1 h with different concentrations of CFE. In the absence of CFE, PBMC showed a similar high proliferation to all three concentrations of ConA up to  $\sim 170\ 000$  cpm as shown by the uptake of  $^3\text{H}$ -thymidine, whereas little proliferation was observed without ConA. From graph A, exposure of the PBMC to different concentration of CFE from strain JRMT12 (this study) gave a dose-dependent suppression of PMBC proliferation. Pre-incubation of PBMC for 1 h with CFE at  $5\ \mu\text{g}/\text{ml}$  followed by addition of ConA at any concentration showed a slight suppression of PBMC proliferation but this was more marked at  $10\ \mu\text{g}/\text{ml}$  and  $20\ \mu\text{g}/\text{ml}$  of CFE.

Graph B shows the effect of pre-treatment of the PBMC with CFE prepared previously from the wild-type strain, 85020. Without ConA, minimal proliferation of PBMC was observed even with increasing concentrations of CFE. When PBMC were incubated with different concentrations of ConA alone, proliferative responses up to  $\sim 170\ 000$  cpm were observed but after pre-treatment with the CFE, there was no clear dose-dependent inhibition of proliferation. CFE at  $5\ \mu\text{g}/\text{ml}$  slightly reduced PBMC proliferation and it appeared to have a greater

suppressive effect at 10 µg/ml. However, at 20 µg/ml, PBMC proliferation had increased. This contrast with Ataei's finding (2007) whereby CFE from 85020 at 2 µg/ml greatly suppressed PBMC proliferation in response to presence of ConA.

Taking account of the results of the first assay with a freshly-prepared CFE, it was concluded that the putative active components responsible for proliferation inhibition in CFE prepared by Ataei (2007) might be labile, as the CFE had been prepared two years previously even though it had been stored at -80°C. However, fresh CFE, from JRMT12 generated some dose response in terms of suppression of PBMC proliferation.

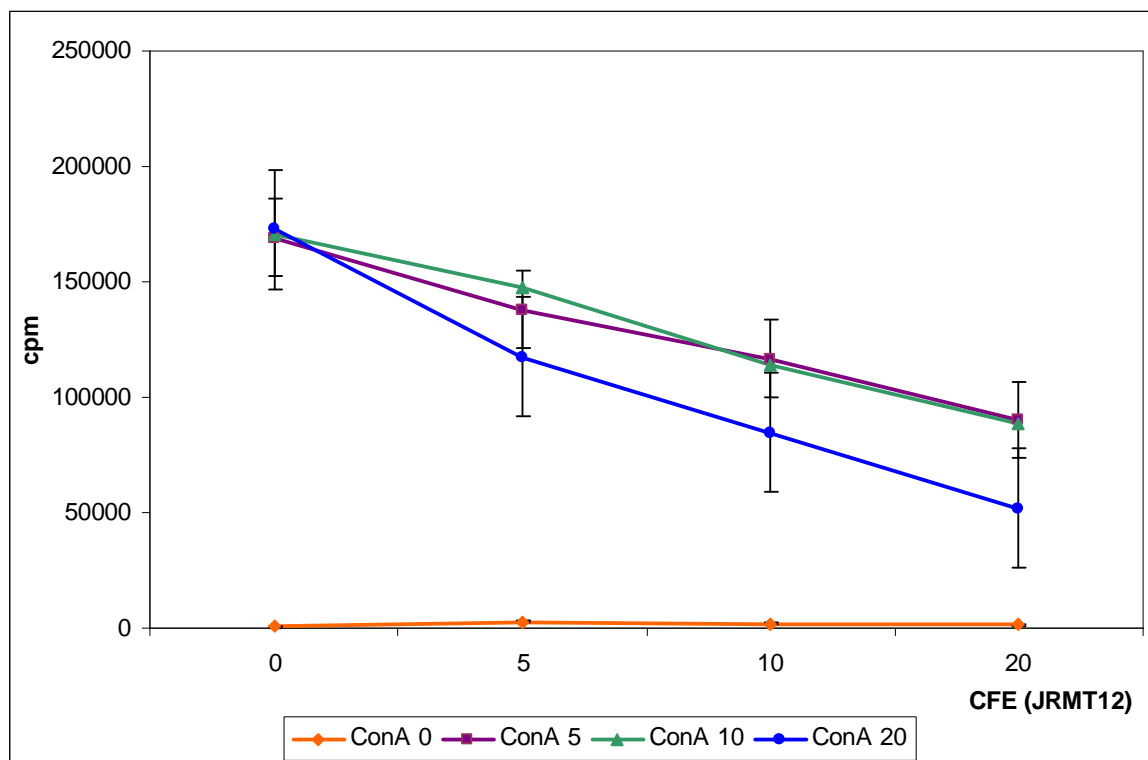
This assay was repeated twice, with PBMC obtained from normal calves at MRI, and treated *in vitro* with a freshly-prepared CFE from the wild-type strain, 85020 and with the CFE prepared from the mutant strain, JRMT12. However, in these assays, no clear suppression of the PBMC proliferation was observed and results from the initial assay were not reproduced.

**Figure 37. Effect of CFE from *P. multocida* B:2 on the proliferative response of PBMC to ConA.**

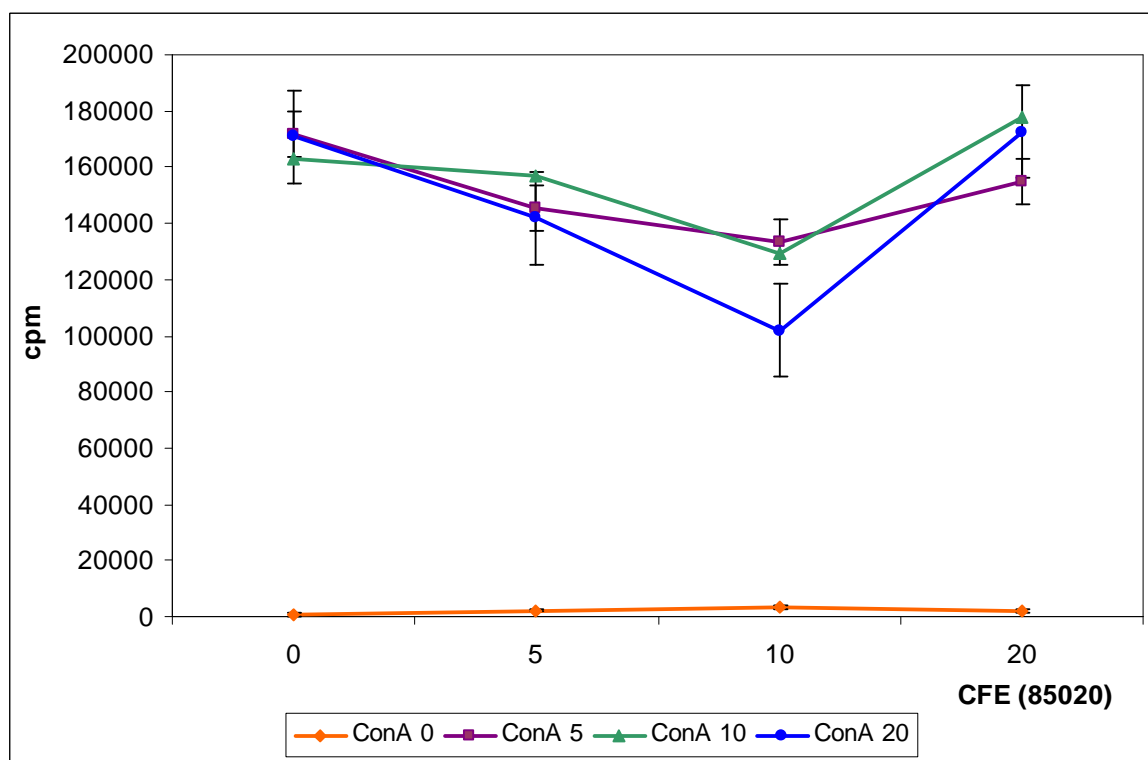
The data represent proliferative responses of normal calf PBMC after incubation for 1 h with CFE at different concentration (0, 5, 10 and 20 µg/ml) before addition of 0, 5, 10 or 20 µg/ml of concanavalin A (ConA). Proliferation was detected by measurement of tritiated thymidine incorporation and expressed as counts per minute (cpm). All tests were done in triplicate and results are mean values ( $\pm$  SEM).

- A PBMC treated with CFE from *P. multocida* B:2 JRMT12 (this study)
- B PBMC treated with CFE from *P. multocida* B:2 85020 (Ataei, 2007)

A



B



The assay was repeated again using fresh batches of CFE prepared from the same mutant (JRMT12) and wild type (85020) strains. PBMC were obtained from calves at the School of Veterinary Medicine, University of Glasgow. Figure 38 A shows the PBMC response after pre-treatment with CFE from the mutant strain (JRMT12). Without ConA, proliferation was not significant. When CFE was not present in the assay, ConA at 5 µg/ml or 20 µg/ml greatly enhanced PBMC proliferation. Pre-incubation of PBMC with CFE at 1 µg/ml for 1 h before addition of ConA did not show any significant suppression of PBMC proliferation. However, with higher CFE concentrations, a reduction of PBMC proliferation was observed, especially with ConA at 20 µg/ml. Thus, this experiment showed a similar result to the first assay (Figure 37 A) where PBMC proliferation was suppressed by CFE from strain JRMT12 in a dose-dependent manner.

Figure 38 B shows the PBMC response after treatment with CFE prepared from the wild type, 85020. However, the results are similar to those observed in the first assay (Figure 37 B). PBMC proliferation was not significantly suppressed when pre-incubated with CFE from strain 85020, followed by addition of ConA.

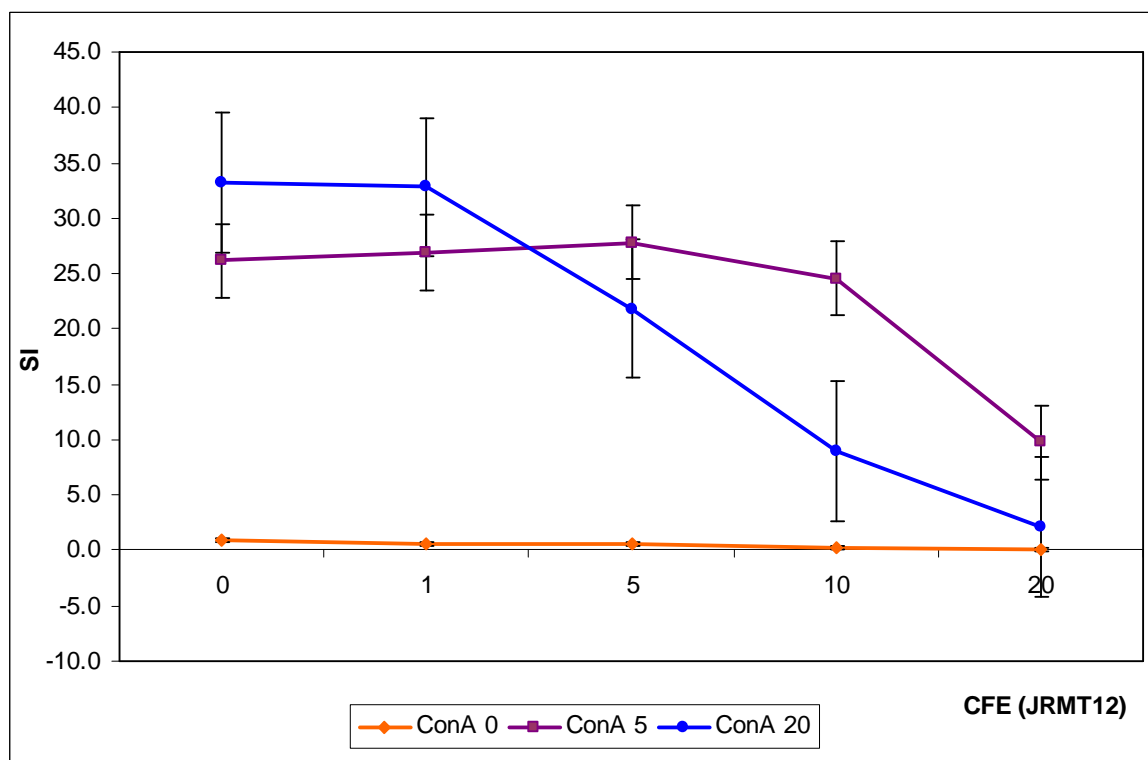
**Figure 38. Effect of new preparations of CFE *P. multocida* B:2 on proliferative response of PBMC to ConA.**

The data represent proliferative responses of normal calf PBMC after incubation for 1 h with CFE at different concentration (0, 1, 5, 10 and 20 µg/ml) before addition of 0, 5, or 20 µg/ml of concanavalin A (ConA). Proliferation was detected by measurement of tritiated thymidine incorporation and expressed as stimulation index (SI). Which shows the ratio of incorporation in treated (CFE was added) compared to untreated cells. PBMC were cultured in triplicate and results are mean values ( $\pm$  SEM).

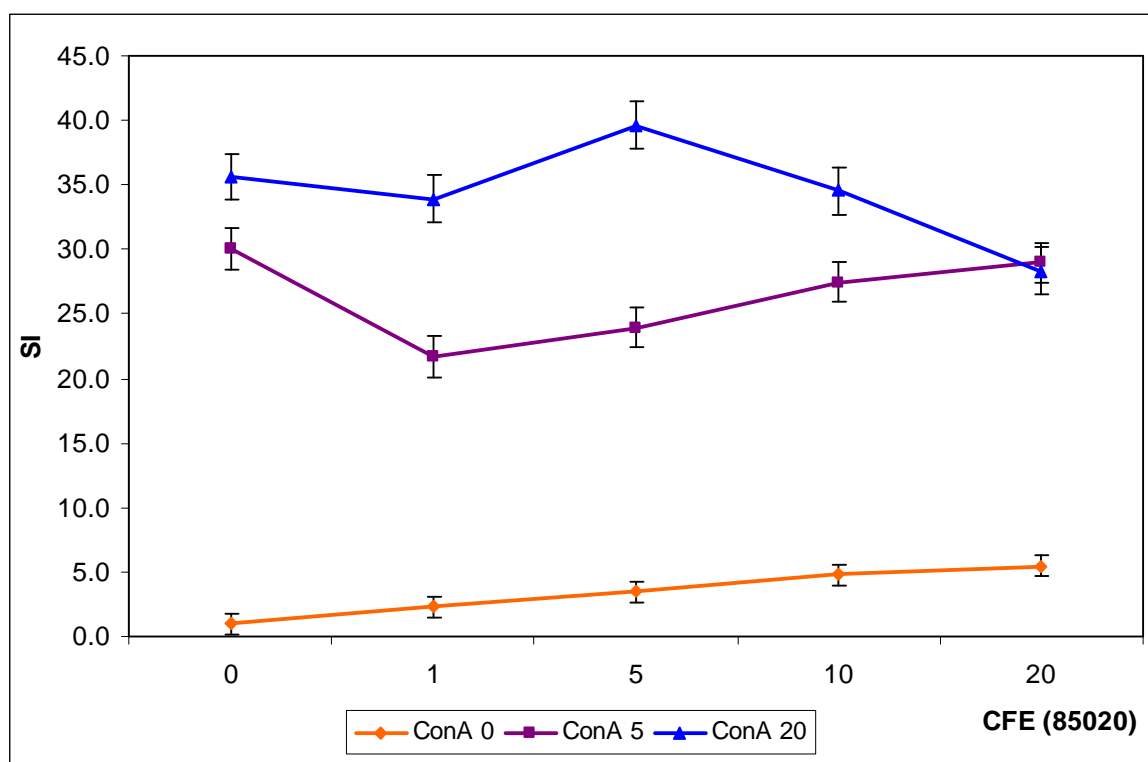
- A PBMC treated with CFE from *P. multocida* B:2 JRMT12
- B PBMC treated with CFE from *P. multocida* B:2 85020



A



B



The assay was again repeated, with the same prepared CFE from the previous experiment and PBMC obtained from calves at the School of Veterinary Medicine, University of Glasgow. Results showed no clear suppression of the PBMC proliferation and data from the initial assay were not reproduced. Despite irreproducibility and inconsistencies in the data obtained, a trend towards suppression on PBMC proliferation had been observed with CFE prepared from strain JRMT12.

## 4.0 DISCUSSION

### 4.1 Interaction between mammalian cells and *Pasteurella*

*P. multocida* B:2 causes haemorrhagic septicaemia (HS) in cattle and buffaloes. The successful transmission of disease by the intranasal and oral routes, producing a syndrome with clinical signs and lesions resembling natural disease indicates that these may be the natural routes of infection (De Alwis, 1992). However, a feature of the HS disease is the rapid spread of infecting bacteria from the respiratory tract to the blood and lymph to cause a fatal septicaemia in less than 48 h. To pass into the bloodstream, the bacteria must migrate through the epithelial layer into the pulmonary interstitium. The potential of *Pasteurella* for attachment to and invasion of mammalian cells may constitute a mechanism that enables the bacteria to invade the blood stream. In this study, two strains of *P. multocida* B:2 were assessed for their interactions with several types of mammalian cells. Beside the parent strain, *P. multocida* B:2 85020 (HS-associated strain obtained from Sri Lanka), a marker-free *aroA* deletion derivative of this strain, JRMT12, were observed for their ability to adhere to and invade mouse macrophage-like, J774.2 cells, bovine lymphoma, BL-3 cells and embryonic bovine lung, EBL cells. For comparison, bovine *P. multocida* A:3, bovine *M. haemolytica* A:1 and *E. coli* XL-1 Blue were included.

As attachment is a primary prerequisite for bacterial infection, many studies have examined potential receptors and ligands during host-pathogen interactions. *P. multocida* serotype A:3 was found to adhere to the mucosal epithelium of the nasopharynxes of rabbits (Glorioso *et al.*, 1982). The study showed that bacteria specifically attached to squamous epithelial cells of the pharyngeal mucosa both *in vivo* and *in vitro* and to some tissue culture cell lines such as HeLa cells. The attachment to pharyngeal and HeLa cells was inhibited by N-acetyl-D-glucosamine. These findings suggested that this amino sugar may be a component of the receptor on both cell surfaces and that fimbriae may have mediated adhesion (Glorioso *et al.*, 1982). However, they also found that the hyaluronic acid capsule of the A:3 strain reduced adhesion, possibly because of its high-charge density which increased repulsion between the animal cell and the bacteria (Jones, 1977). It was suggested in another study that the hyaluronic acid capsule was not involved in the adherence process during pathogenesis but

played a role in increasing resistance to cellular defence mechanisms during *Pasteurella* infections (Maheswaran & Thies, 1979).

Adherence of a *P. multocida* serotype A strains to HeLa cells was also shown by Esslinger *et al.* (1994). The strain adhered strongly to HeLa cells and alveolar macrophages from rabbits, mice, cattle and horses. They also showed that by pre-treating the *Pasteurella* with hyaluronidase or pre-incubating the HeLa cells with hyaluronic acids, bacteria adherence was dramatically reduced. They thus suggested that hyaluronic acid in the capsule of the type A strain played a role in adhesion and subsequent colonization of the bacteria (Esslinger *et al.*, 1994). These data contradict the earlier study of Glorioso *et al.* (1982), but were confirmed in another study when acapsulated strain of *P. multocida* A:3 was found to adhere to turkey air sac macrophages in culture but were not internalized, while non-capsulated variants of the A:3 strain showed little or no adherence and also were not internalized (Pruimboom *et al.*, 1996). Depolymerization of the bacterial capsule with hyaluronidase increased phagocytosis by macrophage cultures, and addition of hyaluronic acid to the macrophages inhibited bacterial adherence. The study suggested that capsular hyaluronic acid facilitates adherence to, but not internalization of, macrophages cultures. It also suggested that a host-specific glycoprotein receptor is involved for recognition of this bacterial polysaccharide.

*In vitro* adherence of *P. multocida* A:3 and a type D:1 strain, isolated from a rabbit with septicaemia, towards explants of tracheal mucosa, lung and aorta from freshly killed rabbits were assessed by Al-Haddawi *et al.* (2000). Under a scanning electron microscope, the type D strain was found to adhere more to trachea and aorta when compared to the type A strain. However, the type A strain adhered to the lung explants more efficiently. The results were obtained after 45 min of incubation, but prolonged incubation to 2 h found that both strains adhered at a similar rate to the lung explants. It was noted that the capsular material of type A strain and the toxin of the type D strain may have influenced the adherence to lung tissue in the rabbit. This study also suggested, from the ability of the type D strain to adhere to aorta, that the expression of receptors on the endothelium could possibly explain the ability of certain strains to cause septicaemia (Al-Haddawi *et al.*, 2000).

*P. multocida* types A, D and B:2 strains are known to possess type 4 fimbriae [designated PtfA] (Ruffolo *et al.*, 1997; Dabo *et al.*, 2007; Siju *et al.*, 2007). Under microaerophilic conditions, *P. multocida* showed an increased expression of the fimbriae, which were observed to form bundles. Purification of fimbriae with high performance reverse phase liquid chromatography isolated a single 18-kDa subunit and the first 21 amino acids shared a very high similarity with the N-terminal amino acid sequence of type 4 fimbrial subunits from other bacteria. The gene *ptfA* which coded for type 4 fimbrial protein from *P. multocida* B:2 was later studied and characterized (Siju *et al.*, 2007). This study revealed that type 4 fimbriae are probably one of the most important surface components that mediate colonization of host surfaces and which correlate to bacterial virulence.

It has also been shown known that many pathogens, including members of the family *Pasteurellaceae*, exploit host extracellular matrix (ECM) molecules for virulence through adherence and colonization. ECM is a mixture of many glycoproteins including fibronectin, fibrinogen, collagen, elastin, laminin and glycosaminoglycans present in the cell membrane of eukaryotic cells (Kreis & Vale, 1993). The broad host range characteristics of *P. multocida* A:3 suggest recognition of host cell surface components (ECM molecules) common to multiple animal species and tissue types. Recent studies have investigated the binding of *P. multocida* A to ECM molecules including fibronectin (Fn) (Dabo *et al.*, 2005). Bacteria bound both soluble and immobilized Fn and preferentially bound the N-terminal heparin-binding fragment (Hep-1) of Fn, similar to that described for other bacterial pathogens (Dabo *et al.*, 2005). OmpA, TonB-dependent receptor HgbA (a hemoglobin-binding protein A) and transferrin-binding protein A (TbpA) were among the *P. multocida* and *M. haemolytica* proteins identified as putative Fn-binding proteins. The OmpA protein was found to bind Madin-Darby bovine kidney (MDBK) cells via heparin and/or Fn bridging (Dabo, 2003) and ELISA study using bovine fibronectin as the substrate demonstrate antibody to the 45 kDa OmpA of *M. haemolytica* A1 bound specifically to the fibronectin but not to fibrinogen (Lo & Sorensen, 2007). This study was further elaborated by Kisiela & Czuprynski (2009) who demonstrated that OmpA and lipoprotein 1 (Lpp1) were involved in adherence of bovine *M. haemolytica* A1 towards bovine bronchial epithelial cells.

*M. haemolytica* has been reported to adhere to epithelial cells of the bovine respiratory tract (Clarke *et al.*, 2001) and Mardin-Darby bovine kidney (MDBK) cells (Galdiero *et al.*, 2002). *M. haemolytica* field isolates from ovine mastitis were also found to adhere to a primary culture of ovine mammary epithelium (Vilela *et al.*, 2004). In another study, confluent bovine aortic endothelial cells (BAEC) were infected with *P. multocida* serotype B and *M. haemolytica* serotype A:1 at MOI 10, 50, 100 or 1000 bacteria/cell. An association assay was carried out at 30 or 60 min post-infection. The infected cells were fixed with methanol and Giemsa staining was utilized to illustrate cell-association of bacteria. Assessment of adherence showed no significance differences between the two species at the different bacteria:cell ratios (Galdiero *et al.*, 2001). Although the above studies did not indicate potential adherence substances, they did demonstrate adherence of *P. multocida* to different cell types, tissues or organs and often reflected a serogroup-specific host preference and pathogenicity.

In this study, in the absence of killing of extracellular bacteria (by omitting gentamicin and polymyxin B) the number of intracellular plus adherent bacteria of different strains of *P. multocida* B:2, *P. multocida* A:3 and *M. haemolytica* A:1 with EBL cells could be determined. By comparison with the number of intracellular bacteria (after using gentamicin and polymyxin B) to kill extracellular bacteria, the number of adherent bacteria could then be assessed. After incubation for 1 or 3 h with EBL cells, all strains tested showed a similar rate of adherence, although the attenuated derivative *P. multocida* B:2 JRMT12 adhered to EBL cells slightly better than its parent strain, 85020 (Table 10). This might be due to modification in the surface properties associated with altered aromatic acid biosynthesis in the JRMT12 strain. The other strain, *P. multocida* A:3 and *M. haemolytica* A:1 adhered to EBL cells at a similar rate to JRMT12 (Table 11). These findings correspond to all previous studies mentioned above. However, experiments here were not extended to investigate host-interaction receptors between mammalian cells and *P. multocida* B:2 strains. In further experiments, it would be of interest to determine the effect of Fn on the adherence of these strains to mammalian cells.

A variety of pathogenic bacterial species adhere to non-phagocytic mammalian cells but not all bacteria-host cell interactions result in cellular entry. Avian serogroup A strains of *P. multocida* have been reported to invade cultured

mammalian cells (Al-haj Ali *et al.*, 2004) as have *P. multocida* serotype B strains when investigated for their ability to adhere to and invade bovine aortic endothelial cells (BAEC) (Galdiero *et al.*, 2001). Preliminary data (Tabatabaei, 2000; Merza, 2008) showed that *P. multocida* B:2 can enter and survive within mouse macrophage-like cells, J774.2 and bovine lymphoma cells, BL-3. In the host, survival within leukocytes may be a feature that facilitates rapid systemic infection.

Our study showed that *P. multocida* B:2 has the ability to invade J774.2, BL-3 and EBL cells at MOI 100:1. At lower MOIs, invasion was less pronounced and at higher MOIs little enhancement of invasion was seen (Tables 7 & 9). Much of the knowledge regarding bacterial internalisation and intracellular survival has been gained from studies using *in vitro* assay in which cultured mammalian cells are infected with bacteria for a pre-determined time. Bacteria recovered after antibiotic treatment to kill extracellular bacteria are presumed to be internalised within the cells. A combination of gentamicin and polymyxin B antibiotics at 50 µg/ml of each reduced the number of viable *P. multocida* B:2 JRMT12 by > 99.9% after 30 min incubation and essentially killed all bacteria after incubation for 60 min. Both *P. multocida* B:2 strains were found to be internalised in J774.2, BL-3 and EBL cells at 3 h post-invasion (Tables 5, 6, 8 & 9). It was mentioned above that all other *Pasteurella* strains tested in this study were able to adhere to EBL cells; however very low number of them were found intracellularly. The same results were observed when J774.2 cells were infected with either *P. multocida* A:3 or *E. coli* XL-1 Blue, very low number of these strains were internalised by the phagocytic cell lines (Table 7).

*P. multocida* B:2 JRMT12 was found to survive intracellularly for at least 7 h with a slow decrease with time in the number of viable internal bacteria. An EBL monolayer was exposed to JRMT12 in the standard invasion assay for 3 h and this was followed by prolonged incubation for 5 or 7 h, either with gentamicin and polymyxin B each at 10 µg/ml or 50 µg/ml or in the absence of antibiotic. These conditions were created in order to eliminate the possibility of any extracellular bacteria replicating if there was no antibiotics present in the assay. Antibiotics at 50 µg/ml were maintained in the assay to eliminate extracellular bacteria but ingestion of the assay medium by mammalian cells might result in the possibility of killing of intracellular bacteria. Hence, in parallel, a lower level of antibiotics

(10 µg/ml) was added, sufficient to prevent replication of any remaining extracellular bacteria but at the same time, ingestion of assay medium by the cell would be less likely to result in short-term killing of intracellular bacteria. However, the data obtained showed no significance difference in bacterial numbers recovered, either with or without the presence of antibiotics (Table 12). A previous study had shown an apparent increase of bacterial counts 6 h post-infection by *P. multocida* B:2 strains of J774.2 cells but fewer bacteria were recovered when the assay was done in the presence of antibiotics at a low level (Merza, 2008). This could be due to the fact that the cell line used was actively phagocytic. Thus the possibility of medium ingestion would be more likely when compared to EBL cells used in our study.

As mentioned above, infection of BAEC with *P. multocida* B at MOI 100:1 found the bacteria to be internalized at 4 h post-infection (Galdiero *et al.*, 2001). They also found that bacterial internalization was dependent on microfilament and microtubule stability. The study used cytochalasin D, an inhibitor of actin polymerization, colchicine and nocodazole, inhibitors of microtubule formation, and taxol, which stabilizes the microtubules, to determine the involvement of microfilaments and microtubules in these processes. In the presence of cytochalasin D, invasion was reduced by 60%; it was reduced by 3% in the presence of colchicine and by 5% in the presence of nocodazole (Galdiero *et al.*, 2001). Thus, *P. multocida* invasion was principally dependent on actin filament formation.

In an invasion inhibition assay in the present study, EBL monolayers were pre-incubated with 1, 2, 4 and 8 µg/ml of cytochalasin D (CD) for 1 h. After infection of 3 h with the JRMT12 strain, CD was active at 1 µg/ml in completely preventing invasion. The assay was repeated with pre-incubation of the EBL monolayer with 1 µg/ml of CD but the monolayer was washed three times with PBS before adding the bacteria at MOI 100:1. Incubation was then followed as for the standard invasion assay but also prolonged as for the intracellular survival assay (total 7 h). Table 13 shows that the effect of CD was not reversible, at least during the 2 h period when washed EBL cells were incubated with bacteria prior to antibiotic treatment. In comparison with the above study by Galdiero *et al.* (2001) which showed only 60% of inhibition during invasion of BAEC by *P. multocida*, invasion was totally inhibited in this study when CD was pre-exposed



to the EBL cells before bacterial infection. Nevertheless, all data concur that entry of *P. multocida* B:2 into mammalian cells might be by actin-dependent phagocytosis.

A summary of *Pasteurella* adherence to and invasion of mammalian cells is listed below in Table 15.

**Table 15. Summary of *Pasteurella* interactions with mammalian cells.**

Pathogen	Properties	Cells	Reference
<i>P. multocida</i> A:3	Adherence	mucosal epithelium of rabbit nasopharynges and HeLa cells	Glorioso <i>et al.</i> , 1982
<i>P. multocida</i> A	Adherence	alveolar macrophages (from rabbits, mice, cattle and horses) and HeLa cells	Esslinger <i>et al.</i> , 1994
<i>P. multocida</i> A:3 (capsulated)	Adherence	air sac macrophage of turkey	Pruimboom <i>et al.</i> , 1996
<i>P. multocida</i> A:3	Adherence	explants of tracheal mucosa, lung and aorta from rabbit	Al-Haddawi <i>et al.</i> , 2000
<i>P. multocida</i> D:1	Adherence		
<i>P. multocida</i> B:2	Adherence & Invasion	Mouse macrophage-like J774.2 cells	Tabatabaei, 2000
<i>M. haemolytica</i> A:1	Adherence	Bovine aortic endothelial (BAEC) cells	Galdiero <i>et al.</i> , 2001
<i>P. multocida</i> B	Adherence & Invasion		
<i>M. haemolytica</i> A	Adherence	Bovine upper respiratory tract tissues	Clarke <i>et al.</i> , 2001
<i>M. haemolytica</i>	Adherence	Mardin-Darby bovine kidney (MDBK) cells	Galdiero <i>et al.</i> , 2002
<i>P. multocida</i> A	Invasion	Chicken embryo fibroblast (CEF) cells	Al-haj Ali <i>et al.</i> , 2004
<i>M. haemolytica</i> (isolates from ovine mastitis)	Adherence	Ovine mammary epithelium	Vilela <i>et al.</i> , 2004
<i>P. multocida</i> B:2	Adherence & Invasion	Mouse macrophage-like J774.2 cells and bovine lymphoma (BL-3) cells	Merza, 2008
<i>M. haemolytica</i> A:1	Adherence	Bovine bronchial epithelial cells	Kisiela & Czuprynski, 2009

Localization of internalized bacteria was determined by TEM examination of an infected EBL monolayer. In previous studies the appearance of vacuoles has been observed in phagocytic cells such as macrophages, in the presence of the intracellular pathogen (Shah *et al.*, 1996). In J774.2 cells, extensive vacuolation was seen after infection with *P. multocida* B:2 (Merza, 2008). Both of these studies showed dramatic effects on the appearance and viability of macrophages after infection with *P. multocida* B:2. In the present study, in order to determine bacterial cytotoxic activity towards mouse macrophage-like J774.2 cells and EBL cells (which are not normally considered phagocytic), trypan blue exclusion staining was used to distinguish between live and dead cells. Staining was done before and after exposure of the cells to bacteria. The data showed no toxic effects of any of the bacterial strains used for either J774.2 or EBL cells. Galdiero *et al.* (2001) assessed cytotoxicity by measuring the release of lactic dehydrogenase from BAEC cells and their findings were in agreement with our study, as they reported little or no cytotoxicity of their B serotype strain. TEM micrographs in the present study showed pre-existing vacuoles in non-infected EBL cells and exposure to bacterial strains did not extensively alter their morphologies. Thus the vacuolating effect of *P. multocida* B:2 noted above may be restricted to professional phagocytes.

A micrograph prepared from a sample taken 2 h post-infection demonstrated JRMT12 bacteria in the process of being taken up by an EBL. Protruding arms (pseudopod-like elongations) extending from the EBL cell to surround the bacteria were found in this micrograph agreeing with earlier data which indicated that bacteria enter through phagocytosis. Observation of filamentous structures on the bacterial periphery might be indication of adherence mechanisms. At 3 h post-infection, electron-dense *P. multocida* B:2 JRMT12 were observed individually inside tight membrane bound cytoplasmic vacuoles, but rarely (if ever) free in the cytoplasm of EBL cells, although the vacuole membrane were sometime difficult to see.

Micrographs on other *Pasteurella* strains demonstrated bacteria adhering to EBL cells or existing extracellularly at 2 h post-infection. *M. haemolytica* A:1 adherence to these cells appeared to be low even compared to *P. multocida* A:3. Neither of these strains was found intracellularly even at 3 h post-infection, agreeing with the data of the previous invasion assays (section 3.2.4.3). These

data also agree with the previous literature mentioned earlier, indicating that both *P. multocida* A:3 and *M. haemolytica* A:1 adhere to mammalian cells but were not found intracellularly.

The morphological assessment by TEM showed bacteria co-localising in a low percentage of mammalian cells rather than being invasive for the majority of mammalian cells. These results raise the question of whether the differentiation or proliferation states of the mammalian cells modify their susceptibility to *P. multocida* B:2. Enteropathogenic *E. coli* (EPEC) pathogenesis was dependent on cell differentiation states (Gabastou *et al.*, 1995). Infection of Caco-2 cells with EPEC provided evidence that intestinal cell differentiation could alter EPEC pathogenesis. The study found that EPEC:cell clusters increased as a function of the epithelial cell differentiation while efficient cell entry by EPEC bacteria occurred in Caco-2 cells where differentiation had recently been initiated and decreased when the cells were fully differentiated. Thus, the mature cell up-regulates intestinal colonization but down-regulates intestinal cell invasion by EPEC (Gabastou *et al.*, 1995). Another study, with *Listeria monocytogenes*, showed that entry into intestinal cell lines did not involve mammalian cell metabolism. The observation shows that *L. monocytogenes* entry escalated during the mammalian cell proliferation process rather than during the differentiation state of the cells (Velge *et al.*, 1997). In our study, *P. multocida* B:2 was found to invade selective cells after monolayer infection. Assessment of target cell conditions during infection would be worth investigating. Experiments could recruit carboxyfluorescein diacetate succinimidyl ester (CFDA-SE) to monitor the extent of mammalian cell proliferation (Fuller *et al.*, 2001) simultaneously with fluorescent dyes such as acetomethoxy derivate of calcein (calcein-AM) to measure cell viability by determining functionality of intracellular esterases (Calvinho & Oliver, 1998). Both of these stains could evaluate the growth stages of cells during bacterial invasion.

In this section, the capacity of *P. multocida* B:2 strains to be internalized and persist in mammalian cells has been discussed. The *P. multocida* A:3 strain and the *M. haemolytica* A:1 strain showed a capacity to adhere to EBL cells, but only the B:2 strain was found intracellularly. The pathogenesis of HS strains is very complex and further investigations are necessary to improve our understanding of this process. However, the recognition that the B:2 strain expresses the

capacity to adhere to and invade mammalian cells suggests that molecular studies to identify the components involved in these processes and the relevance of target cell cycle to pathogenesis may help to improve our understanding of the pathogenicity of HS. Moreover, the collective data also serves as important preliminary work that established that the JRMT12 strain could act as a suitable carrier vehicle for bacteria-mediated gene transfer (bactofection), the transkingdom transfer of DNA from bacteria to other organisms.

## 4.2 Construction of a *Pasteurella* eukaryotic expression plasmid

Bactofection uses bacteria as a vehicle for DNA vaccination. Generally, the vector bacterium will carry a plasmid able to express heterologous gene(s) under the control of a eukaryotic promoter. After entry of the bacterium into the mammalian cell, progressive destruction of the bacterium will release the plasmid into the mammalian cell cytosol where the heterologous gene can then be expressed. Such a delivery system has many benefits such as the ability to target sites of the immune system open only to intracellular pathogens. One of the most important components in bacteria-mediated gene transfer is the suitability of the eukaryotic expression plasmid to the carrier bacterium and to the target host cells.

The eukaryotic expression plasmid pCMV-sCRIPt is a pUC-based plasmid designed to allow replication in *E. coli* together with replication and protein expression in mammalian systems. It was found in this study that the plasmid failed to propagate in *P. multocida* B:2 after electroporation. The inability of *Pasteurella* (*Mannheimia*) strains to maintain other plasmids with different origins of replication has been shown in previous studies. Non-*Pasteurella* broad-host-range plasmids such as pRK290 and pSa4 were transferred into *M. haemolytica* A1 of bovine origin either by conjugation or electroporation. However, none was found to propagate in this strain (Craig *et al.*, 1989). The study suggested that *M. haemolytica* possessed an active DNA restriction system that might prevent the function of a non-suitable plasmid in the bacterium. It was later found that *M. haemolytica* A1 harbours a type I restriction enzyme, *phal*, and a type II restriction enzyme *hsdM* (Hill & Lainson, 2003). Another study on *P. multocida* type D found a restriction-modification system in the toxigenic strain, LFB3

(Hoskins, 1997). Plasmid DNA transformed in this strain was resistant to *Pst*I, and sensitive to *Dpn*I digestion. Since the discovery of DNA restriction systems in *Pasteurellaceae*, researchers have needed to develop a plasmid that can be delivered between members of *Pasteurellaceae* family and to other Gram-negative bacteria, such as *E. coli*, to facilitate genetic studies (Azad *et al.*, 1994; Wood *et al.*, 1995).

As outlined in Figure 12, Chapter 3, two plasmids were selected in order to develop a *Pasteurella* eukaryotic expression plasmid. Plasmid pAKA16, developed in this laboratory (Azad *et al.*, 1994) was derived from a plasmid isolated from a bovine *M. haemolytica* A:1 strain and was selected for its stability and ready amplification in *P. multocida* B:2 and also in *E. coli*. The commercial *E. coli* eukaryotic expression vector pCMV-sCRIPT was selected based on its size and properties. The proposed strategy illustrated in Figure 12 showed the isolation of the *Pasteurella* origin of replication from plasmid pAKA16 to replace the ColE1 origin of replication on plasmid pCMV-sCRIPT. The origin of replication from plasmid pAKA16 (*ori*P) was identified and sequenced (Figure 15). The sequence had two open reading frames (ORF). The first ORF was located downstream of a set of genes recognized as the putative *ori*P gene; 51 bp of the sequence within this gene was highly matched with several native *Pasteurellaceae* plasmids, pJR1 (from *P. multocida*), pD70 (from *M. haemolytica*), pIG1 (from *P. multocida*) and pAB2 (from *M. haemolytica*), and was located in the replication origin in each of these plasmids. Short 16 bp direct repeats were found within the 51 bp homologous sequence. Direct repeats and inverted repeats are common characteristics found within the region involved in replication in native *Pasteurellaceae* plasmids. One study showed that plasmid pIG1, isolated from *P. multocida* serotype D, harboured three major inverted repeats of 20, 16 and 38 bp in its putative origin of replication gene (Wright *et al.*, 1997). Interestingly, the authors reported that the same 16 bp and 38 bp inverted repeats were also present in the plasmid pYFC1 (from *M. haemolytica*) and plasmid pLS88 (from *H. ducreyi*), while all three inverted repeats were found in pAB2; a plasmid isolated from *M. haemolytica*. In addition to that, the 20-bp inverted repeat is found to be associated with the *bla* gene in *H. influenzae* and *A. pleuropneumoniae*. It is located immediately downstream of the *bla* gene in these organisms which is thought to be in the terminator region of this gene coding for the ROB-1  $\beta$ -lactamase enzyme (Maclean *et al.*,

1992). None of the inverted repeats were found in our putative *oriP* gene. This might indicate a different type of sequence for the replication origin of our native *Pasteurella* plasmid. A study of multiresistance in *P. multocida* isolated 13 native plasmids from clinical strains. It was noted that none of the replication origin regions among these 13 plasmids were identical, although they were highly similar (San Millan *et al.*, 2009). This might suggest that there is more than one pattern of *oriP* gene replication in native *Pasteurella* plasmids which may harbour similar direct repeats or inverted repeats, but the relevance of either the direct or inverted repeats to replication of these *Haemophilus*, *Actinobacillus* & *Pasteurella* (HAP) plasmids is unclear.

The second ORF in Figure 15 was highly matched with part of the mobilization gene, *mbeAY* from plasmid pIG1 (Wright *et al.*, 1997). From here, isolation of the putative *oriP* gene was continued as illustrated in Figure 12. Removal of the pUC origin of replication from plasmid pCMV-sCRIPT was done in parallel. However, attempts to transform the ligation mixture of the plasmid and the *oriP* gene failed due to unknown reasons. This may have been due to DNA restriction barriers that may not have allowed the transformed plasmid to propagate in *P. multocida* B:2.

Another commercial pUC-based eukaryotic expression plasmid pEGFP-N1 was recruited for use in this study. The plasmid was derived from plasmid pUC18 and has an advantage when compared to the previously selected plasmid, pCMV-sCRIPT. It harbours a reporter gene, EGFP, which encodes a red-shifted variant of the wild type green fluorescent protein (GFP). The EGFP gene is located downstream of the viral immediate early promoter of cytomegalovirus ( $P^{CMV_{IE}}$ ). An ability to propagate this plasmid in *P. multocida* B:2 would help to monitor intracellular trafficking of the plasmid via GFP expression and also for future antigenic protein expression in mammalian cells.

Having a similar origin of replication as plasmid pCMV-sCRIPT, plasmid pEGFP-N1 was expected to behave similarly after electroporation into *Pasteurella*. However, plasmid pEGFP-N1 was recovered from positive transformants at 36h post-electroporation. The only difference from previous electroporation with plasmid pCMV-sCRIPT was the extended incubation time. Small colonies were observed only after 36h. This indicated that suppression of plasmid DNA propagation was overcome, with a delay in replication and ability to express the

antibiotic-resistance gene. As discussed above, an active DNA restriction system has been identified in *Pasteurellaceae* bacteria which acts as a defence mechanism against foreign DNA. In order to achieve successful transformation, it was proposed that DNA must be modified by *phal* (Briggs *et al.*, 1994). However, Hill & Lainson (2003) found that a strain of *M. haemolytica* A1 positive for both *hsdM* and *phal* was able to be transformed with plasmid DNA extracted from *E. coli* which was contrary to the suggestion of Briggs *et al.* (1994) that the origin of plasmid DNA influences transformation efficiency. They indicated that plasmid DNA purified from methylase positive and negative bacteria of different species can be cross-transferred at the same transformation rate.

In order to determine if there was any enzyme modification in the *E. coli* plasmid propagating in *P. multocida*, pEGFP-N1 purified from *P. multocida* after electroporation was re-electroporated into *E. coli* XL-1 BLUE and *P. multocida* B:2 JRMT12. In parallel, purified plasmid from *E. coli* XL-1 BLUE was also electroporated into *P. multocida* B:2 JRMT12 and *E. coli* XL-1 BLUE for comparison. Similar numbers of colonies were found after incubation for 18 h in *E. coli* XL-1 BLUE either harbouring pEGFP-N1 purified from *P. multocida* or from *E. coli*. After incubation for 36 h, similar numbers of colonies were found in *P. multocida* B:2 JRMT12 either harbouring pEGFP-N1 purified from *P. multocida* or *E. coli*. This suggested that transfer of plasmid from methylase-negative *E. coli* XL-1 BLUE to methylase-positive *P. multocida* B:2 is possible, showing that the source of genetic material is not a barrier to transformation. However, the delay of *P. multocida* strain recovery on the selective plate would suggest that the plasmid DNA had to undergo some adaptation in order to replicate, and this would need further investigation.

Other pUC-based plasmids, pGEM-oriP and pCMV-sCRIP, were then electroporated into *P. multocida* B:2 JRMT12. Plasmid pAKA16 was included for comparison. In parallel, all plasmids were also electroporated into *E. coli* XL-1 BLUE. Colonies were observed on all *E. coli* transformants at 18 h after electroporation, while in *P. multocida* only colonies electroporated with pAKA16 were recovered at 18 h after electroporation. However, colonies were observed for all other transformants after incubation for 36 h. There was no significant difference in the number of colonies on each individual selective plate among the same strain harbouring different plasmids. This showed that the effect was

not confined to plasmid pEGFP-N1 but that all pUC-based plasmids were capable of propagation in *P. multocida* B:2 JRMT12 when the incubation time after electroporation was extended to at least 36 h.

Plasmid-containing *P. multocida* B:2 were able to stably maintain the pEGFP-N1™ plasmid for at least 14 days with the absence of an antibiotic selection. Plasmid purified from all strains showed no alteration in DNA size after restriction enzyme analysis. Comparison of growth rate between *P. multocida* B:2 JRMT12 and *E. coli* XL-1 BLUE whether harbouring pEGFP-N1 or not showed a similar pattern with no obvious difference. However, *P. multocida* B:2 JRMT12 harbouring plasmid pEGFP-N1, cultured in BHI broth with kanamycin (50 µg/ml), entered exponential phase at a slower rate when compared to the strain cultured in BHI broth without antibiotic (Figure 11). Thus, the delay may have been caused by the time taken to express sufficient enzyme needed for resistance to the antibiotic. However, both strains showed insignificant differences in the slope of the exponential phase. When pEGFP-N1 was purified from both strains at the same OD<sub>600nm</sub>, the concentration of plasmid DNA obtained was similar from each. Thus, pEGFP-N1 was stably maintained in *P. multocida* B:2 even in the absence of antibiotic.

### **4.3 Development of *P. multocida* B:2 bacteriofection model system**

Bacteriofection (bacteria-mediated expression plasmid DNA transfer) can be applied for genetic vaccination, gene therapy and production of therapeutic proteins (Liu, 2011). Delivery of naked plasmid DNA by intramuscular, intradermal or oral administration in genetic vaccination offers the possibility of both antigen presentation and immune modulation. However, this route of vaccination always results in low efficiency of delivery. The use of bacteria as carriers for mucosal applications of DNA vaccines addresses some of the problems of naked DNA vaccination and provides additional benefits, such as adjuvant effects and the ability to target inductive sites of the immune system. The progress in bioengineering of attenuated strains of many otherwise pathogenic bacteria and use of these as vaccine vectors provides a means of using bacteria as efficacious delivery vehicles for transporting plasmid DNA containing heterologous genes expressing protective antigens into mammalian



cells. Attenuated bacterial strains such as *Listeria monocytogenes*, different strains of *Salmonella* and *Shigella* act as bacterial vectors for transkingdom transfer of plasmid. For example, a protective response was observed in BALB/c mice against a lethal challenge with *L. monocytogenes* after immunization with attenuated *Salmonella typhimurium* carrying a listeriolysin-encoding expression plasmid (Darji *et al.*, 2000). In another study, a diaminopimelate auxotroph mutant (*dap*<sup>-</sup>) of *Shigella flexneri* harbouring plasmid pCMV $\beta$ , which synthesized  $\beta$ -galactosidase under the control of a eukaryotic promoter (Sizemore *et al.*, 1995), was used to infect mammalian cells which showed expression of  $\beta$ -galactosidase at 48 h post-invasion. Furthermore, after intranasal infection of mice, both humoral and cellular anti- $\beta$ -galactosidase responses were detected, indicating that *in vivo* delivery of plasmid DNA by this strain stimulated immune responses to plasmid-encoded antigen. Another recent study enhanced the ability of *Listeria* to act as delivery vector. An engineered attenuated strain of *L. monocytogenes* underwent self-destruction in the cell cytosol when it produced a phage lysin under the control of the *actA* promoter, which is preferentially activated in the host cytosol (Yoshikawa *et al.*, 2009). This demonstrated an efficient delivery strategy in transferring plasmids (after programmed bacterial lysis in the cytosol) from the bacteria into epithelial or endothelial cells.

The success of gene therapy has been mainly hampered by the lack of efficient vectors that can target transgene expression to the right cells *in vivo*, but at the same time do not induce adverse effects or vector-specific immune responses. Bactofection is a serious alternative to counter the inability of non-replicating vectors to target specific tissue layers and also to facilitate cell to cell spread. The almost unlimited coding capacity that could be incorporated into a bacterial plasmid should allow the transfer of large genomic fragments and by using appropriate recombinant bacterial carriers, homologous recombination might also be possible. It has been shown that bactofection by *Salmonella typhimurium* can deliver plasmid encoding a tumor-expressed antigen that can lead to induction of humoral and cellular immune response in the host and provide a protective defence against the tumour (Xiang *et al.*, 2000). In another study, treatment of malignant melanoma has been successfully achieved by combining classical gene therapy with *Salmonella*-mediated vaccination against murine VEGFR-2 (Lu *et al.*, 2008). Here, synergism was achieved with oral

vaccination of the vaccine *Salmonella* strain combined with direct intratumoral injection of plasmid vector encoding the chemokine IP-10 (CXCL10) resulting in an anti-tumour effect.

The development of bacteria as efficient transfer vehicles for the therapy of monogenic defects would appear to offer potential because although most of the bacterial therapeutic mechanisms of action are still being understood some are showing promising results in clinical trials. *Listeria* has long been considered for therapeutic agents using the anticancer-vaccination approach. In one study, safety of a live-attenuated *L. monocytogenes* that secreted the HPV16 E7 antigen fused to the *Listeria* protein Listeriolysin O (LLO) has been demonstrated in a clinical phase I trial in patients with cervical cancer (Maciag *et al.*, 2009) and phase II trials are in progress. This is an example of a promising future in implementing bactofection for anti-tumour therapy.

The utilization of bacterial systems for therapeutic purposes is further enhanced by genetic modification of the vectors which makes them a very promising tool for targeted delivery of genes and their products. Alternative gene therapy (AGT) is based on bacterial protein delivery of bacterially-expressed therapeutic proteins to the host organism using genetically-modified bacteria. Pawelek *et al.* (1997) have shown that using hyperinvasive *Salmonella* can lead to accumulation of bacteria to high levels in individual organs and solid tumours. Furthermore, high levels of expression of transgenes have been observed in cells following plasmid transfer from bacteria (Darji *et al.*, 2000). In AGT, bacteria persisting in target tissues produce the therapeutic polypeptide *in situ*, thus ideally providing a local distribution of drug without increasing its systemic levels. For this, primarily oncolytic or tumour-colonizing bacterial strains such as *Clostridia*, *Bifidobacteria* or *Salmonella* have been demonstrated to be useful for treatment (Zheng *et al.*, 2000; Van Mellaert *et al.*, 2006).

In the future, a long term aim of the laboratory would be to apply bactofection in genetic vaccination against cattle diseases. Hence, in this study, one interest was to visualize intracellular trafficking of the plasmid in and out of the *Pasteurella* in the EBL cells. As mentioned in Chapter I, one of the vital components for bactofection is the expression plasmid. The plasmid DNA backbone needs to contain the requisite genes for optimal prokaryote propagation, selection, delivery and expression in eukaryotic cells. In order to

demonstrate this, the plasmid DNA must first be able to propagate in *P. multocida* B:2, second should preferably be able to express a reporter protein in *Pasteurella* and third should be able to express a reporter protein in mammalian cells.

As discussed in section 4.2, the commercial eukaryotic expression plasmid, pEGFP-N1 was shown to replicate stably in *P. multocida* B:2. Transfection of pEGFP-N1 into an EBL monolayer showed EBL cells expressing GFP after incubation for 48 h (Figure 18). In addition, *P. multocida* B:2 JRMT12 harbouring this plasmid was observed to be able to release this plasmid in EBL cells in order to express GFP from the eukaryotic promoter. This was demonstrated when an infected EBL cell monolayer was shown to express GFP at 24 h post-invasion (Figure 19). According to the invasion data reported in section 3.2, bacteria were found intracellularly in EBL cells at 3 h post-invasion. TEM micrographs (Figure 11) showed *P. multocida* B:2 JRMT12 to reside in the vacuoles of the EBL cells. To visualize the fate of *P. multocida* B:2 JRMT12 pEGFP-N1<sup>+</sup> in EBL cells, a reporter protein expressed by *Pasteurella* from a prokaryotic promoter was needed to be incorporated into the plasmid backbone. Hence, the strategy used was to recruit another *Pasteurella* promoter and prokaryote reporter gene into plasmid pEGFP-N1, in order to allow visualization of the bacterial strain intracellularly.

Plasmid pMK-Express (Bossé *et al.*, 2009) is a broad-host range plasmid that can propagate in HAP (*Haemophilus*, *Actinobacillus* & *Pasteurella*) bacteria. An *A. pleuropneumoniae* promoter, *sodC*, was incorporated into plasmid pMK-Express downstream of the *gfpmut3* gene coding for GFP. It was found that this constitutive promoter was active and able to express the GFP protein from this promoter in *Pasteurella* (Bossé *et al.*, 2009). Section 3.4.2.1 showed that the plasmid, pMK-Express, after electroporation into our strain, JRMT12, was stably propagated and that expression of GFP was visualized from *P. multocida* B:2 JRMT12 pMK-Express<sup>+</sup> when viewed under fluorescence microscopy (FM) (Figure 21). The strategy in Figure 22 was used to recruit another prokaryotic reporter protein, in this case red fluorescent protein (RFP), to help differentiate prokaryotic and eukaryotic expression. Plasmid pMK-Express and plasmid pDsRed-Monomer were exploited to develop plasmid pMK-RED. After electroporation, *P. multocida* B:2 JRMT12 pMK-RED<sup>+</sup> was observed to express RFP

by fluorimetry and also after FM viewing (Figures 23 & 24). FM imaging also shows localization of the bacteria after invasion of EBL monolayer (Figure 25). This confirmed the ability of *P. multocida* B:2 JRMT12 pMK-RED<sup>+</sup> to utilize the prokaryotic *sodC* promoter to express rfp protein from the DsRed.M1 gene.

In developing attenuated bacteria to mediate gene delivery or bactofection, most studies examined bacterial behaviour after entering mammalian cells. Although the principal of the delivery system is generally known, there are still differences observed among bacterial strains especially in the hostile environment inside mammalian cells. Bacteria such as *S. flexneri*, *L. monocytogenes* or *E. coli*, carrying the virulence plasmid of *S. flexneri*, invade their host cells and escape from a vacuole into the cytosol. Once in the cytosol they die for one of three reasons; they can be auxotrophic or conditionally express autolysins or are killed by the addition of antibiotics to the cultures. This result in lysis of the bacteria and the expression plasmids are released. Some of these plasmids find their way into the nucleus where the open reading frames are expressed under the control of the eukaryotic transcription elements (Grillot-Courvalin *et al.*, 1998; Anderson *et al.*, 2000; Darji *et al.*, 2000; Hense *et al.*, 2001). Bacteria such as *S. typhimurium*, *S. typhi* or *E. coli* expressing the invasion gene, *inv* of *Y. pseudotuberculosis* invade their host cells and remain in the vacuole. There they die due to metabolic attenuation and release their expression plasmids. By an unknown mechanism, these plasmids cross the vesicular membrane and reach the cell nucleus of the host cells where they are expressed (Leung & Finlay 1991; Grillot-Courvalin *et al.*, 1998; Fennelly *et al.*, 1999). This technology has not only been demonstrated in mammalian cells. A plant pathogen, *Agrobacterium tumefaciens*, adheres tightly to its host cells via cellulose fibrils and contains a plasmid that encodes most of the apparatus that is necessary for transfer of an expression cassette also encoded by the plasmid. Although wounded plants are its natural targets, plasmid transfer by *A. tumefaciens* has also been demonstrated to yeast and fungi. *In vitro*, it can also target human cell lines (Kunik *et al.*, 2001). This clearly demonstrated bacterial versatility as delivery vectors.

The mechanism of *Pasteurella* entry into mammalian cells has thus far not been studied in detail. In order to help understand this in the vaccine strain, JRMT12, development of a plasmid with both prokaryotic and eukaryotic expression

systems using different reporter genes was developed as indicated in Figure 26. The “traffic light plasmid” termed pSRG was specifically developed to have the *Pasteurella* promoter, *sodC*, downstream of a DsRed.M1 gene coding for RFP together with the virally derived promoter,  $P_{CMV_{IE}}$ , for optimal expression in a eukaryote, downstream of the EGFP gene coding for GFP. The plasmid, pSRG, at 5700 bp was successfully propagated and maintained stably in the vaccine strain, JRMT12, for at least 14 days without the present of selective antibiotic. Sequence confirmation of the sodRED fragment from pSRG is shown in Figure 32. Assessment of RFP expression through the bacterial growth curve showed that JRMT12, harbouring pSRG, expressed RFP at its maximum during the early exponential phase.

Visualization of *P. multocida* B:2 JRMT12 pSRG<sup>+</sup> was undertaken (section 3.4.2.1). The 3D image showed *P. multocida* B:2 JRMT12 pSRG<sup>+</sup> expressing RFP from individual bacteria and the counterstain with Cy5 Dye indicated the outline of the bacterial cells. All images demonstrated the ability of the mutant strain to express RFP from the *sodC* promoter. It was also observed that the majority of the bacteria were expressing RFP at this stage.

Transfection of plasmid pSRG into an EBL monolayer promoted expression of GFP at 24 h post-transfection (Figure 35). After 24 h, only 67% cells were observed to express GFP, but more cells (up to 15% more) were observed to express GFP after 48 h. 3D images of the monolayer shows selected EBL cells with expressed GFP in the cytoplasm after the cell barrier was counterstained with Cell Mask™ plasma membrane stain. The images showed that there were areas within the cell barrier without GFP that can be presumed to be the nuclear compartment. This indicated that GFP expression only occurred in the cytoplasm of the mammalian cells. It would be of interest to counterstain the nuclear compartment to confirm this and also to determine the duration of expression of the GFP in the EBL cells.

The data discussed above showed the functionality of both the prokaryotic and eukaryotic promoters in the construct, pSRG, in two separate experiments. An invasion assay utilizing *P. multocida* B:2 JRMT12 pSRG<sup>+</sup> was then done to monitor bacterial entry, plasmid release and protein expression within the mammalian cells after the standard 3 h invasion time and also at 5 h post-invasion (Figure 36). At 3 h post-invasion bacteria were seen intracellularly when RFP expression

was detected below the cell surface. Fluorescence intensity increased as the sectioning moved deeper into the cell and decreased as it got nearer to the bottom surface of the EBL cell. This co-localization of RFP was again clearly demonstrated in the 3D-images. In some cells, localization of green fluorescence was shown to occur but only in the cytoplasm of the EBL cell and not in the nucleus. Thus, FM images suggested that, at 3 h post-invasion, RFP-expressing bacteria were found intracellularly in EBL cells. Some of these cells were expressing GFP indicating bacterial lysis and free plasmid being delivered into the cytoplasm. At this stage, 44% of the EBL cells analyzed were found to harbour rfp-expressing *P. multocida* B:2 JRMT12 pSRG<sup>+</sup> but only 17% were expressing gfp.

Images captured at 5 h post-invasion showed EBL cells to have a positive response in all fluorescent light paths. At this stage, it was very interesting still to see viable *P. multocida* B:2 JRMT12 pSRG<sup>+</sup> in the EBL cells. This confirmed the data on intracellular survival of the bacteria which found that viable intracellular bacteria could still be detected from 3 h to 7 h post-invasion (Table 12). However, this did not suggest that the bacteria were replicating in the vacuoles as the data in the table showed a gradual decrease in the number of viable bacteria in the EBL cells at 3 h to 7 h post-invasion. Also at this stage, some EBL cells with viable *P. multocida* B:2 JRMT12 pSRG<sup>+</sup> were expressing GFP, an indicator of bacterial lysis and the presence of pSRG in the EBL cell cytoplasm. The 3D images created a better visualization of the model system to demonstrate localization of expression of each fluorescent protein.

Other EBL cells captured at 5 h post-invasion responded negatively under the filter light path which detected RFP expression. Such cells were thus found to be *Pasteurella*-negative yet were expressing GFP. This suggested that all the internal bacteria were lysed and free plasmid DNA was delivered outside of the vacuoles. From 60 analyzed EBL cells at 5 h post-invasion, 53% were found to be expressing GFP yet 20% of those cells still harboured viable *P. multocida* B:2 JRMT12 pSRG<sup>+</sup> because they also expressed RFP. The 3D images showed localization of eukaryotic GFP expression in the cytosol of the EBL cell.

A clear observation after standard invasion time (3 h) was that infected cells that expressed GFP could still harbour viable *P. multocida* B:2 JRMT12 pSRG<sup>+</sup> expressing RFP. The phenomenon was also observed at 5 h post-invasion, but at

this stage the majority of the gfp expressing cells were *Pasteurella*-negative. This suggested that there was killing of the bacteria from an early stage of infection. As this continued, plasmid DNA was released and transferred from the vacuoles into the cytoplasm and then, presumably, delivered to the nuclear compartment by an unknown mechanism.

Vacuolar compartments contain many enzymes that could degrade bacterial cells and constituents. Prevention of intravacuolar growth probably results from a combination of inhibitory factors including the acidic pH of the vacuole, the presence of lysosomal enzymes and the limited availability of nutrients such as iron (Byrd & Horwitz, 1989). The adaptation of other facultative intracellular pathogens to the vacuolar environment has been widely studied, especially for *L. monocytogenes*, *S. flexneri* and *S. typhimurium*. While *Listeria* and *Shigella* destroy or exit the initial membrane-bound vacuole and replicate in host cell cytoplasm, *Salmonella* is known to remain in the vacuole after entry into the host cell. *Salmonella* used for bactofection then die due to metabolic attenuation and release their expression plasmid into the host cytoplasm. It has also been shown that many of the bacterial pathogens which have evolved to grow within a vacuole manage to activate mechanisms to prevent acidification of the vacuole and/or the fusion of the vacuole with lysosomes (Falkow *et al.*, 1992).

It is probable that, instead of replicating, *Pasteurella* JRMT12 was lysed in the vacuole compartment. Bacterial components might then be subjected to degradation by lysosomal enzymes and eventually processed for presentation to APCs to trigger an immune response. As with *Salmonella*, after lysis of *P. multocida* B:2 JRMT12 pSRG<sup>+</sup>, plasmid DNA was presumably transferred from the vacuolar compartment into the cytoplasm. FM observation showed infected EBL cells expressing GFP from plasmid pSRG at 3 h and 5 h post-invasion. Intriguingly, it will be interesting to understand the mechanism by which free plasmid DNA is excluded from degradation by lysosomal nuclease, DNase II, an acidic endonuclease that cleaves the phosphodiester bonds between the nucleotide subunits of nucleic acids. One study showed that plasmid DNA protection in a lysosomal compartment could be achieved by the presence of a bacterial acid nuclease inhibitor. Purified DMI-2, a polyketide metabolite of a *Streptomyces* strain that inhibits acid DNase, was used in a transfection process.

It was found that DMI-2 conferred protection to the plasmid DNA from lysosomal hydrolysis after transfection into a lung adenocarcinoma cell line (Ross *et al.*, 1998). This suggests a possibility for *Pasteurella* to express acid nuclease inhibitors *in vivo* for protection against nuclease degradation. It would be interesting to study the response of *Pasteurella* bacterial components towards lysosomal enzymes *in vitro*.

A study with a diaminopimelate auxotroph mutant (*dap*<sup>-</sup>) of *Shigella*, or the same mutation in invasive *E. coli*, demonstrated the suicidal fate of the bacteria upon host-entry caused by their inability to synthesize cell wall (Sizemore *et al.*, 1997). The bacterial vectors harboured a eukaryotic expression plasmid, pCMV $\beta$ , which synthesizes  $\beta$ -galactosidase. More than one percent of invaded mammalian cells were found expressing transfected  $\beta$ -galactosidase after 48 h of infection. Furthermore, introducing these bacterial strains intranasally into mice allowed detection of both humoral and cellular anti- $\beta$ -galactosidase responses. This study indicated that *in vivo* delivery of plasmid DNA by these bacterial strains stimulated immune responses to plasmid-encoded antigen. Yet, the transfer mechanism of plasmid DNA to the nucleus after bacterial cell lysis remains unexplained.

Despite the ability of plasmid DNA to express antigen in mammalian cells, it apparently occurs in only a low percentage of cells. Employing a gene that mediates bacterial exit from the entry vesicle, such as the *hly* gene coding for listeriolysin O (LLO), could increase the number of plasmid DNA molecules released into the cytoplasm. In a recent study, a *dap* auxotroph strain of *E. coli* with a low-copy-number plasmid pGB2 which expressed the *inv* (*Yersinia* invasion) gene and the *hly* gene were transformed with a eukaryotic expression vector with a GFP reporter gene (Grillot-Courvalin, 2011). The bacteria, made invasive by possession of the *inv* gene, entered non-phagocytic cells expressing  $\beta$ 1-integrins and expression of LLO from the *hly* gene enabled the *dap* auxotroph strain of *E. coli* to escape the entry vesicle. 20% of infected HeLa, CHO and COS-1 cells showed GFP expression by 48 h post-invasion. Bacteria were shown to localize in the cell phagolysosomes within 1-3 h, but viable intracellular bacteria were found to be completely eliminated at 72 h post-invasion. This study indicated that the genes incorporated in the low-copy-number plasmid pGB2 showed functionality by increasing the number of eukaryotic expression plasmid



molecules delivered to the cytoplasm demonstrated by the percentage increment of GFP-expressing cells. It would be of interest to determine the optimal copy number of a plasmid DNA needed for maximum transcription and protein expression of heterologous proteins in the mammalian cells. It is a question as to whether the transfer of plasmid DNA from the cytoplasm to the nuclear compartment is a matter of hit and miss or whether the presence of multiple copies of the DNA would lead to biological pressure forcing the nucleus to take up more and more plasmid DNA.

Future work on this project may want to improve visualization of *Pasteurella* after bactofection, from the entry mechanism up to bacteriolysis in the vacuoles and then the fate of plasmid DNA giving rise to protein expression. An obvious possibility is via live-cell imaging. For FM live-imaging, an environmental chamber is attached to the microscope stage, providing a mechanism for viewing and imaging living cells on the stage while at the same time keeping the culture very close to the optimum growth conditions for extended periods of time. Recent availability of fluorescent protein dyes that can be visualized at various wavelengths and used simultaneously would certainly improve monitoring of cellular processes in living systems. Thus, microscopic imaging coupled with the advancing technology of fluorescent proteins as optical markers should provide ease of viewing during host-pathogen interactions. This is important in understanding the progression of a disease such as HS where bacteria must cross the epithelial cell layer to reach the blood stream.

In order to visualize the attachment/adhesion process or the entry state of the fluorescence-expressing bacteria during *in vitro* infection of mammalian cells, the membrane can be labelled with plasma membrane stain and the cytoskeleton can be immunolabeled with fluorescent phalloidin such as Alexa Fluor 594-conjugated phalloidin (Kraning-Rush *et al.*, 2011). Once the bacteria have been internalized in the cell, fusion of the lysosome with the vacuoles containing bacteria (bacterial compartment) can be detected when the lysosome is labelled with NBD-labeled calix[4]arene (NBDCalAm) (Mueller *et al.*, 2011). Here, the period after invasion up to bacterial lysis can be followed. At the same time, the experiment could also recruit 4'-6-Diamidino-2-phenylindole (DAPI) stain which forms fluorescent complexes with natural double-stranded DNA. This would help to visualize the nuclear compartment of the mammalian cell. The

transfer mechanism of plasmid DNA from the vacuoles to the nucleus is uncertain and the possibility of tracking this is very intriguing. Employing a plasmid DNA stain such as *Label IT® Tracker™* (Mirus Bio, USA) might allow the plasmid DNA movement when it is in the bacteria and its fate after bacterial cell lysis to be tracked. Two studies have visualized plasmid DNA during transfection before and after mammalian cell entry (Cohen *et al.*, 2009; Watt *et al.*, 2002). Manipulation of all the current technologies in fluorescence microscopy to enhance live-cell imaging would certainly make it possible to develop a better understanding of *P. multocida* B:2 infection.

Other than that, the duration of bacterial invasion required to allow protein expression by mammalian cells could be monitored concurrently with the above experiments. Application of flow-cytometry for example, could provide data such as the concentration of plasmid DNA needed in the nuclear compartment to trigger mammalian target protein expression and concentration of the target protein expressed by the mammalian cells. Data such as this could also provide information on dosage-response of various tissues of the host towards the invading pathogen by determining the concentration of heterologous antigenic protein expression needed to trigger mammalian cell activation and to recruit APCs during the development of immune responses.

#### **4.4 Development of bacterial DNA vaccines**

Triggering immune responses for an effective vaccine or therapy will likely require humoral as well as cellular immunity. In that case, while a major impetus for the development of DNA vaccines has been to find a means to generate cellular immunity, any vaccine technology will also need to be able to generate T-cell help and a humoral response. Thus, it is essential to develop innate responses that activate the adaptive response for vaccine purposes (Liu, 2011). The use of live attenuated bacteria as carriers for DNA vaccines (bactofection) shows a very promising approach. It has encountered major bottlenecks, such as difficulties in antigen expression, lack of post-translational modifications and batch-to-batch variability. Nevertheless, it possesses advantages such as built-in immune stimulatory properties which stimulate all three arms of adaptive immunity (antibodies, helper T cells and cytolytic T-lymphocytes), allows specific targeting of plasmid to APCs, and amenability for

mucosal administration (Becker & Guzmán, 2008; Loessner *et al.*, 2008; Liu, 2011). Indeed, live-attenuated bacterial vaccine (LBV) may have features such as cellular tropism, cell-to-cell spread and dissemination within the body and these properties are controllable. Reviews on current LBV show that attenuation, with a deletion in a gene that is essential for metabolism, will not allow them to overcome the immune system of the host (Loessner *et al.*, 2008). Methods such as nutrient deficiency, use of common antibiotics or inducible suicide genes could be introduced into the host for further control of the bacterium used (Curtiss, 2002).

A successful carrier for a prophylactic vaccine requires certain criteria in order to elicit sufficient protection *in vivo*. Most of them have been mentioned above but added to these is the strength of antigen expression in the host. Although most eukaryote promoters have been codon optimized, antigen-encoding genes may also be modified to produce a protein that is secreted, membrane-bound, cytosolic or associated with an organelle (Haddad *et al.*, 1997; Ashok & Rangarajan, 2002). Furthermore, in order to strengthen the end production of the LBV-bactofection (LBV-B) system, accommodating potential molecules with immunomodulatory properties (such as cytokines or chemokines) can augment the elicited immune responses against a plasmid encoded-antigen. One improved technology for the LBV-B system recruited interference RNA (RNAi) for gene silencing to induce vigorous cell apoptosis (Li *et al.*, 2007) which could stimulate cell-mediated immune responses and/or divert them from the optimal response pattern. Another novel strategy to enhance the LBV-B system was shown to employ a direct translation system for RNA. This elegant approach was based on the genetic fusion, at the 5'-end of the mRNA, of an internal ribosome entry site, IRES<sub>EMCV</sub> element. A self-destructing *L. monocytogenes* used this system to directly deliver translation-competent mRNA into the cytosol which showed an earlier translation than when DNA plasmid alone was delivered (Loeffler *et al.*, 2006). Cytoplasmic delivery *in vivo* could also be enhanced with a helper plasmid DNA encoding several genes which enhance bacterial infection and intracellular lysis (refer to section 4.3).

Thus, the transkingdom transfer of plasmid DNA has been systematically studied within the last two decades. The easy manipulation of DNA plasmids makes them rapid to construct and able to express critical attributes for making vaccines

against many emerging pandemic threats (Becker *et al.*, 2008; Liu, 2011). In many research areas, LBV-B combining multiple components from various origins have been used to optimize such a system and, perhaps in the future, it is only a matter of pick-and-use in order to fulfil all requirements in tailoring an ideal vaccine or therapeutic carrier. However, rapid development of the LBV-B mostly accommodates the need for vaccine therapy for human diseases, and not many have been developed in the veterinary field especially for bovine diseases. Table 15 below shows some licensed DNA vaccines employing DNA plasmids to elicit protection (Liu, 2011). These licensed vaccines include those for a viral disease in fish, a viral disease in horses, and an immunotherapeutic vaccine for cancer in dogs, as well as delivery of growth hormone to pigs. Proven efficacy of these DNA plasmids and their acceptance as licensed products together with a better understanding of why the plasmids are effective in these animals will, it is hoped, guide efforts to make DNA vaccines effective for bovine diseases.

**Table 16. Licensed veterinary products employing DNA plasmids.**

Year	Label	Company	Indication	Species	Gene(s) encoded
2005	West Nile-Innovator <sup>®</sup>	Fort Dodge Animal Health, Fort Dodge, IA, USA	West Nile virus	Horses	PreM-E
2005	Apex-IHN <sup>®</sup>	Novartis Animal Health, Basel, Switzerland	Infectious haematopoietic necrosis virus	Salmonid fish	Glycoprotein
2008	LifeTide <sup>®</sup> SW 5	VGX <sup>™</sup> Animal Health Inc., The Woodlands, TX, USA	Increase litter survival	Breeding sows	Growth hormone releasing hormone
2010	Oncept <sup>™</sup>	Merial, Lyon, France	Melanoma	Dogs	Human tyrosinase

Table based on the review by Liu, 2011.

In order for the LBV-B system to find use for treatment of HS and other bovine diseases, some roadblocks should be overcome. It is essential to elucidate the underlying molecular events leading to DNA transfer from the bacteria to the cytosol and to the nucleus. This study has developed a tool to allow visualization

of *P. multocida* B:2 JRMT12 during and after mammalian cell invasion. Plasmid pSRG, constructed in this study, enabled tracking of protein expression and further use of modern synthetic molecule component such as fluorescent markers or DNA staining will promote further understanding on the fate of plasmid DNA after bacterial lysis. Analyzing further a possible *P. multocida* B:2 immunosuppressive effect will help in understanding bacterial physiology during infection. It could be that this unique feature of the B:2 bacteria, to persist longer *in vivo* due to an immunosuppressive effect, might actually play a role in eliciting efficient expression of other immune responses in the host as suggested above. Finally, recruiting several immunomodulatory components or functional antigen molecules to combine into a *Pasteurella* LBV-B system would enhance its application as a versatile vaccine and provide a major contribution to veterinary science.

The ultimate aim of the laboratory is to develop a DNA vaccine, via the LBV-B system, expressing heterologous protective antigen(s) from other bovine pathogens. Our interest would include vaccines that at present can only control but fail to eradicate the disease, for example, against *Brucella abortus*, a zoonotic Gram-negative pathogen that causes abortion and infertility in ruminants. It causes serious medical problems and severe economic losses for livestock producers. The ability of *Brucella* to maintain long-term residence intracellularly is associated with chronic infection (Gyles *et al.*, 2010). It is not a commensal pathogen, thus maintenance of brucellosis in an animal requires continual infection of susceptible hosts. As a facultative intracellular parasite, *Brucella* remains enclosed in the phagosomal compartment. To survive in this hostile environment, the bacteria have developed a successful system for intracellular adaptation. Vaccination has proved to be an effective tool in controlling brucellosis but vaccination alone has not been effective in eradicating the disease (Nicoletti, 1990; Schurig *et al.*, 2002). Current vaccines used live attenuated bacteria, including the *B. abortus* B19 strain, against bovine brucellosis and this has been shown to induce high levels of protection in cattle (Baldi *et al.*, 1996). However this vaccine has several disadvantages: immune responses to the vaccine can interfere with diagnosis; it may result in abortions when administered to pregnant animals; it can be infectious for humans and has weak immunogenic properties (Schurig *et al.*, 2002; Ashford *et al.*, 2004; Shumilov *et al.*, 2010).

Beside *Brucella*, another bovine pathogen of interest is *Mycobacterium bovis*. Its infection causes bovine tuberculosis which poses financial burdens and health risks for the cattle industry throughout the world. Studies have indicated that mycobacteria have evolved as pathogens to survive in macrophages and to overcome multifactorial hostile innate and acquired host immune mechanisms, so they can survive and eventually multiply and transmit to other animals (Schlesinger *et al.*, 1990; Bartow & McMurray, 1998). The *M. bovis* Bacillus Calmette-Guerin (BCG) vaccine has been demonstrated to provide widely unpredictable efficacy in cattle (Buddle, 2001). The inconsistencies suggested that protection conferred by BCG against bovine tuberculosis is influenced by the exposure of animals to environmental mycobacteria which interfere with the acquisition of full immunity after vaccination (Brandt *et al.*, 2002). Vaccination against mycobacterium diseases enables a reduction in clinical signs and limits the spread of bacteria but is not sufficient to eliminate the infection (Buddle, 2001).

Studies have shown that BCG combined with certain subunit vaccines enhanced protection in animals when compared with BCG alone (Skinner *et al.*, 2003; Wedlock *et al.*, 2008). Several DNA vaccines have also been developed for these purposes. One was reported that by combining BCG with antigens expressed from a DNA vaccine, higher levels of protection against tuberculosis were induced than with BCG alone in a mouse model when the animals were sensitized to environmental mycobacteria before vaccination (Donnelly *et al.*, 2005). Another study of interest used a single combined DNA vaccine expressing antigens from *B. abortus* and *M. bovis* which elicited protective immunity in cattle against these two infectious diseases (Hu *et al.*, 2009). In this study, plasmid DNA, pJW4303, incorporated coding regions from mycobacterial antigens (Ag85B, MPT64 and MPT83) and *Brucella* antigens (BCSP31, SOD and L7/L12) amplified from *M. tuberculosis* H37Rv and *B. abortus* strain 544 chromosomal DNA. BCSP31 is a 31 kDa protein; SOD is a Cu-Zn superoxide dismutase; and L7/L12 is a ribosomal protein. It was previously demonstrated that using these combined antigens in a DNA vaccine conferred protective immune responses in mice against *B. abortus* infections (Yu *et al.*, 2007). AG85B is an antigen complex including 85A, B and C recognized by T-cells; MPT64 is antigen restricted to strains of *M. tuberculosis* and is found to stimulate T-cell

responses; and MPT83 is lipoylated and glycosylated protein that remains attached to the cell surface with exposure of some epitopes (Cai *et al.*, 2005).

It would be of interest to incorporate some or all these antigens addressing both diseases caused by these pathogens into our *P. multocida* system. Each gene would be amplified by PCR and cloned into pSRG to replace the GFP gene, placing these bacterial genes under the control of the eukaryotic promoter. It would need to be established initially that the antigen(s) were expressed in, for example, EBL cells by antibody detection before attempting to use the *P. multocida* B:2 JRMT12 carrier system to deliver plasmid DNA in mouse model of infection. If this was successful, our expectations would be for the model system to elicit protection in cattle against challenge with *P. multocida* B:2, *M. bovis* and/or *B. abortus* with a single vaccine.

#### **4.5 Possible immunosuppressive effect of *P. multocida* B:2 infection**

Bacterial pathogens, by definition, have acquired some ability to overcome host defence mechanisms (Brunham *et al.*, 1993). A variety of bacterial components and products play different roles in modulating host immune reactions, most of them are stimulatory but a minority are inhibitory. It has been suggested that every component of bacteria with adjuvant activity can also impose suppressive effects on the immune system depending on timing, dose and selection of antigen (Schwab, 1975). Virulent Gram-negative bacteria (e.g. *Salmonella*, *Shigella*, *Pseudomonas aeruginosa*), which are able to cause septicaemia and endotoxaemia, affect the immune system by the suppression of phagocytosis and cell-mediated immunity (Vorob'ev *et al.*, 2001). The *in vitro* immunomodulatory effects of *P. multocida* serotype D (the causative agent of atrophic rhinitis) was investigated in a study on mouse splenocytes. This study showed treatment of splenocytes with either purified porin or LPS stimulated IL-1 $\alpha$ , IL-6, TNF- $\alpha$ , IFN- $\gamma$  and IL-12 mRNA while no effect was detected on IL-4 and IL-10. It was concluded that these *P. multocida* components were able to modulate immunological responses by affecting the release of different cytokines (Iovane *et al.*, 1998). The immunosuppressive properties of *P. multocida* D were also shown in another study where intranasal challenge of pigs and mice with a toxigenic strain or its

cell free extract (CFE) reduced the IgG response of these animals (Jordan *et al.*, 2003).

It has been shown that outer membrane protein (OMP) preparation of *P. multocida* B:2 is antiphagocytic as it was able to interfere with phagocytosis of opsonised *Candida albicans* by murine peritoneal cells *in vivo*. It was suggested that the antiphagocytic mechanisms induced by OMP enhanced the virulence of the organism (Srivastava, 1998). The immunosuppressive effects of *Yersinia*, which is close taxonomically to *Pasteurella*, have been extensively studied and the mechanisms involved in T cell suppression have been revealed (Sing *et al.*, 2002). *Yersinia pseudotuberculosis* (the causative agent of gastroenteritis and lymphadenitis in humans) is likely to be in contact with lymphocytes in the intestinal Peyer's patches, lymph nodes, spleen and liver in which the organism colonises and multiplies. Preliminary studies reported that T cells transiently exposed to *Yersinia* were suppressed for TCR (T cell receptor) stimulation (Yao *et al.*, 1999). Further *in vitro* studies showed that YopH (*Yersinia* outer protein H), which was known as being antiphagocytic and had protein tyrosine kinase activity (Sing *et al.*, 2002), specifically suppressed T cells by inhibiting the adaptor molecules LAT (linker for activation T cells) and SLP-76 (SH2-domain-containing leukocyte protein of 76 kDa) (Gerke *et al.*, 2005).

Prior to the present study, Ataei (2007) investigated a possible contributory role of cellular immunity against HS in calves given single IM dose of  $10^8$  CFU on the JRMT12 vaccine strain and after challenge with the wild type *P. multocida* B:2 strain 85020. Also, in lymphocyte stimulation assay, the effects of *P. multocida* infection on PBMC isolated from calves at different times after challenge were assessed. He observed a possible immunosuppressive effect of the challenge with *P. multocida* B:2 on the proliferation responses of calf PBMC to ConA. This observation does not appear to have been reported previously since the immunomodulatory effects of *P. multocida* B:2 have not been well studied. In addition, Ataei (2007) assessed the possible immunomodulatory effect *in vitro* using a cell-free extract (CFE) from *P. multocida* B:2 85020. He demonstrated that 2 µg/ml was the optimal concentration of CFE in which peripheral blood mononuclear cells (PBMC) ( $5 \times 10^4$ /ml) grew normally but where the proliferative response to concanavalin A (ConA) was suppressed. He also observed that ConA at 0.2 µg/ml was the optimum concentration with which PBMC were able to



proliferate strongly and the suppressive effect of CFE was also observed. In his experiments, it was shown that the proliferative response of normal PBMC to ConA was 60-100 times that of non-stimulated control cells and that it was markedly suppressed when PBMC were pre-incubated with the optimal concentration of CFE of *P. multocida* B:2 85020 for 1 h before adding the ConA. The addition of 85020 (wild-type) CFE caused a 3-5 fold decrease in the proliferative response of PBMC to ConA. Suppressive effects on PBMC were also tested with other strains of *Pasteurella*, *Staphylococcus aureus* and *E. coli*. Only CFE from *P. multocida* serotype D and A3 (causative agent of pneumonia in cattle) suppressed the PBMC proliferation response to ConA. However, the effect were less marked than that of the CFE from the B:2 strain. Ataei (2007) also suggested that the active part of the suppressive agent(s) was likely to be protein, as he showed that heating the CFE at 80°C for 5 min completely destroyed the suppressive properties. An OMP preparation of *P. multocida* B:2 85020 markedly suppressed the proliferative response of PBMC to ConA. Furthermore, suppressive effects were not altered even after dialysis of the CFE at 10 000 Da cut-off.

Based on previous data obtained in the laboratory by Ataei (2007), immunosuppression was a concern, especially in the development of JRMT12 as a potential vaccine strain. Hence, in this study, the vaccine strain, *P. multocida* B:2 JRMT12, as well as the parent strain, 85020, were used to assess their possible immunosuppressant effect on PBMC obtained from calves. In the first assay, CFE of JRMT12 was compared with CFE of 85020 which had been used previously by Ataei (2007). In agreement with Ataei (2007), it was shown that in the absence of CFE, PBMC showed a similar high proliferation to all three concentrations of ConA, whereas little proliferation was observed without ConA. This mitogen, ConA, belongs to the family of lectins (carbohydrate-binding proteins derived from plants and bacteria). It has potent T-cell mitogenic activity and has been extensively used to study the *in vitro* lymphocyte response (Mukherjee *et al.*, 2005). However, the exact mechanism involved of T cell proliferation *in vitro* by ConA is poorly understood. A dose-dependent suppression of PBMC proliferation was observed when PBMC were pre-exposed to different concentration of CFE from JRMT12. This showed that attenuation of this mutant strain did not alter the presence of component(s) responsible for suppressing PBMC proliferation. The parent strain 85020 was reported to harbour

major immunogenic proteins of 37 and 50 kDa (predicted to be OmpA and OmpH respectively) in an outer membrane protein (OMP) preparation (Ataei *et al.*, 2009) which corroborated to other studies reporting similar results on immunogenic proteins of *P. multocida* B:2 (Pati *et al.*, 1996; Verma & Jaiswal, 1997; Malik & Monga, 2002).

The strain JRMT12 has been reported to act as an effective live-attenuated vaccine strain to protect calves against challenge with the virulent parent strain, 85020. Protection against experimental HS was observed when two doses intramuscularly were given to the animal at 4 weeks apart (Hodgson *et al.*, 2005; Dagleish *et al.*, 2007). In these studies, they found out that, after primary vaccination with the JRMT12 strain, an acute phase protein response and an increase in rectal temperature were observed, indicating that the bacteria persisted long enough to promote an inflammatory response. These data indicate that the vaccine strain had immunogenic proteins equivalent to those of the parent strain sufficient for it to promote protection after challenge. It would be interesting to verify the existence of OmpA and OmpH in JRMT12, as OMP in *Yersinia* have been shown to have immunosuppressive effects on T cells which could account for the resistance of the bacterium to immunity elements in the host (Yao *et al.*, 1999; Sing *et al.*, 2002; Gerke *et al.*, 2005). This observation of immunosuppressive effects of OMP of *P. multocida* may be applicable to understanding the pathogenicity of this organism and the development of the immune response during infection.

However, in the present study, many discrepancies between experiments were observed. During the initial assay, CFE of the mutant strain, JRMT12 was assessed in parallel with CFE of the wild-type, 85020 which had been used previously by Ataei (2007) in his study and stored at -80°C. The results obtained showed an unclear pattern of dose-dependence for the CFE of 85020 in inhibiting PBMC proliferation. There was an inconsistent suppression of PBMC proliferation, especially after pre-incubation with CFE at 20 µg/ml. Even at 10 µg/ml, PBMC proliferation was not highly suppressed as was observed with the CFE from the mutant strain or as reported by Ataei (2007). It was concluded, that putative active components responsible for proliferation inhibition in the CFE might be labile and subject to deterioration with time and conditions of storage. Thus assessments were continued using freshly prepared CFE from the wild-type and

the vaccine strains. Again, consistent results were not obtained. One repeat assay showed a dose-dependant suppression of lymphocyte proliferation in response to ConA by CFE from JRMT12, similar to the first assay, but CFE from 85020 still did not show a clear suppressive effect. The inconsistency of the data was disappointing and further work is required to understand the reasons why the active component(s) of CFE apparently vary in concentration or activity. Difficulties in obtaining fresh blood from calves prevented further investigation of this phenomenon. If the reported immunosuppression of *P. multocida* and its component is a real effect not an artefact, the mechanism of this process requires further investigation. One possible approach would be to assess the interaction of live *P. multocida* B:2 bacteria with PBMC, as demonstrated earlier in this study with other mammalian cells.

Immunosuppression of PBMC by CFE *in vitro* could probably be an artefact of disruption in relation to the receptor binding between the PBMC with ConA that trigger and accelerate proliferation. Ataei (2007) suggested that CFE suppressive properties *in vitro* are more likely to be clinically reflected as a chronic manifestation, yet in HS, the disease is usually acute. Although *P. multocida* B:2 is known as the causative agent of HS, the organism exists in the tonsils and nasopharynx of some apparently healthy carrier cattle and buffaloes (De Alwis, 1999). Carrier status is actually a chronic infection with the bacterium but how the organism survives in the carrier host tonsils, which are in close contact with lymphatic organs, is not yet understood. In this and the Ataei (2007) study, *in vitro* experiments showed that *P. multocida* contains a component(s) with the potential to inhibit PBMC. The suppressive properties of the organism would be a possible explanation of its survival in carrier animals. Other possible consequences of immunosuppression can be in converting a latent carrier to an active carrier. In the active carriers, the bacterium is present in the nasopharynx and, from this site, is shed in nasal secretions. Latent carriers harbour the organism in tonsils in which the bacterium is believed to multiply and intermittently spill over into nasopharynx (De Alwis, 1990). The mechanisms involved in converting a latent carrier to an active carrier have not been revealed. It was shown that stressful conditions and even administration of immunosuppressive preparations (dexamethasone and methylprednisolone acetate) were not able to cause latent carriers to shed the organism in their nasal secretions (De Alwis, 1999).

Ataei (2007) went on to examine the specific suppression of B cell and T cell subpopulations ( $CD4^+$ ,  $CD8^+$  and  $\gamma\delta^+$ ) in normal calf PBMC using fluorescence activated cell sorter (FACS) analysis. Cell populations were identified by indirect immunofluorescence staining of corresponding cell markers using mouse monoclonal antibodies against them as primary antibody and FITC-conjugated goat antibodies specific for the mouse Ig isotype as the secondary antibody. This experiment revealed the proliferative status of each population by assessing the ratio of proliferating and non-proliferating fractions. From this analysis, Ataei (2007) found that  $CD4^+$  and  $CD8^+$  T cells were the principal cells which proliferated in response to ConA and whose proliferation was suppressed by a CFE of *P. multocida* B:2. ConA increased the percentage of proliferating  $CD4^+$  T cells by 10-fold compared to the control cells, but CFE treatment before addition of ConA allowed only a 3-fold increase. Yet, the suppression of  $CD4^+$  T cells was not due to an adverse toxic effect of CFE on the cells, as CFE alone did not decrease the number of these cells. Mitogen stimulation of lymphocytes *in vitro* is believed to mimic stimulation by specific antigens fairly closely. Stimulation of T cell receptors with ConA induces a signal transduction pathway which stimulates IL-2 secretion and up-regulation of the  $\alpha$  subunit of the IL-2 receptor, CD25 (the  $\beta$  and  $\gamma$  subunits are constitutively expressed). Secreted IL-2 functions in an autocrine and paracrine manner by binding to the full receptor ( $\alpha$ ,  $\beta$  and  $\gamma$  subunits) to initiate proliferation of stimulated lymphocytes (Peltier *et al.*, 2008). IL-2 is a crucial element in cell-mediated immune responses both *in vivo* and *in vitro*; in cattle, IL-2 levels can be used to measure specific cellular immune responses (Miller-edge & Splitter, 1986). Stimulation of bovine lymph node cells with ConA causes a biphasic IL-2 secretion. The first phase of IL-2 production occurs after 3 h and the second phase between 10 and 16 h. This study also showed the accumulation of IL-2 mRNA before each phase of IL-2 secretion (Weinberg *et al.*, 1988). In the 2-signal model of mitogen activation of T cells, the first signal occurs with mitogen and monocytes (another population of cells in PBMC) which cause the production of the second signal that is IL-2 (Gelfand *et al.*, 1985). IL-1, which is secreted by monocytes, acts as the first signal and induces the expression of IL-2 receptors in a subpopulation of T cells which, after activation by IL-2, culminates in DNA synthesis and proliferation of these cells (Conti 1991; Conti *et al.*, 1991). *In vitro* experiments on bovine PBMC have indicated that monocytes are necessary for optimum stimulation of T cells

(Pontarollo *et al.*, 2002). According to the 2-signal model of T cell activation, suppression could be at the point of IL-2 secretion and/or induction of CD25. The mechanism of suppression by ovine uterine serpin (OvUs; an immunosuppressive protein secreted by the ewe uterus during pregnancy) on the proliferative response of PBMC has been investigated. This study showed that OvUs inhibited ConA-induced expression of CD25 in  $\gamma\delta^-$  cells but not  $\gamma\delta^+$  T cells. The study also revealed that OvUs suppressed lymphocyte proliferation by blocking CD25 expression. It was also suggested that the lack of suppressive effect of OvUs on ConA stimulated CD25 expression in  $\gamma\delta^+$  T cells may indicate a different mechanism of activation of these cells or insensitivity to inhibition by OvUs (Peltier *et al.*, 2008). This study supports a role for CD25 in the suppression observed in the Ataei (2007) *in vitro* experiments, where *P. multocida* CFE was shown to inhibit the proliferative response in  $\gamma\delta^-$  T cells (including  $CD4^+$  and  $CD8^+$  T cells) but not  $\gamma\delta^+$  T cells.

Interactions between host cells and pathogens are extremely complex and the involvement of multiple inter-dependent pathways in signalling and regulatory systems has made it very difficult to study these interactions. Therefore, it is difficult to predict the combined behaviour by just investigating the interactions between bacteria and individual components of the immune system. However, further investigation in this area could be informative and helpful in understanding the process of disease development by providing information on mechanisms that the pathogen uses to overcome or escape the host immune system. It would also be useful to know if the immunosuppressive effects of *P. multocida* B:2 CFE and OMP were reproducible because they could have a bearing on the efficacy of an attenuated B:2 *aroA* strain inducing rapid and sustained immune responses. Thus observations make this area of study important but the inconsistency in the data obtained needs to be investigated further. In this regard, it should be noted that Hodgson *et al.* (2005) observed only a low antibody response after primary vaccination of calves with *P. multocida* B:2 JRMT12 and only after a secondary booster vaccination, 4 weeks later, was a high IgG response obtained. This delay in response to vaccination (with *P. multocida*) had been noted previously (Chandrasekaran *et al.*, 1994; Shah & Graaf, 1997) and may be related to the possible immunosuppressive effects of *P. multocida* B:2. The corollary of any immunosuppressive effect is

that it may allow the attenuated strain to persist longer in the host and thus allow more time for a protective immune response to eventually develop.

## 4.6 Summary and conclusions

Both *P. multocida* B:2 strains were capable of adhering to and invading J774.2, BL-3 and EBL cells. All of the *Pasteurella* and *Mannheimia* strains tested were able to adhere to EBL cells but only B:2 strains were taken up intracellularly in significant numbers. The vaccine strain, JRMT12, was found to survive intracellularly in EBL cells for at least 7 hours and the invasion inhibition assay suggested that its entry into the cells was by an actin-dependent process. Transmission electron micrographs showed that JRMT12 resided in the vacuolar compartments of the EBL cells.

A novel 'traffic light' expression plasmid, pSRG, was created. *P. multocida* B:2 JRMT12 was shown by fluorescence microscopy to be able to express the reporter protein, red fluorescent protein, from the prokaryotic expression system of this plasmid and this was used to monitor the viability and intracellular location of the bacterium. Expression of green fluorescent protein from the eukaryotic expression system of pSRG demonstrated the ability of the plasmid to be delivered from the intracellular environment of the bacterium into the intracellular environment of the eukaryotic cell. This, in principal, has shown a potential use of the vaccine strain as a vehicle for the intracellular delivery of protective antigens (bactofection).

A reported immunosuppressive effect of *P. multocida* B:2 on lymphocyte proliferation was investigated because of its relevance to any future use of the JRMT12 strain for immunization purposes. However, the results were not consistently reproducible and further investigation in this area would be desirable.

## 5.0 BIBLIOGRAPHY

- Aalbaek, B., Eriksen, L., Rimler, R. B., Leifsson, P. S., Basse, A. & Christiansen, T. (1999). Typing of *Pasteurella multocida* from haemorrhagic septicaemia in Danish fallow deer (*Dama dama*). *APMIS : Acta Pathologica, Microbiologica, Et Immunologica Scandinavica* **107**, 913-920.
- Ackermann, M. R., Rimler, R. B. & Thurston, J. R. (1991). Experimental model of atrophic rhinitis in gnotobiotic pigs. *Infection and Immunity* **59**, 3626-3629.
- Adamson, M. R., Morrow, C.J., Johnson, R.B., Townsend, K. M., Dawkins, H.J.S. and Spencer, T. L. (1993). Molecular epidemiology of *Pasteurella multocida* using ribotyping. In B. E. Patten, T. L. Spencer, R. B. Johnson, D. Hoffmann and L. Lehane (eds), *Pasteurellosis in Production Animals, An International workshop held at Bali, Indonesia, 10-13 August 1992. ACIAR Proceedings* **43**, 69-76.
- Akagi, T., Kaneko, T., Kida, T., & Akashi, M. (2005). Preparation and characterization of biodegradable nanoparticles based on poly(gamma-glutamic acid) with l-phenylalanine as a protein carrier. *Journal of Controlled Release : Official Journal of the Controlled Release Society* **108**, 226-236.
- Al-Haddawi, M. H., Jasni, S., Zamri-Saad, M., Mutalib, A. R., Zulkifli, I., Son, R. & Sheikh-Omar, A. R. (2000). *In vitro* study of *Pasteurella multocida* adhesion to trachea, lung and aorta of rabbits. *Veterinary Journal* **159**, 274-281.
- Al-Haddawi, M. H., Jasni, S., Zamri-Saad, M., Mutalib, A. R., Son, R. & Sheikh-Omar, A. R. (2000). Ultrastructural observation of nasal and pulmonary intracellular *Pasteurella multocida* A:3 in rabbits. *Veterinary Research Communications* **24**, 153-167.
- Al-haj Ali, H., Sawada, Takuo, Hatakeyama, H., Katayama, Y., Ohtsuki, N. & Itoh, O. (2004). Invasion of chicken embryo fibroblast cells by avian *Pasteurella multocida*. *Veterinary Microbiology* **104**, 55-62.
- Amonsin, A., Wellehan, J. F. X., Li, L., Laber, J. & Kapur, V. (2002). DNA fingerprinting of *Pasteurella multocida* recovered from avian sources. *Society* **40**, 3025-3031.

- Anderson, R. J., Pasetti, M. F., Sztein, M. B., Levine, M. M. & Noriega, F. R. (2000). DeltaguaBA attenuated *Shigella flexneri* 2a strain CVD 1204 as a *Shigella* vaccine and as a live mucosal delivery system for fragment C of tetanus toxin. *Vaccine* **18**, 2193-202.
- Angen, O., Mutters, R., Caugant, D. A., Olsen, J. E. & Bisgaard, M. (1999). Taxonomic relationship of the [*Pasteurella*] *haemolytica* complex as evaluated by DNA-DNA hybridizations and 16s rRNA sequencing with proposal of *Mannheimia haemolytica* gen. nov., comb. nov., *Mannheimia granulomatis* comb. nov., *Mannheimia glucosida* sp. *International Journal of Systematic Bacteriology* **49**, 67-86.
- Ashford, D. A., Pietra, J., Lingappa, J., Woods, C., Noll, H., Neville, B., Weyant, R., Bragg, S. L., Spiegel, A. R., Tappero, J. & Perkins, B.A. (2004). Adverse events in humans associated with accidental exposure to the livestock brucellosis vaccine RB51. *Vaccine* **22**, 3435-3439.
- Ashok, M. S., & Rangarajan, P. N. (2002). Protective efficacy of a plasmid DNA encoding Japanese encephalitis virus envelope protein fused to tissue plasminogen activator signal sequences: studies in a murine intracerebral virus challenge model. *Vaccine* **20**, 1563-1570.
- Ataei, S. (2007). Immune responses of calves after vaccination with a live attenuated derivative of *Pasteurella multocida* B:2. PhD thesis. University of Glasgow.
- Ataei, S., Burchmore, R., Hodgson, C. J., Finucane, A., Parton, R. & Coote, J. G. (2009). Identification of immunogenic proteins associated with protection against haemorrhagic septicaemia after vaccination of calves with a live-attenuated *aroA* derivative of *Pasteurella multocida* B:2. *Research in Veterinary Science* **87**, 207-210.
- Azad, A. K., Coote, J. G., & Parton, R. (1994). Construction of conjugative shuttle and suicide vectors for *Pasteurella haemolytica* and *P. multocida*. *Gene* **145**, 81-85.
- Azad, A. K. (1992). Analysis of plasmid DNA from *Pasteurella haemolytica* and construction of cloning vectors. PhD thesis. University of Glasgow.
- Baalsrud, K. J. (1987). Atrophic rhinitis in goats in Norway. *Veterinary Record*, **121**, 350-353.



- Bain, R. V., & Knox, K. W. (1961). The antigens of *Pasteurella multocida* type I. II. Lipopolysaccharides. *Immunology* 4, 122-129.
- Bain, R. V. S. (1963). Haemorrhagic septicaemia. *FAO Agricultural Studies*. No. 62, Food and Agricultural Organization United Nations, Rome, Italy.
- Bain, R. V. S., De Alwis, M. C. L., Carter, G. R. and Gupta, B. K. (1982). Haemorrhagic septicaemia FAO Animal Production and Health Paper. No. 33. Food and Agriculture Organisation of the United Nations, Rome.
- Bal, S. M., Ding, Z., Kersten, G. F. A., Jiskoot, W. & Bouwstra, J. A. (2010). Microneedle-based transcutaneous immunisation in mice with N-trimethyl chitosan adjuvanted diphtheria toxoid formulations. *Pharmaceutical Research* 27, 1837-1847.
- Baldi, P. C., Giambartolomei, G. H., Goldbaum, F. A., Abdon, L. F., Velikovskiy, C. A., Kittleberger, R. & Fossati, C. A. (1996). Humoral immune response against lipopolysaccharide and cytoplasmic proteins of *Brucella abortus* in cattle vaccinated with *B. abortus* S19 or experimentally infected with *Yersinia enterocolitica* serotype 0:9. *Clinical and Diagnostic Laboratory Immunology* 3, 472-476.
- Baldwin, M. R., Lakey, J. H. & Lax, A. J. (2004). Identification and characterization of the *Pasteurella multocida* toxin translocation domain. *Molecular Microbiology* 54, 239-250.
- Bartow, R. A. & McMurray, D. N. (1998). Lymphocytes expressing Fc gamma receptors suppress antigen-induced proliferation in cells from guinea pigs infected with virulent *Mycobacterium tuberculosis*. *Cellular Immunology* 184, 51-57.
- Basagoudanavar, S. H., Singh, D. K. & Varshney, B. C. (2006). Immunization with outer membrane proteins of *Pasteurella multocida* (6:B) provides protection in mice. *Journal of Veterinary Medicine* 53, 524-530.
- Becker, P. D. & Guzmán, C. A. (2008). Genetic immunization. Bacteria as DNA vaccine delivery vehicles. *Human Vaccines* 4, 189-202.
- Benvenisty, N. & Reshef, L. (1986). Direct introduction of genes into rats and expression of the genes. *Proceedings of the National Academy of Sciences of the United States of America* 83, 9551-9555.

- Birnboim, H. C. & Doly, J. (1979). A rapid alkaline extraction procedure for screening recombinant plasmid DNA. *Nucleic Acids Research* **7**, 1513-1523.
- Bisgaard, M., Frederiksen, W., Mannheim, W. and R. Mutters. (1994). Zoonoses caused by organisms classified with Pasteurellaceae. In: G. W. Beran (Ed.) Handbook of Zoonoses, 2nd ed. CRC Press. London, UK. pg 203-208.
- Blackall, P. J., Fegan, N., Pahoff, J. L., Storie, G. J., McIntosh, G. B. & Cameron, R. D. (2000). The molecular epidemiology of four outbreaks of porcine pasteurellosis. *Veterinary microbiology* **72**, 111-20.
- Blackall, P. J., Christensen, H., Beckenham, T., Blackall, L. L. & Bisgaard, M. (2005). Reclassification of *Pasteurella gallinarum*, [*Haemophilus*] *paragallinarum*, *Pasteurella avium* and *Pasteurella volantium* as *Avibacterium gallinarum* gen. nov., comb. nov., *Avibacterium paragallinarum* comb. nov., *Avibacterium avium* comb. nov. and *Avibacterium*. *International Journal of Systematic and Evolutionary Microbiology* **55**, 353-362.
- Boot, R. & Bisgaard, M. (1995). Reclassification of 30 *Pasteurellaceae* strains isolated from rodents. *Laboratory Animals* **29**, 314-319.
- Bossé, J. T., Durham, A. L., Rycroft, A. N., Kroll, J. S. & Langford, P. R. (2009). New plasmid tools for genetic analysis of *Actinobacillus pleuropneumoniae* and other *pasteurellaceae*. *Applied and Environmental Microbiology* **75**, 6124-6131.
- Boyce, J. D. & Adler, B. (2000). The capsule is a virulence determinant in the pathogenesis of *Pasteurella multocida* M1404 (B:2). *Infection and Immunity* **68**, 3463-3468.
- Boyce, John D, & Adler, B. (2001). Acapsular *Pasteurella multocida* B:2 can stimulate protective immunity against *Pasteurellosis*. *Infection and Immunity* **69**, 1943-1946.
- Boyce, J. D., Harper, M., St. Michael, F., John, M., Aubry, A., Parnas, H., Logan, S. M., Wilkie, I. W., Ford, M., Cox, A. D. & Adler, B. (2009). Identification of novel glycosyltransferases required for assembly of the *Pasteurella multocida* A:1 lipopolysaccharide and their involvement in virulence. *Infection and Immunity* **77**, 1532-1542.

- Bradley, D. E., Taylor, D. E. & Cohen, D. R. (1980). Specification of surface mating systems among conjugative drug resistance plasmids in *Escherichia coli* K-12. *Journal of Bacteriology* **143**, 1466-1470.
- Brandt, L., Cunha, J. F., Olsen, A. W., Chilima, B., Hirsch, P., Appelberg, R. & Andersen, P. (2002). Failure of the *Mycobacterium bovis* BCG Vaccine : some species of environmental mycobacteria block multiplication of BCG and induction of protective immunity to tuberculosis. *Infection and Immunity* **70**, 672-678.
- Briggs, R. E., Tatum, F. M., Casey, T. A. & Frank, G. H. (1994). Characterization of a restriction endonuclease, *Phal*, from *Pasteurella haemolytica* serotype A1 and protection of heterologous DNA by a cloned *Phal* methyltransferase gene. *Applied and Environmental Microbiology* **60**, 2006-2010.
- Brunham, R. C., Plummer, F. A. & Stephens, R. S. (1993). Bacterial antigenic variation, host immune response, and pathogen-host coevolution. *Nature* **61**, 2273-2276.
- Buchanan, R. E. (1925). General Systematic Bacteriology, Williams & Wilkins Co., Baltimore/London. pg 414.
- Buddle, B M. (2001). Vaccination of cattle against *Mycobacterium bovis*. *Tuberculosis* **81**, 125-132.
- Burril, T. J. (1883). New species of Micrococcus. *America Naturalist* **17**, 319-320.
- Buttenschon, J. and Rosendal, S. (1990). Phenotypical and genotypical characteristics of paired isolates of *Pasteurella multocida* from the lungs and kidneys of slaughtered pigs. *Veterinary Microbiology* **25**, 67-75.
- Byrd, T. F. & Horwitz, M. A. (1989). Interferon gamma-activated human monocytes downregulate transferrin receptors and inhibit the intracellular multiplication of *Legionella pneumophila* by limiting the availability of iron. *The Journal of Clinical Investigation* **83**, 1457-1465.
- Cai, H., Tian, X., Hu, X. D., Li, S. X., Yu, D. H. & Zhu, Y. X. (2005). Combined DNA vaccines formulated either in DDA or in saline protect cattle from *Mycobacterium bovis* infection. *Vaccine* **23**, 3887-3895.
- Caley, I. J., Betts, M. R., Irlbeck, D. M., Davis, N. L., Swanstrom, R., & Frelinger, J. (1997). Humoral, mucosal, and cellular immunity in response

- to a human immunodeficiency virus type 1 immunogen expressed by a Venezuelan equine encephalitis virus vaccine vector. *Journal of Virology* **71**, 3031-3038.
- Calvinho, L. F. & Oliver, S. P. (1998). Invasion and persistence of *Streptococcus dysgalactiae* within bovine mammary epithelial cells. *Journal of Dairy Science* **81**, 678-686.
- Carter G. R. (1955). *America Journal of Veterinary Research* **16**, 481-484. In C. Adlam and J. M. Rutter (eds). *Pasteurella* and pasteurellosis. Academic Press, New York, pg 68-73.
- Carter, G. R. (1984). Serotyping of *Pasteurella multocida*. In *Methods in Microbiology*. T. Bergman (ed.), Academic Press, London, pg 16.
- Carter G. R. and De Alwis, M. C. L. (1989). Haemorrhagic septicaemia. In C. Adlam and J. M. Rutter (eds). *Pasteurella* and pasteurellosis. Academic Press, New York, pg 37-73.
- Carter, G. R. and Chengappa, M. M. (1991). Rapid presumptive identification of type B *Pasteurella multocida* from Haemorrhagic septicaemia. *Veterinary Record* **128**, 526.
- Carlton L. Gyles, John F. Prescott, Glenn Songer, C. (Ed.). (2010). Pathogenesis of bacterial infections in animals (4th ed., p. 660). Iowa, USA: Blackwell Publishing.
- Chabri, F., Bouris, K., Jones, T., Barrow, D., Hann, A., Allender, C. (2004). Microfabricated silicon microneedles for nonviral cutaneous gene delivery. *British Journal of Dermatology* **150**, 869-877.
- Chandrasekaran, S., Kennett, L., Yeap, P. C., Muniandy, N., Rani, B. & Mukkur, T. K. (1994). Characterization of immune response and duration of protection in buffaloes immunized with haemorrhagic septicaemia vaccines. *Veterinary Microbiology* **41**, 213-219.
- Chandrasekaran, S., Yeap, P. C. & Chuink, B. H. (1981). Biochemical and serological studies of *Pasteurella multocida* isolated from cattle and buffaloes in Malaysia. *British Veterinary Journal* **137**, 361-367.
- Chanter, N. and Rutter, J. M. (1989). Pasteurellosis in pigs and the determinants of virulence of toxigenic *Pasteurella multocida*. In C. Adlam and J. M.

- Rutter (Eds.) *Pasteurella* and Pasteurellosis. Academic Press. London, UK. pg 161-195.
- Chen, S. C., Jones, D. H., Fynan, E. F., Farrar, G. H., Clegg, J. C. & Greenberg, H. B. (1998). Protective immunity induced by oral immunization with a rotavirus DNA vaccine encapsulated in microparticles. *Journal of Virology* **72**, 5757-5761.
- Chengappa, M. M., Carter, G. R. & Chang, T. S. (1979). A streptomycin-dependent live *Pasteurella multocida* type-3 vaccine for the prevention of fowl cholera in turkeys a streptomycin-dependent live *Pasteurella multocida* type-3 vaccine for the prevention of fowl cholera in turkeys. *Avian Diseases* **23**, 57-61.
- Choi-Kim, K., Maheswaran, S. K., Felice, L. J. and Molitor, T. W. (1991). Relationship between the iron regulated outer membrane proteins and the outer membrane proteins of *in vivo* grown *Pasteurella multocida*. *Veterinary Microbiology* **28**, 75-92.
- Christensen, D., Korsholm, K. S., Andersen, P. & Agger, E. M. (2011). Cationic liposomes as vaccine adjuvants. *Expert Review on Vaccines* **4**, 513-521.
- Christensen, H. (2003). Genetic relationships among avian isolates classified as *Pasteurella haemolytica*, "*Actinobacillus salpingitidis*" or *Pasteurella anatis* with proposal of *Gallibacterium anatis* gen. nov., comb. nov. and description of additional genomospecies within *Gallibac*. *International Journal of Systematic and Evolutionary Microbiology* **53**, 275-287.
- Christensen, H., Bisgaard, M., Albaek, B. & Olsen, J. E. (2004). Reclassification of Bisgaard taxon 33, with proposal of *Volucribacter psittacida* gen. nov., sp. nov. and *Volucribacter amazonae* sp. nov. as new members of the *Pasteurellaceae*. *International Journal of Systematic and Evolutionary Microbiology* **54**, 813-818.
- Christensen, H., Angen, Ø., Olsen, J. E., & Bisgaard, M. (2004b). Revised description and classification of atypical isolates of *Pasteurella multocida* from bovine lungs based on genotypic characterization to include variants previously classified as biovar 2 of *Pasteurella canis* and *Pasteurella avium*. *Microbiology* **150**, 1757-67.

- Christensen, H. & Bisgaard, M. (2006). The genus *Pasteurella*. *Prokaryotes* **6**, 1062-1090.
- Christensen, H., Dziva, F., Olsen, J. E. & Bisgaard, M. (2002). Genotypic heterogeneity of *Pasteurella gallinarum* as shown by ribotyping and 16S rRNA sequencing. *Avian Pathology* **31**, 603-10.
- Christensen, J. P. & Bisgaard, M. (1997). Avian pasteurellosis: Taxonomy of the organisms involved and aspects of pathogenesis. *Avian Pathology* **26**, 461-483.
- Christensen, J. P., Diet, H. H. & Bisgaard, M. (1998). Phenotypic and genotypic characters of isolates of *Pasteurella multocida* obtained from back-yard poultry and from two outbreaks of avian cholera in avifauna in Denmark. *Avian Pathology* **27**, 373-381.
- Christensen, J. P. & Bisgaard, M. (2000). Fowl cholera. *Revue Scientifique Et Technique-Office International Des Epizootie* **19**, 626-637.
- Clarke, J. M., Morton, R. J., Clarke, C. R., Fulton, R. W. & Saliki, J. T. (2001). Development of an ex vivo model to study adherence of *Mannheimia haemolytica* serovar 1 to mucosal tissues of the respiratory tract of cattle. *American Journal of Veterinary Research* **62**, 805-811.
- Cobb, B. D. & Clarkson, J. M. (1994). A simple procedure for optimising the polymerase chain reaction (PCR) using modified Taguchi methods. *Nucleic Acids Research* **22**, 3801-3805.
- Cohen, R. N., Macaraeg, N., Lee, A. P. & Szoka, F. C. (2009). Quantification of plasmid DNA copies in the nucleus after lipoplex and polyplex transfection. *Journal of Controlled Release : Official Journal of the Controlled Release Society* **135**, 166-174.
- Conti, P. (1991). Human recombinant interleukin-1 receptor antagonist inhibits lymphocyte blastogenesis induced by concanavalin A restorative effect of hrIL-1. *FEBS Letters* **286**, 137-141.
- Conti, P., Reale, M., Barbacane, R. C., Panara, M. R., Bongrazio, M., Dempsey, R. A. & Dinarello, C. A. (1991). Reduced mitogen stimulation of DNA synthesis in human lymphocytes by a human recombinant interleukin-1 receptor antagonist. *Immunology Letters* **28**, 19-25.

- Cossart, P. & Lecuit, M. (1998). Interactions of *Listeria monocytogenes* with mammalian cells during entry and actin-based movement: bacterial factors, cellular ligands and signaling. *The EMBO Journal* **17**, 3797-3806.
- Courvalin, P., Goussard, S. & Grillot-Courvalin, C. (1995). Gene transfer from bacteria to mammalian cells. *Comptes rendus de l'Académie des sciences. Série 3, Sciences de la vie* **318**, 1207-1212.
- Craig, F. F., Coote, J. G., Parton, R., Freer, J. H. & Gilmour, N. J. (1989). A plasmid which can be transferred between *Escherichia coli* and *Pasteurella haemolytica* by electroporation and conjugation. *Journal of General Microbiology* **135**, 2885-2890.
- Curtiss, R. I. (2002). Bacterial infectious disease control by vaccine development. *Journal of Clinical Investigation* **110**, 1061-1066.
- Dabo, S. (2003). Molecular and immunological characterization of *Pasteurella multocida* serotype A:3 OmpA: evidence of its role in *P. multocida* interaction with extracellular matrix molecules. *Microbial Pathogenesis* **35**, 147-157.
- Dabo, S. M., Confer, A. W. & Hartson, S. D. (2005). Adherence of *Pasteurella multocida* to fibronectin. *Veterinary Microbiology* **110**, 265-275.
- Dabo, S. M., Taylor, J. D. & Confer, A. W. (2007). *Pasteurella multocida* and bovine respiratory disease. *Animal Health Research Reviews / Conference of Research Workers in Animal Diseases* **8**, 129-150.
- Dagleish, M. P., Hodgson, J. C., Ataei, S., Finucane, A., Finlayson, J. & Sales, J. (2007). Safety and protective efficacy of intramuscular vaccination with a live *aroA* derivative of *Pasteurella multocida* B:2 against experimental hemorrhagic septicemia in calves. *Infection and Immunity* **75**, 5837-5844.
- Darji, A., Lage, S. zur, Garbe, L., Chakraborty, T. & Weiss, S. (2000). Oral delivery of DNA vaccines using attenuated *Salmonella typhimurium* as carrier. *FEMS Immunology and Medical Microbiology* **27**, 341-349.
- Darji, A., Guzman, C. A., Gerstel, B., Wachholz, P., Timmis, K. N., Chakraborty, T. (1997). Oral somatic transgene vaccination using attenuated *S. typhimurium*. *Cell* **91**, 765-775.

- Davies, R. L. & Quire, M. (1996). Intra-specific diversity within *Pasteurella trehalosi* based on variation of capsular polysaccharide, lipopolysaccharide and outer membrane proteins. *Microbiology* **142**, 551-560.
- De Alwis, M. C. L., Gunatileke, A. A. P. & Wickremasinghe, W. A. T. (1978). Duration of immunity to haemorrhagic septicaemia in cattle and buffaloes following immunization with alum precipitated and oil adjuvant vaccines. *Ceylon Veterinary Journal* **26**, 35-41.
- De Alwis, M. C. L., Carter, G. R. & Chengappa, M. M. (1980). Production and characterization of streptomycin dependent mutants of *Pasteurella multocida* from bovine haemorrhagic septicaemia. *Canadian Journal of Comparative Medicine* **44**, 418-422.
- De Alwis, M. C. L., Wijewardana, T. G., Gomis, A. I. U. & Vipulasiri, A. A. (1990). Persistence of the carrier status in haemorrhagic septicaemia (*Pasteurella multocida* serotype 6:b infection) in buffaloes. *Tropical Animal Health Production* **22**, 185-194.
- De Alwis, M. C. L. (1992). *Pasteurellosis in Production Animals: A Review*. *ACIAR Proceedings* **43**, 256.
- De Alwis, M. C. L. (1995). Haemorrhagic septicaemia (*Pasteurella multocida* serotype B:2 and E:2 infection) in cattle and buffaloes. In W. Donachie, F. A. Lainson and J. C. Hodgson (Eds.) *Haemophilus, Actinobacillus and Pasteurella*. Plenum Press. London, UK. pg 9-24.
- De Alwis, M. C. (1999). Haemorrhagic septicaemia--a general review. *ACIAR Proceedings* **57**, 99-112.
- De Ley, J., Mannheim, W., Muttters, R., Piechulla, K., Tytgat, R., Segers, P. (1990). Inter- and intrafamilial similarities of rRNA cistrons of the *Pasteurellaceae*. *International Journal of Systematic Bacteriology* **40**, 126-137.
- Delpy, L. P. & Rastegar, R. (1938). *Bulletin Academy Veterinary France* **9**, 256.  
*In Verma & Jaiswal (1998).*
- Dewhirst, F. E., Paster, B. J., Olsen, I. & Fraser, G. J. (1992). Phylogeny of 54 representative strains of species in the family Pasteurellaceae as determined by comparison of 16S rRNA sequences. *Journal of Bacteriology* **174**, 2002-2013.



- Dewhirst, F. E., Paster, B. J., Olsen, I., & Fraser, G. J. (1993). Phylogeny of the *Pasteurellaceae* as determined by comparison of 16S ribosomal ribonucleic acid sequences. *Zentralblatt für Bakteriologie* **279**, 35-44.
- Dietrich, G., Bubert, A., Gentschev, I., Sokolovic, Z., Simm, A. & Catic, A. (1998). Delivery of antigen-encoding plasmid DNA into the cytosol of macrophages by attenuated suicide *Listeria monocytogenes*. *Nature* **16**, 181-185.
- DiGiacomo, R. F., Deeb, B. J., Giddens, W. E., Bernard, B. L. & Chengappa (1989). Atrophic rhinitis in New Zealand white rabbits infected with *Pasteurella multocida*. *American Journal of Veterinary Research* **50**, 1460-1465.
- Donate, A., Coppola, D., Cruz, Y. & Heller, R. (2011). Evaluation of a novel non-penetrating electrode for use in DNA vaccination. *PloS One* **6**, 1-6.
- Donnelly, J. J., Wahren, B. & Liu, Margaret A. (2005). DNA Vaccines: Progress and Challenges. *Journal of Immunology* **175**, 633-639.
- Dower, W. J., Miller, J. F. & Ragsdale, C. W. (1988). High efficiency transformation of *E. coli* by high voltage electroporation. *Nucleic Acids Research* **16**, 6127-6145.
- Edelman, R. (1980). Vaccine Adjuvants. *Clinical Infection and Disease* **2**, 370-383.
- Eriksen, L., Aalbæk, B., Leifsson, P. S., Basse, A., Christiansen, T. & Rimler, R. B. (1999). Hemorrhagic Septicemia in Fallow Deer ( *Dama dama* ) caused by *Pasteurella multocida multocida*. *Journal of Zoo and Wildlife Medicine* **30**, 285-292.
- Esslinger, J., Seleim, R. S., Herrmann, G. & Blobel, H. (1994). Adhesion of *Pasteurella multocida* to HeLa cells and to macrophages of different animal species. *Revue De Medecine Veterinaire* **145**, 49-53.
- Falkow & Isberg & Portnoy. (1992). The interaction of bacteria with mammalian cells. *Annual Review of Cell Biology* **8**, 333-363.
- Feingold, D. S., HsuChen, C. C. & Sud, I. J. (1974). Basis for the selectivity of action of the polymyxin antibiotics on cell membranes\*. *Annals of the New York Academy of Sciences* **235**, 480-492.

- Fennelly, G. J., Khan, S. A., Abadi, M. A., Wild, T. F. & Bloom, B. R. (1999). Mucosal DNA vaccine immunization against measles with a highly attenuated *Shigella flexneri* vector. *Journal of immunology* **162**, 1603-1610.
- Foged, C., Brodin, B., Frokjaer, S. & Sundblad, A. (2005). Particle size and surface charge affect particle uptake by human dendritic cells in an *in vitro* model. *International Journal of Pharmaceutics* **298**, 315-322.
- Frank, G. H. (1989). Pasteurellosis of cattle. In C. Adlam and J. M. Rutter (Ed.) *Pasteurella* and Pasteurellosis. Academic Press. London, UK. pg 197-222.
- Frederiksen, W. (1989). Pasteurellosis of man, p. 303-320. In C. Adlam and J. M. Ruter (ed.), *Pasteurella* and pasteurellosis. Academic Press, London, UK.
- Fuller, M. E., Mailloux, B. J., Zhang, P., Streger, S. H., Hall, J. A., Vainberg, S. N., Beavis, A. J., Johnson, W. P., Onstott, T. C. & DeFlaun, M. F. (2001). Field-scale evaluation of CFDA/SE staining coupled with multiple detection methods for assessing the transport of bacteria in situ. *FEMS Microbiology Ecology* **37**, 55-66.
- Furie, R. A., Cohen, R. P., Hartman, B. J. & Roberts, R. B. (1980). *Pasteurella multocida* infection: report in urban setting and review of spectrum of human disease. *New York State Journal of Medicine* **80**, 1597-1602.
- Fynan, E. F., Webster, R. G., Fuller, D. H., Haynes, J. R., Santoro, J. C. & Robinson, H. L. (1993). DNA vaccines: protective immunizations by parenteral, mucosal, and gene-gun inoculations. *Proceedings of the National Academy of Sciences of the United States of America* **90**, 11478-11482.
- Gabastou, J. M., Kernéis, S., Bernet-Camard, M. F., Barbat, A., Coconnier, M. H., Kaper, J. B. & Servin, A. L. (1995). Two stages of enteropathogenic *Escherichia coli* intestinal pathogenicity are up and down-regulated by the epithelial cell differentiation. *Research in Biological Diversity* **59**, 127-134.
- Galdiero, M., Palomba, E., De, L., Vitiello, M. & Pagnini, P. (1998). Effects of the major *Pasteurella multocida* porin on bovine neutrophils. *American Journal Of Veterinary Research* **59**, 1270-1274.

- Galdiero, M., De Martino, L., Pagnini, U., Pisciotta, M. G. & Galdiero, E. (2001). Interactions between bovine endothelial cells and *Pasteurella multocida*: association and invasion. *Research in Microbiology* **152**, 57-65.
- Galdiero, M., Pisciotta, M. G., Marinelli, A., Petrillo, G. & Galdiero, E. (2002). Coinfection with BHV-1 modulates cell adhesion and invasion by *P. multocida* and *Mannheimia (Pasteurella) haemolytica*. *The New Microbiologica* **25**, 427-436.
- Gardlik, R., Behuliak, M., Palffy, R., Celec, P. & Li, C. J. (2011). Gene therapy for cancer: bacteria-mediated anti-angiogenesis therapy. *Gene Therapy* **18**, 425-431.
- Gardner, I. A., Kasten, R., Eamens, G. J., Snipes, K. P. & Anderson, R. J. (1994). Molecular fingerprinting of *Pasteurella multocida* associated with progressive atrophic rhinitis in swine herds. *Journal of Veterinary Diagnostic Investigation* **6**, 442-447.
- Gelfand, E. W., Cheung, R. K., Mills, G. B. & Grinstein, S. (1985). Mitogens trigger a calcium-independent signal for proliferation in phorbol-ester-treated lymphocytes. *Letters to Nature* **315**, 419-420.
- Gerke, C., Falkow, S. & Chien, Y.-Hsiu. (2005). The adaptor molecules LAT and SLP-76 are specifically targeted by *Yersinia* to inhibit T cell activation. *The Journal of Experimental Medicine* **201**, 361-371.
- Gilkeson, G. S., Bloom, D. D., Pisetsky, D. S. & Clarke, S. H. (1993). Molecular characterization of anti-DNA antibodies induced in normal mice by immunization with bacterial DNA. Differences from spontaneous anti-DNA in the content and location of VH CDR3 arginines. *Journal of Immunology* **151**, 1353-64.
- Gill, H. S. & Prausnitz, M. R. (2007). Coated microneedles for transdermal delivery. *Journal of Control Release* **117**, 227-237.
- Glorioso, J. C., Jones, Garth W, Rush, H. G., Pentler, L. J., Darif, A. & Coward, J. (1982). Adhesion of type A *Pasteurella multocida* to rabbit pharyngeal cells and its possible role in rabbit respiratory tract infections. *Infection and Immunity* **35**, 1103-1109.

- Gould-Fogerite, S., Kheiri, M., Zhang, F., Wang, Z., Scolpino, A. & Feketeova, E. (1998). Targeting immune response induction with cochleate and liposome-based vaccines. *Advanced Drug Delivery Reviews* **32**, 273-287.
- Gould-fogerite, S. & Mannino, R. J. (1996). Mucosal and systemic immunization using cochleate and liposome vaccines. *Journal of Liposome Research* **6**, 357-379.
- Graydon R. J., Patten, B. E. & Hamid, H. (1993). The pathology of experimental haemorrhagic septicaemia in cattle and buffalo. In B. E. Patten, T. L., Spencer, R. B., Johnson, D., Hoffmann and Lehane, L. (eds), Pasteurellosis In Production Animals, an international workshop held at Bali, Indonesia, 10-13 August 1992. *ACIAR Proceedings* **43**, 105-107.
- Gregoriadis, G. (1990). Immunological adjuvants: a role for liposomes. *Immunology Today* **11**, 89-97.
- Gregoriadis, G., Gursel, I., Gursel, M. & McCormack, B. (1996). Liposomes as immunological adjuvants and vaccine carriers. *Journal of Controlled Release* **41**, 49-56.
- Gregoriadis, G., Saffie, R. & De Souza, J. B. (1997). Liposome-mediated DNA vaccination. *FEBS Letters* **402**, 107-110.
- Griffiths, E. (1995). Assuring the Safety and Efficacy of DNA Vaccines. *Annals of the New York Academy of Sciences* **772**, 164-169.
- Grillot-Courvalin, C., Goussard, S., Huetz, F., Ojcius, D. M. & Courvalin, P. (1998). Functional gene transfer from intracellular bacteria to mammalian cells. *Nature Biotechnology* **16**, 862-866.
- Grillot-Courvalin, C., Goussard, S. & Courvalin, P. (2002). Wild-type intracellular bacteria deliver DNA into mammalian cells. *Cellular Microbiology* **4**, 177-186.
- Grillot-Courvalin, C., Goussard, S. & Courvalin, P. (2011). Bacterial vectors for delivering gene and anticancer therapies. *Microbe* **6**, 115-121.
- Gunawardana, G. A., Townsend, K. M. & Frost, A. J. (2000). Molecular characterisation of avian *Pasteurella multocida* isolates from Australia and Vietnam by REP-PCR and PFGE. *Veterinary Microbiology* **72**, 97-109.

- Guroff, R. M. (2007). Replicating and non-replicating viral vectors for vaccine development. *Current Opinion in Biotechnology* **18**, 546-556.
- Gurunathan, S., Klinman, D. M. & Seder, R. A. (2000). DNA vaccines: immunology, application, and optimization\*. *Annual Review of Immunology* **18**, 927-974.
- Gyles, C. L., Prescott, J. F., Songer, G. & Thoen, C. O. (2010). Pathogenesis of bacterial infections in animals 4th Ed., Iowa, USA: Blackwell Publishing. 660 pg.
- Haddad, D., Liljeqvist, S., Stahl, S., Andersson, I., Perlmann, P., Berzins, K. & Ahlborg, N. (1997). Comparative study of DNA-based immunization vectors: effect of secretion signals on the antibody responses in mice. *FEMS Immunology & Medical Microbiology* **18**, 193-202.
- Harper, M., Boyce, J. D., Wilkie, I. W. & Adler, B. (2003). Signature-tagged mutagenesis of *Pasteurella multocida* identifies mutants displaying differential virulence characteristics in mice and chickens. *Infection and Immunity* **71**, 5440-5446.
- Harper, M., Cox, A. D., Adler, B. & Boyce, J. D. (2011). *Pasteurella multocida* lipopolysaccharide: the long and the short of it. *Veterinary Microbiology*, Article in Press.
- Harper, M., St Michael, F., John, M., Vinogradov, E., Adler, B. & Boyce, J. D. (2011). *Pasteurella multocida* Heddleston serovars 1 and 14 express different lipopolysaccharide structures but share the same lipopolysaccharide biosynthesis outer core locus. *Veterinary Microbiology* **150**, 289-296.
- Hartmann, L., Schroder, W. & Lubke-Becker, A. (1996). A comparative study of the major outer membrane proteins of the avian haemophili and *Pasteurella gallinarum*. *Zentralbl Bakteriologie* **284**, 47-51.
- Heddleston, K. L., Gallagher, J. E. and Rebers, P. A. (1972). Fowl Cholera: Gel Diffusion and Precipitin Test for Serotyping *Pasteurella multocida* from Avian Species. *Avian Disease* **16**, 925-936.
- Heddleston, K. L. and Rebers, P. A. (1975). Properties of free endotoxin from *Pasteurella multocida*. *American Journal of Veterinary Research* **36**, 574-673.

- Hense, M., Domann, E., Krusch, S., Wachholz, P., Dittmar, K. E. J., Rohde, M., Wehland, J., Chakraborty, T. & Weiss, S. (2001). Eukaryotic expression plasmid transfer from the intracellular bacterium *Listeria monocytogenes* to host cells. *Cellular microbiology* **3**, 599-609.
- Herrmann, J. E., Chen, S. C., Jones, D. H., Tinsley-Bown, A., Fynan, E. F., Greenberg, H. B. (1999). Immune responses and protection obtained by oral immunization with rotavirus VP4 and VP7 DNA vaccines encapsulated in microparticles. *Virology* **259**, 148-53.
- Hill, E. & Lainson, F. (2003). Survey of restriction-modification systems and transformation in *Mannheimia haemolytica* and *Pasteurella trehalosi*. *Veterinary Microbiology* **92**, 103-109.
- Hirsh, D. C., Hansen, L. M., Dorfman, L. C., Snipes, K. P., Carpenter, T. E., Hird, D. W. (1989). Resistance to antimicrobial agents and prevalence of R plasmids in *Pasteurella multocida* from turkeys. *Antimicrobial Agents and Chemotherapy* **33**, 670-673.
- Hirsh, D. C., Martin, L. D., & Rhoades, K. R. (1985). Resistance plasmids of *Pasteurella multocida* isolated from turkeys. *American Journal of Veterinary Research* **46**, 1490-1493.
- Hodgson, J. C., Finucane, A., Dagleish, M. P., Ataei, S., Parton, R. & Coote, J. G. (2005). Efficacy of vaccination of calves against hemorrhagic septicemia with a live *aroA* derivative of *Pasteurella multocida* B:2 by two different routes of administration. *Infection and Immunity* **73**, 1475-1481.
- Holt, J. (Ed.). (1994). *Bergey's manual of determinative bacteriology* (9th ed., p. 787). Baltimore, MD: Lippincott Williams & Wilkins.
- Homchampa, P., Strugnell, R. & Adler, B. (1992). Molecular analysis of the *aroA* gene of *Pasteurella multocida* and vaccine potential of a constructed *aroA* mutant. *Molecular Microbiology* **6**, 3585-3593.
- Homchampa, P., Strugnell, R. & Adler, B. (1994). *Pasteurella haemolytica*. *Science* **42**, 35-44.
- Homchampa, P., Strugnell, R. & Adler, B. (1997). Cross protective immunity conferred by a marker-free *aroA* mutant of *Pasteurella multocida*. *Vaccine* **15**, 203-208.

- Hornef, M. W., Wick, M. J., Rhen, M. & Normark, S. (2002). Bacterial strategies for overcoming host innate and adaptive immune responses. *Nature Immunology* **3**, 1033-1040.
- Hoskins, I. C. & Lax, A. J. (1997). Identification of restriction barriers in *Pasteurella multocida*. *FEMS Microbiology Letters* **156**, 223-226.
- Hu, S. P., Felice, L. J., Sivanandan, V. & Maheswaran, S. K. (1986). Siderophore production by *Pasteurella multocida*. *Infection and Immunity* **54**, 804-10.
- Hu, X.-D., Yu, D.-H., Chen, S.-T., Li, S.-X. & Cai, Hong. (2009). A combined DNA vaccine provides protective immunity against *Mycobacterium bovis* and *Brucella abortus* in cattle. *DNA and Cell Biology* **28**, 191-199.
- Hubbert, W. T. & Rosen, M. N. (1970). *Pasteurella multocida* infection due to animal bite. *America Journal of Public Health* **60**, 1103-1108.
- Hunt, M. L., Adler, B. & Townsend, K. M. (2000). The molecular biology of *Pasteurella multocida*. *Veterinary Microbiology* **72**, 3-25.
- Ibrahim, R. S., Sawada, T., Shahata, M. & Ibrahim, A. (2000). Cross-protection and antigen expression by chicken embryo-grown *Pasteurella multocida* in chickens. *Journal of Comparative Pathology* **123**, 278-84.
- Ikeda, J. S. & Hirsh, D. C. (1990). Possession of identical nonconjugative plasmids by different isolates of *Pasteurella multocida* does not imply clonality. *Veterinary Microbiology* **22**, 79-87.
- Iovane, G., Pagnini, P., Galdiero, M., Cipollaro de l'Ero, G., Vitiello, M. & D'Isanto, M. (1998). Role of *Pasteurella multocida* porin on cytokine expression and release by murine splenocytes. *Veterinary Immunology and Immunopathology* **66**, 391-404.
- Jablonski, L., Sriranganathan, N., Boyle, S. M. & Carter, G. R. (1992). Conditions for transformation of *Pasteurella multocida* by electroporation. *Cell* **473**, 63-68.
- Jacques, M. & Mikael, L. G. (2002). Virulence factors of *Pasteurellaceae*, formidable animal pathogens. *ASM News* **68**, 175-179.
- Jain, D., Jain, V. & Singh, R. (2011). Novel antigen delivery technologies: a review. *Drug Delivery and Translational Research* **1**, 103-112.

- Johnson, R. H. and Rumans, L. W. (1977). Unusual infections caused by *Pasteurella multocida*. *The Journal of the American Medical Association* **237**, 146-147.
- Jones, F. L. Jr., Smull, C. E. (1973). Infections in man due to *Pasteurella multocida*. *Pennsylvania Medicine* **76**, 41-44.
- Jones, G. W. (1977). The attachment of bacteria to the surfaces of animal cells. *J. L. Reissig (ed.), Microbial interactions. Chapman & Hall, Ltd., London*, pg. 139-176.
- Jones, T.O. & Hussaini, S. N. (1982). Outbreaks of *Pasteurella multocida* septicaemia in fallow deer (*Dama dama*). *Journal of Veterinary Record* **110**, 451-452.
- Jordan, R. W., Hamilton, T. D. C., Hayes, C. M., Patel, D., Jones, P. H. & Roe, J. M. (2003). Modulation of the humoral immune response of swine and mice mediated by toxigenic *Pasteurella multocida*. *FEMS Immunology & Medical Microbiology* **39**, 51-59.
- Joseph, P. G. & Hedger, R. S. (1984). Serological response of cattle to simultaneous vaccinations against foot-and-mouth disease and haemorrhagic septicaemia. *Journal of Veterinary Record* **114**, 494-496.
- Kaneda, Y., Iwai, K. & Uchida, T. (1989). Introduction and expression of the human insulin gene in adult rat liver. *The Journal of Biological Chemistry* **264**, 12126-12129.
- Kasten, R. W., Carpenter, T. E., Snipes, K. P. & Hirsh, D. C. (1997). Detection of *Pasteurella multocida*-specific DNA in turkey flocks by use of the polymerase chain reaction. *Avian Diseases* **41**, 676-682.
- Kasten, R. W., Hansen, L. M., Hinojoza, J., Bieber, D., Ruehl, W. W. & Hirsh, D. C. (1995). *Pasteurella multocida* produces a protein with homology to the P6 outer membrane protein of *Haemophilus influenzae*. *Infection and Immunity* **63**, 989-993.
- Kisiela, D. I. & Czuprynski, C. J. (2009). Identification of *Mannheimia haemolytica* adhesins involved in binding to bovine bronchial epithelial cells. *Infection and Immunity* **77**, 446-55.



- Klavinskis, L. S., Gao, L., Barnfield, C., Lehner, T. & Parker, S. (1997). Mucosal immunization with DNA-liposome complexes. *Vaccine* **15**, 818-820.
- Knox, K. W. & Bain, R. V. (1960). The antigens of *Pasteurella multocida* type I. II. Lipopolysaccharides. *Immunology* **3**, 352-362.
- Kock, S. A., Lanske, B., Uberschar, S. & Atkinson, M. J. (1995). Effects of the *Pasteurella multocida* toxin on osteoblastic cells *in vitro*. *Veterinary Pathology* **32**, 274-279.
- Kraning-Rush, C. M., Carey, S. P., Califano, J. P., Smith, B. N. & Reinhart-King, C. A. (2011). The role of the cytoskeleton in cellular force generation in 2D and 3D environments. *Physical Biology* **8**, 1-9.
- Kreis, T. and Vale, R. (1993). Guidebook to the extracellular matrix and adhesion proteins. Sambrook & Tooze Publication at Oxford University Press, Oxford.
- Krusch, S., Domann, E., Frings, M., Zelmer, A., Diener, M. & Chakraborty, T. (2002). *Listeria monocytogenes* mediated CFTR transgene transfer to mammalian cells. *The Journal of Gene Medicine* **4**, 655-67.
- Kuhnert, P., Korczak, B., Falsen, E., Straub, R., Hoops, A. & Boerlin, P. (2004). *Nicoletella semolina* gen. nov., sp. nov., a new member of *Pasteurellaceae* isolated from horses with airway disease. *Journal of Clinical Microbiology* **42**, 5542-5548.
- Kunik, T., Tzfira, T., Kapulnik, Y., Gafni, Y., Dingwall, C. & Citovsky, V. (2001). Genetic transformation of HeLa cells by *Agrobacterium*. *Proceedings of the National Academy of Sciences of the United States of America* **98**, 1871-1876.
- Lainson, F. A., Aitchison, K. D., Donachie, W. & Thomson, J. R. (2002). Typing of *Pasteurella multocida* isolated from pigs with and without porcine dermatitis and nephropathy syndrome. *Infection and Immunity* **40**, 588-593.
- Landry, S. & Heilman, C. (2005). Future directions in vaccines: the payoffs of basic research. *Health Affairs (Project Hope)* **24**, 758-769.
- Lee, C.-H., Wu, C.-L. & Shiau, A.-L. (2005). Systemic administration of attenuated *Salmonella choleraesuis* carrying thrombospondin-1 gene leads

- to tumor-specific transgene expression, delayed tumor growth and prolonged survival in the murine melanoma model. *Cancer Gene Therapy* **12**, 175-184.
- Lee, J. W., Park, J.-hwan & Prausnitz, M. R. (2008). Dissolving microneedles for transdermal drug delivery. *Biomaterials* **29**, 2113-2114.
- Lee, M. D., Wooley, R. E. & Glisson, J. R. (1994). Invasion of epithelial cell monolayers by turkey strains of *Pasteurella multocida*. *Avian Diseases* **38**, 72-77.
- Lee, M. D. & Wooley, R. E. (1995). The effect of plasmid acquisition on potential virulence attributes of *Pasteurella multocida*. *Avian Diseases* **39**, 451-457.
- Lehmann, K. B. and Neumann, R. O. (1899). Bakteriologische Diagnostik. L.F. Lehmanns Verlg./ Munchen, 2. Auf., II. Band, pg. 408-413.
- Lemichez, E., Flatau, G., Gauthier, M., Chardin, P., Paris, S. & Fiorentini, C. (1997). Toxin-induced activation of the G protein p21 Rho by deamidation of glutamine. *Nature* **387**, 729-33.
- Leung, K. Y. & Finlay, B. B. (1991). Intracellular replication is essential for the virulence of *Salmonella typhimurium*. *Proceedings of the National Academy of Sciences of the United States of America* **88**, 11470-11474.
- Li, D., Liu, Y., Zhang, Y., Xu, J., Hong, K., Sun, M. & Shao, Y. (2007). Adjuvant effects of plasmid-generated hairpin RNA molecules on DNA vaccination. *Vaccine* **25**, 6992-7000.
- Liu, M. A. (2003). REVIEW. DNA vaccines :A review. *Journal of Internal Medicine* **253**, 402-410.
- Liu, M. A. (2011). DNA vaccines : A historical perspective and view to the future. *Immunological Reviews* **239**, 62-84.
- Lo, R. Y. C. & Sorensen, L. S. (2007). The outer membrane protein OmpA of *Mannheimia haemolytica* A1 is involved in the binding of fibronectin. *FEMS Microbiology Letters* **274**, 226-31.
- Loeffler, D. I. M., Schoen, C. U., Goebel, W. & Pilgrim, S. (2006). Comparison of different live vaccine strategies in vivo for delivery of protein antigen or antigen-encoding DNA and mRNA by virulence-attenuated *Listeria monocytogenes*. *Infection and Immunity* **74**, 3946-3957.

- Loessner, H., Endmann, A., Leschner, S., Bauer, H., Zelmer, A., Lage, S., Westphal, K. & Weiss, S. (2008). Improving live attenuated bacterial carriers for vaccination and therapy. *International Journal of Medical Microbiology* **298**, 21-26.
- Lu, X.-ling, Jiang, X.-bing, Liu, R.-en & Zhang, S.-min. (2008). The enhanced anti-angiogenic and antitumor effects of combining flk1-based DNA vaccine and IP-10. *Vaccine* **26**, 5352-5357.
- Lubke, A., Hartmann, L., Schroder W. & Hellmann E. (1994). Isolation and partial characterization of the major protein of the outer membrane of *Pasteurella haemolytica* and *Pasteurella multocida*. *Zentralbl. Bakteriologie* **281**, 45-54.
- Lundstrom, K. (2005). Biology and application of alphaviruses in gene therapy. *Gene Therapy* **12**, 92-97.
- Lundstrom, K. (1997). Alphaviruses as expression vectors. *Current Opinion in Biotechnology* **8**, 578-582.
- Maciag, P. C., Radulovic, S. & Rothman, J. (2009). The first clinical use of a live-attenuated *Listeria monocytogenes* vaccine: A Phase I safety study of Lm-LLO-E7 in patients with advanced carcinoma of the cervix. *Vaccine* **27**, 3975-3983.
- Maclean, I. W., Slaney, L., Juteau, J. M., Levesque, R. C., Albritton, W. L. & Ronald, A. R. (1992). Identification of a ROB-1 beta-lactamase in *Haemophilus ducreyi*. *Antimicrobial Agents and Chemotherapy* **36**, 467-469.
- Maheswaran, S. K. & Thies, E. S. (1979). Influence of encapsulation on phagocytosis of *Pasteurella multocida* by bovine neutrophils. *Infection and Immunity* **26**, 76-81.
- Malik, P. & Monga, D. P. (2002). Comparative analysis of the outer membrane protein profiles of isolates of the *Pasteurella multocida* (B:2) associated with haemorrhagic septicaemia. *Veterinary Research Communications* **26**, 513-522.
- Manning, P. J., DiGiacomo, R. F. & DeLong, D. (1989). Pasteurellosis in laboratory animals. In C. Adlam and J. M. Rutter (Eds.) *Pasteurella and Pasteurellosis*. Academic Press. London, UK. pg. 263-302.

- Mannino, R. J. & Gould-fogerite, S. (1988). Liposome mediated gene transfer. *BioTechniques* **6**, 682-689.
- Mannino, R. J. & Gould-fogerite, S. (1997). Antigen cochleate preparations for oral and systemic vaccination. In *New Generation Vaccines*, eds. ML Levine, GC Woodrow, JB Kaper, GS Cobon. New York: Marcel Dekker. 2nd ed.
- Marandi, M. V. & Mittal, K. R. (1995). Identification and characterization of outer membrane proteins of *Pasteurella multocida* serotype D by using monoclonal antibodies. *Journal of Clinical Microbiology* **33**, 952-957.
- Marandi, M. V. & Mittal, K. R. (1996). Characterization of an outer membrane protein of *Pasteurella multocida* belonging to the OmpA family. *Veterinary Microbiology* **53**, 303-314.
- Mario Jacques, L. G. M. (2002). Virulence factors of *Pasteurellaceae*, formidable animal pathogens. *ASM News* **68**, 175-179.
- Marsh, J. L., Erfle, M. & Wykes, E. J. (1984). The pIC plasmid and phage vectors with versatile cloning sites for recombinant selection by insertional inactivation. *Gene* **32**, 481-485.
- Mbuthia, P. G., Christensen, H., Boye, M., Majken, K., Petersen, D. & Bisgaard, M. (2001). Specific detection of *Pasteurella multocida* in chickens with fowl cholera and in pig lung tissues using fluorescent rRNA in situ hybridization. *Society* **39**, 2627-2633.
- Merza, M. (2008). Adherence to and invasion of mammalian cell lines by *Pasteurella multocida* B:2. MSc thesis. University of Glasgow.
- Miflin, J. K. & Blackall, P.J. (2001). Development of a 23S rRNA-based PCR assay for the identification of *Pasteurella multocida*. *Letters in Applied Microbiology* **33**, 216-221.
- Miller-edge, M. & Splitter, G. (1986). Detection of impaired T cell-mediated immune responses to herpesvirus (BHV-1) in cattle. *Veterinary Immunology and Immunopathology* **13**, 1-18.
- Mohan, K., Kelly, P. J., Hill, F. W. G., Muvavarirwa, P. & Pawandiwa, A. (1997). Phenotype and serotype of *Pasteurella multocida* isolates from diseases of dogs and cats in Zimbabwe. *Comparative Immunology, Microbiology and Infectious Diseases* **20**, 29-34.

- Mueller, A., Lalor, R., Cardaba, C. M. & Matthews, S. E. (2011). Stable and sensitive probes for lysosomes: cell-penetrating fluorescent calix[4]arenes accumulate in acidic vesicles. *Cytometry. Part A : The journal of the International Society for Analytical Cytology* **79**, 126-136.
- Mukherjee, S., Ahmed, A. & Nandi, D. (2005). CTLA4-CD80 / CD86 interactions on primary mouse CD4<sup>+</sup> T cells integrate signal-strength information to modulate activation with Concanavalin A. *Journal of Leukocyte Biology* **78**, 144-157.
- Mutters, R., Ihm, P., Pohl, S., Frederiksen, W. & Mannheim, W. (1985). Reclassification of the genus *Pasteurella trevisan* 1887 on the basis of deoxyribonucleic acid homology, with proposals for the new species *Pasteurella dagmatis*, *Pasteurella canis*, *Pasteurella stomatis*, *Pasteurella anatis*, and *Pasteurella langaa*. *International Journal of Systematic Bacteriology* **35**, 309-322.
- Mutters, R., Christensen, H. & Bisgaard, M. (2003). Genus *Pasteurella* Trevisan 1887, 94, AL nom. cons. opin. 13, Jud. Comm. 1954. In: Bergey's Manual of Systematic Bacteriology, 2nd ed. Springer-Verlag. New York, NY. 2.
- Myint, A., Jones, T. O. & Nyunt, H. H. (2005). Efficacy and cross-protectivity of a live intranasal aerosol haemorrhagic septicaemia vaccine. *Veterinary Records* **156**, 41-45.
- Myint, A., Carter, G. R. & Jones, T. O. (1987). Prevention of experimental haemorrhagic septicaemia with a live vaccine. *Journal of Veterinary Record* **23**, 500-501.
- Nagai, S., Someno, S. & Yagihashi, T. (1994). Differentiation of toxigenic from nontoxigenic isolates of *Pasteurella multocida* by PCR. *Journal of Clinical Microbiology* **32**, 1004-1010.
- Nagy, L. K. & Penn, C. W. (1974). Capsule and somatic antigen of *Pasteurella multocida*, types B and E. *Research in Veterinary Science* **16**, 251-259.
- Nandedkar, T. D. (2009). Nanovaccines: recent developments in vaccination. *Journal of Biosciences* **34**, 995-1003.
- Nicolau, C., Le Pape, A., Soriano, P., Fargette, F. & Juhel, M. F. (1983). *In vivo* expression of rat insulin after intravenous administration of the liposome-

- entrapped gene for rat insulin I. *Proceedings of the National Academy of Sciences of the United States of America* **80**, 1068-1072.
- Nicolettil, P. (1990). Vaccination against *Brucella*. *Advances in Biotechnological Processes* **13**, 147-168.
- Nielsen, J. P., Foged, N. T., Sørensen, V., Barfod, K., Bording, A. & Petersen, S. K. (1991). Vaccination against progressive atrophic rhinitis with a recombinant *Pasteurella multocida* toxin derivative. *Canadian Journal of Veterinary Research* **55**, 128-138.
- Niethammer, A. G., Xiang, R., Becker, J. C., Wodrich, H., Pertl, U. & Karsten, G. (2002). A DNA vaccine against VEGF receptor 2 prevents effective angiogenesis and inhibits tumor growth. *Nature Medicine* **8**, 1369-1375.
- Ochman, H., Gerber, A. S. & Hartl, D. L. (1988). Genetic applications of an inverse polymerase chain reaction. *Genetics* **120**, 621-623.
- OIE. (2004). Haemorrhagic septicaemia. In *Manual of Diagnostic Tests and Vaccines for Terrestrial Animals*. *World Organisation for Animal Health*.
- Olsen, I., Dewhirst, F. E., Paster, B. J. & Busse, H. J. (2003). Family Pasteurellaceae. In *Bergey's Manual of Systematic Bacteriology*, 2nd ed. Springer-Verlag. New York, 2.
- Olsen, J. E., Bisgaard, M., Kuhnert, P. & Christensen, H. (2005). The current status of *Pasteurellaceae* systematics. In *ASM Conference on Pasteurellaceae*. *American Society for Microbiology*. October 23-26, 2005. Kohala Coast, Big Island, Hawaii, USA, pg. 14.
- Pabs-Garnon, L. F. & Soltys, M. A. (1971). Multiplication of *Pasteurella multocida* in the spleen, liver and blood of turkeys inoculated intravenously. *Canadian Journal of Comparative Medicine. Revue canadienne de médecine comparée* **35**, 147-149.
- Paglia, P., Medina, E., Arioli, I., Guzman, C. A. & Colombo, M. P. (1998). Gene transfer in dendritic cells, induced by oral DNA vaccination with *Salmonella typhimurium*, results in protective immunity against a murine fibrosarcoma. *Blood* **92**, 3172-3176.
- Paglia, P., Terrazzini, N., Schulze, K., Guzmán, C. A. & Colombo, M. P. (2000). In vivo correction of genetic defects of monocyte/macrophages using

- attenuated *Salmonella* as oral vectors for targeted gene delivery. *Gene therapy* **7**, 1725-1730.
- Pati, U. S., Srivastava, S. K., Roy, S. C. & More, T. (1996). Immunogenicity of outer membrane protein of *Pasteurella multocida* in buffalo calves. *Veterinary Microbiology* **52**, 301-311.
- Pawelek, J. M., Low, K. B. & Bermudes, D. (1997). Tumor-targeted *Salmonella* as a Novel Anticancer Vector. *Cancer Research* **57**, 4537-4544.
- Pei, S., Doye, A. & Boquet, P. (2001). Mutation of specific acidic residues of the CNF1 T domain into lysine alters cell membrane translocation of the toxin. *Molecular Microbiology* **41**, 1237-1247.
- Peltier, M. R., Liu, W.-J. & Hansen, P. J. (2008). Regulation of lymphocyte proliferation by uterine serpin-interleukin-2. in: interleukin-2 mRNA production, CD25 expression and responsiveness. *Proceedings of the Society for Experimental Biology and Medicine* **223**, 75-81.
- Penn, C. W. & Nagy, L. K. (1976), Res. Veterinary Science, 20, 90-96. Cited by Frederiksen, W. (1989). A note on the name *Pasteurella multocida*. In C Adlam and J.M Rutter (Eds), *Pasteurella* and Pasteurellosis. London: Academic Press, pg. 35-36.
- Petersen, S. K., Foged, N. T., Bording, A., Nielsen, J. P., Riemann, H. K. & Frandsen, P. L. (1991). Recombinant derivatives of *Pasteurella multocida* toxin: candidates for a vaccine against progressive atrophic rhinitis. *Infection and Immunity* **59**, 1387-1393.
- Pontarollo, R. A., Rankin, R., Babiuk, L. A., Godson, D. L., Griebel, P. J. & Hecker, R. (2002). Monocytes are required for optimum in vitro stimulation of bovine peripheral blood mononuclear cells by non-methylated CpG motifs. *Veterinary Immunology and Immunopathology* **84**, 43-59.
- Pruimboom, I. M., Rimler, R. B., Ackermann, M. R. & Brogden, K. A. (1996). Capsular hyaluronic acid-mediated adhesion of *Pasteurella multocida* to turkey air sac macrophages. *Avian Diseases* **40**, 887-893.
- Pálffy, R., Gardlík, R., Hodosy, J., Behuliak, M., Resko, P. & Radvánský, J. (2006). Bacteria in gene therapy: bactofection versus alternative gene therapy. *Gene Therapy* **13**, 101-105.

- Rabier, M. J., Tyler, N. K., Walker, N. J., Hansen, L. M., Hirsh, D. C. & Tablin, F. (1997). *Pasteurella multocida* enters polarized epithelial cells by interacting with host F-actin. *Veterinary Microbiology* **54**, 343-55.
- Rafat, M., Cl  roux, C. A., Fong, W. G., Baker, A. N., Leonard, B. C. & O'Connor, M. D. (2010). PEG-PLA microparticles for encapsulation and delivery of Tat-EGFP to retinal cells. *Biomaterials* **31**, 3414-3421.
- Ratledge, C. & Dover, L. G. (2000). Iron metabolism in pathogenic bacteria. *Annual Review of Microbiology* **54**, 881-941.
- Rebers, P. A., Heddleston, K. L. & Rhoades, K. R. (1967). Isolation from *Pasteurella multocida* of a lipopolysaccharide antigen with immunizing and toxic properties. *Journal of Bacteriology* **93**, 7-14.
- Rhodes, K. R. & Rimler R. B. (1989) Fowl cholera, p 95-113. In C. Adlam and J. M. Ruter (ed.), *Pasteurella* and pasteurellosis. Academic Press, London, UK.
- Rimler, R. B., Rebers, P. A. & Phillips, M. (1984). Lipopolysaccharides of the Heddleston serotypes of *Pasteurella multocida*. *American Journal of Veterinary Research* **45**, 759-763.
- Rimler, R. B. & Rhoades, K. R. (1989). Solubilization of membrane-associated cross-protection factor(s) of *Pasteurella multocida*. *Avian Diseases* **33**, 258-263.
- Robinson, H. L., Hunt, L. A. & Webster, R. G. (1993). Protection against a lethal influenza virus challenge by immunization with a haemagglutinin-expressing plasmid DNA. *Vaccine* **11**, 957-960.
- Robinson, R. (1944). Human infection with *Pasteurella septica*. *British Medical Journal* **2**, 725.
- Rosenbusch, C. & Merchant, I. A. (1939). *Journal Bacteriology*, **37**, 69-89. Cited by Frederiksen, W. (1989). A note on the name *Pasteurella multocida*. In C. Adlam and J. M. Rutter (Eds), *Pasteurella* and Pasteurellosis. London:Academic Press, pg. 35-36.
- Ross, G. F., Bruno, M. D., Uyeda, M., Suzuki, K., Nagao, K., Whitsett, J. A. & Korfhagen, T. R. (1998). Enhanced reporter gene expression in cells transfected in the presence of DMI-2, an acid nuclease inhibitor. *Gene Therapy* **5**, 1244-1250.



- Rudin, A., Healey, A., Phillips, C. A., Gump, D. W. & Forsyth, B. R. (1970). Antibacterial activity of gentamicin sulfate in tissue culture. *Applied Microbiology* **20**, 989-90.
- Ruffolo, C. G. & Adler, B. (1996). Cloning, sequencing, expression, and protective capacity of the *oma87* gene encoding the *Pasteurella multocida* 87 kda outer membrane antigen. *Infection and Immunity* **64**, 3161-3167.
- Ruffolo, C. G., Tennent, J. M., Michalski, W. P. & Adler, B. (1997). Identification, purification, and characterization of the type 4 fimbriae of *Pasteurella multocida*. *Infection and Immunity* **65**, 339-343.
- Ruffolo, C. G., Jost, B. H. & Adler, B. (1998). Iron-regulated outer membrane proteins of *Pasteurella multocida* and their role in immunity. *Veterinary Microbiology* **59**, 123-137.
- Sabri, M Y., Zamri-Saad, M., Mutalib, A. R., Israf, D. A. & Muniandy, N. (2000). Efficacy of an outer membrane protein of *Pasteurella haemolytica* A2, A7 or A9-enriched vaccine against intratracheal challenge exposure in sheep. *Veterinary Microbiology* **73**, 13-23.
- Saharee A. A., Salim, N. (1991). The epidemiology of haemorrhagic septicaemia in cattle and buffaloes in Malaysia. In *FAO*, 109-112.
- Saharee A. A., Salim, N. (1993). Haemorrhagic septicaemia carriers among cattle and buffalo in Malaysia. *ACIAR Proceedings* **42**, 89-91.
- Sambrook, J., Fritsch, E. F. & Maniatis, T. (1989). *Molecular cloning: A laboratory manual* (2nd ed.). Cold Spring Harbor Laboratory Press, Cold Spring Harbor, New York, USA.
- San Millan, A., Escudero, J. A., Gutierrez, B., Hidalgo, L., Garcia, N., Llagostera, M., Dominguez, L. & Gonzalez-Zorn, B. (2009). Multiresistance in *Pasteurella multocida* is mediated by coexistence of small plasmids. *Antimicrobial Agents and Chemotherapy* **53**, 3399-3404.
- Sanger, F., Nicklen, S. & Coulson, A. R. (1977). DNA sequencing with chain-terminating inhibitors. 1977. *Proceedings of the National Academy of Sciences of the United States of America* **74**, 5463-5467.

- Sarah, S. O., Zamri-Saad, M., Zunita, Z. & Raha, A. R. (2006). Molecular cloning and sequence analysis of *gdhA* gene of *Pasteurella multocida* B:2. *Journal of Animal and Veterinary Advances* **5**, 1146-1149.
- Schaffner, W. (1980). Direct transfer of cloned genes from bacteria to mammalian cells. *Proceedings of the National Academy of Sciences of the United States of America* **77**, 2163-2167.
- Schlesinger, L. S., Bellinger-Kawahara, C. G., Payne, N. R. & Horwitz, M. A. (1990). Phagocytosis of *Mycobacterium tuberculosis* is mediated by human monocyte complement receptors and complement component C3L. *The Journal of Immunology* **144**, 2771-2780.
- Schurig, G. G., Sriranganathan, N. & Corbel, M. J. (2002). Brucellosis vaccines : past , present and future. *Veterinary Microbiology* **90**, 479-496.
- Schwab, J. H. (1975). Suppression of the immune response by microorganisms. *Bacteriological Reviews* **39**, 121-43.
- Scott, P. C., Markham, J. F. & Whithear, K. G. (1999). Safety and efficacy of two live *Pasteurella multocida aroA* mutant vaccines in chickens. *Avian Diseases* **43**, 83-88.
- Seow, Y. & Wood, M. J. (2009). Biological gene delivery vehicles: beyond viral vectors. *Molecular Therapy : The journal of the American Society of Gene Therapy* **17**, 767-777.
- Shah, N. H., Biewenga, J. & Graaf, F. K. de. (1996). Vacuolating cytotoxic activity of *Pasteurella multocida* causing haemorrhagic septicaemia in buffalo and cattle. *FEMS Microbiology Letters* **143**, 97-101.
- Shah, N. H. & Graaf, F. K. de. (1997). Protection against haemorrhagic septicaemia induced by vaccination of buffalo calves with an improved oil adjuvant vaccine. *FEMS Microbiology Letters* **155**, 203-207.
- Shelke, N. B., Kadam, R., Tyagi, P., Rao, V. R. & Kompella, U. B. (2010). Intravitreal poly(l-lactide) microparticles sustain retinal and choroidal delivery of TG-0054, a hydrophilic drug intended for neovascular diseases. *Drug Delivery and Translational Research* **1**, 76-90.

- Shen, H., Kanoh, M., Liu, F., Maruyama, S. & Asano, Y. (2004). Modulation of the immune system by *Listeria monocytogenes*-mediated gene transfer into mammalian cells. *Microbiology and Immunology* **48**, 329-337.
- Shumilov, K. V., Sklyarov, O. & Klimanov, A. (2010). Designing vaccines against cattle brucellosis. *Vaccine* **28**, 31-34.
- Siju, J., Kumar, A. A., Shivachandra, S. B., Chaudhuri, P., Srivastava, S. K. & Singh, V. P. (2007). Cloning and characterization of type 4 fimbrial gene (*ptfA*) of *Pasteurella multocida* serogroup B:2 (strain P52). *Veterinary Research Communications* **31**, 397-404.
- Sing, A., Roggenkamp, A., Geiger, A. M. & Heesemann, J. (2002). *Yersinia enterocolitica* evasion of the host innate immune response by V antigen-induced IL-10 production of macrophages is abrogated in IL-10-deficient mice. *Journal of Immunology* **168**, 1315-1321.
- Sizemore, D. R., Branstrom, A. A. & Sadoff, J. C. (1997). Attenuated bacteria as a DNA delivery vehicle for DNA-mediated immunization. *Vaccine* **15**, 804-807.
- Sizemore, D. R., Branstrom, A. A. & Sadoift, J. C. (1995). Attenuated *Shigella* as a DNA delivery vehicle for DNA-mediated immunization. *Science* **270**, 299-302.
- Skinner, M. A., Buddle, B. M., Wedlock, D. N., Keen, D., Lisle, G. W. D. & Tascon, R. E. (2003). A DNA Prime-*Mycobacterium bovis* BCG boost vaccination strategy for cattle induces protection against bovine tuberculosis. *Infection and Immunity* **71**, 4901-4907.
- Srivastava, S. K. (1998). outer membrane protein of *Pasteurella multocida* serotype B:2 is immunogenic and antiphagocytic. *Indian Journal of Experimental Biology* **36**, 530-532.
- Staddon, J. M., Chanter, N., Lax, A. J., Higgins, T. E. & Rozengurt, E. (1990). *Pasteurella multocida* toxin, a potent mitogen, stimulates protein kinase C-dependent and -independent protein phosphorylation in Swiss 3T3 cells. *Journal of Biological Chemistry* **265**, 11841-11848.
- Syamsudin, A. (1993). Control of haemorrhagic septicaemia in Indonesia-A short history. *ACIAR Proceedings* **43**, 180-181.

- Tabatabaei, M. (2000). Construction and characterisation of attenuated derivatives of *Pasteurella multocida* serotype B:2 strains. PhD thesis. Univeristy of Glasgow.
- Tabatabaei, M., Liu, Z., Finucane, A., Parton, R. & Coote, J. (2002). Protective immunity conferred by attenuated *aroA* derivatives of *Pasteurella multocida* B:2 strains in a mouse model of hemorrhagic septicemia. *Infection and Immunity* **70**, 3355-3362.
- Tang, D., De vit, M. & Johnston, S. A. (1992). Genetic immunization is a simple method for eliciting an immune response. *Letters to Nature* **356**, 152-154.
- Talmage, W. & Dixon, F. J. (1953). The influence of adjuvants on the elimination of soluble protein antigens and the associated antibody responses. *Journal of Infectious Diseases* **93**, 176-180.
- Thomas, J. (1970). Studies on haemorrhagic septicaemia oil-adjuvant vaccine III. serological studies. *Kajian Veterinaire (Singapore)* **2**, 103-112.
- Thomsen, D. R., Stenberg, R. M., Goins, W. F. & Stinski, M. F. (1984). Promoter-regulatory region of the major immediate early gene of human cytomegalovirus. *Proceedings of the National Academy of Sciences of the United States of America* **81**, 659-663.
- Tomer, P., Chaturvedi, G. C., Minakshi, M., P. & Monga, D. P. (2002). Comparative analysis of the outer membrane protein profiles of isolates of the *Pasteurella multocida* (B:2) associated with haemorrhagic septicaemia. *Veterinary Research Communications* **26**, 513-522.
- Tomer, P., Chaturvedi, G. C., & Monga, D. P. (2004). Detection of fimbriae on Haemorrhagic septicaemia associated *Pasteurella multocida* (B:2) isolated. *The Indian Journal of Animal Sciences* **74**,12.
- Townsend, K. M., Frost, A. J., Lee, C. W., Papadimitriou, J. M. & Dawkins, H. J. (1998). Development of PCR assays for species- and type-specific identification of *Pasteurella multocida* isolates. *Journal of Clinical Microbiology* **36**, 1096-100.
- Tsuji, A. M., Matsumoto, M. & Tsuji, M. (1989). Pathogenesis of Fowl Cholera : Influence of encapsulation on the fate of *Pasteurella multocida* after intravenous inoculation into turkeys. *Avian Diseases* **33**, 238-247.

- Tubulekas, I., Berglund, P., Fleeton, M. & Liljestrom, P. (1997). Alphavirus expression vectors and their use as recombinant vaccines: A mini review. *Gene* **190**, 191-195.
- Ulmer, J. B., Donnelly, J. J., Parker, S. E., Rhodes, G. H., Felgner, P. L. & Dwarki, V. J. (1993). Heterologous protection against influenza by injection of DNA encoding a viral protein. *Science* **259**, 1745-1749.
- Urashima, M., Suzuki, H., Yuza, Y., Akiyama, M., Ohno, N. & Eto, Y. (2000). An oral CD40 ligand gene therapy against lymphoma using attenuated *Salmonella typhimurium*. *Blood* **95**, 1258-1263.
- Van Mellaert, L., Barbé, S. & Anné, J. (2006). *Clostridium* spores as anti-tumour agents. *Trends in Microbiology* **14**, 190-196.
- Vanden Bush, T. J. & Rosenbusch, R. F. (2002). *Mycoplasma bovis* induces apoptosis of bovine lymphocytes. *FEMS Immunology and Medical Microbiology* **32**, 97-103.
- Veken, J. W., Oudega, B., Luirink, J. & Graaf, F. K. de. (1994). Binding of bovine transferrin by *Pasteurella multocida* serotype B:2,5, a strain which causes haemorrhagic septicaemia in buffalo and cattle. *FEMS Microbiology Letters* **115**, 253-257.
- Veken, J. W., Shah, N. H., Klaasen, P., Oudega, B. & Graaf, F. K. de. (1996). Binding of host iron-binding proteins and expression of iron-regulated membrane proteins by different serotypes of *Pasteurella multocida* causing haemorrhagic septicaemia. *Microbial Pathogenesis* **21**, 59-64.
- Velge, P., Bottreau, E., Van-Langendonck, N. & Kaeffer, B. (1997). Cell proliferation enhances entry of *Listeria monocytogenes* into intestinal epithelial cells by two proliferation-dependent entry pathways. *Journal of Medical Microbiology* **46**, 681-692.
- Verma, R. & Jaiswal, T. N. (1997). Protection, humoral and cell-mediated immune responses in calves immunized with multiple emulsion haemorrhagic septicaemia vaccine. *Vaccine* **15**, 1254-1260.
- Verma, R. & Jaiswal, T. N. (1998). Haemorrhagic septicaemia vaccines. *Vaccine* **16**, 1184-1192.

- Vilela, C. L., Fitzpatrick, J. & Morgan, K. L. (2004). *In vitro* adherence and invasion of ovine mammary epithelium by *Mannheimia (Pasteurella) haemolytica*. *Veterinary Journal* **167**, 211-213.
- Vorob'ev, A. A. & Khoroshko N. V. (2001). Persistence of *Escherichia coli* recombinant strains in experimental animals. *Zh Mikrobiol Epidemiology Immunobiology* **4**, 120-122.
- Watts, A. M. & Kennedy, R. C. (1999). DNA vaccination strategies against infectious diseases. *International Journal for Parasitology* **29**, 1149-1163.
- Watt, M. V., Duzeski, J. L., Loomis, A. G., Machnik, K. J., Noble, M. A., Sebestyen, M. G. & Hagstrom, J. E. (2002). Intracellular Localization and Expression of Labeled Plasmid DNA using Label IT® Tracker™ Nucleic Acid Labeling Kits. *Technical Report, Mirus Corp.*
- Weber, D. J., Wolfson, J. S., Swartz, M. N. & Hooper, D.C. (1984) *Pasteurella multocida* infections. Report of 34 cases and review of the literature. *Medicine* **63**, 133-154.
- Wedlock, D. N., Denis, M., Painter, G. F., Ainge, G. D., Vordermeier, H. M., Hewinson, R. G. & Buddle, B. M. (2008). Enhanced protection against bovine tuberculosis after coadministration of *Mycobacterium bovis* BCG with a mycobacterial protein vaccine-adjuvant combination but not after coadministration of adjuvant alone. *Infection and Immunity* **15**, 765-772.
- Wei, B. D. & Carter, G.R. (1978). Live streptomycin-dependent *Pasteurella multocida* vaccine for the prevention of hemorrhagic septicaemia. *American Journal of Veterinary Research* **39**, 1534-1537.
- Weinberg, A. D., Magnuson, N. S., Reeves, R., Wyatt, C. R. & Magnuson, J. A. (1988). Discrete phases of IL-2 production in bovine IL-2 lymphocytes. *Journal of Immunology* **141**, 1174-1179.
- Weiss, S. & Chakraborty, T. (2001). Transfer of eukaryotic expression plasmids to mammalian host cells by bacterial carriers. *Current Opinion in Biotechnology* **12**, 467-72.
- Wendorf, J., Singh, M., Chesko, J., Kazzaz, J., Soewanan, E. & Ugozzoli, M. (2006). A practical approach to the use of nanoparticles for vaccine delivery. *Particle Characterization* **95**, 2738-2750.

- Williams, R. S., Johnston, S. A., Riedy, M., DeVit, M. J., McElligott, S. G. & Sanford, J. C. (1991). Introduction of foreign genes into tissues of living mice by DNA-coated microprojectiles. *Proceedings of the National Academy of Sciences of the United States of America* **88**, 2726-2730.
- Wolff, J. A., Malone, R. W., Williams, P., Chong, W., Acsadi, G. & Jani, A. (1990). Direct gene transfer into mouse muscle i. *Science* **247**, 1465-1468.
- Wood, A. R., Lainson, F. A., Wright, F., Baird, G. D., & Donachie, W. (1995). A native plasmid of *Pasteurella haemolytica* serotype A1: DNA sequence analysis and investigation of its potential as a vector. *Research in Veterinary Science* **58**, 163-168.
- Wright, C. L., Strugnell, R. A. & Hodgson, A. L. (1997). Characterization of a *Pasteurella multocida* plasmid and its use to express recombinant proteins in *P. multocida*. *Plasmid* **37**, 65-79.
- Wu, G. Y. & Wu, C. H. (1987). Receptor-mediated *in vitro* gene transformation by a soluble DNA carrier system. *The Journal of Biological Chemistry* **262**, 4429-4432.
- Wu, X.-M., Todo, H. & Sugibayashi, K. (2007). Enhancement of skin permeation of high molecular compounds by a combination of microneedle pretreatment and iontophoresis. *Journal of Controlled Release : Official Journal of the Controlled Release Society* **118**, 189-195.
- Xiang, R., Lode, H. N., Chao, T. H., Ruehlmann, J. M., Dolman, C. S., Rodriguez, F., Whitton, J. L., Overwijk, W. W., Restifo, N. P. & Resfield, R. A. (2000). An autologous oral DNA vaccine protects against murine melanoma. *Proceedings of the National Academy of Sciences of the United States of America* **97**, 5492-5497.
- Yang, N. S., Burkholder, J., Roberts, B., Martinell, B. & McCabe, D. (1990). *In vivo* and *in vitro* gene transfer to mammalian somatic cells by particle bombardment. *Proceedings of the National Academy of Sciences of the United States of America* **87**, 9568-9572.
- Yao, T., Meccas, J., Healy, J. I., Falkow, S. & Chien, Y. (1999). Suppression of T and B lymphocyte activation by a *Yersinia pseudotuberculosis* virulence factor, *yopH*. *The Journal of Experimental Medicine* **190**, 1343-1350.

- Yeo, B. K. & Mokhtar, I. (1993). Haemorrhagic septicaemia of buffalo in Sabah, Malaysia. *ACIAR Proceedings* **43**, 112-115.
- Yoshida, A., Nagata, T., Uchijima, M., Higashi, T. & Koide, Y. (2000). Advantage of gene gun-mediated over intramuscular inoculation of plasmid DNA vaccine in reproducible induction of specific immune responses. *Vaccine* **18**, 1725-1729.
- Yoshikawa, Y., Ogawa, M., Hain, T., Yoshida, M., Fukumatsu, M., Kim, M., Mimuro, H., Nakagawa, I., Yanagawa, T., Ishii, T., Kakizuka, A., Sztul, E., Chakraborty, T. & Sasakawa, C. (2009). *Listeria monocytogenes* ActA-mediated escape from autophagic recognition. *Nature Cell Biology* **11**, 1233-1240.
- Yu, D.-H., Hu, X.-D., Cai, H. & Li, M. (2007). A combined DNA vaccine encoding BCSP31, SOD, and L7/L12 confers high protection against *Brucella abortus* 2308 by inducing specific CTL responses. *DNA and Cell Biology* **26**, 435-443.
- Zamri-Saad, M. (2005). Attempts to develop vaccines against Haemorrhagic septicaemia: A Review. Proceeding of Regional Symposium on Haemorrhagic Septicaemia, 1<sup>st</sup> - 2<sup>nd</sup> December 2005, Putrajaya, Malaysia, pg. 1-11.
- Zamri-Saad, M., Ernie, Z. A. & Sabri, M. Y. (2006). Protective effect following intranasal exposure of goats to live *Pasteurella multocida* B:2. *Tropical Animal Health and Production* **38**, 541-546.
- Zhao, G., Pijaon, C., Choi, K., Maheswaran, S. K. & Trigo, E. (1995). Expression of iron-regulated outer membrane proteins by porcine strains of *Pasteurella multocida*. *Canadian Journal of Veterinary Research* **59**, 46-50.
- Zheng, L. M., Luo, X., Feng, M., Li, Z., Le, T., Ittensohn, M., Trailsmith, M., Bermudes, D., Lin, S. L. & King, I. C. (2000). Tumor amplified protein expression therapy: *Salmonella* as a tumor-selective protein delivery vector. *Oncology research* **12**, 127-135.







## Appendix 2

### Preparation of antibiotic solutions

Stock solutions of antibiotics were made at the following concentrations (% w/v): ampicillin (1%), kanamycin (1%) and chloramphenicol (1%). Chloramphenicol was dissolved in ethanol. All other antibiotics were dissolved in distilled water and filter sterilised by passing the solution through an Acrodisc of 0.45 µm pore size (Milipore). All antibiotic solutions were stored at -20° C

### Phosphate-buffered saline (PBS)

Sodium chloride	128 mM
Potassium chloride	2.7 mM
Potassium di-hydrogen orthophosphate	1.5 mM
di-potassium hydrogen phosphate	5.0 mM

### Tris-Borate-EDTA (TBE) buffer

(5 x stock solution)

1 litre

Tris-base	54 g
Boric acid	27.5 g
EDTA (0.5 M stock) pH 8.0	20 ml

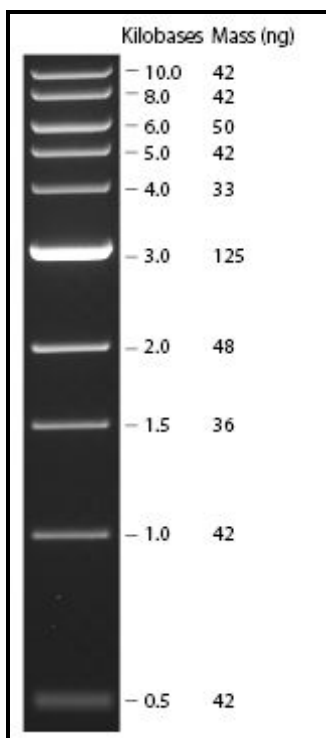
### DNA loading buffer

(6 x stock solution)

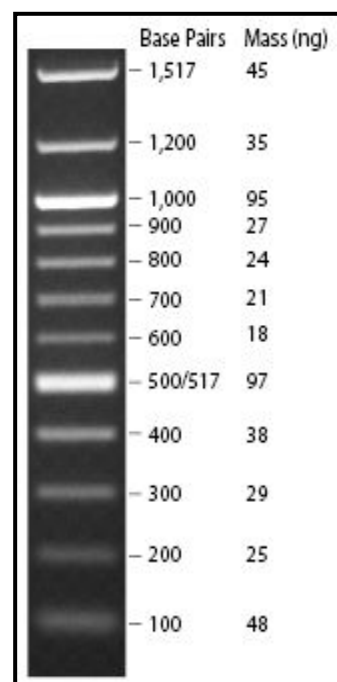
Tris	60 mM
EDTA	6 mM
Sucrose	40%
Bromophenol blue	0.25%

**DNA ladder**

Quick-Load™ 1 kb DNA Ladder



Quick-Load™ 100 bp DNA Ladder



## Appendix 3

### **QIAprep® Spin Miniprep Kit for plasmid DNA purification.**

The kit (cat. nos. 27104 and 27106) can be stored at room temperature (15-25°C) for up to 12 months. More information in *QIAprep Miniprep Handbook, December 2006* at [www.qiagen.com/handbooks](http://www.qiagen.com/handbooks). All centrifugation steps are carried out at 13,000 rpm in a conventional table-top centrifuge.

1. Pellet 1-5 ml bacterial overnight culture by centrifugation at >8000 rpm (6800 x g) for 3 min at room temperature (15-25°C).
2. Resuspend pelleted bacterial cells in 250 µl Buffer P1 and transfer to a microcentrifuge tube.
3. Add 250 µl Buffer P2 and mix thoroughly by inverting the tube 4-6 times until the solution becomes clear. Do not allow the lysis reaction to proceed for more than 5 min. If using LyseBlue reagent, the solution will turn blue.
4. Add 350 µl Buffer N3 and mix immediately and thoroughly by inverting the tube 4-6 times. If using LyseBlue reagent, the solution will turn colorless.
5. Centrifuge for 10 min at 13,000 rpm (~17,900 x g).
6. Apply the supernatant from step 5 to the QIAprep spin column by decanting or pipetting. Centrifuge for 30-60 s and discard the flow-through.
7. Recommended: Wash the QIAprep spin column by adding 0.5 ml Buffer PB. Centrifuge for 30-60 s and discard the flow-through.
8. Wash the QIAprep spin column by adding 0.75 ml Buffer PE. Centrifuge for 30-60 s and discard the flow-through. Transfer the QIAprep spin column to the collection tube.
9. Centrifuge for 1 min to remove residual wash buffer.
10. Place the QIAprep column in a clean 1.5 ml microcentrifuge tube. To elute DNA, add 50 µl Buffer EB (10 mM Tris-Cl, pH 8.5) or water to the center of the QIAprep spin column, let stand for 1 min, and centrifuge for 1 min.
11. Plasmid DNA is stored in -20°C till further used.

### **QIAquick® Gel Extraction Kit for purification of DNA from agarose gel.**

The QIAquick Gel Extraction Kit (cat. nos. 28704 and 28706) can be stored at room temperature (15-25°C) for up to 12 months. More information in *QIAquick Spin Handbook, March 2008* at [www.qiagen.com/handbooks](http://www.qiagen.com/handbooks). All centrifugation steps are carried out at 17,900 x g (13,000 rpm) in a conventional table-top centrifuge.

1. Excise the DNA fragment from the agarose gel with a clean, sharp scalpel.
2. Weigh the gel slice in a colorless tube. Add 3 volumes Buffer QG to 1 volume gel (100 mg ~ 100  $\mu$ l). For >2% agarose gels, add 6 volumes Buffer QG.
3. Incubate at 50°C for 10 min (or until the gel slice has completely dissolved). Vortex the tube every 2-3 min to help dissolve gel.
4. After the gel slice has dissolved completely, check that the color of the mixture is yellow. If the color of the mixture is orange or violet, add 10  $\mu$ l 3 M sodium acetate, pH 5.0, and mix. The color of the mixture will turn yellow.
5. Add 1 gel volume of isopropanol to the sample and mix.
6. Place a QIAquick spin column in a provided 2 ml collection.
7. To bind DNA, apply the sample to the QIAquick column and centrifuge for 1 min. Discard flow-through and place the QIAquick column back into the tube.
8. If the DNA will subsequently be used for sequencing, add 0.5 ml Buffer QG to the QIAquick column and centrifuge for 1 min. Discard flow-through and place the QIAquick column back into the same tube.
9. To wash, add 0.75 ml Buffer PE to QIAquick column and centrifuge for 1 min. Discard flow-through and place the QIAquick column back into the tube.
10. Centrifuge the QIAquick column once more in the provided 2 ml collection tube for 1 min at 17,900 x g (13,000 rpm) to remove residual wash buffer.
11. Place QIAquick column into a clean 1.5 ml microcentrifuge tube.
12. To elute DNA, add 50  $\mu$ l Buffer EB (10 mM Tris-Cl, pH 8.5) or water to the center of the QIAquick membrane and centrifuge the column for 1 min. For increased DNA concentration, add 30  $\mu$ l Buffer EB to the center of the QIAquick membrane, let the column stand for 4 min, and then centrifuge for 1 min.

#### **QIAquick® PCR Purification Kit for cleaning up DNA after PCR.**

The QIAquick PCR Purification Kit (cat. nos. 28104 and 28106) can be stored at room temperature (15-25°C) for up to 12 months. More information in *QIAquick Spin Handbook, March 2008* at [www.qiagen.com/handbooks](http://www.qiagen.com/handbooks). All centrifugation steps are carried out at 17,900 x g (13,000 rpm) in a conventional table-top centrifuge at room temperature.

1. Add 5 volumes Buffer PB to 1 volume of the PCR reaction and mix. If the color of the mixture is orange or violet, add 10  $\mu$ l 3 M sodium acetate, pH 5.0, and mix. The color of the mixture will turn yellow.

2. Place a QIAquick column in a provided 2 ml collection.
3. To bind DNA, apply the sample to the QIAquick column and centrifuge for 30-60 s. Discard flow-through and place the QIAquick column back in the tube.
4. To wash, add 0.75 ml Buffer PE to the QIAquick column centrifuge for 30-60 s. Discard flow-through and place the QIAquick column back in the tube.
5. Centrifuge the QIAquick column once more in the provided 2 ml collection tube for 1 min to remove residual wash buffer.
6. Place each QIAquick column in a clean 1.5 ml microcentrifuge tube.
7. To elute DNA, add 50  $\mu$ l Buffer EB (10 mM Tris·Cl, pH 8.5) or water (pH 7.0-8.5) to the center of the QIAquick membrane and centrifuge the column for 1 min. For increased DNA concentration, add 30  $\mu$ l elution buffer to the center of the QIAquick membrane, let the column stand for 1 min, and then centrifuge.

**MinElute<sup>®</sup> Reaction Cleanup Kit for cleaning DNA after enzymatic reactions.**

The MinElute Reaction Cleanup Kit (cat. nos. 28204 and 28206) can be stored at room temperature (15-25°C) for up to 12 months. Store spin columns at 2-8°C upon arrival. More information in the *MinElute Handbook* which can be found at [www.qiagen.com/handbooks](http://www.qiagen.com/handbooks). This protocol is for cleanup of up to 5  $\mu$ g DNA (70 bp to 4 kb) from enzymatic reactions. All centrifugation steps are carried out at 17,900 x g (13,000 rpm) in a conventional table-top centrifuge at room temperature (15-25°C).

1. Add 300  $\mu$ l Buffer ERC to the enzymatic reaction (sample volume 20-100  $\mu$ l) and mix. If the enzymatic reaction is in a volume of <20  $\mu$ l, adjust the volume to 20  $\mu$ l. If the enzymatic reaction exceeds 100  $\mu$ l, split your reaction, add 300  $\mu$ l Buffer ERC to each aliquot, and use the appropriate number of MinElute columns.
2. Check that the color of the mixture is yellow (similar to Buffer ERC without the enzymatic reaction). If the color of the mixture is orange or violet, add 10  $\mu$ l 3 M sodium acetate, pH 5.0, and mix. The color of the mixture will turn to yellow.
3. Place a MinElute column in a provided 2 ml collection tube.
4. Apply sample to the MinElute column and centrifuge for 1 min. Discard flow-through and place the MinElute column back into the tube.

5. Add 750  $\mu$ l Buffer PE to the MinElute column and centrifuge for 1. Discard flow-through and place the MinElute column back into the same collection tube.
6. Centrifuge the column in a 2 ml collection tube (provided) for 1 min. Residual ethanol from Buffer PE will not be completely removed unless the flow-through is discarded before this additional centrifugation.
7. Place each MinElute column into a clean 1.5 ml microcentrifuge tube.
8. To elute DNA, add 10  $\mu$ l Buffer EB (10 mM Tris·Cl, pH 8.5) or water to the center of the MinElute membrane. (Ensure that the elution buffer is dispensed directly onto the membrane for complete elution of bound DNA.) Let the column stand for 1 min, and then centrifuge the column for 1 min.

## PROMEGA pGEM<sup>®</sup>-T Easy Vector Systems

### Cloning PCR Products with pGEM<sup>®</sup>-T Easy Vectors

#### *Ligation Using 2X Rapid Ligation Buffer*

1. Briefly centrifuge the pGEM<sup>®</sup>-T Easy Vectors and Control Insert DNA tubes to collect contents at the bottom of the tube.
2. Set up ligation reactions as described below. Vortex the 2X Rapid Ligation Buffer vigorously before each use. Use 0.5 ml tubes known to have low DNA binding capacity.

Reagents	Standard Reaction	Positive Control	Background Control
2X Rapid Ligation Buffer, T4 DNA Ligase	5 $\mu$ l	5 $\mu$ l	5 $\mu$ l
pGEM <sup>®</sup> -T or pGEM <sup>®</sup> -T Easy Vector (50ng)	1 $\mu$ l	1 $\mu$ l	1 $\mu$ l
PCR product	X $\mu$ l	–	–
Control Insert DNA	–	2 $\mu$ l	–
T4 DNA Ligase (3 Weiss units/ $\mu$ l)	<u>1<math>\mu</math>l</u>	<u>1<math>\mu</math>l</u>	<u>1<math>\mu</math>l</u>
Deionized water to a final volume of	10 $\mu$ l	10 $\mu$ l	10 $\mu$ l

3. Mix the reactions by pipetting. Incubate the reactions 1 hour at room temperature. Alternatively, incubate the reactions overnight at 4°C for the maximum number of transformants.

### **Transformation into High Efficiency Competent *E. coli* Cells**

1. Prepare LB/ampicillin/IPTG/X-Gal plates.
2. Centrifuge the ligation reactions briefly. Add 2  $\mu$ l of each ligation reaction to a sterile 1.5 ml tube on ice. Prepare a control tube with 0.1 ng of uncut plasmid.



3. Place the High Efficiency Competent *E. coli* Cells in an ice bath until just thawed (5 minutes). Mix cells by gently flicking the tube.
4. Carefully transfer 50  $\mu$ l of cells to the ligation reaction tubes from Step 2. Use 100  $\mu$ l of cells for the uncut DNA control tube. Gently flick the tubes and incubate on ice for 20 min.
5. Heat-shock the cells for 45-50 seconds in water bath at exactly 42°C. DO NOT SHAKE. Immediately return the tubes to ice for 2 minutes.
6. Add 950  $\mu$ l room temperature SOC medium to the ligation reaction transformations and 900  $\mu$ l to the uncut DNA control tube. Incubate for 1.5 hours at 37°C with shaking (~150 rpm).
7. Plate 100  $\mu$ l of each transformation culture onto duplicate LB/ampicillin/IPTG/X-Gal plates. For the uncut DNA control, a 1:10 dilution with SOC is recommended.
8. Incubate plates overnight at 37°C. Select white colonies.

## Appendix 4

### Cell culture

#### J774.2 or BL-3 complete medium

Heat-inactivated FBS (Sigma, UK)	10% (v/v)
L-glutamine (Gibco, UK)	1% (v/v)
Penicillin/Streptomycin (Sigma, UK)	1% (v/v)
Fungizone (Amphotericin B) (Gibco, UK)	1% (v/v)
Add RPMI (1640) medium (Sigma, UK)	up to 200 ml

#### J774.2 or BL-3 assay medium

As above but without antibiotics and fungizone.

#### EBL complete medium

Heat-inactivated FBS (Sigma, UK)	10% (v/v)
L-glutamine (Gibco, UK)	1% (v/v)
Penicillin/Streptomycin (Sigma, UK)	1% (v/v)
Fungizone (Amphotericin B) (Gibco, UK)	1% (v/v)
Add MEM (M2279) medium (Sigma, UK)	up to 200 ml

#### EBL assay medium

As above but without antibiotics and fungizone.

### Cell counting using a haemocytometer

As manufacturer's instructions ([www.abcam.com/technical](http://www.abcam.com/technical)).

#### Preparing haemocytometer

1. Ensure the haemocytometer is clean using 70% ethanol.
2. Moisten the shoulders of the haemocytometer and affix the coverslip using gentle pressure and small circular motions. The phenomenon of Newton's rings can be observed when the coverslip is correctly affixed, thus the depth of the chamber is ensured.

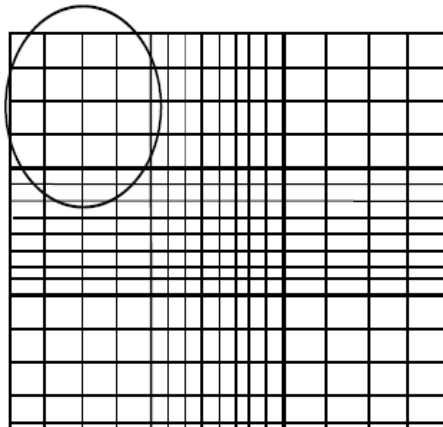
#### Preparing cell suspension

1. Make sure the cell suspension to be counted is well mixed by either gentle agitation of the flask containing the cells (or other appropriate container). A serological pipette may be used if required.
2. Before the cells have a chance to settle take out about 1 ml of cell suspension using a serological pipette and place in an eppendorf tube.

- Using a 100  $\mu\text{l}$  pipette, mix the cells in this sample again (gently to avoid lysing them). Take out 100  $\mu\text{l}$  and place into a new eppendorf, add 100  $\mu\text{l}$  trypan blue and mix gently again.

### Cell counting

- Using the pipette, draw up some cell suspension containing trypan blue. Carefully fill the haemocytometer by gently resting the end of the pipette tip at the edge of the chambers. Take care not to overfill the chamber. Allow the sample to be drawn out of the pipette by capillary action, the fluid should run to the edges of the grooves only.
- Focus on the grid lines of the haemocytometer using the x10 objective of the microscope. Focus on one set of 16 corner squares (shown below).



- Using a hand tally counter, count the number of cells in this area of 16 squares. When counting, always count only live cells that look healthy (unstained by Trypan Blue). Count cells that are within the square and any positioned on the right hand or bottom boundary line. Dead cells stained blue with trypan blue can be counted separately for a viability count.
- Move the haemocytometer to another set of 16 corner squares and carry on counting until all 4 sets of 16 corner squares are counted.
- The haemocytometer is designed so that the number of cells in one set of 16 corner squares is equivalent to the number of cells  $\times 10^4$  /ml

Therefore, to obtain the count:

The total count from 4 sets of 16 corner =

$[(\text{cells/ml} \times 10^4) \times 4 \text{ squares from one haemocytometer grid}]$

Divide the count by 4, and then multiply by 2 to adjust for the 1:2 dilutions in trypan blue. These two steps are equivalent to dividing the cell count by 2.

Viability

1. The trypan blue is used to stain any dead cells. Cells looking faint or dark blue within the grid being counted are counted as dead cells. To check the viability of the cells requires:

- **Live cell count** (not including trypan blue cells)
- **Total cell count** including those stained with trypan blue.

$$\frac{\text{Live cell count}}{\text{Total cell count}} = \% \text{ Viability}$$

**Concanavalin A (ConA)**

ConA (Sigma, UK) 5 mg

RPMI 1640 (Sigma, UK) 10 ml

Aliquot of 200 µl kept in -20°C. Before use, mixed with 800 µl of RPMI 1640.

**Red blood cell (RBC) lysis buffer**

(10 x stock solution), pH 7.4

NH<sub>4</sub>Cl 1.5 M

NaHCO<sub>3</sub> 0.1 M

diNaEDTA 1 mM

dH<sub>2</sub>O 900 ml

**Wash buffer**

FBS 2%

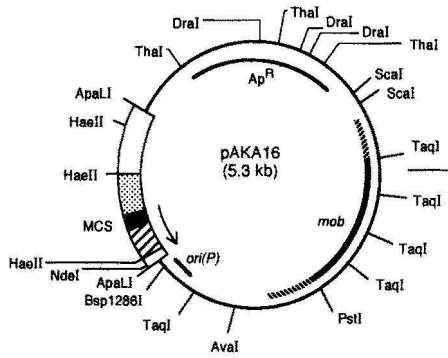
Penicillin/Streptomycin 1%

Hank's balance salt solution (HBSS) (Sigma, UK) 98 ml

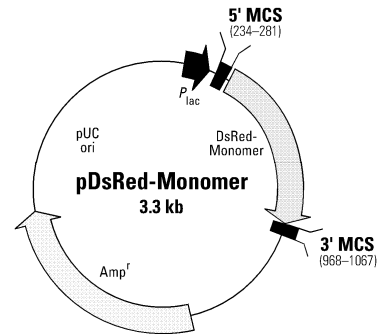
# Appendix 5

## Plasmid DNA

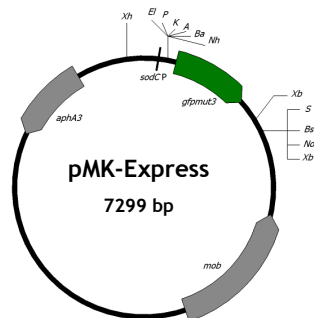
pAKA 16 (Azad *et al.*, 1994)



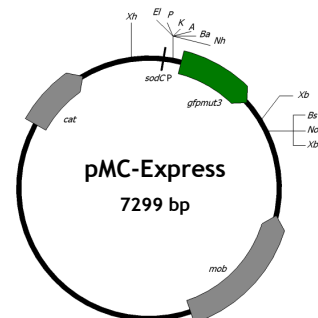
pDsRed-Monomer (ClonTech, USA)



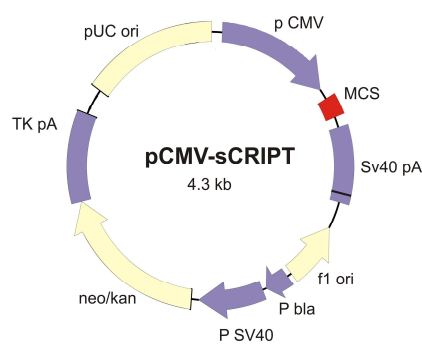
pMK-Express (Bossé *et al.*, 2010)



pMC-Express (Bossé *et al.*, 2010)



pCMV-sCRIP (Stratagene, UK)



pEGFP-N1 (ClonTech, USA)

